

THE ORIGIN OF THE NINETYEAST RIDGE
AND THE NORTHWARD MOTION OF INDIA,
BASED ON DSDP PALEOLATITUDES

by

JOHN WENTWORTH PEIRCE

A.B., Dartmouth College
(1968)

SUBMITTED IN PARTIAL FULFILLMENT OF THE REQUIREMENTS FOR
THE DEGREE OF DOCTOR OF PHILOSOPHY

at the

MASSACHUSETTS INSTITUTE OF TECHNOLOGY

and the

WOODS HOLE OCEANOGRAPHIC INSTITUTION

January, 1977

Signature of Author _____

Joint Program in Oceanography, Massachusetts Institute of
Technology - Woods Hole Oceanographic Institution, and the
Department of Earth and Planetary Sciences, Massachusetts
Institute of Technology, December, 1976

Certified by _____

Thesis Supervisor

Accepted by _____

Chairman, Joint Oceanography Committee in Earth Sciences,
Massachusetts Institute of Technology - Woods Hole
Oceanographic Institution

Lindgren
~~WITHDRAWN~~
NOV 8 1976
FROM
MIT LIBRARIES

TABLE OF CONTENTS

Subject	Page No.
1. List of Figures	5
2. List of Tables	8
3. Biographical Sketch	9
4. List of Publications	11
5. Acknowledgements	12
6. Abstract	14
7. Chapter I - Overview	16
8. Chapter II - Paleomagnetic results of basalt samples from DSDP Leg 26, southern Indian Ocean ...	36
a. Abstract	37
b. Introduction	37
c. Natural remanent magnetization, coercivity, and susceptibility	37
d. Viscous remanent magnetization	39
e. Inclinations and reversals	40
f. Paleolatitudes	43
g. Acknowledgements	47
h. References	47
9. Chapter III - Assessing the reliability of DSDP paleolatitudes	48
a. Abstract	50
b. Introduction	52
c. Limitations of DSDP paleolatitudes	54
d. Secondary magnetization	59
e. Age of paleolatitudes	62
f. Corrected paleolatitudes	63
g. Confidence limits	67
h. Rating criteria	69
i. Discussion	77
(1) Poles for the Pacific plate	78
(2) Poles for the Australian plate	89

j.	Origin of the Ninetyeast Ridge	94
k.	Conclusions	95
l.	Acknowledgements	99
m.	References	112
10.	Chapter IV - The origin of the Ninetyeast Ridge and the northward motion of India, based on DSDP paleolatitudes	124
a.	Abstract	126
b.	Introduction	128
c.	Tectonics of the Indian Ocean	129
d.	Previous evidence for northward motion	138
e.	Basalt paleolatitudes	139
f.	Geology of the basalt sections	143
	(1) Site 213	147
	(2) Site 214	148
	(3) Site 215	150
	(4) Site 216	151
g.	Sediment paleolatitudes	152
h.	Magnetic stability of sediments	161
	(1) Site 213	161
	(2) Site 214	162
	(3) Site 215	162
	(4) Site 216	163
	(5) Site 217	164
i.	Paleomotion of the Ninetyeast Ridge	165
j.	Skewness of magnetic anomalies	179
k.	Anomaly identification	185
l.	Previous Ninetyeast Ridge models and their predicted paleolatitudes	189
	(1) Migrating spreading center-transform junction model	190
	(2) Hotspot model	191
	(3) Two hotspot model	192
m.	Implications for the origin of the Ninetyeast Ridge	194
n.	Summary	206
o.	References	223
11.	Appendix I - Basalt specimen directions	234
12.	Appendix II - Stereonet plots and alternating field demagnetization curves for representative basalt pilot specimens	241
13.	Appendix III - Sediment specimen directions	253

14. Appendix IV - Stereonet plots and alternating field demagnetization curves for representative sediment pilot specimens 262
15. Appendix V - Deskewed magnetic anomalies from the east central Indian Ocean 274

LIST OF FIGURES

Chapter I	Page No.
1. Smith and Hallam reconstruction of Gondwanaland	19
2. Sketch map of the Indian Ocean about 53 mybp	21
3. Bathymetry of the Indian Ocean	23
4. Hotspot model for the origin of the Ninetyeast Ridge	27
Chapter II	
1 - 6. Progressive alternating field demagnetization curves for DSDP Leg 26 basalt specimens	40
7. Median destructive field, Curie temperature, and NRM intensity at DSDP Site 257	43
8 - 11. Graphs of viscous remanent magnetization acquisition in 1000 hours	43
12 - 13. Graphs of shock remanent magnetization acquisition for sample 257-11-3-130	45
14. Magnetic inclinations versus depth for DSDP Leg 26 basalt specimens	45
15. Histograms of magnetic inclinations at DSDP Sites 256 and 257	46
16. Loci of virtual geomagnetic poles of DSDP Leg 26 basalts compared with apparent polar wandering curves	46
Chapter III	
1. Paleolatitude correction parameter	70
2. Histograms of paleolatitude ratings	75
3a. Paleolatitude histograms versus age for DSDP Site 10	79

3b. Paleolatitude histograms versus age for DSDP Site 66	79
4. Upper Cretaceous paleomagnetic pole for the Pacific plate	83
5. Middle Cretaceous paleomagnetic pole for the Pacific plate	86
6. Middle Cretaceous paleomagnetic pole for the Wharton Basin	90
7. Loci of possible paleomagnetic pole positions for DSDP Sites 212 and 213 in the Wharton Basin	92
8. Chart of the Indian Ocean	96

Chapter IV

1. Bathymetric chart of the Indian Ocean	132
2. Tectonic summary diagram of the eastern Indian Ocean	134
3. Evolution of the eastern Indian Ocean	136
4. Uncorrected paleolatitudes for basalt cooling units	144
5. Histograms of uncorrected paleolatitudes for sediment samples	156
6. Paleomotion of DSDP Site 216	166
7. Comparison of estimates of the paleomotion of DSDP Site 216	171
8a. Reconstruction of the Indian Ocean, 34 mybp	176
8b. Reconstruction of the Indian Ocean, 51.5 mybp	176
9. Lunes of possible paleomagnetic pole positions	181
a. For the Indian plate, anomalies 22 - 26	
b. For the Indian plate, anomalies 25 - 33	
c. For the Wharton Basin plate, anomalies 25 - 33	
10. Deskewed magnetic anomalies in the east central Indian Ocean	186

11. Comparison of measured and predicted paleo- latitudes on the Ninetyeast Ridge	196
Appendix II - Stereonet plots and alternating field demagnetization curves for representative basalt pilot specimens	242
Appendix IV - Stereonet plots and alternating field demagnetization curves for representative sediment pilot specimens	263
Appendix V - Deskewed magnetic anomalies from the east central Indian Ocean	275

LIST OF TABLES

Chapter II	Page No.
1. Paleomagnetic results from basalt samples, DSDP Leg 26	38
2. Site means and paleolatitudes	44
Chapter III	
1. Summary of DSDP paleolatitudes, Legs 1 - 33	100
Chapter IV	
1. Basalt paleolatitudes	209
2. Apparent cooling units, Site 213	210
3. Apparent cooling units, Site 214	212
4. Apparent cooling units, Site 215	214
5. Apparent cooling units, Site 216	215
6. Sediment paleolatitudes	216
7. Rotations used to compute paleolatitudes for DSDP Site 216 in Figure 7	221
Appendix I	
1. Basalt specimen directions	235
Appendix III	
1. Sediment specimen directions	254

BIOGRAPHICAL SKETCH

I was born in Boston, Massachusetts, on October 17, 1946. I grew up in the Boston area, and went to high school at Saint Mark's School, Southboro, Massachusetts. It was there that I first developed an interest in scientific research.

I graduated from Dartmouth College (Hanover, New Hampshire) in 1968 with a Bachelor of Arts degree, awarded with highest distinction in my major field, Earth Sciences. My experiences at Dartmouth included a field course on Central American volcanoes and a summer working on the active rift zones of Iceland.

After college I served in the United States Navy's nuclear submarine program. My experience there included three Polaris patrols, reactor refueling, and shipyard overhaul. I was honorably discharged as a Lieutenant in 1972.

In the fall of that year I entered the MIT-WHOI Joint Program in Oceanography. Since then, my work has concentrated on using paleomagnetism as a tool to solve problems in plate tectonics. In particular, my recent interest has been the application of paleomagnetic techniques to learn more about

the detailed nature of the genesis of ocean crust at plate boundaries.

I am presently an Assistant Professor in the Department of Geology at Dalhousie University in Halifax, Nova Scotia.

LIST OF PUBLICATIONS

1. Peirce, J.W., Chemical changes during palagonitization under marine and non-marine conditions, Science in Iceland, 2, 31-36, 1970.
2. Peirce, J.W., C.R. Denham, and B.P. Luyendyk, Paleomagnetic results from basalt samples, DSDP Leg 26, (extended abstract), EOS Trans. Am. Geophys. Un., 54, 1027-1029, 1973.
3. Peirce, J.W., C.R. Denham, and B.P. Luyendyk, Paleomagnetic results of basalt samples from DSDP Leg 26, Southern Indian Ocean, in Davies, T.A., B.P. Luyendyk, et al., Initial Reports of the Deep Sea Drilling Project, XXVI, Washington (U.S. Govt. Printing Office), 517-527, 1974.
4. Sclater, J.G., C.O. Bowin, R.N. Hey, H.L. Hoskins, J.W. Peirce, J.D. Phillips, and C.R. Tapscott, The Bouvet triple junction, J. Geophys. Res., 81, 1857-1869, 1976; abstract: Peirce, J.W., et al., EOS Trans. Am. Geophys. Un., 56, 452, 1975.
5. Peirce, J.W., Assessing the reliability of DSDP paleolatitudes, J. Geophys. Res., in press, 1976; abstract: Peirce, J.W., EOS Trans. Am. Geophys. Un., 57, 405-406, 1976.
6. Peirce, J.W., The origin of the Ninetyeast Ridge and the northward motion of India, based on DSDP paleolatitudes, for submission to Geophys. Jour. Roy. astr. Soc., in preparation, 1976.

ACKNOWLEDGEMENTS

My original interest in the Ninetyeast Ridge was kindled by a seminar in Indian Ocean tectonics, organized by Bruce Luyendyk. It was he who gave me the opportunity to work on the paleomagnetism of DSDP Leg 26 basalts. Chuck Denham patiently taught me many of the intricacies of paleomagnetism research and helped me earn my credentials as a paleomagnetist. I am especially indebted to Bruce, Chuck, John Sclater, and Tanya Atwater for helping me develop my ideas about the Ninetyeast Ridge into a successful National Science Foundation grant proposal.

Out of the many scientists and staff at Woods Hole and elsewhere who have assisted me in this project, I would particularly like to acknowledge the following people: Chuck Helsley (University of Texas at Dallas) and Norman Watkins (University of Rhode Island) for the use of their cryogenic magnetometers; the WHOI Digital Data Library, especially Bob Groman and Steve Gegg, for their patience in the face of a stream of computer questions; Linda Meinke (MIT) for her assistance with the Indian Ocean magnetism data; Sandy Bernardo for her typing assistance and her skillful editing of my tables; Jake Peirson for sheltering me from the combined

bureaucracies of MIT and WHOI; and the WHOI Education Office and the National Science Foundation (Grant DES-74-22552) for financial support of this work.

My thesis committee (Chuck Denham, John Sclater, Carl Bowin, Jim Heirtzler, Peter Molnar, and Hans Schouten) has provided me with continuing encouragement, timely advice, and cogent criticisms over the duration of this project.

Thought-provoking discussions with John Sclater and Carl Bowin on the details of my model for the origin of the Ninetyeast Ridge were especially helpful in the preparation of the final draft of Chapter IV.

No graduate experience would be worthwhile without the constant exchange of ideas and the support of one's colleagues. In addition to those people cited above, I would like to give due credit to the friendship and intellectual stimulation which I have shared with many of my fellow students in the Joint Program, especially Jamie Austin, Scott Briggs, Keith Loudon, and Chris Tapscott.

And last, but certainly not least, I am particularly grateful to my best friend, Nancy Hetherington, for her moral support during the final harrowing months of thesis preparation as well as her assistance in assembling the final draft.

THE ORIGIN OF THE NINETYEAST RIDGE
AND THE NORTHWARD MOTION OF INDIA,
BASED ON DSDP PALEOLATITUDES

by

John Wentworth Peirce

Submitted to the Massachusetts Institute of Technology -
Woods Hole Oceanographic Institution Joint Program in
Oceanography on August 19, 1976 in partial fulfillment of
the requirements for the degree of Doctor of Philosophy.

ABSTRACT

This thesis is a collection of papers on the paleomagnetism of samples from several Deep Sea Drilling Project (DSDP) sites in the Indian Ocean. These papers present the basic paleomagnetic data, discuss the statistical methods for analyzing such data from DSDP cores, and examine the implications of the paleolatitudes for the origin of the Ninetyeast Ridge and the northward motion of India.

Rarely do DSDP paleolatitudes approach the reliability of good continental pole positions. However, the reliability of such paleolatitudes can be markedly improved by using comparisons with paleolatitudes of different ages from the same site, paleolatitudes of similar ages from different sites on the same plate, estimates of paleolatitude from the skewness of marine magnetic anomalies, and continental paleopole positions.

Using such comparisons, a new paleomagnetic pole of upper Cretaceous age has been defined for the Pacific plate. A middle Cretaceous pole has been defined for the Wharton Basin plate, and it suggests that there may have been left lateral motion between Australia and the Wharton Basin.

Paleolatitudes from the Ninetyeast Ridge are consistent with the pole position for the Deccan Traps. These data indicate that India and the Ninetyeast Ridge moved northwards with respect to the South Pole at 14.9 ± 4.5 cm/yr from 70 to 40 mybp and at $5.2 \pm .8$ cm/yr from 40 mybp until the present. However, when this paleomotion is compared to the Australian paleomagnetic data (by removing the relative motion components), a major inconsistency appears between 40 and 50 mybp. The Australian data indicate that India should be 13° further north than the positions implied by the Ninetyeast Ridge data.

Basal paleolatitudes on the Ninetyeast Ridge indicate that its volcanic source was approximately fixed in latitude near 50°S , supporting the hypothesis that the ridge is the trace of the Kerguelen hotspot on the northward moving Indian plate. There is considerable geologic evidence in favor of such an hypothesis, and there is none to contradict it.

Thesis Supervisor: Charles R. Denham

Title: Assistant Scientist

Chapter I

OVERVIEW

The Indian Ocean has the most complicated tectonic history of any of the world's oceans because its floor has been shaped by the complex breakup and dispersal of the Gondwanaland continent. This huge landmass was made up of South America and the continental blocks which now surround the Indian Ocean (Wegener, 1912a, 1912b, 1915; Du Toit, 1937; Smith and Hallam, 1970; Figure 1). In the early Cretaceous Gondwanaland started to break up, and the formation of the Indian Ocean began (McKenzie and Sclater, 1971; Sclater and Fisher, 1974). The Indian subcontinent moved rapidly northward, and eventually it began to collide with Asia. Two long aseismic ridges, the Ninetyeast Ridge to the east, and the Chagos-Laccadive Ridge to the west, marked the transform faults which once bounded the oceanic portion of the Indian plate. Both of these transform faults had active portions which were thousands of kilometers in length. To the east of India lay the Sunda plate (not subducted) and the Wharton Basin-Australian plate (see sketch map, Figure 2). To the west lay the African plate and the Chagos Transform Fault.

Although we now know the basic steps by which the Indian Ocean evolved, it was not until the International Indian Ocean Expedition (1960-65) that a coherent image of

the shape of the floor of the ocean began to emerge (Figure 3). Only then did the presence of the long, linear, aseismic ridge now named the Ninetyeast Ridge become known. It was so named because it strikes nearly due north along the 90th meridian from about 31°S until it is buried by the sediments of the Bengal Fan near 9°N (Heezen and Tharp, 1965).

The Ninetyeast Ridge is a curious feature which dominates the topography of the eastern Indian Ocean. It is some 4500 km. long, roughly 50-100 km. wide, and its relief above the surrounding ocean floor averages about 2 km. The earliest explanation for the origin of the ridge interpreted it as a horst (Francis and Raitt, 1967). Le Pichon and Heirtzler (1968) recognized that the ridge marked the old boundary between the Australian and the Indian plates, and they suggested that its elevation was caused by the edge of one plate overriding the other. The gravity and seismic data presented by Bowin (1973) indicate that the ridge is nearly isostatically compensated, and they are not compatible with either the horst or the overriding plate theory. In order to maintain a small free air gravity anomaly and still provide the 7-8 km/sec material detected by seismic refraction (Francis and Raitt, 1967), he proposed that a mixture of gabbro and serpentized peridotite was emplaced at depth at the same

FIGURE I

Reconstruction of Gondwanaland made using the poles of rotation listed in Smith and Hallam (1970), except that the sign of the longitude of the Antarctica/India pole has been corrected to $+7.7^\circ$. Also Ceylon has been moved into the space south of India to avoid overlap with Antarctica. Paleographic coordinates based on the Cygnet volcanic complex (104 mybp) paleomagnetic pole for Australia. These coordinates are only approximate as Gondwanaland had certainly begun to break up by this time. The map projection is Lambert equal area, centered at the South Pole.

60°

SMITH & HALLAM RECONSTRUCTION

120°

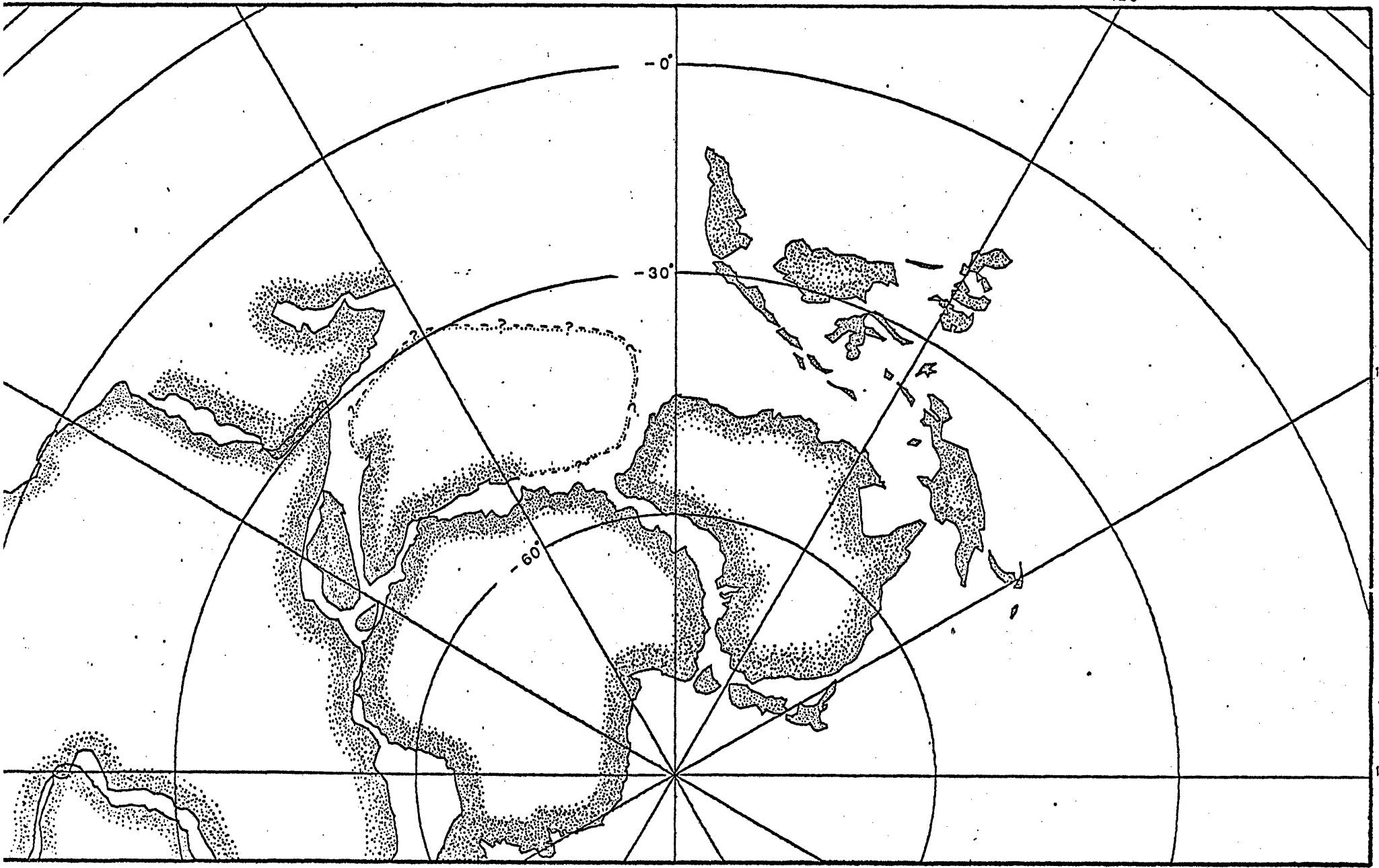


FIGURE 2

Sketch map of the Indian Ocean about 53 mybp.
Note the relative positions of the four plates
involved and the length of the Ninetyeast
Transform Fault. The position of the Ninetyeast
Ridge is delineated by DSDP sites 214, 216, and
217. Lambert equal area projection, centered
at the South Pole.

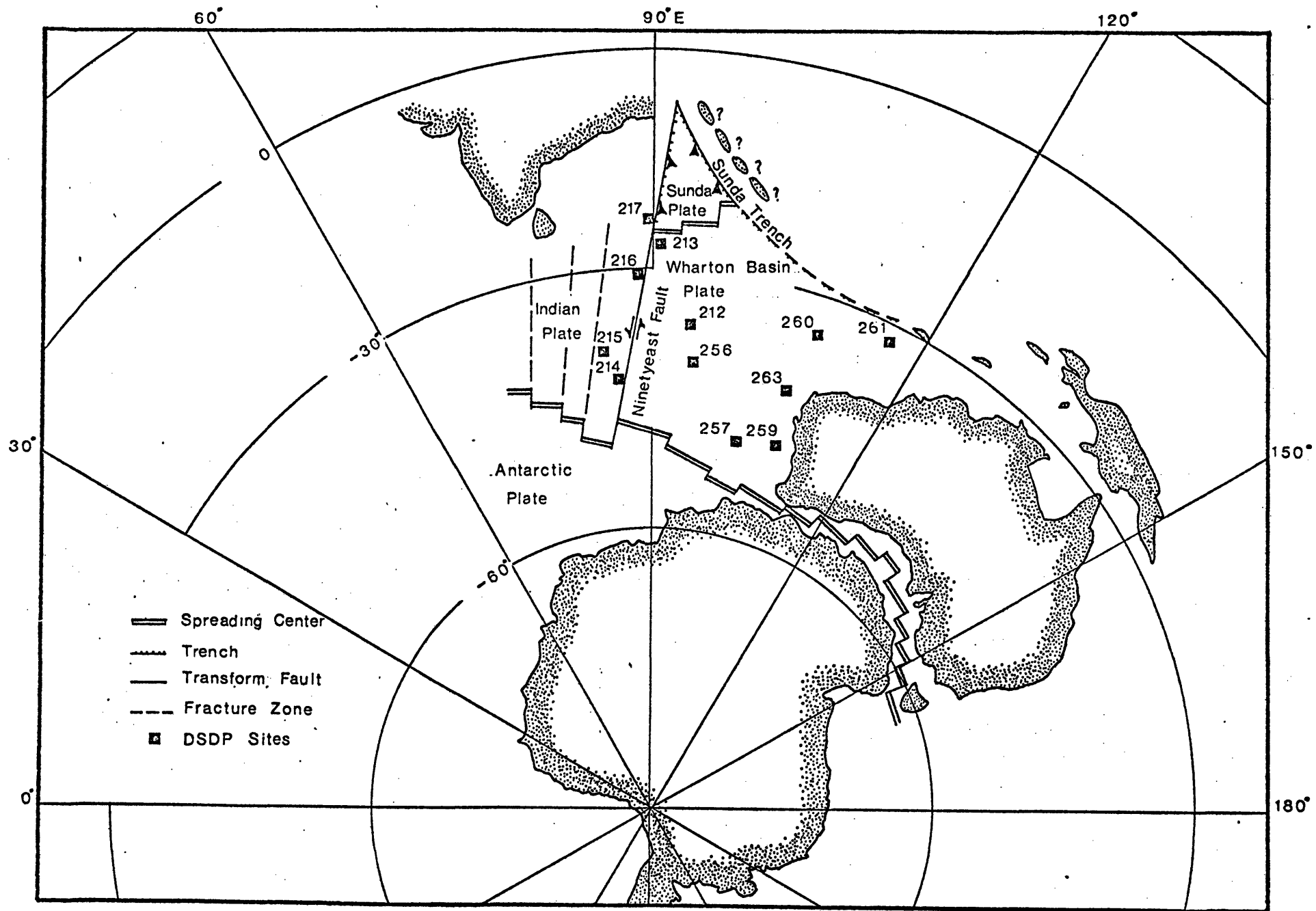
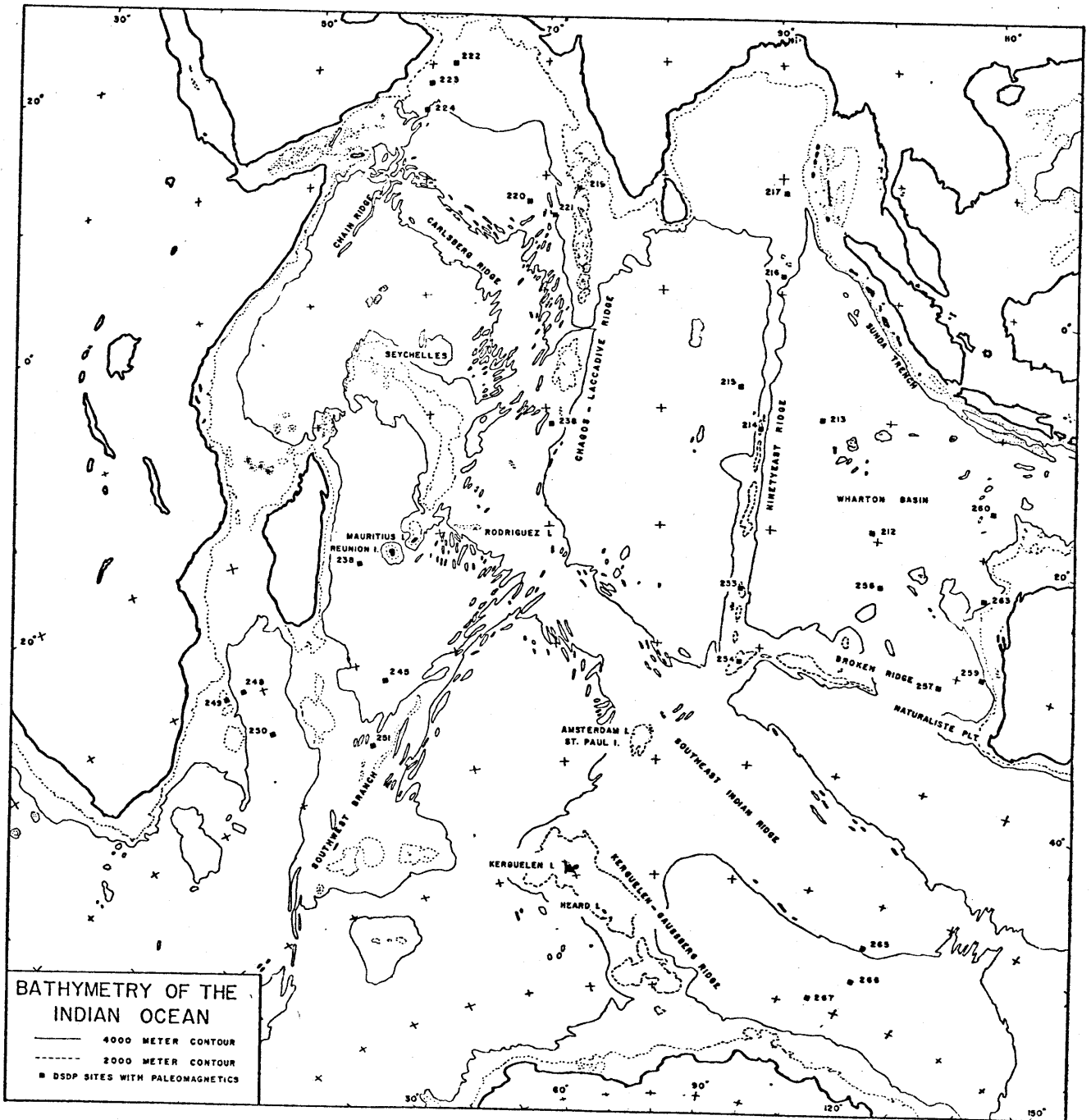


FIGURE 3

Bathymetric chart of the Indian Ocean. Contours from recently published Russian bathymetric chart (Burakova, ed., no publ. date). Squares indicate the positions of DSDP sites for which some paleomagnetic data has been reported.



time as the volcanic pile was being built at the surface. He favored a modification of the hotspot model (Wilson, 1965; Morgan, 1971, 1972a, 1972b) as the emplacement mechanism.

Basically, the hotspot model postulates that there are deep volcanic sources in the mantle which create rising plumes in the aesthenosphere. These plumes impinge on the underside of the lithosphere, and the material in them penetrates the plate and creates a pile of excess volcanics at the surface. Furthermore, these plumes are postulated to be fixed, or nearly fixed, with respect to geographic coordinates. If the plate above is moving over the plume some of the excess volcanics are carried away and a new pile is created in their place, much as smoke signals drift off to leeward in a slow breeze and are replaced by more from the same source. The surface manifestation of this process is an island/seamount chain (such as the Hawaii/Emperor seamount chain, Wilson, 1965) if the delivery of the volcanics to the surface is discontinuous, or a continuous ridge if the delivery process is continuous (see sketch, Figure 4).

A more recent theory for the origin of the Ninetyeast Ridge is that it is the line of excess volcanics produced at the migrating junction of a spreading center and a major

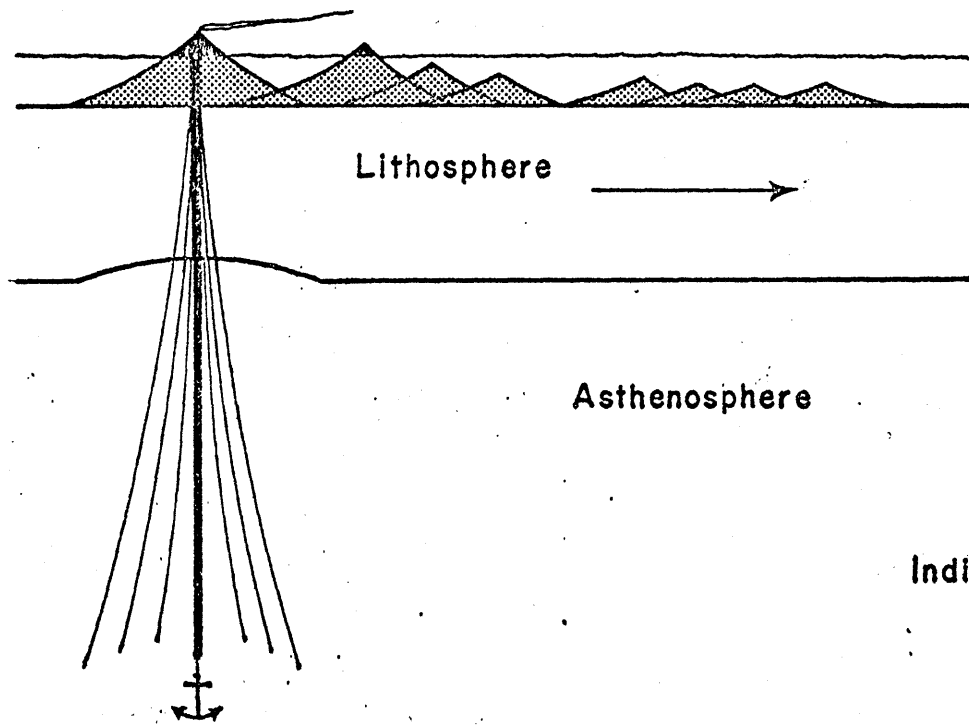
transform fault (Sclater and Fisher, 1974). The location of this junction is not assumed to be fixed in any way with respect to present geographic coordinates, and it is assumed to be free to migrate according to the kinematics of the plate system.

Both the hotspot model and the migrating ridge-transform junction model fit the available data in 1974, but both had significant shortcomings which were difficult to explain. The hotspot model did not predict any correlation between the age of the ridge and the age of the Indian plate to the west, to which it was presumably attached. However, the Deep Sea Drilling Project results from Legs 22 and 26 (Von der Borch, Sclater et al., 1974; Davies, Luyendyk et al., 1974) indicate very similar ages for both the ridge and the plate along the entire length of the ridge. Sclater and Fisher's (1974) model explained this age relationship. However, their model predicted that the excess volcanics should have been created at the plate boundary, and presumably some of them should have ended up on the Antarctic plate and formed a "mirror image" ridge counterbalancing the Ninetyeast Ridge. There appeared to be no such ridge on the Antarctic plate with the correct orientation.

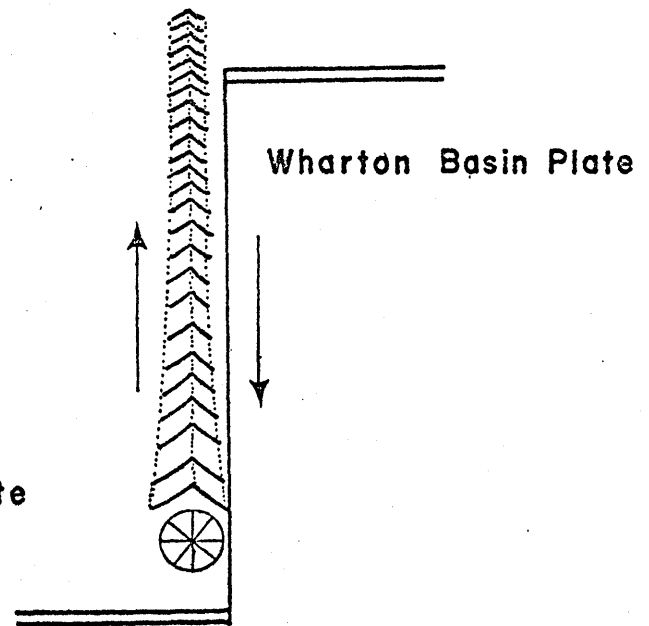
FIGURE 4

Sketch of the model for the generation of the
Ninetyeast Ridge by a hotspot.

HOTSPOT PRODUCTION OF THE NINETYEAST RIDGE



Indian Plate



Recently, Luyendyk and Rennick (in press, 1976) sought to explain these two inconsistencies in the earlier models by invoking a two hotspot hypothesis for the origin of the ridge. They postulated that Amsterdam and St. Paul Islands and Kerguelen and Heard Islands mark the present positions of two hotspots, and they suggested that both contributed to the formation of the Ninetyeast Ridge. Because one or the other hotspot always remained near the Antarctic-Indian plate boundary, they could explain the close age correspondence between the ridge and the adjacent plate. Because the Kerguelen hotspot spent a large portion of time under the Antarctic plate they also required a "mirror image" ridge to satisfy their model. They demonstrated that the Kerguelen-Gaussberg Ridge, which strikes to the southeast from Kerguelen Island, did mark the trace of the Kerguelen hotspot under the Antarctic plate if one assumed that the Ninetyeast Ridge was also a hotspot trace. This relationship had not been known previously because the absolute motion vector of the Antarctic plate is quite different from its relative motion vector with respect to India, and previous investigators had been led astray by their intuition.

These hypotheses each predict the latitude at which the volcanic basement of the ridge was formed as a function of time. These predicted paleolatitudes differ considerably from one model to the next for certain parts of the ridge. Thus it is possible, at least in theory, to test one hypothesis against the others. There have been five Deep Sea Drilling Project sites drilled on the ridge, as well as others on either side of it. Because of the large volume of material recovered at these sites, it is possible to directly measure the paleolatitudes along the length of the ridge.

The following chapters develop these ideas using the paleomagnetic data from DSDP sites 213, 214, 215, 216, 217, 253, and 254. Supporting data is drawn from other DSDP sites in the Wharton Basin.

The chapters are arranged in chronological order as they have appeared or will appear in the literature. Chapter II, "Paleomagnetic results of basalt samples from DSDP Leg 26, Southern Indian Ocean", (Peirce et al., 1974) was the most complete paleomagnetic study of DSDP basalts from one leg prior to the attempts at deep basalt penetration on DSDP Leg 34. During my initial year of work on the Ninetyeast Ridge rocks I became increasingly aware of the inadequacy of the statistics then used to analyze DSDP paleomagnetism data. A preprint of a new statistical approach by Allan Cox (in preparation, 1976) stimulated the analysis which culminated in Chapter III, "Assessing the reliability of

DSDP paleolatitudes", (Peirce, in press, 1976). With a rational statistical method with which to place the data in a realistic perspective finally available, I completed the work on the Ninetyeast Ridge samples. Those results and their implications for the origin of the ridge are discussed in Chapter IV, "The origin of the Ninetyeast Ridge and the northward motion of India, based on DSDP paleolatitudes".

Analysis of these paleomagnetic data leads to the following conclusions:

(1) The Ninetyeast Ridge is attached to the Indian plate and it has moved northwards about 5000 km. since the late Cretaceous.

(2) The rate of northward motion of India was 14.9 ± 4.5 cm/yr from 70 to 40 million years before present (mybp) when it slowed to a rate of $5.2 \pm .8$ cm/yr. The latter rate has continued to the present. The time of slowing roughly corresponds to the collision of India and Asia in the Eocene.

(3) The basal paleolatitudes for four sites on the ridge are all near 50°S , supporting a Kerguelen hotspot model for the origin of the ridge as suggested by Morgan (1972a, 1972b).

(4) There are serious errors in the paleolatitudes of previous reconstructions of the Indian Ocean (Sclater and Fisher, 1974). Australian paleomagnetic poles were used as the paleolatitude reference for these maps, and there are large, presently unresolvable, differences between the Australian and the Indian plate paleomagnetic data sets. In order to compare these data sets one must correct for the relative motions of the plates. Thus, the source of the error may be in the relative motion estimates for India/Antarctica and Australia/Antarctica, as well as in the paleomagnetic data itself.

Although the paleomagnetic data strongly support the Kerguelen hotspot model for the origin of the Ninetyeast Ridge, the major firm conclusion is that the volcanic source which created the ridge was nearly fixed in latitude. To date there has been no mechanism supported by the available evidence which can explain the reason for the existence of rising plumes of hot material from deep in the mantle. As such plumes have been proposed as a plate driving mechanism (Morgan, 1971), the proof or disproof of their existence is a major unsolved problem. This thesis strongly supports the existence of one such plume, but a plausible mechanism for its existence remains to be demonstrated.

References

- Bowin, C.O., Origin of Ninetyeast Ridge from studies near the equator: Jour. Geophys. Research, 78, 6029-6043, 1973.
- Cox, A., Paleolatitudes determined from paleomagnetic data from vertical cores: in preparation, 1976.
- Davies, T.A., B.P. Luyendyk, et al., Initial Reports of the Deep Sea Drilling Project, XXVI, Washington, D.C. (U.S. Gov't Printing Office), 982 pp., 1974.
- Du Toit, A.L., 1937, Our Wandering Continents: Edinburgh and London, Oliver and Boyd, 366 pp.
- Francis, T.J.G. and R.W. Raitt, Seismic refraction measurements in the southern Indian Ocean: Jour. Geophys. Research, 72, 3015-3041, 1967.
- Heezen, B.C. and Tharp, M., Physiographic Diagram of the Indian Ocean (with descriptive sheet), New York, Geol. Soc. Am., 1965.
- LePichon, X. and J.R. Heirtzler, Magnetic anomalies in the Indian Ocean and sea floor spreading: Jour. Geophys. Research, 73, 2101-2117, 1968.
- Luyendyk, B.P. and W. Rennick, The tectonic origin of aseismic ridges in the Eastern Indian Ocean: submitted to Bull. Geol. Soc. Am., in press, 1976.

McKenzie, D. and J.G. Sclater, The evolution of the Indian Ocean since the Late Cretaceous: Geophys. J.R. astr. Soc., 25, 437-528, 1971.

Morgan, W.V., Convection plumes in the lower mantle: Nature, 230, 42-43, 1971.

Peirce, J.W., C.R. Denham, and B.P. Luyendyk, Paleomagnetic results of basalt samples from DSDP Leg 26, southern Indian Ocean, In: Davies, T.A., B.P. Luyendyk, et al., Initial Reports of the Deep Sea Drilling Project, XXVI, Washington (U.S. Govt. Printing Office), p. 517-527, 1974.

Peirce, J.W., Assessing the reliability of DSDP paleolatitudes: J. Geophys. Res., in press, 1976.

Sclater, J.G. and R.L. Fisher, The evolution of the east central Indian Ocean, with emphasis on the tectonic setting of the Ninetyeast Ridge: Geol. Soc. Amer. Bull., 85, 683-702, 1974.

Smith, A.G. and A. Hallam, The fit of the southern continents: Nature, 225, 139-144, 1970.

Von der Borch, C.C., J.G. Sclater, et al., Initial Reports of the Deep Sea Drilling Project, XXII, Washington, D.C. (U.S. Govt. Printing Office), 890 pp., 1974.

Wegener, A., Die entstehung der kontinente: Petermanns Geog.

Mitt, 58, 185-195, 253-256, 305-309, 1912a.

Wegener, A., Die entstehung ver kontinente: Geol. Rundschau,

3, 276-292, 1912b.

Wegener, A., Die Entstehung der Kontinente und Ozeane,

Braunschweig, Vieweg, 1915.

Wilson, J.T., Evidence from oceanic islands suggesting

movement in the earth, In: Symposium on Continental

Drift, Roy. Soc. London Phil. Trans., ser. A., 258,

145-167, 1965.

Chapter II

PALEOMAGNETIC RESULTS OF BASALT SAMPLES
FROM DSDP LEG 26, SOUTHERN INDIAN OCEAN

18. PALEOMAGNETIC RESULTS OF BASALT SAMPLES FROM DSDP LEG 26, SOUTHERN INDIAN OCEAN¹

John W. Peirce, Woods Hole Oceanographic Institution, Woods Hole, Massachusetts and Massachusetts Institute of Technology, Cambridge, Massachusetts
 and

Charles R. Denham and Bruce P. Luyendyk², Woods Hole Oceanographic Institution, Woods Hole, Massachusetts

ABSTRACT

Magnetic measurements were made on 67 basalt samples from Sites 250, 251, 253, 254, 256, and 257 of Leg 26, Deep Sea Drilling Project. Paleolatitudes estimated from the inclinations after alternating-field demagnetization at 100 oe are compatible with apparent polar wandering curves (except Site 256) and reconstructions of the Indian Ocean based on lineated magnetic anomalies (except Sites 250 and 256). The samples displayed low coercivities (95-oe average median destructive field), except at Site 254 (383-oe median destructive field). Intensities of natural remanent magnetization are lower than are typical of dredged basalts, and low-field susceptibilities are higher. Viscous remanent magnetization was shown experimentally to be high in many specimens and could account for a large portion of their original intensity. Low coercivities, high viscous remanence, and the limited number of flows sampled all detract from the statistical confidence of the paleolatitude estimates. Site 257 revealed a polarity reversal, which can most likely be attributed to a thin dike or sill injected during a reversed episode subsequent to the emplacement and cooling of the rest of the cored section, which is normally polarized.

INTRODUCTION

Since the tectonic motions of the plates in the Indian Ocean were both rapid and extensive and as they are not yet well understood east of the Ninetyeast Ridge, reliable paleolatitude determinations from there would be valuable. Leg 26 of the Deep Sea Drilling Project recovered long sections of cored basalt from six sites in the Indian Ocean, providing the first opportunity to analyze paleomagnetic variations and properties with depth. Unfortunately, each site probably sampled only a small number of flows, thus leaving the paleolatitude estimates open to considerable interpretation. Nevertheless, paleomagnetic latitudes at Sites 251, 253, 254, and 257 are compatible with reconstructions of the Indian Ocean based on lineated magnetic anomalies (McKenzie and Sclater, 1971; Sclater and Fisher, in press).

Measurements of remanent magnetization were made on 67 samples (72 specimens) from Sites 250, 251, 253, 254, 256, and 257. Twenty-nine specimens were progressively demagnetized in alternating fields to less than 25% of their natural remanent magnetization (NRM) in-

tensity, and a test for viscous remanent magnetization (VRM) was conducted using 20 specimens. Paleolatitude estimates, based on the geocentric dipole assumption, were made using the magnetic inclinations after cleaning in a peak alternating field of 100 oe.

The following abbreviations for paleomagnetic terms are used in this report: AF, alternating field; G, Gauss (emu/cc); H100, AF demagnetized at 100 oe; J_{NRM} , intensity of NRM; MDF, median destructive field; NRM, natural remanent magnetization; oe, oersteds; S , magnetic viscosity coefficient; S/J_{NRM} , normalized viscosity coefficient; SRM, shock remanent magnetization; T_c , Curie temperature; VGP, virtual geomagnetic pole; VRM, viscous remanent magnetization.

NATURAL REMANENT MAGNETIZATION, COERCIVITY, AND SUSCEPTIBILITY

Specimen magnetizations were measured on a spinner magnetometer with coil pickup (Phillips and Kuckes, 1967) operated at 9.5 Hz and 97.5 Hz. A Princeton Applied Research SM-2 spinner magnetometer, operated at 15 Hz, was used for a few oversize specimens. Intensities of NRM ranged from 3.9×10^{-4} G to 4.33×10^{-2} G, the geometric mean for all samples being 3.22×10^{-3} G (Table 1). These values are comparable to those previously reported for DSDP basalts, but are somewhat lower than typical values for dredged basalts (Lowrie et al., 1973).

¹Woods Hole Oceanographic Institution Contribution Number 2968.

²Now at University of California, Santa Barbara, California.

TABLE 1
Paleomagnetic Results from Basalt Samples, DSDP, Leg 26

Sample (Interval in cm)	NRM Incl.	H100 Incl.	J _{nrm} (10 ⁻⁴ G)	MDF	S/J _{nrm} (%)	k (10 ⁻⁴ G/oe)	Remarks
Site 250 (33.46°S, 39.37°E)							
25-2, 140	-77.0	-76.2	108	-	-	9.3	
26-2, 140	-77.3	-62.7	131	-	2.4	12.9	
26-3, 16	-65.5	-59.1	153	-	-	7.5	
26-4, 09	-71.5	-67.5	89.3	-	-	11.8	
26-5, 115	-70.7	-68.6	88.3	-	-	10.9	
26-6, 58	-84.4	-70.0	73.5	40	-	13.4	
Site 251 (36.50°S, 49.48°E)							
31-2, 84	-67.5	-52.8	21.6	72	1.1	3.5	
31-3, 50	-72.2	-50.5	46.1	40	1.6	19.7	
31-4, 48	-26.1	-20.2	7.7	140	8.6	13.2	High VRM
31-5, 105	-69.8	-66.9	104	75	.3	10.4	
Site 253 (24.88°S, 87.37°E)							
58-175 CC	-62.4	-68.5	8.8	145	2.2	31.1	Incls., J _{nrm} , k mean of 3 spec.
Site 254 (30.97°S, 87.90°E)							
31-1, 111	- 2.7	+70.2	4.0	370	6.0	1.9	High VRM
35-1, 54	+62.2	+61.5	11.9	-	-	4.3	
35-1, 107	+70.6	+68.9	3.9	350	3.6	4.4	
35-2, 40	+54.6	+67.0	4.1	-	-	5.5	
35-3, 23	+74.8	+70.9	15.4	-	-	6.4	
35-3, 110	+54.6	+60.1	22.3	-	-	9.4	
36-2, 30	+63.8	+63.9	39.4	-	-	6.9	
36-3, 25	+64.4	+64.1	21.4	-	-	6.8	
36-3, 105	+66.6	+66.1	19.7	430	.2	8.5	
Site 256 (23.46°S, 100.77°E)							
9-2, 12	-48.7	-52.3	56.5	110	.5	12.1	
9-2, 130	-64.7	-56.0	46.8	-	-	10.8	Poor stability
9-3, 35	-56.0	-53.3	16.2	-	-	29.2	
9-3, 129	-19.2	-49.2	92.0	-	-	35.7	
10-2, 68	+50.1	-40.4	33.6	30	?	40.3	Poor stability
10-2, 140	-52.8	-50.4	94.5	-	-	41.7	Poor stability
10-2, 145	-67.5	-60.7	131	-	-	36.9	
10-3, 31	-49.0	-52.1	110	-	-	39.2	Poor stability
10-3, 85	+77.1	+64.1	19.7	?	29.0	41.4	High VRM
10-3, 140	+51.4	+59.5	106	-	-	-	
10-4, 15	+20.6	-42.7	26.1	-	-	35.3	
10-4, 64	+24.9	-45.7	29.8	-	-	22.9	
11-1, 15	-45.0	-58.2	187	60	1.8	40.6	
11-1, 122	-57.8	-41.5	35.2	-	-	41.8	Poor stability
11-2, 15	-64.4	-48.5	37.4	-	-	35.7	Poor stability
11-2, 88	-57.9	-61.3	433	-	-	25.3	
11-3, 15	+12.6	-53.5	34.6	120	7.8	33.9	High VRM
Site 257 (30.99°S, 108.35°E)							
11-2, 74	-49.2	-52.9	22.7	130	2.0	13.4	
11-3, 130	-67.2	-70.5	21.1	135	-	9.0	
12-1, 130	-61.6	-63.6	23.7	125	-	7.9	
12-2, 140	-74.5	-69.7	28.1	-	-	9.3	
12-3, 85	-67.6	-68.1	68.0	100	-	12.2	Mean of 2 spec.
13-2, 80	-38.1	-46.0	21.9	-	-	19.7	
13-2, 88	-54.9	-57.9	44.6	-	-	17.8	
13-2, 120	-44.0	-44.6	44.9	-	-	14.9	
13-2, 137	-40.3	-46.0	15.8	-	-	19.3	
13-3, 15	+47.0	+45.5	20.7	75	-	18.6	Mean of 2 spec.
13-3, 20	+48.3	+46.6	34.3	-	-	18.8	
13-3, 40	-36.5	-35.1	45.2	-	-	18.7	
13-3, 56	-38.7	-37.6	57.9	-	-	18.3	

TABLE 1 – Continued

Sample (Interval in cm)	NRM Incl.	H100 Incl.	J_{nrm} (10^{-4} G)	MDF	S/J_{nrm} (%)	k (10^{-4} G/oe)	Remarks
13-3, 80	-50.0	-48.1	25.0	-	-	-	
13-3, 103	-46.0	-39.7	41.6	-	-	18.8	
13-3, 124	-21.5	-36.9	45.7	-	-	15.4	
13-4, 62	-31.3	-51.9	12.3	-	-	20.2	
14-2, 95	-31.7	-34.8	11.8	-	-	17.8	
14-3, 73	-48.9	-59.2	23.9	-	-	19.7	
14-4, 111	-42.4	-61.3	51.7	65	5.2	42.2	High VRM
14-5, 95	-66.1	-67.4	22.8	-	-	12.7	
Site 257 (30.99°S, 108.35°E)							
15-1, 133	-60.7	-68.1	50.4	70	-	19.2	Mean of 2 spec.
15-2, 111	-70.2	-71.3	23.7	-	-	14.1	
16-1, 124	-67.9	-68.6	36.0	-	-	14.8	
16-2, 145	-48.6	-61.8	17.4	130	-	15.9	Mean of 2 spec.
16-3, 73	-65.0	-70.2	33.1	-	-	20.1	
17-1, 86	-67.5	-71.1	45.0	140	1.0	21.8	H200 Incl.
17-2, 60	-65.0	-66.2	19.9	-	-	13.9	
17-4, 145	-67.7	-68.6	12.1	-	-	16.4	
17-5, 130	-69.1	-71.2	80.7	120	2.7	18.5	H200 Incl.

An alternating field (AF) demagnetizing apparatus with two-axis tumbler and ambient field cancellation to less than 5×10^{-3} oe was used for magnetic cleaning. During progressive AF demagnetization, the magnetization directions usually stabilized after cleaning in a 100-oe peak field.

Except at Site 254, all the specimens which were progressively demagnetized exhibited low coercivities, their MDF's averaging 95 oe for 20 specimens (Table 1). In most of the samples, Ade-Hall (this volume, Chapter 19) found little altered, single-phase titanomagnetite, whose coarse grain size appears to control the coercivity. However, at Site 257, hematite is also present in several samples, contributing to higher MDF and lower NRM intensity (Figure 1).

Only samples from Site 254 show evidence of significant deuteric oxidation. Ade-Hall (this volume, Chapter 20) found exsolved lathes of ilmenite within grains of low-titanium titanomagnetite. The ilmenite divides the titanomagnetite into finer grains, accounting for the high average MDF of 383 at this site.

Low-field magnetic susceptibilities, measured with a Geophysical Specialties bridge, are higher than those for dredged basalts (Fox and Opdyke, 1973) and for previously reported DSDP basalts (Lowrie et al., 1973; Lowrie and Opdyke, 1972, 1973). There is considerable variation between sites, ranging from an arithmetic mean of 6.0×10^{-4} G/oe at Site 254 to one of 32.7×10^{-4} G/oe at Site 256 (Table 1).

VISCOUS REMANENT MAGNETIZATION

When demagnetized in a peak field of 25-50 oe, most of the normally polarized specimens showed an increase of about 5% in intensity (Figures 2-7), accompanied by a slight increase in inclination. This effect is attributed to the addition of an oppositely inclined component of VRM, acquired during upright storage in the northern hemisphere, to the NRM component acquired in the southern hemisphere.

An experiment with VRM, similar to that described by Lowrie (1973), was conducted on 20 specimens to evaluate the materials for paleomagnetic purposes. Each specimen was first demagnetized until less than 10% of its NRM remained. It was then placed in a constant orientation in the earth's field, and its magnetization was measured over a period of 1000 hours at 8-10 logarithmically spaced times. The VRM accumulated since the beginning of the experiment was plotted against the logarithm of time in hours, and the magnetic viscosity coefficient (S) was determined from the slope of the least-squares best-fitting line (Figures 8-11). S ranged from 0.2 to 29% of J_{nrm} (Table 1) for a 10-fold increase in time, implying possible VRM acquisition during the Brunhes normal epoch of 2-290% (see captions of Figures 8-11). An AF of about 100 oe was sufficient for removing an amount equivalent to the inferred Brunhes VRM in all but Site 254 specimens. Site 254 directions showed very little change between 100 and 1300 oe cleaning, indicating that any VRM component had been removed by 100 oe. We found generally high levels of VRM, which may complicate the interpretation of marine magnetic anomalies near Leg 26 sites. On the other hand, the specimens may be reliable paleolatitude indicators provided measures are taken to minimize both long and short-term VRM. We found that measurable amounts of VRM could be acquired over the period of a single measurement, especially at Site 256, where we assign a low reliability because of this behavior.

Two samples were rejected from the paleolatitude calculations as a result of the VRM test. The normalized viscosity coefficient, S/J_{nrm} , was very high at 8.6% for Sample 251A-31-4-48, whose direction differed radically from the other directions at the same site. Specimen 256-10-3-085, with S/J_{nrm} of 29%, was rejected because the intensities during AF demagnetization were so unstable that a demagnetization curve could not be drawn beyond 50-oe peak field.

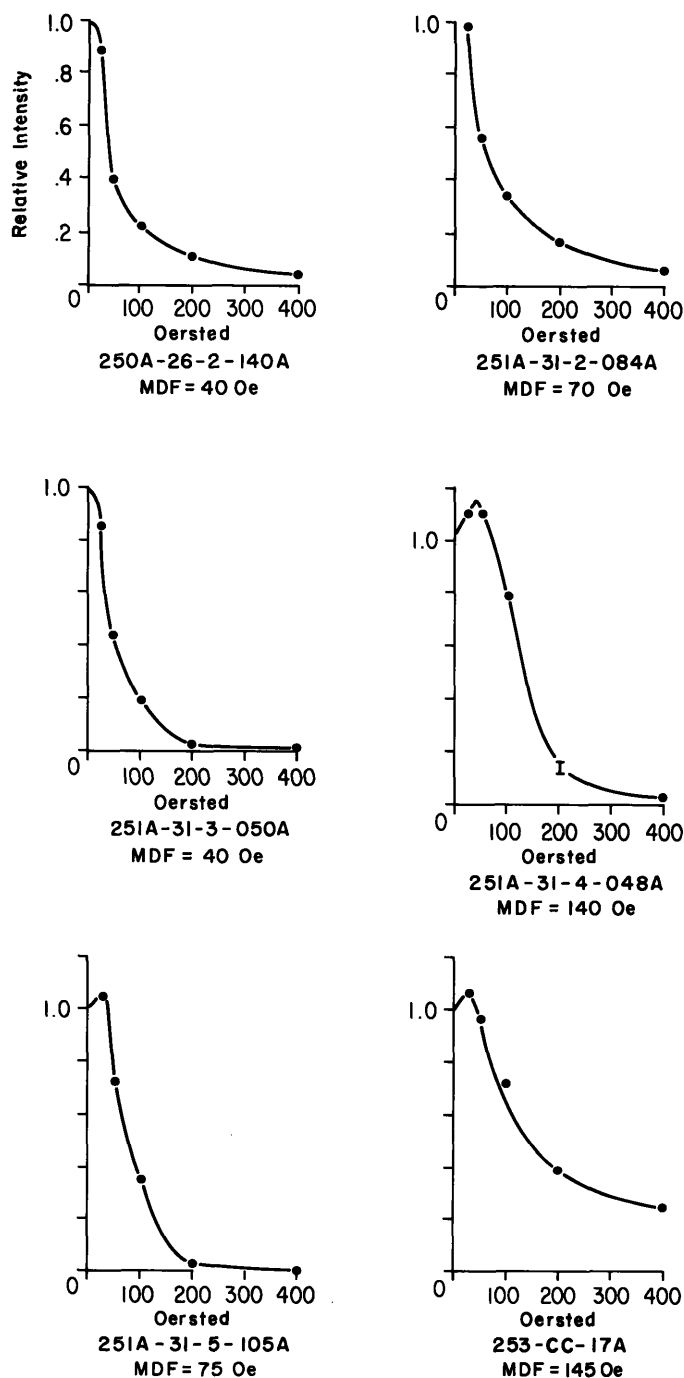


Figure 1. Progressive AF demagnetization curves for DSDP Leg 26 basalt specimens. Intensities are relative to the untreated (NRM) values. Replicate demagnetization and measurements are connected by vertical bars.

Samples 254-31-1-111 and 256-11-3-15, which also displayed high viscosity coefficients, were not rejected, since their magnetic directions moved rapidly at low cleaning fields and stabilized near the 100-oe position, indicating that the large VRM component had been satisfactorily removed.

To supplement the VRM tests, two specimens were tested for the acquisition of shock remanent mag-

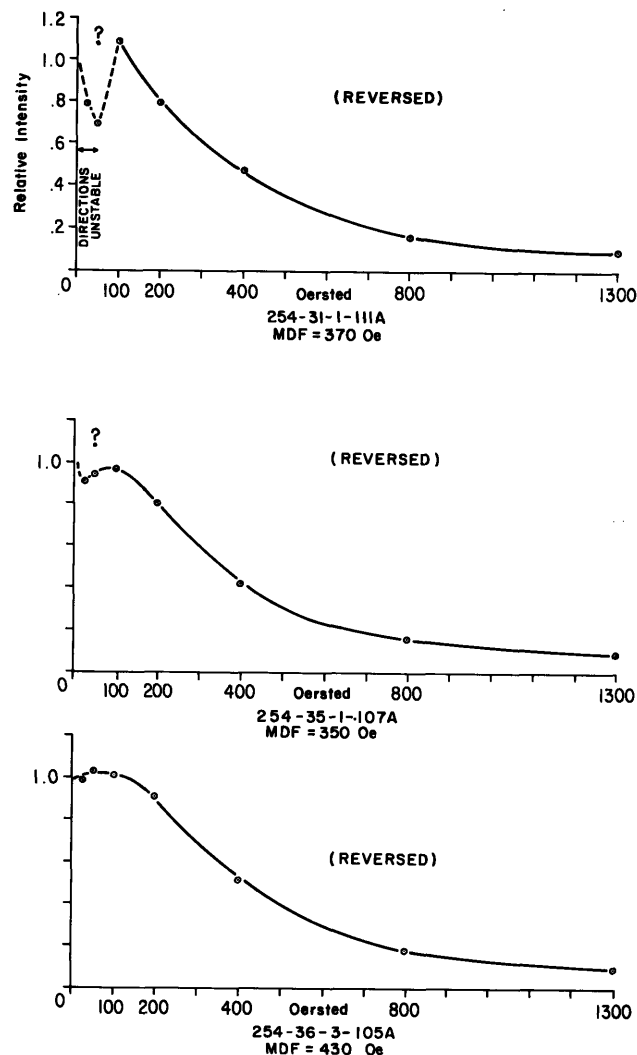


Figure 2. Progressive AF demagnetization curves for DSDP Leg 26 basalt specimens. Intensities are relative to the untreated (NRM) values. Replicate demagnetization and measurements are connected by vertical bars.

netization (SRM). While held in a known orientation, each was given a tap with a screwdriver, whose local field was about 0.5 oe. Both specimens displayed immediate changes in intensity (Figures 12 and 13), amounting to about 5% of NRM and oriented along the direction of the applied earth's field, similar to the behavior observed by Nagata (1971). Since it is difficult to assess the intensity and stability of SRM acquired during DSDP drilling, recovery, and storage operations, we have assumed that its influence is weak in specimens demagnetized in peak alternating fields of 100 oe or higher.

INCLINATIONS AND REVERSALS

The correlation between the polarity of the samples (Figure 14, Table 1) and the polarity of the oceanic magnetic anomalies at the drill sites was poor. Site 250 was drilled on a negative anomaly, yet the samples all had normal inclinations. Conversely, Site 254 samples had very stable reversed inclinations, yet the site lay over a positive anomaly. The positive anomalies at Sites 256

PALEOMAGNETIC RESULTS OF BASALT SAMPLES

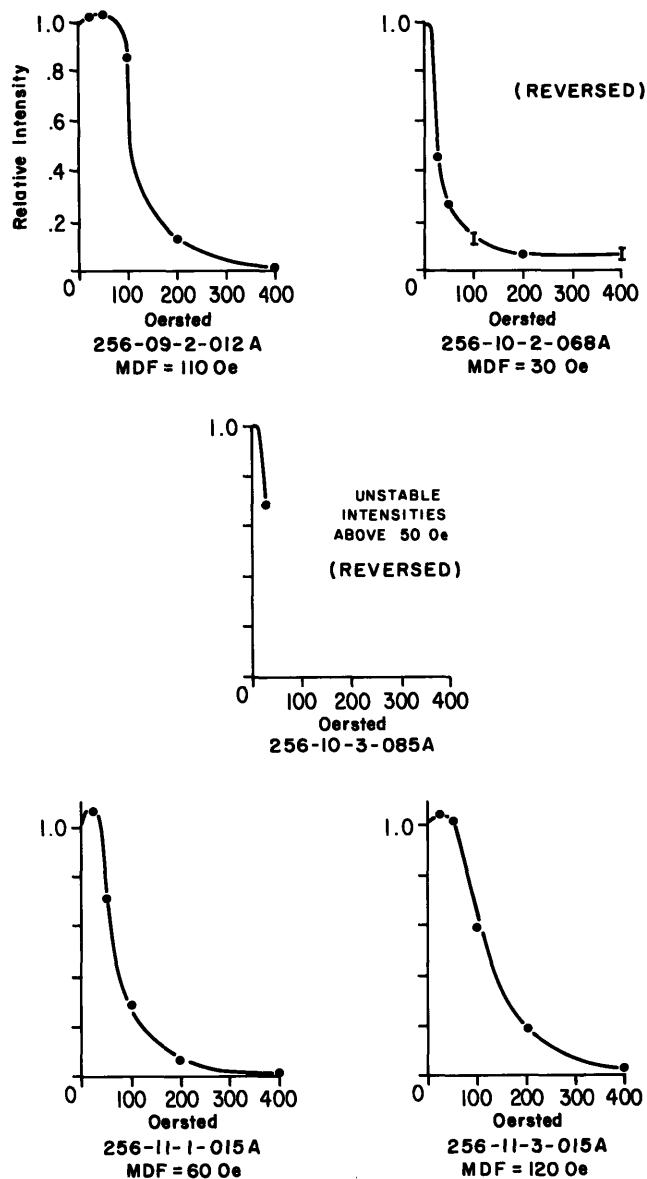


Figure 3. Progressive AF demagnetization curves for DSDP Leg 26 basalt specimens. Intensities are relative to the untreated (NRM) values. Replicate demagnetization and measurements are connected by vertical bars.

and 257 correlate with the predominantly normal inclinations found there. Sites 251 and 253 lay over anomalies of indeterminate polarity, and their samples had normal inclinations. If the classic sea-floor-spreading model applies, then Site 250 could have been located over lavas deposited during a short polarity event, whose extent is too small to be observed in the surface anomaly pattern. At Site 254 on the Ninetyeast Ridge, a simple block model does not apply to the anomaly, and a large mass of normally magnetized rock may lie beneath the drilled section.

At Site 256, we found a cluster of reversed NRM inclinations in Core 10, Sections 2 to 4, as well as another shallow reversed inclination at the bottom of the hole. After cleaning in 100-oe peak alternating field,

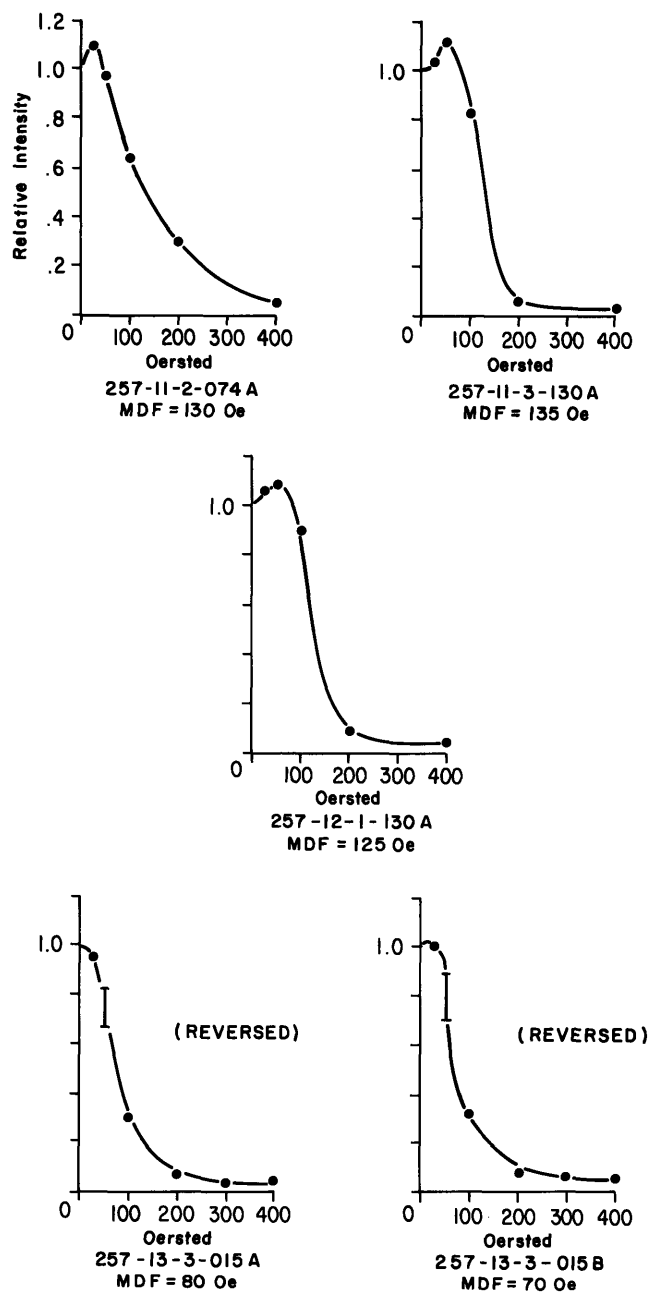


Figure 4. Progressive AF demagnetization curves for DSDP Leg 26 basalt specimens. Intensities are relative to the untreated (NRM) values. Replicate demagnetization and measurements are connected by vertical bars.

only two samples remained reversed. One of these, Sample 10-3-85, varied erratically in intensity when progressively demagnetized, and it was highly affected by VRM ($S/J_{\text{NRM}} = 29\%$). In view of the instability of Sample 10-3-85, the present data are clearly insufficient to establish the existence of a reversed polarity subzone at this level in the core.

At Site 257, we found that the inclinations have a definite bimodal distribution (Figure 15). As shown in Tables 1 and 2, the lower inclinations (average -43.9°) are spatially grouped in Core 13, Section 2 to Core 14,

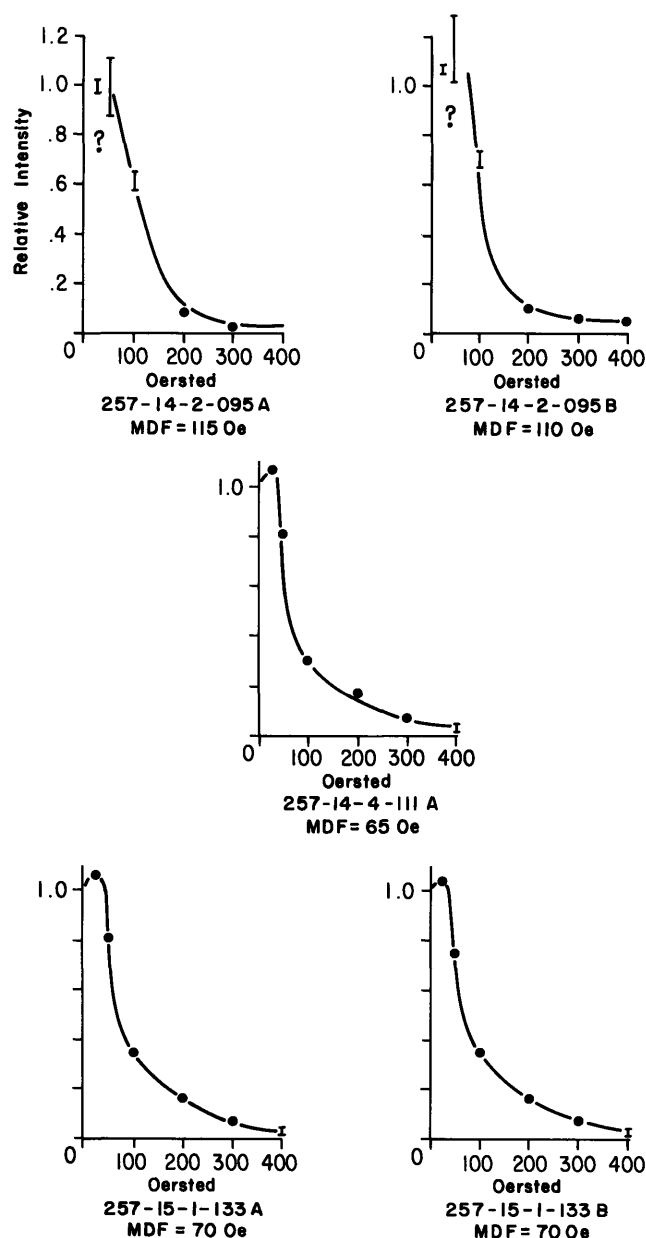


Figure 5. Progressive AF demagnetization curves for DSDP Leg 26 basalt specimens. Intensities are relative to the untreated (NRM) values. Replicate demagnetization and measurements are connected by vertical bars.

Section 2, except for one low inclination at the top of the core. This group includes the two reversed inclinations, which were averaged with opposite signs. Above this group, the mean inclination was -68.0° , compared with -67.1° below it. The difference between the low- and high-inclination groups is equivalent to a difference in paleolatitude of 25° , assuming all had the same declination. Watkins et al. (1972), suggested that the Brunhes secular variation in the Indian Ocean could be modeled by employing an 11.5° dipole wobble, combined with nondipole behavior comparable to that of the present field. This model could produce a variation of 25° in apparent paleolatitude if sampled near the extremes of

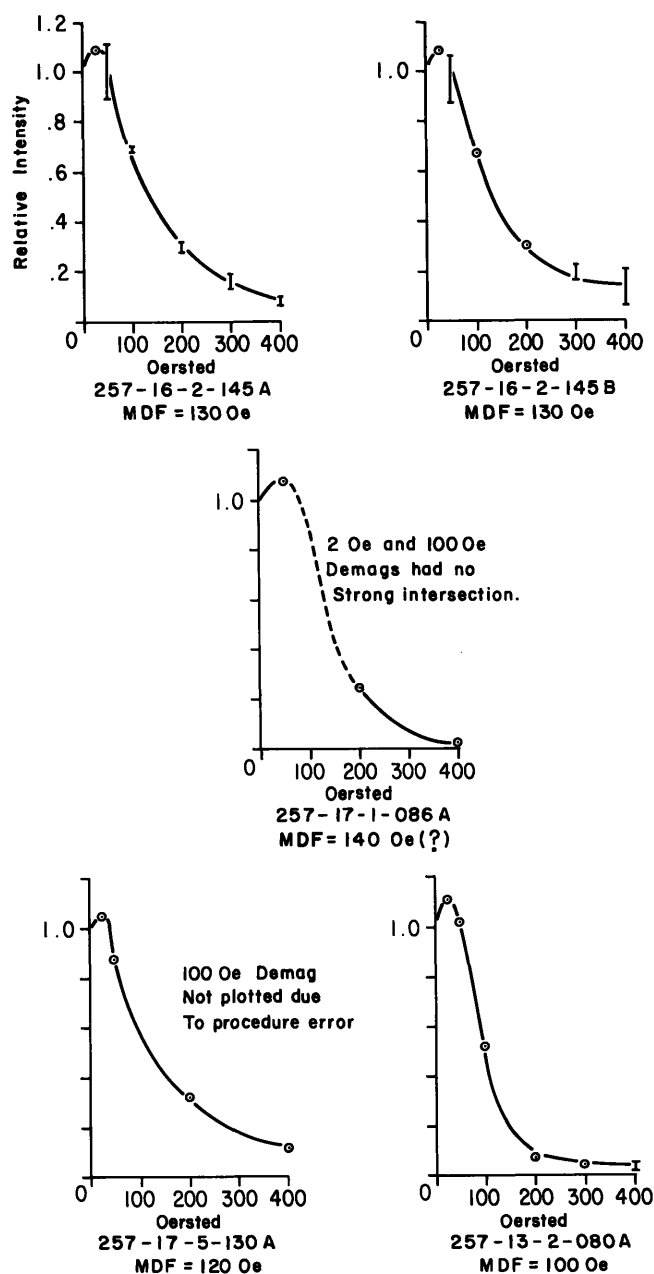


Figure 6. Progressive AF demagnetization curves for DSDP Leg 26 basalt specimens. Intensities are relative to the untreated (NRM) values. Replicate demagnetization and measurements are connected by vertical bars.

the secular variation. Therefore, the difference in inclination may reflect secular variation and suggests that the cored section covers a considerable span of time.

The two reversed samples at Site 257 have inclinations within 2° of the mean of the group of lower inclinations, suggesting that the reversal is real and not due to local reorientation, such as an overturned block at the front of a flow. In contrast to the reversed samples at Site 256, these samples were magnetically stable. This is the first instance in which a reversed subzone has been clearly documented from DSDP basalts. The most likely explanation for the narrow reversed zone is that it is a

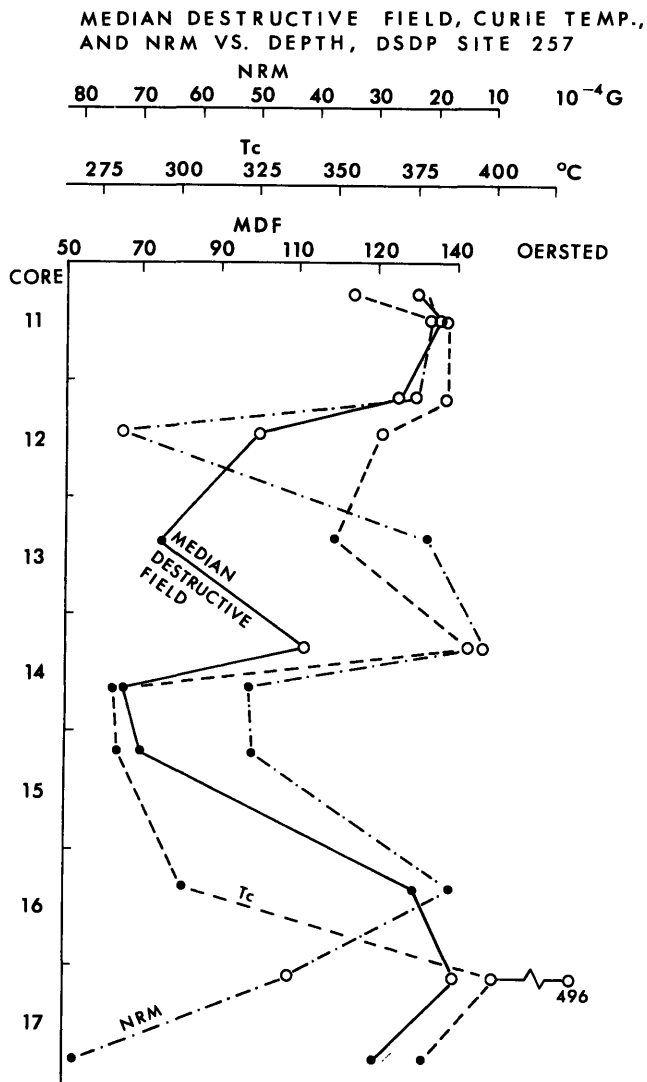


Figure 7. Median destructive field (MDF), Curie temperature (T_c), and NRM intensity at Site 257. Open and closed circles indicate the presence and absence of hematite, respectively. Curie temperatures and hematite determinations are from Ade-Hall this volume, Chapter 20.

dike or sill injected during a reversed polarity event subsequent to the time during which the normally magnetized lavas cooled. On the basis of limited marine magnetic coverage, Site 257 appears not to be located on the boundary between two major blocks of opposite polarity, but it could be near a small block representing a short unseen polarity event. The plate reconstructions of Sclater and Fisher (in press) suggest that the site formed at a spreading center. However, the wide range of preliminary K/Ar dates reported by Rundle et al. (this volume, Chapter 17) argues against a spreading center origin for at least part of the cored interval, in which case the reversed subzone would have little significance. There is no evidence (Ade-Hall, this volume, Chapter 19) suggesting magnetic self-reversal of these samples.

PALEOLATITUDES

Paleomagnetic studies ordinarily assume that the geomagnetic field approximates that of an axially oriented

PALEOMAGNETIC RESULTS OF BASALT SAMPLES

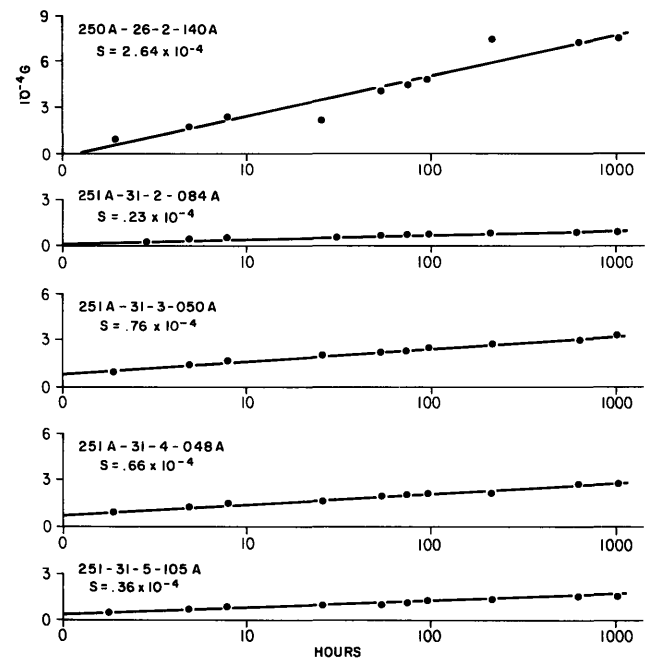


Figure 8. Viscous remanent magnetization (VRM) acquired in the earth's field by initially demagnetized specimens. VRM was calculated as the vectorial difference between the final and initial magnetic remanences. The viscosity coefficient S is the slope of the least-squares best-fitting line through the VRM data when plotted against the logarithm of time. During the Brunhes epoch, specimens could have acquired VRM equaling $9.78S$ ($9.78 = \log$ number of hours in 700,000 years) if the linear extrapolation is valid and initial magnetizations were zero.

geocentric dipole when averaged over a sufficient length of time. Because lavas record the local field direction only at discrete times, the number of flows and the total length of time sampled are vitally important to the statistical confidence which can be ascribed to the data. In the basalt section cored on Leg 26, little information is available about either parameter.

The Leg 26 paleolatitude data can be compared both with published reconstructions for the Indian Ocean and with polar wandering curves. McKenzie and Sclater (1971) and Sclater and Fisher (in press) reconstructed the relative positions of the Indian Ocean continents from sea-floor magnetic data for various times, then rotated the entire set of continents so that the VGP for Australia lay on the South Pole. This gives paleolatitude estimates for the various reconstructions. The data at Sites 250 and 251 on the African plate are limited. The magnetic paleolatitude for Site 250 does not agree with McKenzie and Sclater's (1971) reconstruction for 75 m.y. ago, but compares favorably with the apparent polar wandering curve for Africa, as shown in Figure 16. Site 251 formed near its present latitude, and according to McKenzie and Sclater, did not exist 36 m.y. ago. Our paleolatitude estimate is close to the present latitude, and it is compatible with any age since the middle Tertiary on the polar wandering curve.

On the Ninetyeast Ridge, the single sample from Site 253 bears no statistical significance, but it is not incom-

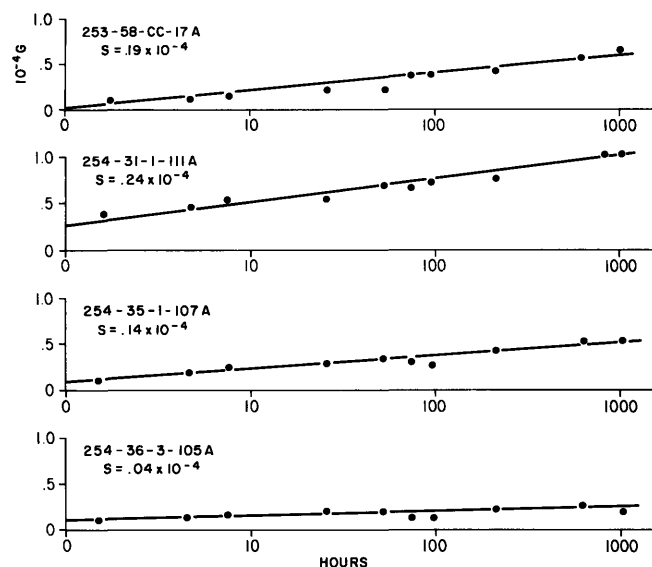


Figure 9. Viscous remanent magnetization (VRM) acquired in the earth's field by initially demagnetized specimens. VRM was calculated as the vectorial difference between the final and initial magnetic remanences. The viscosity coefficient S is the slope of the least-squares best-fitting line through the VRM data when plotted against the logarithm of time. During the Brunhes epoch, specimens could have acquired VRM equaling $9.78S$ ($9.78 = \log$ number of hours in 700,000 years) if the linear extrapolation is valid and initial magnetizations were zero.

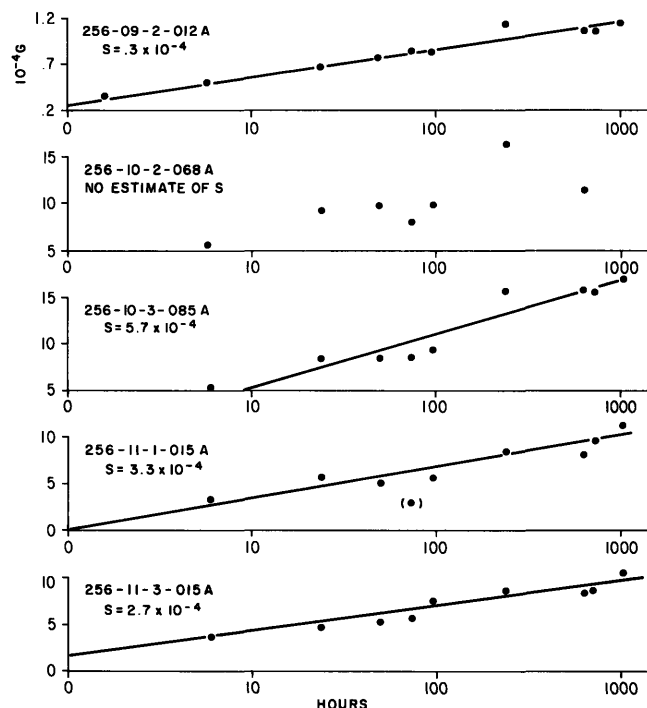


Figure 10. Viscous remanent magnetization (VRM) acquired in the earth's field by initially demagnetized specimens. VRM was calculated as the vectorial difference between the final and initial magnetic remanences. The viscosity coefficient S is the slope of the least-squares best-fitting line through the VRM data when plotted against the logarithm of time. During the Brunhes epoch, specimens could have acquired VRM equaling $9.78S$ ($9.78 = \log$ number of hours in 700,000 years) if the linear extrapolation is valid and initial magnetizations were zero.

TABLE 2
Site Means and Paleolatitudes

Site	(Plate)	N	Mean Incl. \pm sd	Paleo- latitude	Site Latitude	SF Latitude (Age)	MS Latitude (Age)
250	(African)	6	-67.4 ± 6.0	-50.2	-33.5	-	-36 (75)
251	(African)	3	-56.7 ± 8.9	-37.3	-36.5	-	-
253	(Indian)	1	-68.5	-51.8	-24.9	-45 (32)	-43 (45)
254	(Indian)	9	$+65.9 \pm 3.8$	-48.2	-31.0	-52 (32)	-45 (36)
256	(Australian)	16	-51.6 ± 6.7	-32.2	-23.5	-39 (100)	-41 (75)
257	(Australian)	21	-62.2 ± 10.5	-43.5	-31.0	-48 (100)	-52 (75)
257:							
All samples		30	-56.4 ± 12.6	-37.0	(equal wt/sample)		
11-3 to 12-3		4	-68.0 ± 3.1	-51.1	See text for discussion		
13-2 to 14-2		13	-43.9 ± 6.9	-25.7	of these three groupings.		
14-3 to 17-5		12	-67.1 ± 4.2	-49.8			

Note: Mean inclinations are the arithmetic means of the H100 inclinations for each site. Reversed inclinations are averaged as normal at Sites 256 and 257. Site 257 mean is based on equal weight for each core section to correct for unequal sample distribution. SF latitude and MS latitude are the paleolatitudes predicted by the reconstructions of Sclater and Fisher (in press) and McKenzie and Sclater (1971), respectively, determined graphically. Age of reconstruction is given in parentheses in m.y.B.P.

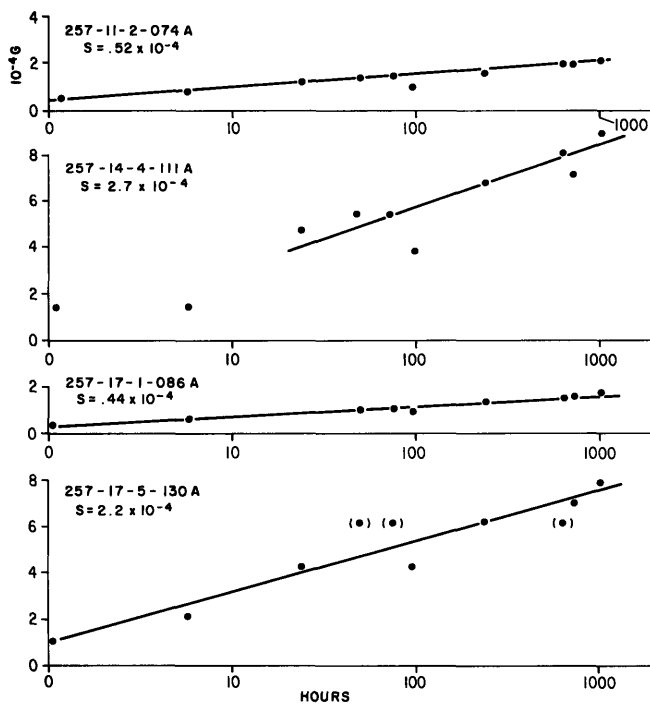


Figure 11. Viscous remanent magnetization (VRM) acquired in the earth's field by initially demagnetized specimens. VRM was calculated as the vectorial difference between the final and initial magnetic remanences. The viscosity coefficient S is the slope of the least-squares best-fitting line through the VRM data when plotted against the logarithm of time. During the Brunhes epoch, specimens could have acquired VRM equaling $9.78S$ ($9.78 = \log$ number of hours in 700,000 years) if the linear extrapolation is valid and initial magnetizations were zero.

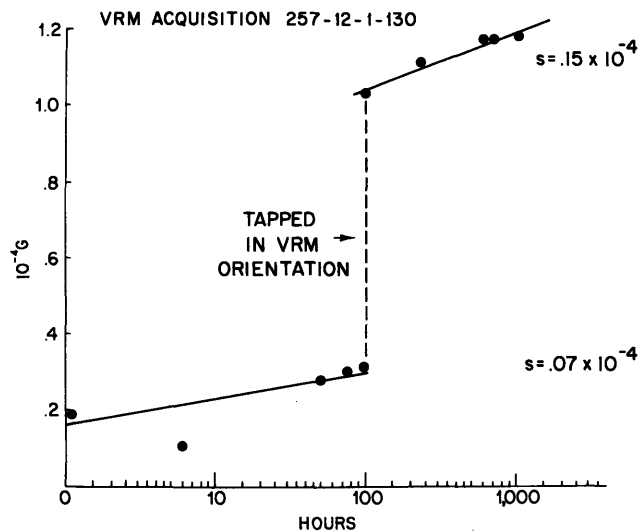


Figure 12. Shock-remanent magnetization (SRM) acquired by Sample 257-12-1, 130 when tapped in its VRM test orientation. The SRM intensity was about 3% of NRM and was oriented in the direction of the applied earth's field.

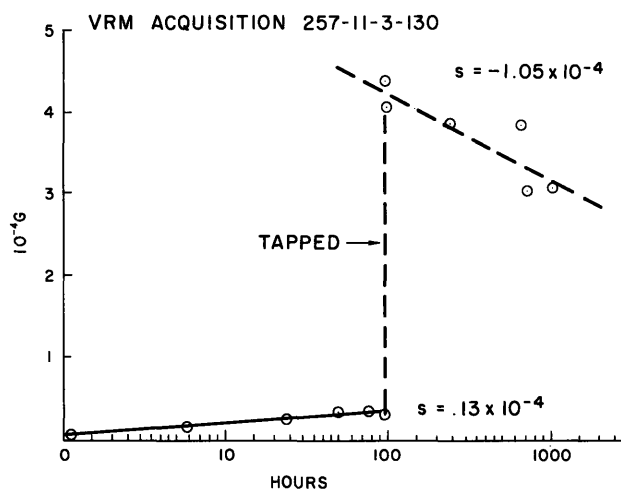


Figure 13. SRM test using Sample 257-11-3, 130, rotated away from the VRM orientation by 180° in the horizontal plane. The SRM lay along the applied earth's field and was about 20% of the specimen's NRM intensity.

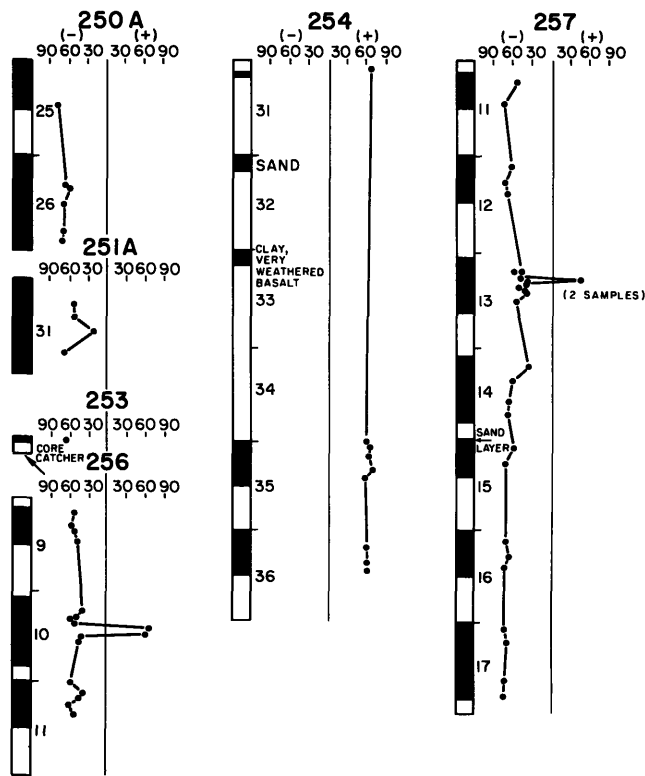


Figure 14. Magnetic inclinations versus depth for DSDP Leg 26 basalt samples after HF demagnetization at 100-oe peak. Core section numbers are adjacent to the core recovery logs (black = recovery; white = no recovery). Since all sites are in the Southern Hemisphere, negative inclination corresponds to normal polarity.

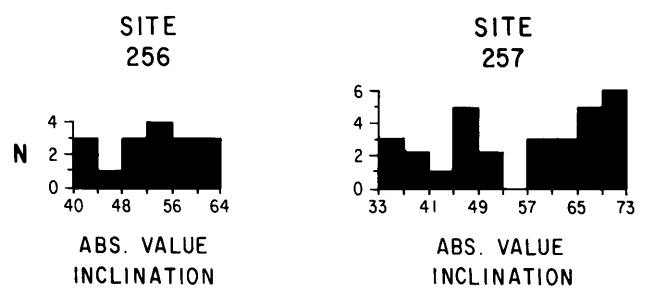


Figure 15. Histograms of magnetic inclinations for Sites 256 and 257 after AF cleaning at 100-oe. Note the bimodal distribution for Site 257.

patible with the reconstructions. At Site 254 our paleolatitude falls midway between the predictions of McKenzie and Sclater (1971) and Sclater and Fisher (in press) and appears to agree with the Indian plate polar wandering curve. It should be noted, however, that no age control is available along the Tertiary portion of the curve, hence the agreement of Site 254 is not very rigorous.

The sites for which we have the most data, 256 and 257, are both on the Australian plate, and their magnetic paleolatitudes are open to interpretation. The latitude we determined for Site 256 lies within 10° of the reconstruction position, but the data must be regarded with low confidence because of the unstable behavior ex-

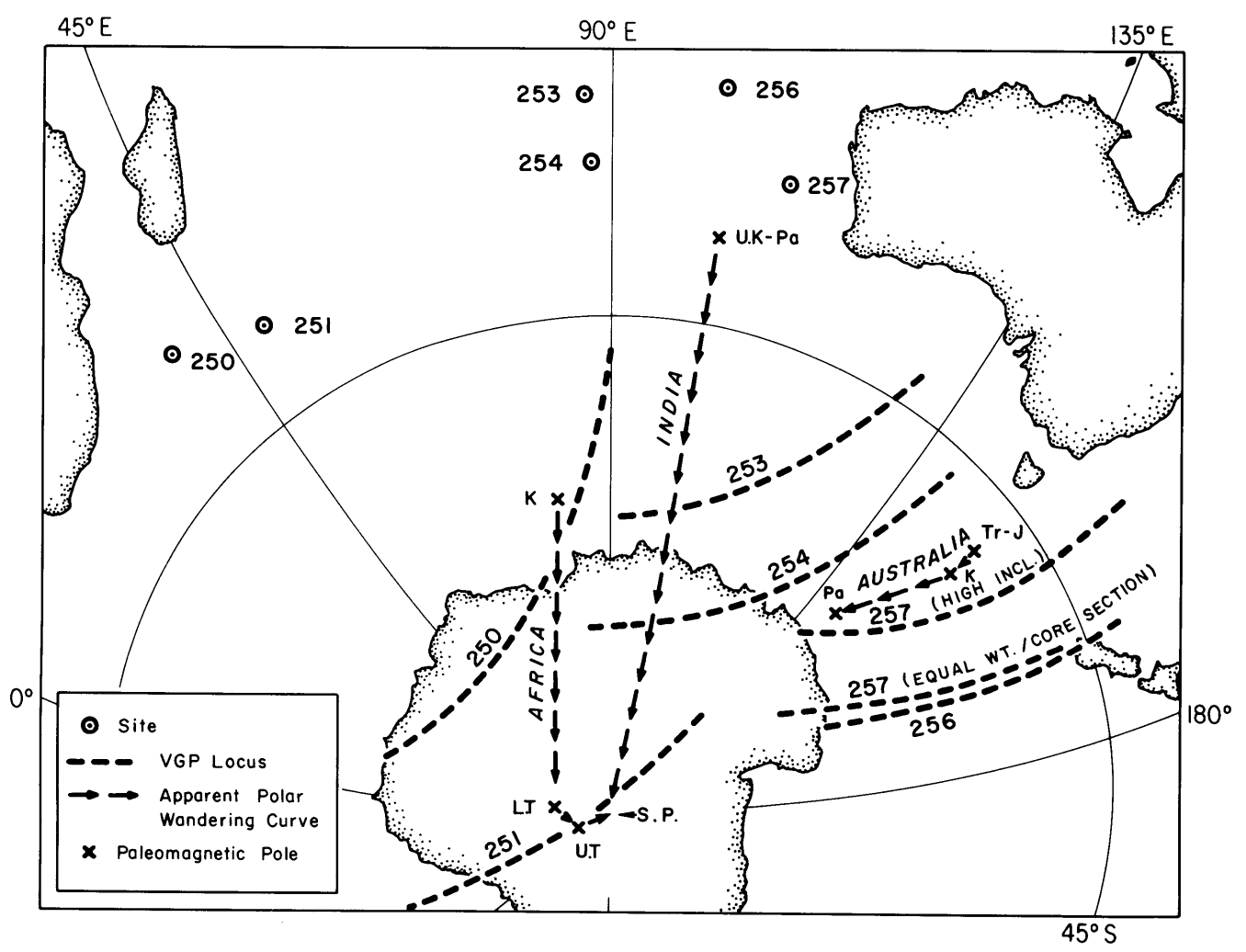


Figure 16. Loci of VGP's from DSDP Leg 26 basalts, compared with apparent polar wandering curves compiled by McElhinny (1973). Catalog numbers of data from McElhinny (1973) are:
 Africa: Cretaceous (K): AF 10.1-2; Lower Tertiary (LT): AF 11.1-2; Upper Tertiary (UT): AF 12.1-4
 India: Upper Cretaceous-Paleocene (UK-Pa): IN 11.2
 Australia: Triassic-Jurassic (TR-J): AU 8.1, 9.1-5; Cretaceous (K): AU 10.1-2; Paleocene (Pa): AU 11.1
 Error bands for the VGP loci were omitted from the diagram to avoid confusion. In the case of Site 257 (equal-weight per core section), the ± 1 SD band is 26° wide and incorporates the VGP locus based on the two groups of higher inclinations. Lambert equal-area projection centered at 60°S, 90°E.

hibited by many of the specimens. The magnetic paleolatitude varies considerably at Site 257, depending on the manner in which the data are averaged (Table 2). Although the group of lower inclinations at this site appears to be anomalous, we presently have no valid reason for discarding it, since its internal consistency is high. The paleolatitude determined from the two groups of higher inclinations agrees well with the reconstructions and the Jurassic-Paleocene polar wandering curve for Australia. If, however, the mean is based on equal-weight per core section, the VGP locus then lies significantly south of the Australian curve, near that of Site 256. McElhinny (in press) found a similar VGP locus for Site 259. Such an occurrence may be coincidental or it may represent motion of these sites relative to the eastern Australian localities used for determining the polar wander curves. It is worth noting that our VGP loci at Sites 256 and 257 approximately parallel the Australian Jurassic-Paleocene polar wandering curve and thus neither support nor contradict the -100 m.y. span of K/Ar ages reported by Snelling and Rundle (this volume) at Site 257.

Because of the limited (and uncertain) number of flows sampled in each Leg 26 hole, the polar wandering curve correlations observed at several of the sites may be misleading. The sediments immediately overlying the basalts could resolve some of the present ambiguities of interpretation and form a more reliable basis for the paleomagnetic reconstruction of the southern Indian Ocean.

ACKNOWLEDGMENTS

Discussions with W. Lowrie and J. M. Ade-Hall broadened our understanding of viscous remanence and magnetic mineralogy. We thank J. G. Sclater for his advice, enthusiastic encouragement, and a preprint of Sclater and Fisher (in press). The authors were supported by ONR contracts N-00014-67-A-0204-0048 (J.W.P.), N00014-66-CO241 NR 083-004 (B.P.L.),

and a Postdoctoral Fellowship from the Woods Hole Oceanographic Institution (C.R.D.).

REFERENCES

- Fox, P. V. and Opdyke, N. D., 1973. Geology of the oceanic crust: magnetic properties of oceanic rocks: *J. Geophys. Res.*, v. 78, p. 5139-5154.
- Lowrie, W., 1973. Viscous remanent magnetization in oceanic basalts: *Nature*, v. 243, p. 27-29.
- Lowrie, W., Lovlie, R., and Opdyke, N. D., 1973. The magnetic properties of Deep Sea Drilling Project basalts from the Atlantic Ocean: *Earth Planet. Sci. Lett.*, v. 17, p. 338-349.
- Lowrie, W. and Opdyke, N. D., 1972. Paleomagnetism of igneous samples. *In* Hayes, D. E., Pimm, A. C., et al., Initial Reports of the Deep Sea Drilling Project, Volume 14: Washington (U.S. Government Printing Office), p. ———, 1973. Paleomagnetism of igneous and sedimentary samples. *In* Edgar, N. T., Saunders, J. B., et al., Initial Reports of the Deep Sea Drilling Project, Volume 15: Washington (U.S. Government Printing Office), p. ———, 1973. Paleomagnetism and plate tectonics: Cambridge (Cambridge University Press). ———, in press. Paleomagnetism of basalt samples, Leg 27. *In* Heirtzler, J. R., Veevers, J. J., et al., Initial Reports of the Deep Sea Drilling Project, Volume 27: Washington (U.S. Government Printing Office).
- McKenzie, D. and Sclater, J. G., 1971. The evolution of the Indian Ocean since the Late Cretaceous: *Roy. Astron. Soc. Geophys. J.*, v. 25, p. 437-528.
- Nagata, T., 1971. Introductory notes on shock remanent magnetization and shock demagnetization of igneous rocks: *Pure Appl. Geophys.*, v. 89, p. 159-177.
- Phillips, J. D. and Kuckes, A. F., 1967. A spinner magnetometer: *J. Geophys. Res.*, v. 72, p. 2209-2212.
- Sclater, J. G. and Fisher, R. L., in press. The evolution of the east central Indian Ocean, with emphasis on the tectonic setting of the Ninetyeast Ridge: *Geol. Soc. Am. Bull.*
- Watkins, N. D., Hajash, A. and Abranson, C. E., 1972. Geomagnetic secular variation during the Brunhes epoch in the Indian and Atlantic regions: *Roy. Astron. Soc. Geophys. J.*, v. 28, p. 1-25.

Chapter III

ASSESSING THE RELIABILITY
OF DSDP PALEOLATITUDES

Assessing the Reliability of
DSDP Paleolatitudes¹

by

John W. Peirce

Woods Hole Oceanographic Institution
Woods Hole, Massachusetts 02543
and
Massachusetts Institute of Technology
Cambridge, Massachusetts 02139

Woods Hole Oceanographic Institution Contribution No. 3719.

Abstract

Published DSDP paleomagnetic data are reviewed and reevaluated in terms of their reliability for paleolatitude calculations. Where possible, new paleolatitudes are calculated from data which were originally used only for paleomagnetic stratigraphy. For basalts, new paleolatitudes are calculated by averaging the data by cooling unit if this was not done previously. In addition, all paleolatitudes are corrected by a small amount because inclination averages without declination control provide low estimates of the true paleolatitude. Standard rating criteria are developed and all paleolatitudes are rated accordingly.

Rarely do DSDP paleolatitudes approach the reliability of good continental pole positions. A paleolatitude determination for a given age at a single DSDP site cannot be considered reliable even if the data on which it is based are coherent. However, the reliability of such paleolatitudes can be markedly improved by using comparisons with paleolatitudes of different ages from the same site, paleolatitudes of similar ages from different sites on the same plate, estimates of paleolatitude from reconstructions based on marine magnetic anomalies, and continental paleopole positions.

A newly calculated paleomagnetic pole for the Pacific plate has been defined by six DSDP sites of upper Cretaceous age. The pole at 61°N , 45°W is generally consistent with other estimates of Pacific plate motion.

A pole for the Wharton Basin (eastern Indian Ocean) has been defined by four sites of middle Cretaceous age. The pole position at 55°S , 165°E is well constrained in latitude, and it suggests that there may have been left lateral motion between the Wharton Basin and the Australian continent.

Basement paleolatitudes from four sites on the Ninetyeast Ridge in the Indian Ocean all are close to 50°S , although they range widely in age. This supports the hypothesis that the Ninetyeast Ridge may be a volcanic trace from a hotspot.

Introduction

Since the beginning of the Deep Sea Drilling Project (DSDP), paleomagnetic measurements have been made in sediments and basalts from over 100 drilling sites. Many of the earlier studies were designed to examine the paleomagnetic stratigraphy of the sediments. Sclater and Cox (1970) pointed out the possibilities of using magnetically determined paleolatitudes of known age to discover the northerly component of absolute motion of DSDP sites. Numerous authors who have tried to determine site paleolatitudes have met with varying success. These results have usually been evaluated within a limited context, using a variety of statistical criteria, and it is often difficult to compare results from different studies.

I have compiled all the DSDP paleomagnetic data for Legs 1-33 published as of November, 1975, and summarized it in Table 1. In addition to listing all the work done by site, paleolatitudes are listed for all those data which seemed well grouped, as well as some statistical parameters. Each paleolatitude determination has been rated according to objective criteria based on the magnitude of the associated

errors. In addition I have indicated whether or not I considered the paleolatitude to be consistent with other independent data.

This assessment points out some of the limitations associated with DSDP paleolatitudes, in addition to providing a compilation of the data in a convenient form.

Limitations of DSDP Paleolatitudes

There are several limitations and assumptions inherent in working with DSDP material which make it difficult to attain the same degree of reliability in the calculated paleolatitudes as one could attain by studying the same section on land. These include:

- (1) The assumption that the cores are drilled vertically;
- (2) The possibility that the drilling process has disturbed the original orientation of the material;
- (3) The limited amount of material which is available to sample at a given level;
- (4) The statistical problems which are caused by the samples being oriented only with respect to the vertical;
- (5) The statistical problems which are caused by an incomplete knowledge of how well the sample set has sampled the secular variation.

The assumption that the cores are drilled vertically is a good one. Typically, measured down hole deviations from vertical are less than 5° (Wolejszo, et al., 1974). These deviations contribute to the total experimental

error in the directions, but they are comparable to, or less than the errors introduced in taking individual specimens from the core.

A related problem is the assumption that the pieces of core have been correctly marked as to which way is up. Individual pieces can be accidentally inverted during handling, and short pieces can be inverted by the drilling process. At least one reversal in basalts has been reported which is probably the result of such an inversion (site 257, Peirce, et al., 1974). In my experience in sampling at the DSDP repository, several accidental inversions were detected by comparing the orientations of unmarked pieces to the photographs taken on board ship.

To obtain reliable paleolatitudes from sediments one needs several samples that are closely grouped in age. Because of the limited volume of the core and the existence of numerous zones of disturbed material, it is often

impossible to get as many samples within a particular biostratigraphic zone as statistical considerations alone would dictate. Disturbed material usually can be avoided successfully, but often there is no evidence of disturbed bedding to identify it clearly. Inclinations which vary erratically between adjacent specimens may be indicative of sampling in disturbed material if the directions are magnetically stable.

There may be an ambiguity as to whether samples are normally or reversely magnetized because inclination alone is a poor indicator of paleofield polarity, especially at low latitudes where the scatter of inclinations due to secular variation is the greatest (Cox, 1970). If several samples are available from each sediment horizon or igneous cooling unit, then they should fall into normal and reversed polarity groups. These groups will often contain some relatively shallow inclinations of the opposite sign to the inferred polarity. However, if only a few samples are available per horizon, or if the site was within about ten degrees of the equator at the time in question, then the polarity ambiguity probably cannot be resolved.

Because there is usually no declination control between adjacent samples, it is not possible to use the customary statistics of directions on a sphere (Fisher, 1953) to analyze the data. Most DSDP paleolatitudes have been calculated by converting the mean inclination to a mean paleolatitude using equation (1) below. Sometimes the median inclination has been used instead to avoid biasing the mean paleolatitude by a few extreme inclinations (Jarrard, 1974). Either approach consistently underestimates the true paleoinclination because the arithmetic mean is only an approximation of the vertical angle of the vectorial mean. Thus, paleolatitude determinations based on inclinations alone must be corrected for this low bias. The method I have used was proposed by Cox (in prep.), and it is discussed in detail in the section on corrected paleolatitudes.

Normally, paleolatitudes are computed from the paleomagnetic inclinations assuming that the time averaged magnetic field of the earth has behaved as a geocentric axial dipole. The geocentric dipole model assumes that the data set has sampled the magnetic field in such a way that

a time averaged value is derived. The samples must span at least 50-100,000 years to adequately sample the longest known periods of secular variation which are about 10^4 years (Cox, 1975). In DSDP sediments the problem is not too severe as each specimen often samples as much as 10^3 - 10^4 years. But in high sedimentation rate environments, each specimen may sample only 50 years or less, and care must be exercised to assure that enough samples are taken to average out secular variation.

In DSDP basalts secular variation usually is not sampled completely enough to average it out. With only a small diameter core to look at, it is often difficult to identify unambiguously the number of cooling units present. If several chilled margins or flow tops are identified, there is still no way of knowing if the cooling units erupted in rapid succession in a few years or if they were erupted over a longer time span. Sometimes clues are provided by interlayered sediments or the variability of inclinations between successive cooling units when a large number are sampled. In all of the studies reviewed here, the time span sampled in the basalts is unknown.

Thus paleolatitudes derived from DSDP sediment data with a large number of samples probably average out secular variation adequately, except where abnormally high sedimentation rates were found. These should approach the reliability of comparable continental paleopole determinations except for the handicap of incomplete orientation. On the other hand, paleolatitudes determined from DSDP basalt data are unlikely to adequately sample secular variation. These cannot be regarded as being as reliable as continental poles from lava flows unless several sites of similar age give consistent results. Lowrie (1974) has compared the observed paleolatitudes of 26 DSDP sites with that predicted by various plate reconstruction models. The correlation coefficient of .712 represents a level of 99% confidence, but it demonstrates the degree of scatter in the data, and much of the scatter may be caused by incomplete averaging of secular variation.

Secondary Magnetization

Secondary magnetization due to viscous remanent magnetization (VRM) is a major component of the natural remanent magnetization (NRM) in many DSDP basalts (Lowrie, 1974; Peirce et al., 1974; Lowrie and Hayes, 1975; Lowrie

and Israfil, 1975). Indeed, at site 57 it was found to be the dominant component of the NRM (Lowrie, 1973).

The magnitude of the VRM vector grows linearly with the logarithm of time (Thellier, 1938; Néel, 1949, 1951), although for certain grain size distributions the slope of the VRM acquisition line may change abruptly as certain viscous time constants are exceeded (Lowrie and Hayes, 1975). If the VRM vector is opposed to the primary magnetization vector, and if it possesses a lower coercivity than the primary magnetization, then an increase in intensity may be observed during careful progressive alternating field (AF) demagnetization (Peirce, et al., 1974).

No studies have been done on the nature of VRM in DSDP sediments. However, many of the DSDP sediment samples I have worked with have components of magnetization which change rapidly during a single measurement, indicative of VRM acquisition. VRM has been found to be the major component of magnetization in some sediments from piston cores (Kent and Lowrie, 1974).

The presence of soft secondary components of magnetization, such as VRM, in most DSDP material make NRM values unreliable

indicators of the paleoinclination. It is not uncommon for inclinations to change by 20° between their NRM and cleaned values, and occasional changes of more than 90° occur. At site 256, where relatively rapid VRM acquisition was observed in some basalt samples, the average change in inclination during the cleaning of 17 samples was 24.2° . The inclinations of four samples changed sign (Peirce, et al., 1974). The combination of the common occurrence of such inclination changes in both sediments and basalts with the scattering of inclinations across the equator by secular variation discussed above can make the NRM values of inclination unreliable indicators of paleofield polarity.

The age of basalt samples is often very hard to define accurately. If the basalt is not a sill, basal sediments may be used as a minimum age if they are fossiliferous, but the length of time between basement formation and initial sediment accumulation remains a question. K/Ar ages are sometimes used, but accuracies of $\pm 10\%$ appear to be rare in DSDP material. Multiple ages are necessary for K/Ar to be reliable, although in some cases they may confuse the picture.

For example, at site 257, the 5 K/Ar ages ranged from 97-192 m.y. (Rundle, et al., 1974). In cases where sites are drilled on specific magnetic anomalies, the age of that anomaly, as determined from independent data, may be taken as basement age if no other dating method exists.

Chemical remanent magnetization (CRM) is a secondary effect which has been inadequately studied in DSDP material. If the CRM is acquired in a different applied field than that in which the primary magnetization was acquired, a complete overprinting can occur and lead to an erroneous paleoinclination. Because CRM in titanomagnetite may have a higher coercivity than the original remanence (Johnson and Merrill, 1973), it is not detectable by standard magnetic cleaning techniques, and it may appear to be very self-consistent. Thus, determinations of paleolatitude at a single site at a single horizon should be regarded with some suspicion until they are corroborated by consistent results from different sites or from different horizons at the same site.

Age of Paleolatitude

When trying to use DSDP paleolatitudes to constrain models of plate reconstructions, it is important to understand

the uncertainty of the age associated with it. Paleontological ages in Tertiary sediments are generally quite good relative to one another if the cores are fossiliferous (± 1 million years (m.y.) for the upper Tertiary, ± 3 m.y. for the lower Tertiary (van Andel, 1972)). In the Cretaceous, many ages are as good as ± 4 m.y. (van Andel, 1972), but they are often considerably worse, especially in the lower Cretaceous. It is also important to place possible age errors in the perspective of the plate motions of interest. For example, a 10 m.y. error in the relative ages of two Tertiary sites in the Antarctic may be tolerable because of the slow motion of the plate. A similar error for two sites of the same age on the Indian Plate would introduce an uncertainty of $10-15^\circ$ because of the rapid motion of India at that time.

Corrected Paleolatitudes

As mentioned above, a paleolatitude determination which is based on inclination data alone will always be low. There are basically two ways to correct for the mean inclination being a biased estimate. One can attempt to measure the dispersion in a data set from the inclinations alone, and

thus make an estimate of the precision parameter (Briden and Ward, 1966). Alternatively, one can assume $K=K_{SV}$, the precision parameter for the dispersion caused by secular variation as measured in continental studies (Cox, in prep.). If several long unbroken pieces of core were recovered, several groups of specimens completely oriented with respect to each other could be sampled. These would yield several independent estimates of K . In practice, however, long unbroken pieces of core are rare, and it is difficult to get enough completely oriented samples to make such estimates. In basalts, unbroken pieces which go across a cooling unit boundary are almost never recovered. Thus it is only possible to estimate the within cooling unit precision parameter for basalts when what is really needed is the between cooling unit precision parameter.

To arrive at the paleolatitudes listed in Table 1 I have used the method proposed by Cox (in prep.) in which a model for secular variation as a function of latitude is assumed. The discussion which follows in this section and in the section on confidence limits summarizes the more complete derivation and analysis given by Cox (in prep.) and applies it to this particular study.

The method requires a set of independent measurements of the inclination of the paleofield. In basalts, each cooling unit provides an instantaneous measurement of the paleofield inclination. However, if the eruptive process is episodic, each cooling unit may not be an independent measurement because several units may be erupted at nearly the same time (Cox, in prep.; Ade-Hall and Ryall, 1975). Therefore, if several adjacent cooling units had nearly the same inclination value, the mean inclination of all of them was taken to be one independent measurement. I have treated each sediment measurement as an independent, instantaneous measurement of the paleofield. Although the assumption that the sediment inclinations are instantaneous measurements is clearly in error, it has no bearing on the final paleolatitude and it insures that conservative confidence limits are assigned. This point is discussed in more detail in the next section.

Each independent inclination was converted to a virtual geomagnetic latitude (VGL) (Grommé and Vine, 1972) by the usual formula for the axial dipole model of the geomagnetic field,

$$\theta_i = \tan^{-1} (.5 \tan I_i), \quad (1)$$

where θ_i is the VGL and I_i is the inclination. Then a factor, $T(\theta)$, was applied to correct for the fact that the mean inclination is a low estimate of the true paleoinclination.

Briefly, the correction factor is derived as follows (Cox, in prep.): the probability distribution function, $F(\theta)$, of vertical borehole inclination values derived by Briden and Ward (1966, Eqn 2) may be expressed as

$$F(\theta) = \frac{K}{2 \sinh(K)} \cos(\theta) \exp(K \sin \theta_0 \sin \theta) I_0(K \cos \theta_0 \cos \theta) \quad (2)$$

where θ = observed paleolatitude
 θ_0 = true paleolatitude
 K = precision parameter
 I_0 = integral form of the zero-order hyperbolic Bessel function

$F(\theta)d\theta$ is the probability that an observed paleolatitude will have a value between θ and $\theta + d\theta$. The expected observed value of the paleolatitude, $E(\theta)$, can be expressed as

$$E(\theta) = \int_0^\pi \theta F(\theta) d\theta \quad (3)$$

$F(\theta)$ is a function of K and θ_0 by equation (1). Making the approximation

$$K = K_{SV} \quad (4)$$

where K_{SV} is the precision parameter describing the dispersion due to secular variation alone, and substituting values for

K_{SV} from model C for secular variation (Cox, 1970), and numerically integrating, $E(\theta)$ can be calculated. The correction factor is simply the difference between the true paleolatitude and the expected observed paleolatitude.

$$T(\theta) = \theta_0 - E(\theta) \quad (5)$$

The best estimate of $E(\theta)$ is the actual observed paleolatitude, θ . Thus the best estimate of the true paleolatitude, θ_E , is

$$\theta_E = \theta + T(\theta) \quad (6)$$

Figure (1) shows the variation of the correction factor with latitude (Cox, in prep.). Note that $T(\theta)$ increases to 18° for $\theta = 72^\circ$, implying that no paleolatitudes greater than 72° should be observed. When $\theta > 72^\circ$, secular variation has not been adequately sampled, and the true paleolatitude must be taken as 90° . Thus for $\theta > 72^\circ$, $T(\theta)$ is set equal to $90^\circ - \theta$ to keep θ_E within a physically realistic domain.

Confidence Limits

The error in θ depends upon the angular variance, S_0^2 , due to secular variation, plus an additional contribution for experimental errors. Following Cox (in prep.), the standard error,

S_M , of θ for large N , is

$$S_M = (S_E^2 + S_O^2)/N_I^{1/2}, \quad (7)$$

where S_E is the standard error in the determination of θ_i , and N_I is the number of independent measurements of the paleofield. For basalts, θ_i is the mean θ calculated from one cooling unit or from a few cooling units erupted in rapid succession, and S_E can be calculated directly from the data. For sediments, θ_i is based only one specimen inclination, and I must therefore assume a value for S_E . Although the reproducibility of a measurement on any specimen of intensity greater than 10^{-6} emu/cc is usually 2° or less, the associated sampling errors are $5-10^\circ$. For DSDP material I feel that a value of 10° is a conservative estimate of the standard error of dispersion due to sampling errors.

Because each sediment sample averages out the higher frequencies of secular variation, the sediment data sets should not show as much dispersion due to secular variation as the basalt data sets show. This will not affect the paleolatitude but it will affect the associated confidence limits. At one extreme, one can assume that no secular variation averaging occurs and use the values for S_O directly from Cox (in prep.).

At the other extreme, one can assume that secular variation is completely averaged out and set $S_0 = 0$. The actual amount of averaging will vary between these extremes, depending on the sedimentation rate. I have chosen the conservative approach and assumed that no secular variation averaging occurs. Thus I always have used too large a value for S_0 , and I have always overestimated the errors.

The 95% confidence range of the paleolatitude is expressed as

$$\theta_E \pm = \theta_E \pm 2 SM + T(\theta_E \pm 2 SM) \quad (8)$$

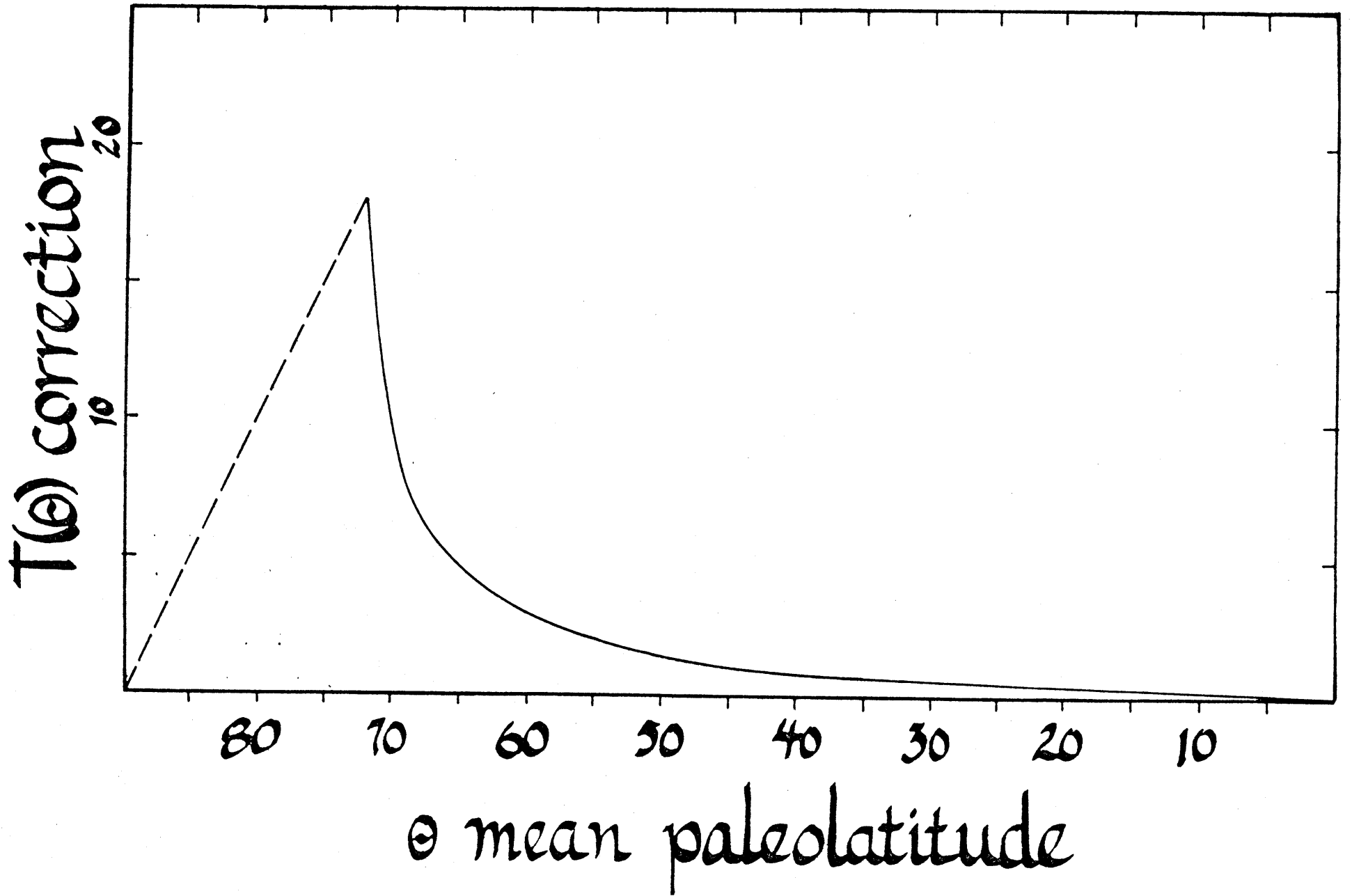
These confidence limits are slightly asymmetric because of the non-linear behavior of $T(\theta)$, but the asymmetry is significant only at high latitudes (Fig. 1). The confidence limit which is polewards of the paleolatitude is always the larger of the two.

Rating Criteria

Because of the wide range of quality and size of the data sets available, it is useful to have a standard scale against which all the data can be compared. The parameter $2 SM$, which

FIGURE 1

Paleolatitude correction, $T(\theta)$, as a function
of mean paleolatitude, θ , (after Cox, in prep.).



is a measure of the statistical reliability of the data, is an appropriate objective criteria to use for such a scale. However, what is important is not the statistical reliability of the data, but its geological reliability. This quality is best tested by considering the consistency of one data set with independent data. Such an assessment is necessarily subjective, as well as being subject to change in the light of new data or models to test against the data.

For the sediments, the parameter 2 SM is independent of the dispersion of the specimen directions, and the confidence limits depend only on the number of samples. In order to filter out data sets which were not sufficiently well grouped to represent the probable behavior of the paleofield, an arbitrary limit of two standard errors (2 SE) of the mean of the inclinations equal to 10° was used. Data sets with greater dispersion than this were omitted, except that three data sets from site 66 were retained because the data were originally used to discuss paleolatitudes.

Considering these ideas, I have rated the data sets in Table 1 according to the following scheme:

(1) Only "stable" inclinations were used, as determined by magnetic cleaning tests. Values of uncleaned natural remanence are not considered reliable, and they were omitted.

(2) An objective rating was assigned according to the value of 2 SM. The ratings assigned were

A	if 2 SM =	$0^{\circ}-5^{\circ}$,
B	"	$5^{\circ}-10^{\circ}$,
C	"	$10^{\circ}-15^{\circ}$,
D	"	$15^{\circ}-20^{\circ}$,
E	"	$> 20^{\circ}$

(3) Consistency of the data with independent evidence is indicated by an asterisk after the rating in Table 1. Inconsistency is indicated by an '-'. In some cases there is no independent evidence to test against, and in others the independent evidence is contradictory. Such cases are indicated by a '?'. References are given in the comments section.

Several consistency tests were used. These tests and references for examples of their application are listed below:

(1) Consistent paleolatitudes in the basal sediments and the basalts, allowing for possible age differences and plate motions (Lowrie and Opdyke, 1973).

(2) A consistent pole defined by the intersection of paleolatitudes of the same age from several sites on the same plate (Cox, in prep.; this paper).

(3) Consistency between the site paleolatitude and a continental apparent polar wandering path or a continental pole of the same age (Peirce et al., 1974; Jarrard, 1974).

(4) Consistent paleolatitudes calculated from the site paleomagnetism data and from plate reconstruction models (Peirce et al., 1974; Lowrie, 1974).

(5) Consistent trends for paleolatitudes of different ages at the same site (Sclater and Cox, 1970; Hammond et al., 1975; Loudon, 1975).

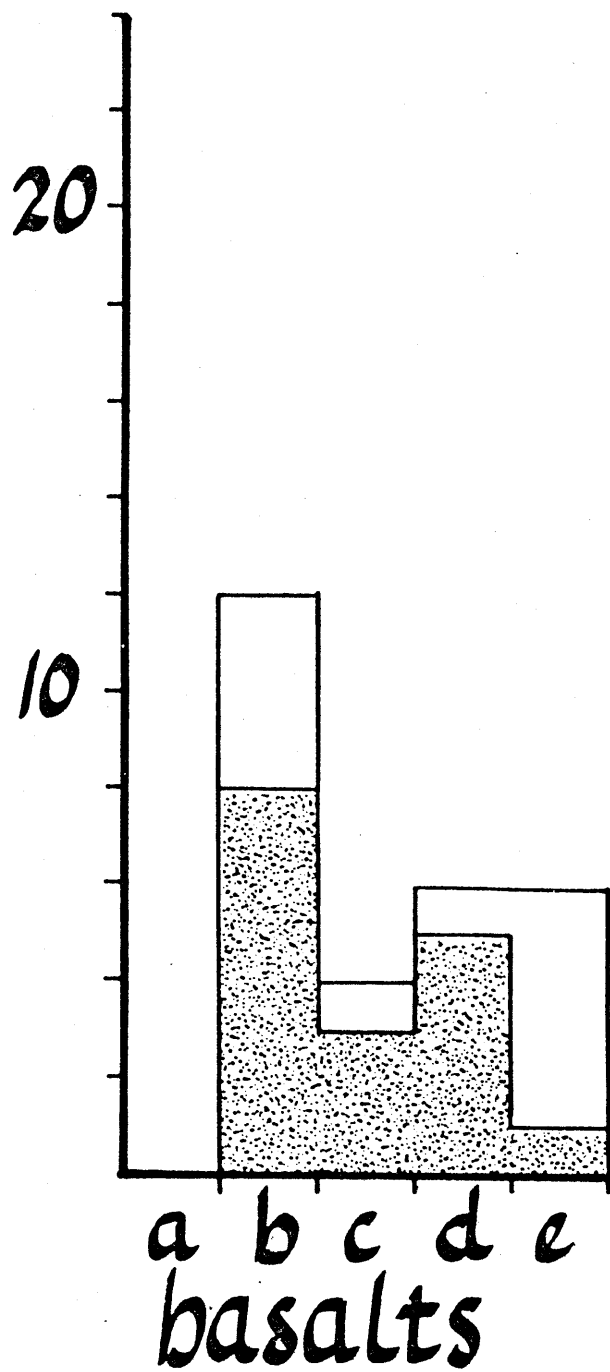
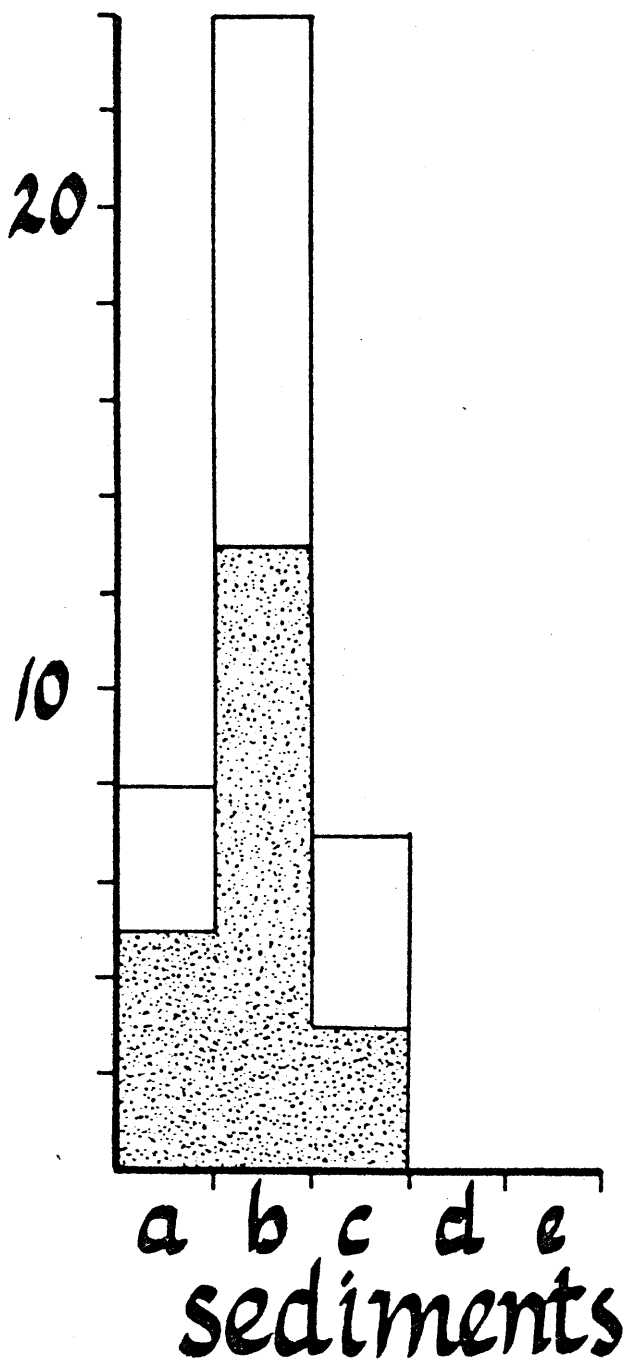
(6) A consistent pole position defined by the intersection of the site paleolatitude and the lunes of confidence derived from the skewness of marine magnetic anomalies (Larson and Chase, 1972; Schouten and Cande, in press). This technique is only applicable to basalts and basal sediments (Larson and Lowrie, 1975; Louden, 1975).

Thirty-nine sediment data sets and twenty-eight basalt data sets were rated in this study. Figure 2a shows the rating histogram for the sediment data, and figure 2b shows the same information for the basalt data. The shaded portions of the two histograms indicate the data which I felt were corroborated by independent evidence.

It is important to note that these rating criteria only indicate how good the data base is for each paleolatitude determination. Because of the assumptions discussed above, the grouping of sediment sample directions has no effect on the rating. The grouping of the within-cooling unit sample directions has a small effect on the rating, but the number of cooling units is the dominant factor.

FIGURE 2

Histograms showing the distribution of ratings for the sediment and basalt data sets. The ratings are indicative of the size of the data base on which the paleolatitudes are based. The shaded portions of the histograms show the number of paleolatitudes which are consistent with independent data.



PALEOLATITUDE RATINGS

Discussion

The concept of using DSDP paleolatitudes to study plate motions was first discussed by Sclater and Cox (1970), using data from site 10 in the North Atlantic. To demonstrate how a consistent trend can be recognized in basically inadequate data, we have shown the histograms for the different age groupings at site 10 (figure 3a). Although none of the inclinations group well except in the lowermost sediments, it is quite evident that the average inclination steepens with younger age. Although very little reliability can be ascribed to specific paleolatitudes at this site, the conclusion that the site has moved northwards with time is clear.

Sclater and Jarrard (1971) concluded that the paleolatitudes found at site 66 in the Pacific were consistent with the 30° of northward motion of the Pacific plate measured by Francheteau et al. (1970) from the magnetic anomalies of seamounts. When viewed in the perspective of the DSDP data base summarized in Table 1, it is clear that the paleolatitudes on which their conclusions were based were unreliable. In contrast to the consistent trend evident in site 10 histograms,

the histograms for different age groupings at site 66 (figure 3b) show no evidence of any grouping of the inclinations at any age and no consistent trend. Because there was no evidence of bedding in the section sampled, there is a possibility that the sampling of disturbed material produced the unreliable results (Jarrard, personal communication). The essentially random distribution of inclinations on the histograms supports this possibility.

Poles for the Pacific plate:

Eight sites on the Pacific plate have upper Cretaceous paleolatitudes calculated for them in Table 1. Sites 57 and 66 were not included in this group. By plotting the locus of possible poles for each site, it is possible to define an upper Cretaceous pole for the Pacific (figure 4) with more confidence than Cox (in prep.) was able to do using only three sites. Six of these paleolatitudes have overlapping confidence intervals which define a polygon of 73% (.95⁶) confidence for the pole.

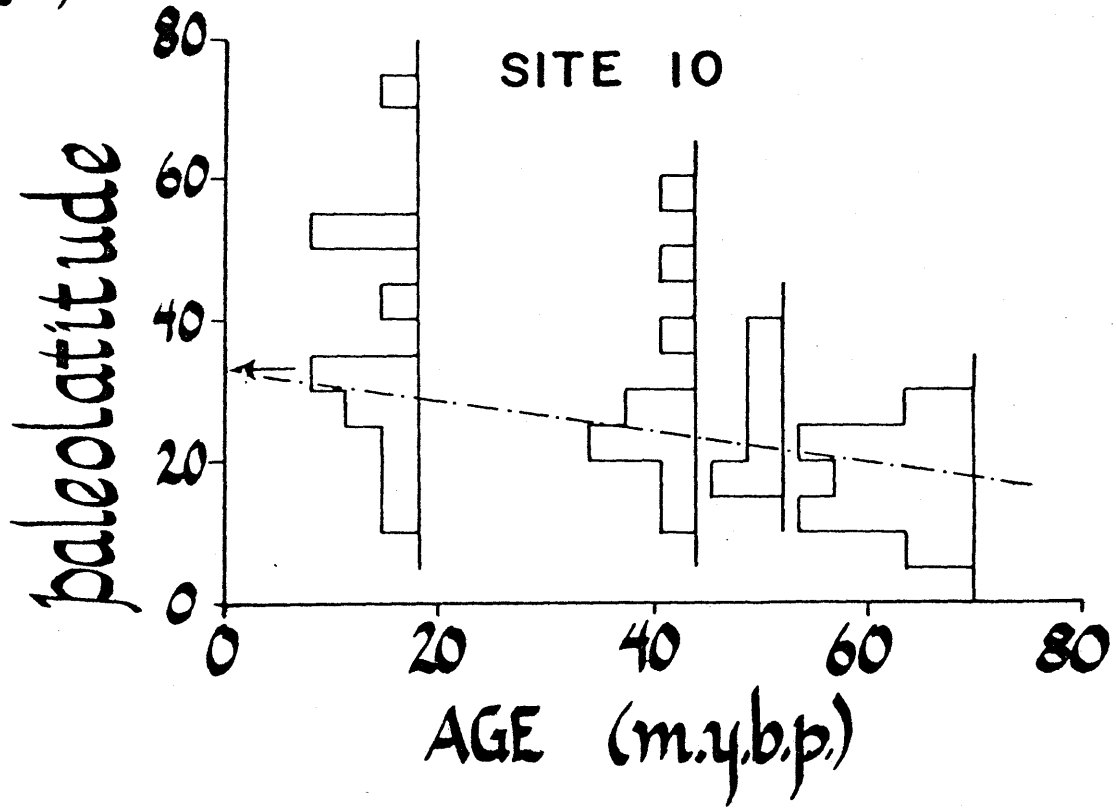
FIGURE 3a.

Paleolatitude histograms plotted versus age for Site 10. Arrow denotes present latitude. This plot demonstrates how the consistency of the trend between poorly defined points can increase the geological reliability associated with individual paleolatitudes.

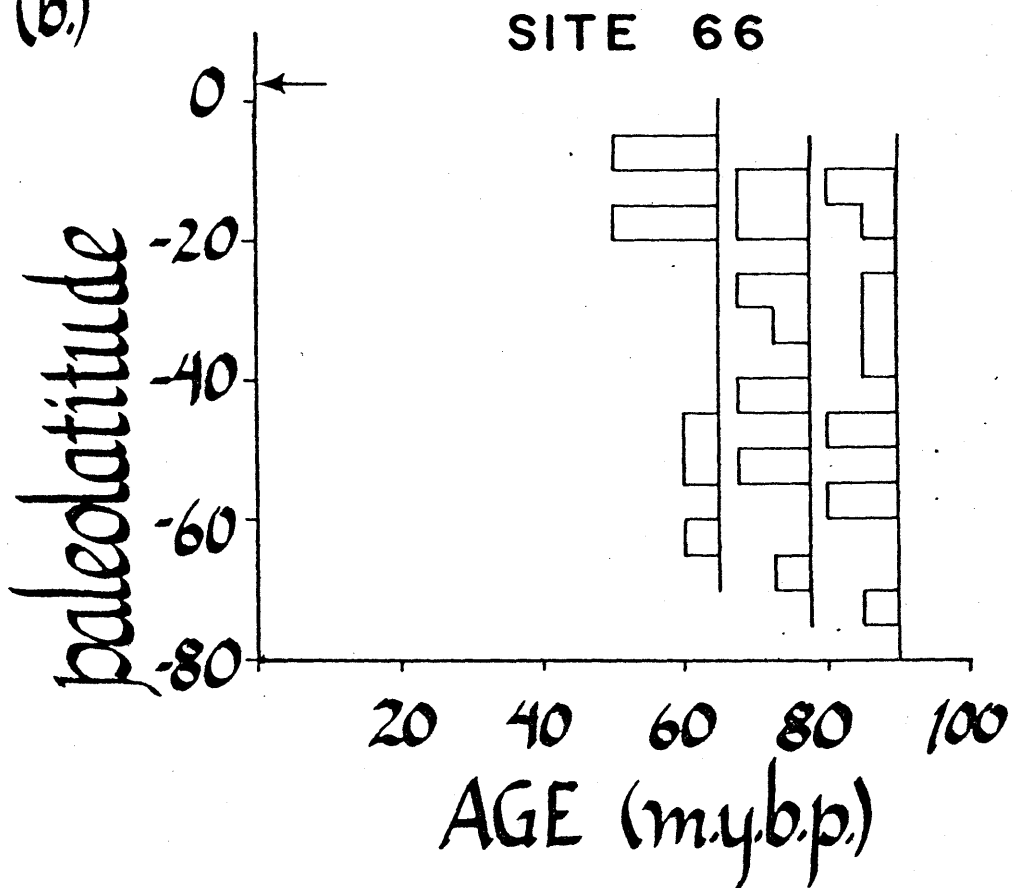
FIGURE 3b.

Paleolatitude histograms plotted versus age for Site 66. Arrow denotes present latitude. This plot demonstrates how the lack of a consistent trend decreases the geological reliability associated with individual paleolatitudes.

(a.)



(b.)



Site 313 is clearly inconsistent with the other data shown on figure 4. This inconsistency is strong evidence either that the site 313 basalts have not correctly recorded the time averaged paleofield or that some assumptions about the age or geology of the site are in error. Figure 4 demonstrates that although individual DSDP paleolatitudes may have large error bands associated with them, the consistency test between different paleolatitude determinations of the same age can be a powerful tool to distinguish between reliable (within the context of a rigid plate model) and unreliable results.

Also shown in figure 4 is the mean pole determined from 26 seamounts (Harrison et al., 1975) and the absolute motion apparent polar wandering path based on the Hawaii Emperor lineation (similar to that used by Clague and Jarrard, 1972).

To compute the polar wandering path I used the following rotations for the absolute motion of the Pacific from Van Andel et al. (in press):

(1) 0-25 m.y.: $.8^{\circ}/\text{m.y.}$ about 67°N , 59°W ;

(2) 25-50 m.y.: $.25^{\circ}/\text{m.y.}$ about 67°N , 59°W ; and

(3) > 50 m.y.: $.8^{\circ}/\text{m.y.}$ about 26.5°N , 127°W .

These rotations are in the opposite sense from those given by Van Andel (in press) because I am defining the motion of the north pole with respect to a fixed Pacific. The last pole given has already been rotated for 50 m.y. from its present position to its given position. As a trial hypothesis I assumed that the absolute motion of the Pacific plate from 50-120 m.y. was defined by Van Andel's pole although the Emperor lineation is probably no older than upper Cretaceous.

There are five sites on the Pacific plate for which middle Cretaceous paleolatitude determinations have been made. Three paleolatitudes (164 and 317 sediments and 303 basalts) have overlapping 95% confidence intervals. The overlap forms a polygon of 85% ($.95^3$) confidence for the middle Cretaceous (fig. 5). The paleolatitude determination for the 317 basalts is 8° steeper than that for the middle Cretaceous sediments, but tectonic tilting may have steepened the observed basalt inclination here between the time of basement formation and the onset of carbonate sedimentation (Cockerham, personal communication).

The paleolatitude determination for site 289 does not appear to be consistent with the other results. However, it is based on only 6 samples from an unknown number of cooling units.

FIGURE 4

Upper Cretaceous paleomagnetic pole for the Pacific plate as defined by DSDP paleolatitudes. The arcs are the loci of positions of the pole for each site. Heavy lines represent sediment data, thin lines represent basalt data, and the dashed lines represent basalt data from only one cooling unit. The diamond shaped outline is defined by the intersection of the 95% confidence bands for sites 163 and 192. The shaded polygon within it is the 73% confidence area defined by the overlapping 95% confidence bands of six sites (all but 61 and 313). The reliability grades assigned to these paleolatitudes are: 61, E; 163, B; 167, A; 171, B; 192, C; 313, E; 315, A; 317, B.

For comparison, the apparent polar wandering path based on the Hawaii-Emperor lineation is shown as stars. The stars represent the absolute motion pole for 25, 50, 60, 70, 80, 90, 100, 110, and 120 million years. See text for poles of rotation and

supporting assumptions. The shaded circle is the pole defined from 26 upper Cretaceous seamounts from Harrison et al. (1975).

The projection is an equal area Schmidt stereo set for the northern hemisphere for Figures 4 and 5, and for the southern hemisphere for Figures 6 and 7.

u. Cretaceous pole for the Pacific

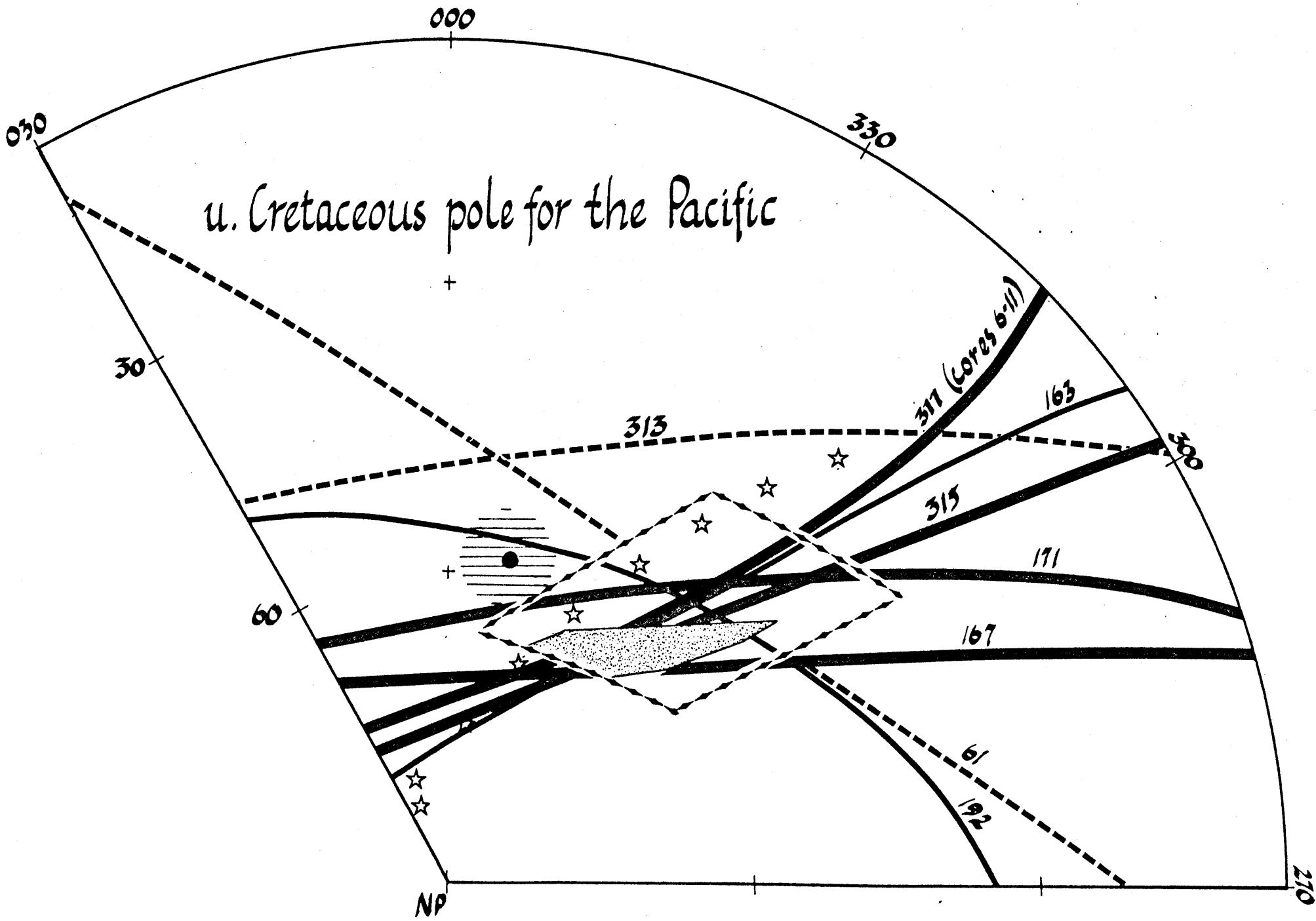
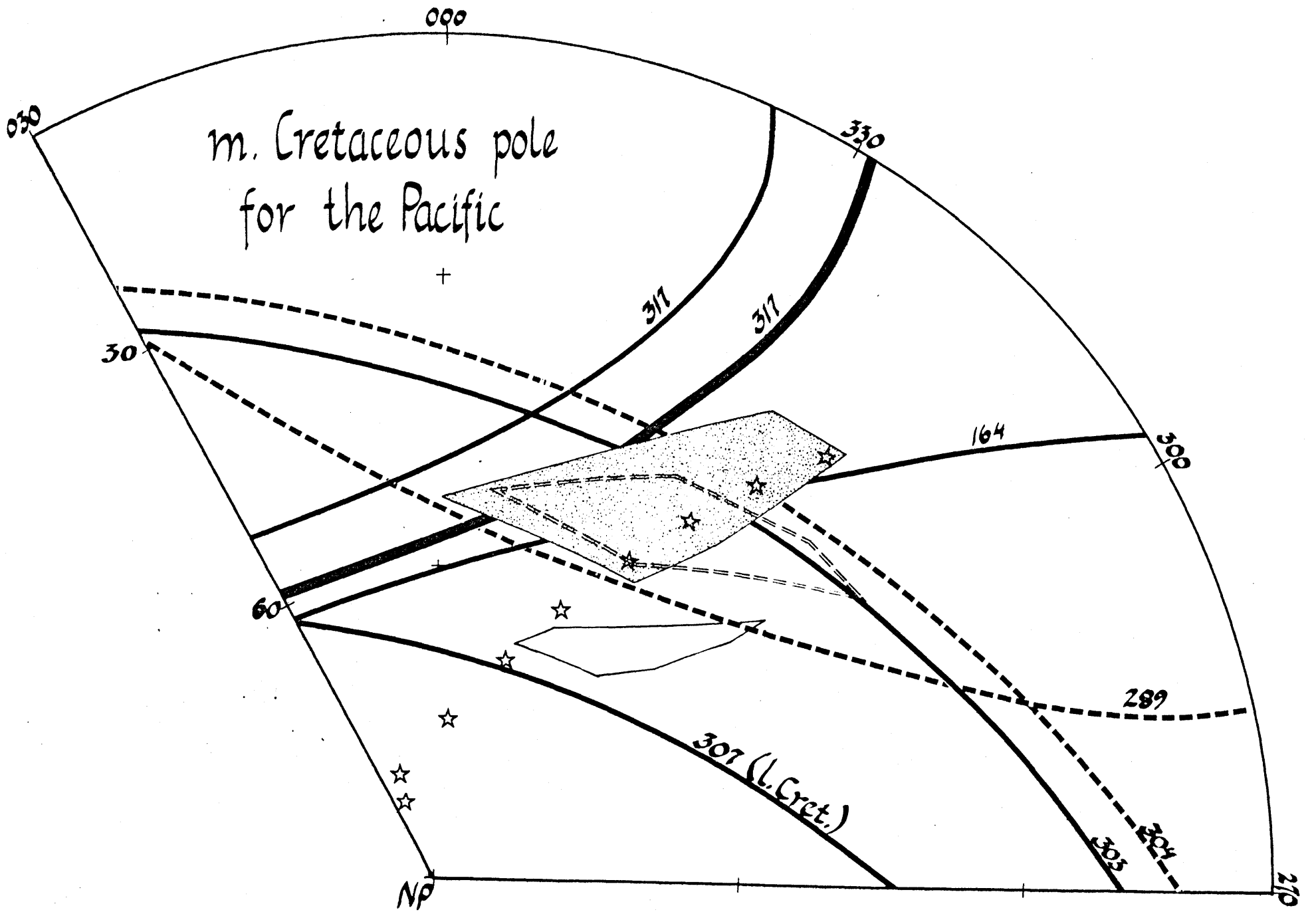


FIGURE 5

Middle Cretaceous paleomagnetic pole for the Pacific plate as defined by DSDP paleolatitudes. The symbols are the same as in Figure 4. The shaded polygon is the 86% confidence limit of sites 164, 304, and 317 (sediments). The double dashed lines outline the polygon of 95% confidence for the pole position defined by Larson and Chase (1972) by phase shifting anomalies M1-M10. The small unshaded polygon is from Figure 4.

Site 307 is of lower Cretaceous age. Its paleolatitude appears to be inconsistent with the middle Cretaceous data because it requires southward motion of the Pacific plate between 125 and 145 mybp.

The reliability grades assigned to these paleolatitudes are: 164, B; 289, none; 303, C; 304, D; 307, B; 317 (sed.), C; 317 (bas.), B.



m. Cretaceous pole
for the Pacific

+

317

317

330

164

300

30

60

289

307 (l. Cret.)

305

204

270

NP

☆

☆

☆

☆

☆

☆

☆

☆

☆

An approximate position for the middle Cretaceous pole is 45°N , 30°W . This is somewhat east of the center of the 95% polygon for the pole by Larson and Chase (1972) from the skewness of anomalies M1-M10 on the Pacific plate (Fig. 5). Thus the DSDP data indicate roughly $10-15^{\circ}$ of northward motion for the Pacific plate between the middle and upper Cretaceous. This is less than half the rate indicated by our extrapolation of the Hawaii-Emperor lineation. I interpret this as an indication that the Pacific plate moved northwards much less rapidly during this time than it did in the upper Cretaceous.

Site 307 is the only site on the Pacific plate with a lower Cretaceous paleolatitude determination. That paleolatitude appears to be inconsistent with the younger data (fig. 5) because it requires southward motion of the site between 145 and 125 m.y.b.p. As a tentative explanation, Larson and Lowrie (1975) speculate that the motion of a then small Pacific plate may have been dominantly rotational during that time. Paleolatitude determinations from a site in the older part of the Phoenix anomalies could be used to test this hypothesis.

A paleomagnetic pole has a longitude ambiguity associated with it because any purely longitudinal translation of a plate

is not recorded paleomagnetically. However, this ambiguity does not exist when comparing an apparent polar wandering path based on absolute motion vectors and a paleomagnetic pole for the same plate because the sites which define each are fixed with respect to each other. Bearing this in mind, figure 4 demonstrates that there is good agreement between the upper Cretaceous latitude of the Pacific predicted by the Hawaii-Emperor lineation, by the DSDP data, and by the seamount data. However, there is a considerable discrepancy in longitude.

Poles for the Australian plate:

In the Indian Ocean it is possible to define a pole for the middle Cretaceous based on five paleolatitudes in the Wharton Basin. As shown in figure 6, four of the pole loci intersect near 55°S , 165°E and the fifth locus passes within 10° . Figure 7 shows the Paleocene pole loci for sites 212 and 213 on the same plate. All these loci lie south of the Australian poles. Although the confidence intervals for the DSDP data overlap some of the circles of 95% confidence for the Australian data, the consistent offset between the two data sets in the direction of minimum error in the DSDP data suggests some left lateral motion

FIGURE 6

Middle Cretaceous paleomagnetic pole for the Wharton Basin, eastern Indian Ocean, as defined by DSDP paleolatitudes. The stippled area is the 81% confidence area for the pole defined by the overlap of the 95% confidence areas for sites 256, 257, 261, and 263. The arrowheads delineate the 95% confidence band for Site 260.

The ellipses numbered 10.1 and 10.2 refer to the 95% confidence areas for the paleomagnetic poles at Mt. Cygnet and Mt. Dromedary (McElhinny, 1973). The five numbered dots are the site positions.

The reliability grades assigned to these paleolatitudes are: 256, C; 257, B; 260, A; 261, B; 263, A.

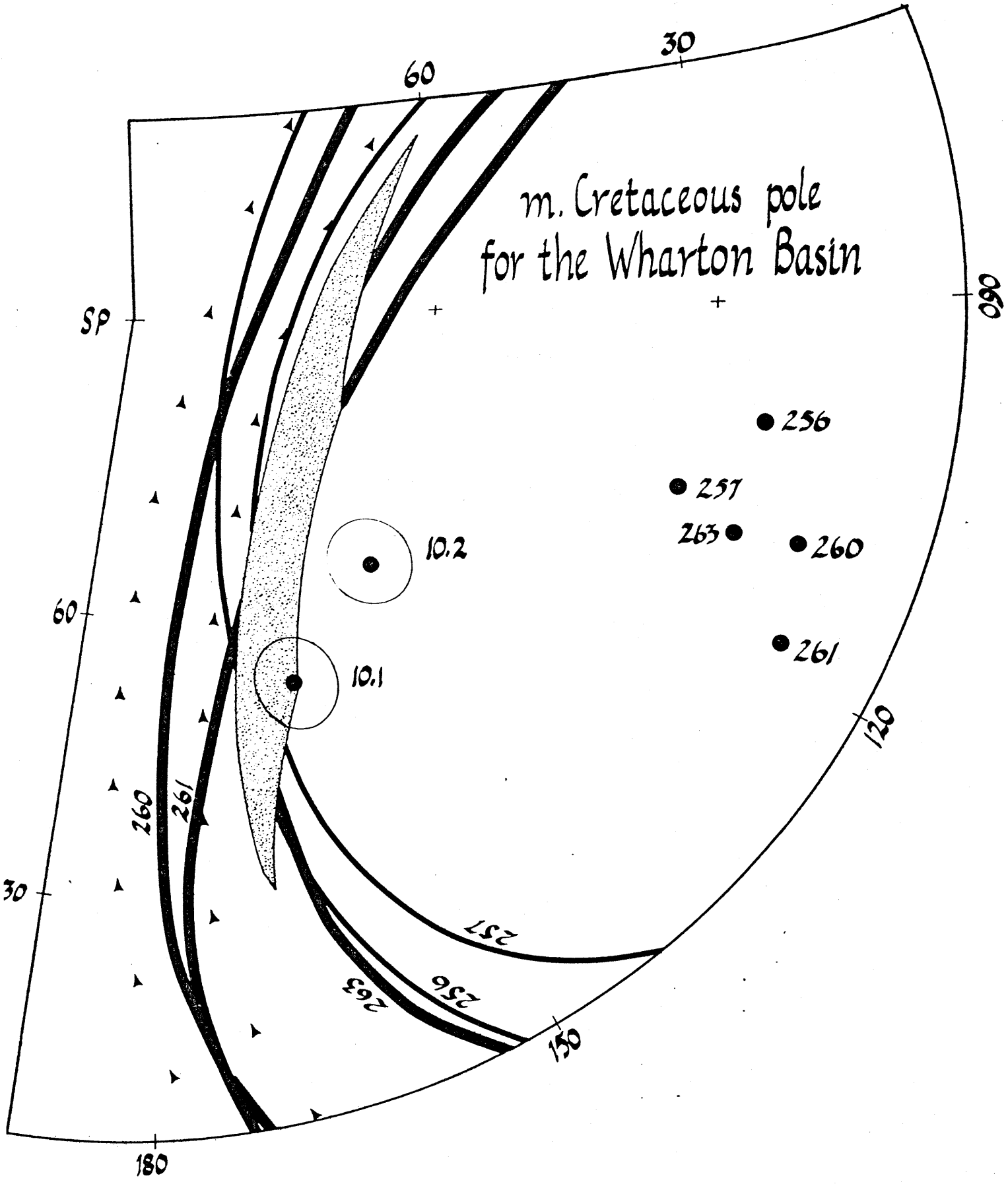
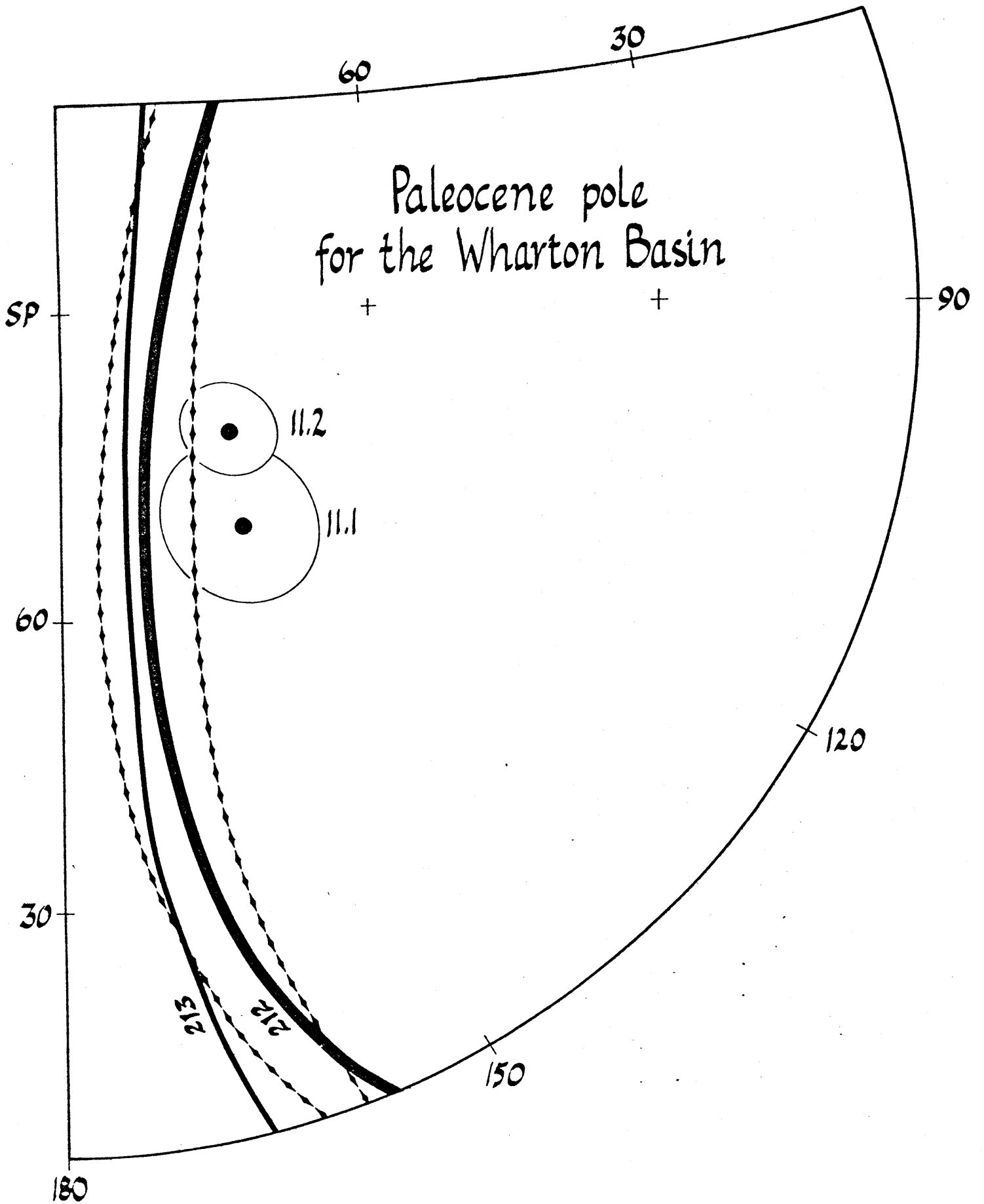


FIGURE 7

Loci of Paleocene pole positions for sites 212 (reliability A) and 213 (reliability B) in the Wharton Basin. The diamond shapes define the 90% confidence area defined by the overlap of the 95% confidence areas of the two sites.

The ellipses numbered 11.1 and 11.2 refer to the 95% confidence areas for the paleomagnetic poles for the Older Volcanics, Victoria, and Barrington Volcano (McElhinny, 1973). The numbered dots are the site positions.



between the Wharton Basin and the Australian continent since the Paleocene. One place this motion may have occurred is along the Darling Fault. (fig. 8). This feature runs for nearly 1000 km along the eastern boundary of the Perth Basin, and there has been 9 km of vertical displacement along it (Brown, et al., 1968). No mention is made in the literature of lateral motion.

Origin of the Ninetyeast Ridge:

There are four sites (214, 216, 253 and 254) on the Ninetyeast Ridge which have paleolatitudes determined from their basement rocks. These sites all lie on the north striking Ninetyeast Ridge and they increase in age from Oligocene to Maestrichtian going from south to north (fig. 8). The data from site 253 is from volcanic sediments (and one basalt sample), while the data for the other three sites come from multiple basalt cooling units. All four paleolatitudes fall in the range 48° - 53° , and only that for site 254 is poorly defined. The close agreement of their basement paleolatitudes supports the hypothesis that the Ninetyeast Ridge is the trace of the Kerguelen hotspot which has remained essentially stationary near 50° S with respect to the spin axis of the earth (Morgan, 1972). The data for site 216

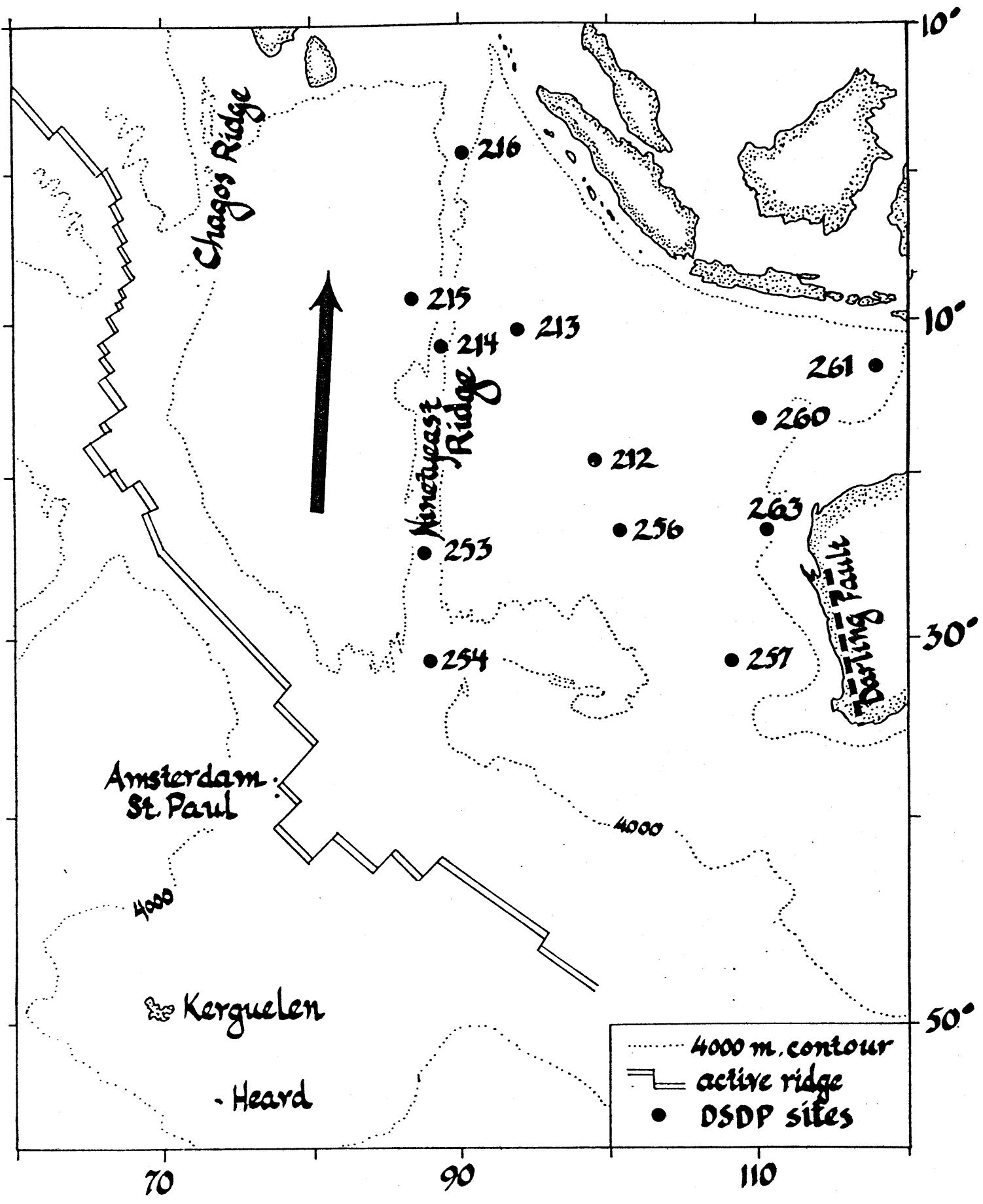
disagree with the paleolatitude predicted by the reconstructions of Sclater and Fisher (1974). They hypothesized that the ridge was the product of excess volcanics produced at the migrating junction of a ridge crest and a major transform fault. The disagreement between the site 216 paleolatitude and their predicted paleolatitude does not disprove their hypothesis for the origin of the ridge; it only suggests that errors exist in their model in the vicinity of the Ninetyeast Ridge. Because the ridge is on the Indian plate now, a spreading center must have existed between site 216 and the Antarctic plate very shortly after basement formation there. That spreading center segment must have been located near 50°S according to the paleolatitude data and not near 40°S as modeled by Sclater and Fisher (1974).

Conclusions

I have presented a rating scheme for DSDP paleolatitudes calculated from the paleomagnetic inclinations in sediments and basalts. In addition I have summarized the paleolatitude determinations in Table I and indicated which data are corroborated by independent evidence. By rating all DSDP

FIGURE 8

Chart of the eastern Indian Ocean showing the relative positions of several DSDP sites for which paleolatitudes have been calculated. Also shown are the Ninetyeast Ridge, Kerguelen Island, and the Darling Fault. The large arrow shows the motion of the Indian plate with respect to Kerguelen prior to the Eocene.



paleolatitudes against these same criteria, their reliability can be viewed with a realistic perspective.

DSDP paleolatitudes have wider bands of confidence than continental poles. Consequently, individual DSDP paleolatitudes are of limited usefulness, but several paleolatitudes of the same age from the same plate can define useful paleomagnetic poles for oceanic plates and provide new constraints for plate reconstruction models. When several sites define a pole, alternative explanations such as secondary magnetization, tectonic tilting, or undetected relative motion between the sites must be sought to explain paleolatitudes which do not agree with that pole.

The paleomagnetic pole for the upper Cretaceous in the Pacific agrees fairly well with the apparent polar wandering curve defined by the Hawaii-Emperor lineation. As the DSDP data fall on one side of the curve and the seamount data (Harrison et al., 1975) fall on the other side of it, I feel that the absolute motion curve is a good first order approximation for an apparent polar wandering curve for the Pacific back to about 100 m.y.b.p. The middle Cretaceous pole for the Wharton Basin lies south of the Australian

paleomagnetic poles and this may indicate some left lateral motion between Australia and the Wharton Basin in the Tertiary.

Four paleolatitudes from basement rocks on the Ninetyeast Ridge all fall close to 50°S , supporting the hypothesis that the Ninetyeast Ridge represents the trace of the Kerguelen hotspot.

Acknowledgements

Allan Cox kindly allowed me to summarize many of the statistical arguments which he has developed in his preprint manuscript. Rob Cockerham, Rick Jarrard, Keith Loudon, and Monte Marshall supplied data from their preprint manuscripts. Jean Guertler measured most of the inclinations included in my unpublished data for Indian Ocean sites. Innumerable discussions with Chuck Denham on the statistics of paleomagnetism stimulated this analysis of the DSDP data. I thank him, Aviva Brecher, Peter Molnar, and Hans Schouten for reviewing the manuscript, and Dorcas Peirce for the calligraphy. This research was supported by NSF grant DES 74-22552 and by the Woods Hole Oceanographic Institution.

Table 1

Summary of DSDP Paleolatitudes, Legs 1-33

Site	Present Position	Age	Type	N	I	+ 2 SM	Corr. P. Lat.	95% P-Lat.	Rating	Ref.	Comments	
1-9	-	-	S	126	-	-	-	-	-	1,2	scattered sampling	
10	32.6°N 52.3°W	Oligo.	S	13/14	53.1	8.0	+36.1	+45.8 +29.3	B*	2,9	cores 2-3	The general trend of northward motion is clearly evident, except for core 5 where low intensities make the data unreliable. Core 12 agrees with (44).
		U. Eoc.	S	9/9	22.3	9.3	+12.6	+22.1 + 3.2	B-	2,9	core 5	
		M. Eoc.	S	10/10	45.7	9.2	+33.9	+43.4 +24.5	B*	2,9	core 7	
		L. Eoc.	S	6/8	42.0	11.6	+25.3	+37.2 +13.5	C*	2,9	core 9	
		L. Maes.	S	18/20	32.2	6.7	+18.6	+25.4 +11.2	B*	2,9	core 11-18	
		L. Maes.	B	6/6	+16.4	19.7	+8.5	+28.6 -11.5	D*	11	$\alpha_{95}=2$, $K=1100$; sill; disagrees with (44)	
12-13	-	-	S	17	-	-	-	-	-	2,3	sparse sampling	
14	28.3°S 20.9°W	L. Mio.	S	5/5	17.3	12.5	- 9.1	-21.9 + 3.6	C-	3	core 2; disagrees with (44)	
		L. Mio.	B	3/3	+70.0	-	+58	-	-	11	$\alpha_{95}=5.2$, $K=552$; sill; disagrees with (44)	
15	30.6°S 18.0°W	Pleis.	S	119	-	-	-	-	-	3	where samples grouped, data scattered only one sample	
		L. Mio.	B	1/1	-43.2	-	+26	-	-	11		
16	30.3°S 15.7°W	L. Plio.	S	13/13	20.8	7.8	-11.4	-19.3 - 3.5	B-	3	Core 4, disagrees with (44)	
17	28.0°S 36.3°W	U. Oligo.	S	42/44	26.2	4.3	-14.7	-19.1 -10.4	A-	3	17B: cores 1, 2, 3-2 to 3-5; disagrees with (44)	
18	28.0°S 8.0°W	Mio.	S	16	-	-	-	-	-	3	sparse sampling only two samples	
		Mio.	B	2/2	-54.7	-	-36	-	-	11		
19	28.5°S 30.6°W	M-L Eoc.	S	5/6	31.1	12.4	-17.7	-30.3 - 5.1	C-	3	cores 8,9; disagrees with basalts and (44)	
		L. Eoc.	B	4/4	-60.8	-	-43	-	-	11	one unit; no sample directions publ.	

Table 1 (continued)

Site	Present Position	Age	Type	N	I	+ 2 SM	Corr. P. Lat.	95% P. Lat.	Rating	Ref.	Comments
20	28.5°S 26.8°W	Oligo.- Maes.	S	7.5	-	-	-	-	-	3	sampling is grouped, but data is widely scattered
21	28.6°S 30.6°W	Camp.	S	7/8	49.7	11.7	-31.5	-43.5 -19.7	B-	3	cores 2,6; disagrees with (44)
22-28	-	-	S	76	-	-	-	-	-	3,4	sparse sampling, weak intensities at 28
29	15.6°N 69.3°W	M. Eocene	S	22/25	29.6	6.0	+17.4	+23.5 +11.3	B*	4	cores 11-16; agrees with (44)
30,31, 33,34	-	-	S	21	-	-	-	-	-	4	sparse sampling
35	40.7°N 127.5°W	Pleis.	S	8/8	67.2	10.3	+53.2	+65.2 +42.1	C-	5	incl. too steep, implies southward motion of Pacific
36	41.0°N 130.1°W	Mio.	S B	1 3/3	- -20	- -	- +10	- -	- -	- 10	only 1 sample only 3 samples
54	15.6°N 140.3°E	L. Mio.	B	3/3	+47	-	+29	-	-	10	only 3 samples
50,51, 55,56	-	-	S	14	-	-	-	-	-	5,6	sparse sampling
57	8.7°N 142.5°E	U. Oligo.	B	7/7	+16	-	+ 8	-	-	12	1 unit; unstable due to high VRM; dipole incl. = 17°; no sample directions publ.
58-60, 68	-	-	S	22	-	-	-	-	-	6,8	sparse sampling
61	12.1°N 147.1°E	Camp.- Sant.	B	5/5	-43	-20.5	-25	-47 - 5	E*	20	1 unit; see fig. 4

Table 1 (continued)

Site	Present Position	Age	Type	N	I	+ 2 SM +I	Corr. P. lat.	95% P. lat.	Rating	Ref.	Comments
66	2.6°N 166.1°W	Tur.- Cen.	S	9/9	38.9	9.5	-26.7	-36.4	B-	7	core 6; See text for discussion
			S	12/12	50.3	8.3	-30.3	-17.0 -38.4	B-	7	core 7
			S	11/11	53.3	8.8	-39.0	-21.4 -48.1 -29.9	B-	7	cores 8-9
77	.5°N 133.2°W	Eoc.	B	1/1	-25	-	-13	-	-	10	only 1 sample
83	4.0°N 95.7°W	Mio.	B	1/1	+40	-	+23	-	-	10	only 1 sample
84	5.8°N 82.9°W	U. Mio.	B	1/1	+17	-	+ 9	-	-	10	only 1 sample
105	34.9°N 69.2°W	Oxford.	B	28/28	-61.2	6.8	+43.2	+50.3 +36.2	B?	37	11 units assumed; consistent with a Jurassic pole for N. America; does not agree with (44)
125	34.6°W 20.6°E	Quat.- L. Plio.	S	39	-	-	-	-	-	13	data scattered
132	40.3°N 11.6°E	Plio.	S	39/43	65.5	4.8	+50.7	+56.2 +45.6	A-	13	incl. steeper than present; cores 7-13
136	34.2°N 16.3°W	Aptian	B	1/1	+11.8	-	+6	-	-	14	only one sample
137	25.9°N 27.1°W	Albian	B	1/1	-	-	-	-	-	14	sample unstable
138	25.9°N 25.6°W	Cen.	B	1/2	+38.7	-	+22	-	-	14	only one stable sample
141	19.4°N 24.0°W	>Mio.	B	2/2	+16.5	-	-	-	-	14	only two samples

Table 1 (continued)

Site	Present Position	Age	Type	N	\bar{I}	+ 2 SM	Corr. P-Lat.	95% P-Lat.	Rating	Ref.	Comments
146	15.1°N	Con.- Tur.	S B	8/8	11.5	9.9	+ 6.0	+16.0	B*	15	similar incl. above and below sill agree with basalt 1 unit
	69.4°W			12/12	+17.0	9.9	+ 8.7	- 4.1 +18.9 - 1.2	B*	15	
150	14.5°N 69.4°W	Con.- Tur.	B	3/3	- 7.7	-	-	+ 4	-	15	only 3 samples
151	15.0°N 73.4°W	Sant.	B	2/2	+22.6	-	12	-	-	15	only 2 samples
153	14.0°W 72.4°W	Tur.	B	3/3	+ 3.2	-	+ 2	-	-	15	only 3 samples
163	11.2°N 150.3°W	1. Camp.	B	21/22	+10.0	8.0	- 5.2	-13.3 + 2.9	B*	20,16	6 units, 1 sample unstable (16); see fig. 4
164	13.2°N 161.5°W	Alb.- Barr.	S	24	-	-	-	-	-	17	data scattered 12 units, 8 independent; see fig. 5
			B	31/31	-27.9	7.0	-15.0	-22.2 -7.9	B*	20	
165, 170, 173	-	-	S	193	-	-	-	-	-	17,18	data scattered; no AF cleaning at 173
166	3.8°N 175.1°W	U. Oligo. U. Eoc.	S	8/13	12.0 or 1.2	-	-	-	-	17	0-3 reversals present, p-lat low, but undefined. Core 9-13.
167	7.1°N 176.8°W	Camp.- Con.	S	48/48	21.4	4.0	-12.5	-16.6 - 8.4	A*	17	see fig. 4 cores 57-62
171	19.1°N 169.5°W	Tur.- Sant.	S	13/16	13.1	7.8	- 6.8	-14.7 + 1.1	B*	17	see fig. 4

Table 1 (continued)

Site	Present Position	Age	Type	N	H	# 2 SM	Corr. P. Lat.	95% P. Lat.	Rating	Ref.	Comments
183	52.6°N 161.2°W	1. Eoc.	B	1/1	+13	-	7	-	-	19	only one sample
191	56.9°N 168.2°W	M. Oligo.	B	2/3	?	-	-	-	-	19	1 unit; one sample unstable; other incls = +32, -11
192	53.0°N 164.7°E	Maes.	B	5/5	+18.7	-	-	-	-	19	3 units (+43, +4, +9) and one xenolith (-44) sampled; scatter too large to rate. 6 units, 4 independent; see fig. 4
		Maes.	B	26/26	+33.3	+10.2	+18.5	+28.5 + 8.1	C*	20	
207	37.0°S 165.4°E	Maes.	S	14/14	+34	-	-	-	-	21	reversed samples; no sample directions publ. normal samples; no sample directions publ.
		Maes.	S	36/36	-57	-	-	-	-	21	
208	26.1°S 165.4°E	Maes.	S	39	?	-	-	-	-	21	only stratigraphy publ.
212	19.2°S 99.3°E	Eoc.- Maes.	S	38/45	45.4	4.7	-29.7	-34.5 -24.9	A*	22	cores 27-29; see fig. 7 core 37; disagrees with Austr. poles
		> Maes.	S	5/5	60.6	13.2	-42.7	-57.2 -29.1	C-	22	
213	10.2°S 93.9°E	Paleo.	S	5/5	-	-	-	-	-	35	apparently disturbed material 10 units of mixed polarities; see fig. 7 and text
		Paleo.	B	35/38	+31.2	6.3	-17.4	-23.8 -11.0	B*	35	
214	11.3°S 88.9°E	Paleo.	B	31/31	+64.8	8.6	-49.3	-59.2 -40.4	B*	35	7 units of mixed polarity; Ninetyeast Ridge; see text
215	8.1°S 86.8°E	Paleo.	S	33/34	55.5	5.3	-38.5	-33.1 -44.0	B-	35	basalts and sediments disagree
			B	28/34	+71.3	7.9	-60.0	-70.2 -50.9	B?	35	11 units, 10 independent, mixed polarity

Table 1 (continued)

Site	Present Position	Age	Type	N	T	+ 2 SM	Corr. P. Lat.	95% P. Lat.	Rating	Ref.	Comments
216	1.5°N 90.2°E	Maes.	B	42/42	+67.1	8.6	-51.1	-61.0 -42.0	B*	35	7 units; Ninetyeast Ridge; see text
219	9.0°N 72.9°E	Pleis.- L. Mio.	S	11	-	-	-	-	-	23, 24	data scattered and some unstable specimens
220	6.5°N 71.0°E	L..Eoc. L. Eoc.	S B	13/14 17/17	19.3 +11.4	5.8 7.4	-14.5 - 5.8	-21.4 - 8.6 -13.4 + 1.6	B- B?	23, 24 23, 24	doesn't agree with basalts 7 units
221	8.0°N 68.4°E	Pleis.- Eoc.	S B	12/13 3/6	20.3 +30.2	8.5	-21.1 -17	-29.7 - 2.4 -	B-	23, 24 23, 24	large time span may account for large 2 SE 5 units samples; (23) considered 3 unreliable
222	20.1°N 61.5°E	Miocene	S	49/55	15.2	4.0	+ 8.0	+12.1 + 4.0	A*	23 24	cores 27-36; 600 m/10 ⁶ yr sed. rate. Agrees with northward motion of India
223	18.7°N 60.1°E	Mio.- U. Paleo.	S B	5/5 7	- +19.4	- -	- -	- -	- -	23 23	data scattered; west of Owen fracture zone 3 basalt and 4 hyaloclastite units sampled, only one sample per unit; data scattered
224	16.5°N 59.7°E	Oligo.	S B	15/15 1/1	10.5 -30.4	7.0	+ 4.9 +17	+12.0 - 2.2 -	B? -	23 23	cores 4-8; west of Owen fracture zone
238	11.2°S 70.5°E	L. Mio.- U. Oligo. L. Oligo.	S B	22 48	30.5 28.2	-	-17 -15	- -	- -	24 24	no sample directions publ. no. of units unknown; no samples directions publ.
239	21.3°S 51.7°E	Camp.	B	2/2	+53.2	-	-34	-	-	25	only 2 samples from 1 unit

Table 1 (continued)

Site	Present Position	Age	Type	N	I	+2 SM	Corr. P. Lat.	95% P. Lat.	Rating	Ref.	Comments
240	3.5°S 50.1°E	Eoc.- Paleo.	B	-	-	-	-	-	-	25	too fractured to sample
245	31.5°S 52.3°E	l. Paleo.	B	2	-	-	-	-	-	25	unstable; K/Ar = 27 ± 3
248	29.5°S 37.5°E	Eoc.- Paleo.	B	3/3	-77.6	-	-72	-	-	25	only 3 samples from 1 unit; K/Ar = 72 ± 7
249	29.9°S 36.1°E	Haut.- Val.	B	2/2	-72.4	-	-60.9	-	-	25	only 2 samples from 1 unit
250	33.5°S 39.4°E	Con.	B	6/6	-67.9	16.3	-50.9	-73.4 -35.3	D-	26	2 units; K/Ar = 59 ± 6; disagrees with (38)
251	36.5°S 49.5°E	L. Mio.	B	3/4	-56.7	-	-	-	-	26	only 3 stable samples from 1 unit; K/Ar = 39 ± 2, 33.7
253	24.9°S 87.4°E	M. Eoc.	S	49/55	-67.6	3.3	-51.9	-55.8 -48.3	A*	36	Ninetyeast Ridge; no sample directions publ.
			B	1/1	-68.5	-	-53	-	-	26	Only 1 sample; K/Ar = 101 ± 3 (?)
254	31.0°S 87.9°E	Oligo.	B	9/9	+67.8	16.2	-50.8	-73.0 -35.3	D*	26	Ninetyeast Ridge; see text; agrees with (38), (39)
256	23.5°S 100.8°E	Albian	B	16/17	-52.4	10.7	-33.7	-45.4 -23.4	C*	35	4 independent units; high VRM is some samples; K/Ar = 92 ± 4; see fig. 6 and text
257	31.0°S 108.4°E	Albian	B	30/30	-61.8	6.4	-45.8	-52.7 -39.2	B*	35	12 units; 2 rev. samples probably inverted; K/Ar = 97, 174, 156, 186; see fig. 6 and text
259	29.6°S 112.7°E	L. Cret.- U. Jur.	B	4/4	?	-	-	-	-	40	1 unit; replicate specimens group but sample incl. scatter: +60.9, +42.0, +81.4, +36.2

Table 1 (continued)

Site	Present Position	Age	Type	N	I	+2 SM	Corr. P. Lat.	95% P. Lat.	Rating	Ref.	Comments
260	16.1°S	Albian	S	61/73	42.6	3.9	-26.7	-30.6	A?	27	see fig. 6 and text
	110.3°E		B	1/1	+50.9	-	-32	-22.7			
261	12.9°S 117.9°E	Aptian L. Cret.- U. Jur. L. Cret.- U. Jur.	S	18/18	52.6	6.8	-34.1	-41.1	B*	27	core 19-23; see fig. 6 and text
			S	12/13	47.4	8.2	-27.0	-27.2	B-	27	core 31-32; disagrees with basalts
			B	9/9	+69.7	11.7	-56.9	-18.6	-76.1	C*	40
263	23.3°S 111.0°E	Alb.- Barr. Alb.- Barr. Alb.- Barr. Alb.- Barr.	S	29/29	55.0	5.4	-36.7	-42.2	(B)*	27	cores 17-19; lith. unit 2 cores 20-23; lith. unit 3 cores 24-29; lith. unit 3 cores 17-29, Nanno age is Alb, dino age is Barr.; see fig. 6
			S	44/53	63.1	4.5	-45.9	-31.2	(A)*	41	
			S	33/52	57.7	5.0	-41.6	-50.6	(B)*	27	
			S	106/134	59.3	2.8	-42.0	-41.2	-46.8	A*	
265	53.5°S 109.9°E	M. Mio.	B	2/2	+49.7	-	-31	-	-	28	only 2 samples; mag. anomalies 5-5b
266	56.4°S 110.1°E	L. Mio.	B	2/2	+71.2	-	-58	-	-	28	only 2 samples; mag. anomalies 6-7
267	59.3°S 104.5°E	M. Oligo.	B	2/2	+81.9	-	-90	-	-	28	only 2 samples; mag. anomalies 15-16
270	77.6°S 178.5°W	Mio.- Oligo.	S	126	45°	-	-	-	-	30	no sample directions or errors publ.
274	69.0°S 173.4°E	L. Oligo.	B	10/10	+74.7	15.9	-65.0	-90.0	D*	28	2 distinct data grouping imply 2 units high VRM in some samples; agrees with Antarctic poles in (42)
								-46.8			

Table 1 (continued)

Site	Present Position	Age	Type	N	I	+ 2 SM	Corr. P. Lat.	95% P. Lat.	Rating	Ref.	Comments	
279	51.3°S 162.6°E	L. Mio.	B	4/4	+66.0	22.9	-49.4	-25.8 -85.0	E?	29	1 unit; high VRM	
280	48.9°S 147.2°E	L. Eoc.	B	7/7	+68.1	23.2	-52.7	-28.5 -90	E?	29	1 unit; high VRM	
282	42.2°S 143.5°E	Eoc.	B	10/10	+66.2	22.7	-49.8	-26.3 -85.7	E?	29	1 unit	
283	43.9°S 154.2°E	Paleo.	B	2/2	-34.7	21.0	-19.4	-40.9 + 1.9	E?	29	1 unit; high VRM	
289	0.5°S 158.5°E	Oligo-Maes.	S	20/20	-	-	-	-	-	43	paleolatitudes trend from 10°S to 1°S generally agree with trend above see fig. 5; K/Ar = 85 ± 10, 77 ± 9	
		Aptian	S	4/4	-	-	-	-	-	43		
		Aptian	B	6/7	-	-	-	-33.5	-	43		
290, 294	-	-	S	58	-	-	-	-	-	31	data have 2 SE > 10, roughly agree with 292 results	
292	15.6°W 124.7°E	U. Mio.	S	13/14	18.2	7.8	+ 8.9	+16.9 + 1.0	B*	31	core 8	Consistent trend shows Phillipine plate formed in southern hemisphere. Basalt incl. agrees with anomaly phase shifting lunes of confidence.
		U. Oligo.	S	10/14	14.4	8.9	+ 7.5	+16.6 - 1.5	B*	31	core 18	
		U. Oligo.	S	14/14	9.6	7.5	+ 5.1	+12.7 - 2.5	B*	31	core 23	
		U. Oligo.	S	18/22	4.1	6.6	+ 1.7	+ 8.4 - 5.0	B*	31	core 31-33	
		L. Oligo-U. Eoc.	S	6/6	.6	11.4	± .3	+12.4 -12.4	C*	31	core 34-38	
		U. Eoc.	S	17/17	10.6	6.8	- 5.0	-11.9 + 2.9	B*	31	core 39	
		U. Eoc.	B	25/35	-21.8	19.8	-11.3	-31.1 + 8.6	D*	31	1 unit	

Table 1 (continued)

Site	Present Position	Age	Type	N	T	+ 2 SM	Corr. P. Lat.	95% P. Lat.	Rating	Ref.	Comments
303	40.6°N 154.5°E	Barr.- Val.	B	5/5	+41.2	11.3	- 5.8	-17.4 + 5.7	C*	32	3 units; agrees with anomaly skewness lunes of confidence; anomaly M-4; see fig. 5
304	39.3°N 155.1°E	Barr.- Val.	B	11/11	21.5	18.8	-11.3	-31.5 + 8.8	D*	32	1 unit; agrees with anomaly skewness lunes of confidence; anomaly M-9; see fig. 5
307	28.6°N 161.0°E	> Val.	B	8/8	+14.2	8.0	+ 7.4	+15.6 - .7	B?	32	6 units; anomaly M-21; agrees with anomaly skewness lunes of confidence; disagrees with other DSDP sites; see fig. 5.
313	20.2°N 171.0°W	Camp.	B	8/8	-36.4	20.4	-20.5	-41.4 + .2	E-	33	1 unit; disagrees with other DSDP sites; see fig. 4
315	4.2°N 158.5°W	Maes.- Sant.	S	77/81	17.8	3.2	- 9.4	-12.7	A*	33	see fig. 4 and text; 315A, cores 16-22, 25, 26
317	11.0°S 162.3°W	Camp.- Apt.	S	24/24	44.0	5.8	-27.1	-33.0 -21.1	B*	33	cores 6-11; see fig. 4
		Apt.- Barr.	S	8/8	59.9	10.6	-41.7	-53.1 -30.9	C*	33	cores 13-15; see fig. 5
		Apt.- Barr.	B	23/23	65.2	7.2	-48.9	-57.2 -41.4	B-	33	10 units; see fig. 5

Notes for Table 1:

Age is the paleontological age of the section. Some K/Ar and magnetic anomaly ages are given in comments. S indicates sediment samples; B indicates basalt or diabase samples. N refers to the number of samples in the data set. Where two numbers are given the first refers to the number of samples used to compute the paleolatitude. See text for an explanation of 2 SM, corrected paleolatitudes, 95% confidence interval, and rating criteria. References are listed below. Numbers in parentheses in comments refer to references.

- | | |
|------------------------------|-------------------------------|
| 1. Opdyke and Phillips, 1969 | 11. Lowrie et al., 1973b |
| 2. Opdyke, 1970 | 12. Lowrie, 1973 |
| 3. Henry and Opdyke, 1970a | 13. Ryan and Flood, 1973 |
| 4. Henry and Opdyke, 1970b | 14. Lowrie and Opdyke, 1972 |
| 5. Doell, 1970 | 15. Lowrie and Opdyke, 1973 |
| 6. Doell, 1971a | 16. Heinrichs, 1973a |
| 7. Sclater and Jarrard, 1971 | 17. Jarrard, 1973 |
| 8. Doell, 1971b | 18. Heinrichs, 1973b |
| 9. Sclater and Cox, 1970 | 19. Whitney and Merrill, 1973 |
| 10. Lowrie et al., 1973a | 20. Marshall, in prep. |

21. Keating, 1974
22. Jarrard and Sclater, 1974
23. Whitmarsh et al., 1974a, 1974b
24. Blow and Hamilton, 1975
25. Wolcejszo et al., 1974
26. Peirce et al., 1974
27. Jarrard, 1974
28. Lowrie and Hayes, 1975
29. Lowrie and Israfil, 1975
30. Allis et al., 1975
31. Louden, 1975
32. Larson and Lowrie, 1975
33. Cockerham and Jarrard, in press
34. Johnson and Ade-Hall, 1975
35. Peirce, unpublished data
36. Cockerham et al., 1975
37. Taylor et al., 1973
38. Mckenzie and Sclater, 1971
39. Sclater and Fisher, 1974
40. McElhinny, 1974
41. Green and Brecher, 1974
42. McElhinny, 1973
43. Hammond et al., 1975
44. Phillips and Forsyth, 1972

REFERENCES

- Ade-Hall, J.M. and P.J.C. Ryall, Geomagnetic field inclinations recorded by the upper part of layer 2 in the vicinity of the crest of the Mid-Atlantic Ridge at 37°N, (abstract), EOS Trans. Am. Geophys. Un., 56, 376, 1975.
- Allis, R.G., P.V. Barrett, and D.A. Christoffel, A paleomagnetic stratigraphy for Oligocene and early Miocene marine glacial sediments at site 270, Ross Sea, Antarctica, In: Hayes, D.E., L.A. Frakes, et al., Initial Reports of the Deep Sea Drilling Project, XXVIII, Washington (U.S. Gov't Printing Office), p. 879-884, 1975.
- Blow, R.A., and N. Hamilton, Paleomagnetic evidence from DSDP cores of northward drift of India, Nature, 257, p. 570-572, 1975.
- Briden, J.C., and M.A. Ward, Analysis of magnetic inclination in bore cores, Pure and Applied Geophysics, 63, pp. 133-152, 1966.
- Brown, D.A., K.S.W. Campbell, and K.A.W. Cook, The Geological Evolution of Australia and New Zealand, Pergamon Press, Oxford, 409 p., 1968.

- Clague, D.A., and R.D. Jarrard, Tertiary Pacific plate motion deduced from the Hawaiian-Emperor chain, Bull. Geol. Soc. Am., 84, p. 1135-1154, 1973.
- Cockerham, R.S., and R.D. Jarrard, in press, Paleomagnetism of some Leg 33 sediments and basalts, In: Initial Reports of the Deep Sea Drilling Project, XXXIII.
- Cockerham, R.S., B.P. Luyendyk, and R. D. Jarrard, Paleomagnetic study of sediments from site 253 DSDP, Ninetyeast Ridge, (abstract), EOS Trans. Am. Geophys. Un., 56, p. 978, 1975.
- Cox, A., Latitude dependence of the angular dispersion of the geomagnetic field, Geophys. J.R. astr. Soc., 20, p. 253-269, 1970.
- Cox, A., The frequency of geomagnetic reversals and the symmetry of the nondipole field, Rev. of Geophys. and Space Phys., 13, p. 35-51, 1975.
- Cox, A., Paleolatitudes determined from paleomagnetic data from vertical cores, in preparation.
- Doell, R.R., Preliminary paleomagnetic results, Leg 5, In: McManus, D.A., et al., Initial Reports of the Deep Sea Drilling Project, V, Washington (U.S. Gov't Printing Office), p. 523-524, 1970.

- Doell, R.R., Preliminary paleomagnetic results, Leg 6, In:
Fischer, A.G., et al., Initial Reports of the Deep Sea
Drilling Project, VI, Washington (U.S. Gov't Printing
Office), p. 961-963, 1971a.
- Doell, R.R., Preliminary paleomagnetic results, Leg 8, In:
Tracy, J.I., Jr., et al., Initial Reports of the Deep
Sea Drilling Project, VIII, Washington (U.S. Gov't
Printing Office), p. 851, 1971b.
- Fisher, R.A., Dispersion on a sphere, Royal Soc. London Proc.,
217, p. 295-305, 1953.
- Francheteau, J., C.G.A. Harrison, J.G. Sclater, and M. Richards,
Magnetization of Pacific seamounts: A preliminary polar
curve for the northeastern Pacific, J. Geophys. Res., 75,
p. 2035-2062, 1970.
- Green, K.E., and A. Brecher, Preliminary paleomagnetic results
for sediments from site 263, Leg 27, In: Veevers, J.J.,
J.R. Heirtzler, et al., Initial Reports of the Deep Sea
Drilling Project, XXVII, Washington (U.S. Gov't Printing
Office), p. 405-414.
- Grommé, C.S., and F.J. Vine, Paleomagnetism of Midway Atoll
lavas and northward motion of the Pacific plate, Earth
and Planet. Sci. Lett., 17, 159-168, 1972.

- Hammond, S.R., L.W. Kroenke, F. Theyer, and D.L. Keeling, Late Cretaceous and Paleogene paleolatitudes of the Ontong Java Plateau, Nature, 255, p. 46-47, 1975.
- Harrison, C.G.A., R.D. Jarrard, V. Vacquier, and R.L. Larson, Paleomagnetism of Cretaceous Pacific seamounts, Geophys. J.R. astr. Soc., 42, p. 859-882, 1975.
- Heinrichs, D.F., Paleomagnetic studies of basalt core from DSDP 163, In: van Andel, T.H., G.R. Heath, et al., Initial Reports of the Deep Sea Drilling Project, XVI, Washington (U.S. Gov't Printing Office), p. 641-645, 1973a.
- Heinrichs, D.F., Paleomagnetic studies of sediments from DSDP site 173, In: Kulm, L.D., R. von Huene, et al., Initial Reports of the Deep Sea Drilling Project, XVIII, Washington (U.S. Gov't Printing Office), p. 843-846, 1973b.
- Henry, K.W., and N.D. Opdyke, Paleomagnetism of specimens from Leg 3 of the Deep Sea Drilling Project, In: Maxwell, A.E., et al., Initial Reports of the Deep Sea Drilling Project, III, Washington (U.S. Gov't Printing Office), p. 667-696, 1970a.
- Henry, K.W., and N.D. Opdyke, Preliminary report on paleomagnetism of Deep Sea Drilling Project, Leg 4 specimens, In: Bader, R.G., et al., Initial Reports of the Deep Sea

Drilling Project, IV, Washington (U.S. Gov't Printing Office), p. 439-454, 1970b.

Jarrard, R.D., Paleomagnetism of Leg 17 sediment cores, In: Winterer, E.L., Ewing, J.I., et al., Initial Reports of the Deep Sea Drilling Project, XVII, Washington (U.S. Gov't Printing Office), p. 365-376, 1973.

Jarrard, R.D., and J.G. Sclater, Preliminary paleomagnetic results, Leg 22, In: von der Borch, C.C., J.C Sclater, et al., Initial Reports of the Deep Sea Drilling Project, XXII, Washington (U.S. Gov't Printing Office), p. 369-375, 1974.

Jarrard, R.D., Paleomagnetism of some Leg 27 sediment cores, In: Veevers, J.J., J.R. Heirtzler, et al., Initial Reports of the Deep Sea Drilling Project, XXVII, Washington (U.S. Gov't Printing Office), p. 415-422, 1974.

Johnson, H.P., and J.M. Ade-Hall, Magnetic results from basalts and sediments from the Nazca plate, Nature, 257, p. 471-473, 1975.

Johnson, H.P., and R.T. Merrill, Low temperature oxidation of a titanomagnetite and the implications for paleomagnetism, J. Geophys. Res., 78, 4938-4949, 1973.

- Keating, B., C.E. Helsley, E.A. Passagno, Jr., Late Cretaceous reversal sequence, Geology, 3, p. 73-76, 1974.
- Kent, D.V., and W. Lowrie, Origin of magnetic instability in sediment cores from the central North Pacific, J. Geophys. Res., 79, p. 2987-3000, 1974.
- Larson, R.L. and C.G. Chase, Late Mesozoic evolution of the western Pacific ocean, Bull. Geol. Soc., 83, p. 3627-3644, 1972.
- Larson, R.L., and W. Lowrie, Paleomagnetic evidence for motion of the Pacific plate from Leg 32 basalts and magnetic anomalies, In: Larson, R.L., R. Moberly, et al., Initial Reports of the Deep Sea Drilling Project, XXXII, Washington (U.S. Gov't Printing Office), p. 571-577, 1975.
- Louden, K.E., Paleolatitudes from DSDP sediments in the West Philippine Basin, (abstract), EOS Trans. AGU, 56, p. 355, 1975.
- Lowrie, W.A., Viscous remanent magnetization in oceanic basalts, Nature, 243, p. 27-29, 1973.
- Lowrie, W., Oceanic basalt magnetic properties and the Vine and Matthews hypothesis, J. Geophys., 40, p. 513-536, 1974.

- Lowrie, W., and D.E. Hayes, Magnetic properties of oceanic basalt samples, In: Hayes, D.E., L.A. Frakes, et al., Initial Reports of the Deep Sea Drilling Project, XXVIII, Washington (U.S. Gov't Printing Office), p. 869-878, 1975.
- Lowrie, W., and M.N. Israfil, Paleomagnetism of basalt samples from Leg 29, In: Kennett, J.P., R.E. Hertz, et al., Initial Reports of the Deep Sea Drilling Project, XXIX, Washington (U.S. Gov't Printing Office), p. 1109-1115, 1975.
- Lowrie, W., R. Løvlie, and N.D. Opdyke, Magnetic properties of Deep Sea Drilling Project basalts from the north Pacific ocean, J. Geophys. Res., 78, p. 7647-7660, 1973a.
- Lowrie, W., R. Løvlie, and N.D. Opdyke, The magnetic properties of Deep Sea Drilling Project basalts from the Atlantic ocean, Earth Planet. Sci. Letters, 17, p. 338-349, 1973b.
- Lowrie, W., and N.D. Opdyke, Paleomagnetism of igneous samples, In: Hayes, D.E., A.C. Pimm, et al., Initial Reports of the Deep Sea Drilling Project, XIV, Washington (U.S. Gov't Printing Office), p. 777-784, 1972.
- Lowrie, W., and N.D. Opdyke, Paleomagnetism of igneous and sedimentary samples, In: Edgar, N.T., J.B. Saunders, et al., Initial Reports of the Deep Sea Drilling Project, XV, (U.S. Gov't Printing Office), p. 1017-1022, 1973.

Marshall, M., Magnetic properties of some DSDP basalts from the north Pacific and Pacific plate tectonics, in preparation.

McElhinny, M.W., Paleomagnetism and plate tectonics, Cambridge Univ. Press, Cambridge, 359 pp., 1973.

McElhinny, M.W., Paleomagnetism of basalt samples, Leg 27, In: Veevers, J.J., J.R. Heirtzler, et al., Initial Reports of the Deep Sea Drilling Project, XXVII, Washington (U.S. Gov't Printing Office), p. 403-404, 1974.

McKenzie, D., and J.G. Sclater, The evolution of the Indian ocean since the late Cretaceous, Geophys. J.R. astr. Soc., 25, p. 437-528, 1971.

Morgan, W.J., Plate motions and deep mantle convection, In: Shagam, R. and others, eds., Studies in earth and space sciences (Hess volume), Geol. Soc. America Mem. 132, p. 7-22, 1972.

Neél, L., Theorie du trainage magnetique des ferromagnetiques en grains fins avec applications aux terres cuites, Ann. Geophys., 5, 99-136, 1949.

Neél, L., Le trainage magnetique, J. Phys. et Radium, 12, 339-351, 1951.

- Opdyke, N.D., Preliminary report of paleomagnetism of Deep Sea Drilling Project Leg 2 specimens, In: Peterson, M.N.A., et al., Initial Reports of the Deep Sea Drilling Project, II, Washington (U.S. Gov't Printing Office), p. 375-385, 1970.
- Opdyke, N.D., and J.D. Phillips, Paleomagnetic stratigraphy of sites 1-7 (Leg 1), In: Ewing, M., et al., Initial Reports of the Deep Sea Drilling Project, I, Washington (U.S. Gov't Printing Office), p. 501-517, 1969.
- Peirce, J.W., C.R. Denham, and B.P. Luyendyk, Paleomagnetic results of basalt samples from DSDP Leg 26, southern Indian Ocean, In: Davies, T.A., B.P. Luyendyk, et al., Initial Reports of the Deep Sea Drilling Project, XXVI, Washington (U.S. Gov't Printing Office), p. 517-527, 1974.
- Phillips, J.D., and D. Forsyth, Plate tectonics, paleomagnetism, and the opening of the Atlantic, Bull. Geol. Soc. Am., 83, p. 1579-1600, 1972.
- Rundle, C.C., M. Brook, N.J. Snelling, P.H. Reynolds, and S.M. Barr, Radiometric age determinations, In: Davies, T.A., B.P. Luyendyk, et al., Initial Reports of the Deep Sea Drilling Project, XXVI, Washington (U.S. Gov't Printing Office), p. 513-516, 1974.

- Ryan, W.B.F., and J.D. Flood, Preliminary paleomagnetic measurements on sediments from the Ionian (site 125) and Tyrrhenian (site 132) Basins of the Mediterranean Sea, In: Ryan, W.B.F., K.J. Hsu, et al., Initial Reports of the Deep Sea Drilling Project, XIII, Washington (U.S. Gov't Printing Office), p. 599-603, 1973.
- Schouten, H., and S.C. Cande, Paleomagnetic poles from marine magnetic anomalies, Geophys. J.R. astr. Soc., in press.
- Sclater, J.G., and A. Cox, Paleolatitudes from JOIDES deep sea sediment cores, Nature, 226, p. 934-935, 1970.
- Sclater, J.G., and R.L. Fisher, The evolution of the east central Indian Ocean, with emphasis on the tectonic setting of the Ninetyeast Ridge, Geol. Soc. Amer. Bull., 85, p. 683-702, 1974.
- Sclater, J.G., and R.D. Jarrard, Preliminary paleomagnetic results, Leg 7, In: Winterer, E.L., et al., Initial Reports of the Deep Sea Drilling Project, p. 1227-1234, 1971.

- Taylor, P.T., N.D. Watkin, and D. Greenewalt, Magnetic property analysis of basalt beneath the quiet zone, EOS Trans. AGU, 54, p. 1030-1032, 1973.
- Theulier, E., Sur l'aimantation des terres cuites et ses applications géophysiques, Ann. Inst. Phys. Globe Univ. Paris Bur. Cent. Magn. Terr., 16, p. 157-302, 1938.
- van Andel, Tj.H., Establishing the age of the oceanic basement, Comments on Earth Sciences: Geophys., 2, p. 159-168, 1971.
- van Andel, Tj.H., G.R. Heath, and T.C. Moore, in press, Cenozoic history of the central Equatorial Pacific: A synthesis based on Deep Sea Drilling Project data, AGU monograph (Woolhard symposium).
- Whitmarsh, R.B., N. Hamilton, and R.B. Kidd, Paleomagnetic results for the Indian and Arabian plates from Arabian Sea cores, In: Whitmarsh, R.B., O.E. Weser, D.A. Ross, et al., Initial Reports of the Deep Sea Drilling Project, XXIII, Washington (U.S. Gov't Printing Office), p. 521-525, 1974.
- Whitmarsh, R.B., O.E. Weser, D.A. Ross, et al., Initial Reports of the Deep Sea Drilling Project, XXIII, Washington (U.S. Gov't Printing Office), Site Reports.

Whitney, J., and R.T. Merrill, Preliminary paleomagnetic results, Leg 19, In: Creger, J.S., D.W. Scholl, et al., Initial Reports of the Deep Sea Drilling Project, XIX, Washington (U.S. Gov't Printing Office), p. 699, 1973.

Wolejszo, J., R. Schlich, and J. Segoufin, Paleomagnetic studies of basalt samples, Deep Sea Drilling Project, Leg 25, In: Simpson, E.S.W., R. Schlich, et al., Initial Reports of the Deep Sea Drilling Project, XXV, Washington (U.S. Gov't Printing Office), p. 555-572, 1974.

Chapter IV

THE ORIGIN OF THE NINETY-EAST RIDGE
AND THE NORTHWARD MOTION OF INDIA,
BASED ON DSDP PALEOLATITUDES

The Origin of the Ninetyeast Ridge
and the Northward Motion of India,
Based on DSDP Paleolatitudes

by

John W. Peirce

MIT-WHOI Joint Program in Oceanography
Woods Hole Oceanographic Institution
Woods Hole, Massachusetts 02543

Woods Hole Oceanographic Institution Contribution No. .

Abstract

Paleomagnetic data are presented from the sediments and basalts at DSDP sites 213, 214, 216, and 217 on or near the Ninetyeast Ridge in the eastern Indian Ocean. The paleolatitudes confirm that the ridge is attached to the Indian plate and that both have moved rapidly northwards since the Late Cretaceous. The Indian plate moved northwards with respect to the south pole at an average rate of 14.9 ± 4.5 cm/yr from 70 mybp until about 40 mybp when it slowed to its present rate of $5.2 \pm .8$ cm/yr.

Basal paleolatitudes on the Ninetyeast Ridge indicate that its volcanic source was approximately fixed in latitude near 50°S , supporting the concept that the ridge is the trace of the Kerguelen hotspot on the northward moving Indian plate. The existence of a "mirror ridge" on the Antarctic plate and the very shallow depths of basement formation on the ridge suggest that the Indian/Antarctic spreading center must have remained near the hotspot from 80 to 40 mybp in spite of one-limb spreading rates of up to 12 cm/yr. This is unexpected in view of the apparently small amount of motion of the Antarctic plate during this time. It is suggested that Antarctica was held nearly fixed by the geometry of other

plate motions, and therefore the Kerguelen hotspot caused asymmetric accretion of new plate material at the southwestern end of the Ninetyeast Ridge. Evidence of such asymmetry has been reported in the form of an 11° southerly migration or jump of that spreading center.

The Ninetyeast Ridge paleolatitudes are consistent with the Deccan Traps paleomagnetic poles. However, a comparison of the Australian paleomagnetic poles and these data shows a major inconsistency between 50 and 40 mybp. Although the reason for this inconsistency is not known, the error may be in the present estimates of the relative motions between India and Antarctica and between Australia and Antarctica as well as the paleomagnetic data itself. The two data sets compare favorably in both rate and paleolatitude back to 40 mybp. Prior to 50 mybp they compare favorably in rate but the DSDP data imply that India was 13° farther south than the Australian poles indicate.

Introduction

There is a wealth of paleontologic, geomagnetic, and tectonic evidence to suggest that the Indian plate has experienced large and rapid northward motion during the Late Cretaceous and Tertiary. One of the remarkable features of the eastern Indian Ocean is the Ninetyeast Ridge, a 5000 km long, linear, aseismic ridge which lies near the 90th meridian. It runs from about 32°S to about 10°N, where it comes buried under the sediments of the Bengal Fan. Legs 22 and 26 of the Deep Sea Drilling Project (DSDP) drilled five holes along the length of the Ninetyeast Ridge. The stratigraphy and paleontology of these sites (von der Borch, Sclater et al., 1974; Davies, Luyendyk et al., 1974; Luyendyk, in press, 1976) provide evidence of extensive northward motion but there is no direct estimate of the rate or the amount of motion.

In this paper I present paleomagnetic data from DSDP sites 214, 216, and 217 on the Ninetyeast Ridge, and also from sites 215 and 213 on either side of it. These data come from several biostratigraphic horizons in the Tertiary and uppermost Cretaceous sediments, as well as from the underlying basalts. They allow a direct, quantitative estimate of the

rates of northward motion of the Indian plate. The tectonic implications of these paleolatitudes for the origin of the Ninetyeast Ridge and the relative motion between India and Australia are discussed in detail.

TECTONICS OF THE INDIAN OCEAN

The floor of the Indian Ocean has been shaped by processes which caused the breakup and dispersal of the Gondwanaland continent. McKenzie and Sclater (1971) used marine magnetic anomalies to reconstruct the evolution of the central Indian Ocean back to 75 million years before present (mybp). Sclater and Fisher (1974) extended that coverage eastward to about 100°E, and they have delineated several north-south fracture zones offsetting east-west trending magnetic anomalies.

The dominant feature in the Indian Ocean is the Ninetyeast Ridge (Figure 1). It had been variously interpreted as a horst (Francis and Raitt, 1967); as the result of overriding plates (LePichon and Heirtzler, 1968); as the trace of a mantle plume (hotspot) beneath the northward moving Indian plate (Morgan, 1972a, 1972b); and as the volcanic mass erupted at the junction of a spreading

center and a transform fault (Sclater and Fisher, 1974). The gravity and seismic data presented by Bowin (1973) indicate that the ridge is nearly isostatically compensated, hence they are not compatible with either the horst or the overriding plate theory.

Bathymetric profiles across the Ninetyeast Ridge are usually asymmetric, often showing a scarp along the eastern side (Laughton et al., 1971). A fracture zone lies near the foot of this escarpment (Bowin, 1973). Sclater and Fisher (1974) found that the crust west of the ridge becomes older to the north while that east of the ridge becomes older to the south (Fig. 2). They postulated that the fracture zone east of the ridge marks an old transform fault (Ninetyeast Fault) which separated the Wharton Basin and the Indian plate during the early Tertiary. A precursor to the present Southeast Indian Ridge lay at the southern end of this transform fault on its western side. On the eastern side of the fault, at the northern end, was an easterly striking spreading center separating the Wharton Basin from the Sunda plate (Figure 3). Figure 3 shows Sclater and Fisher's interpretation of the evolution of the Eastern Indian Ocean in schematic form. Note that the Ninetyeast Ridge is always attached to the Indian plate in this interpretation.

Magnetic anomalies west of the Ninetyeast Ridge appear to be offset about 9° in a left lateral sense along the 86°E fracture zone. The equivalent transform fault on the active SE Indian Ridge is offset about 2° in a right lateral sense. Consequently, Sclater and Fisher (1974) proposed that the ridge segment between 86°E and 90°E jumped about 11° to the south sometime after basement at DSDP site 215 was formed 58-63 mybp, but before anomaly 22 time (53 mybp, according to the revised time scale proposed by Sclater et al., 1974).

The early spreading between India and the Antarctic was in a north-south direction (McKenzie and Sclater, 1971; Sclater and Fisher, 1974, figure 2). Between the time of anomalies 15 and 18 (37.5-43 m.y.B.P., according to the time scale of Sclater et al., 1974), there was a major reorganization of spreading, and the spreading direction changed to northeast-southwest (Sclater et al., 1976). As part of this reorganization, the spreading pattern which was rifting Australia away from Antarctica migrated westward and began to separate Broken Ridge from Kerguelen (McKenzie and Sclater, 1971; Weissel and Hayes, 1972; Bowin, 1974). At about the same time, the spreading center separating the Sunda plate and the Wharton Basin ceased spreading and was

FIGURE 1

Bathymetry of the Indian Ocean. Contours are from a recent Russian chart (Burakova, ed., no publ. date). The small squares indicate the DSDP sites for which some paleomagnetic data have been reported. Note the positions of the Kerguelen - Gaussberg and Broken Ridges relative to the Ninetyeast Ridge.

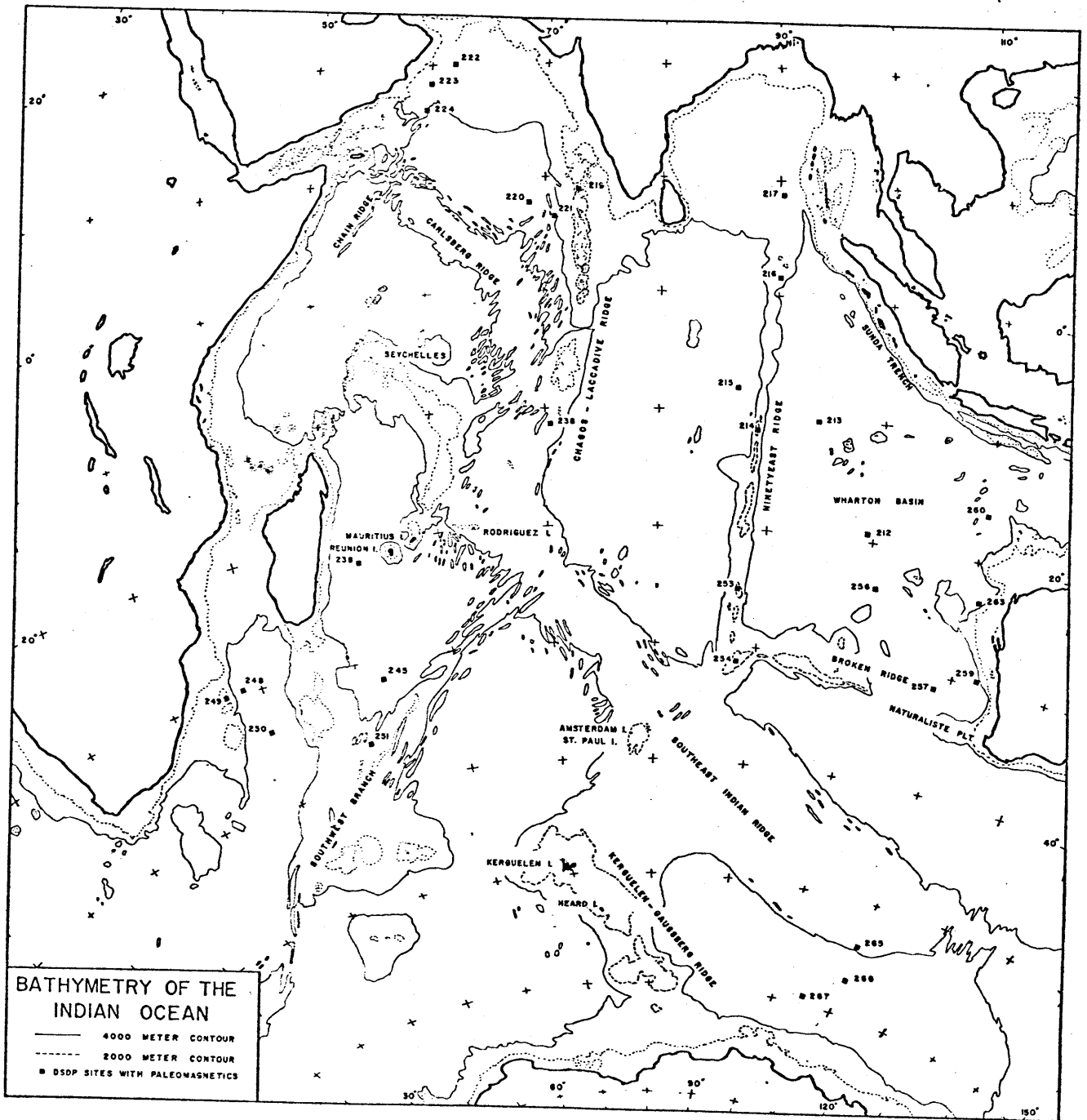
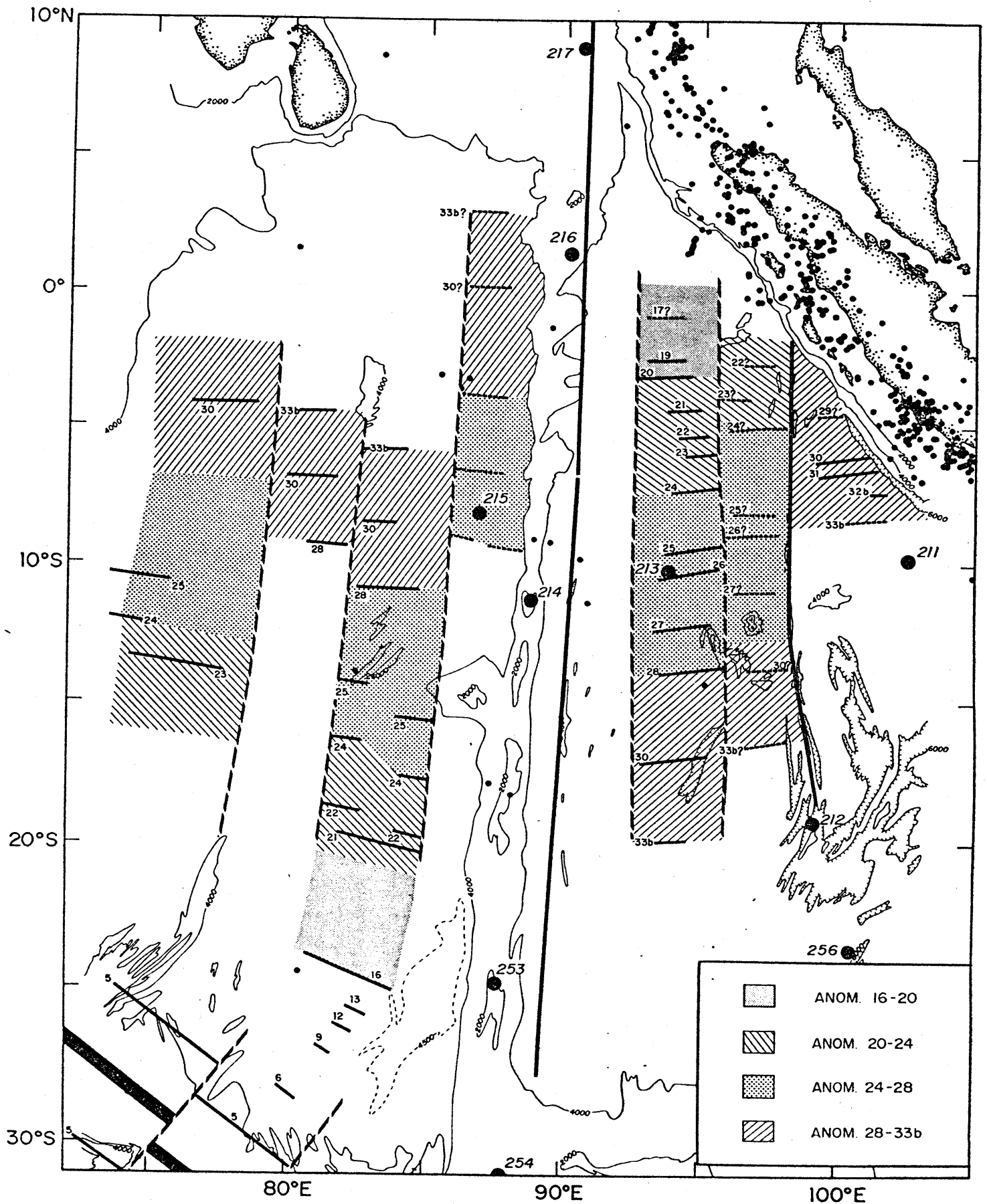


FIGURE 2

Tectonic summary diagram of the eastern Indian Ocean showing the age of oceanic crust on either side of the Ninetyeast Ridge. The light continuous lines are the 2000 and 4000 m contours; the heavy numbered lines indicate identified magnetic anomalies, and the dashed heavy lines represent tentative anomaly identifications. The north-south continuous heavy lines are known fracture zones, and the north-south broken lines represent postulated fracture zones. Large, numbered spots are DSDP sites. Small dots are earthquake epicenters. (From Sclater and Fisher, 1974).







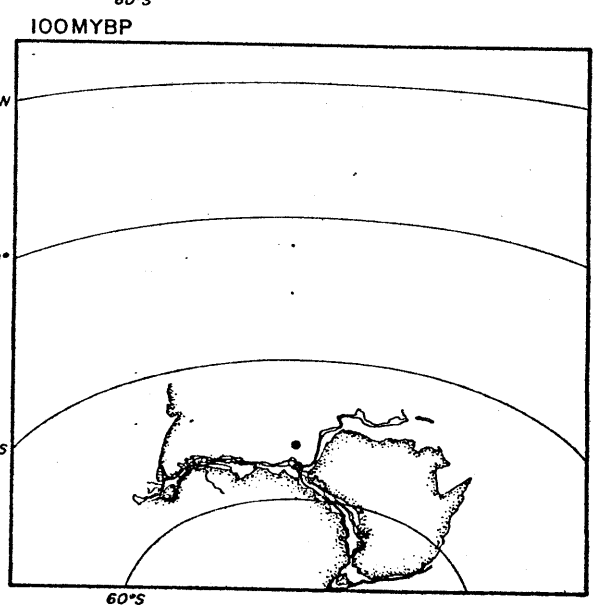
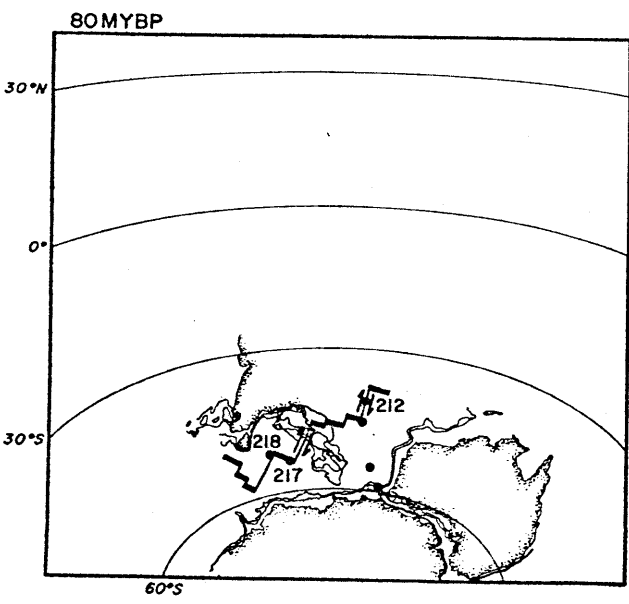
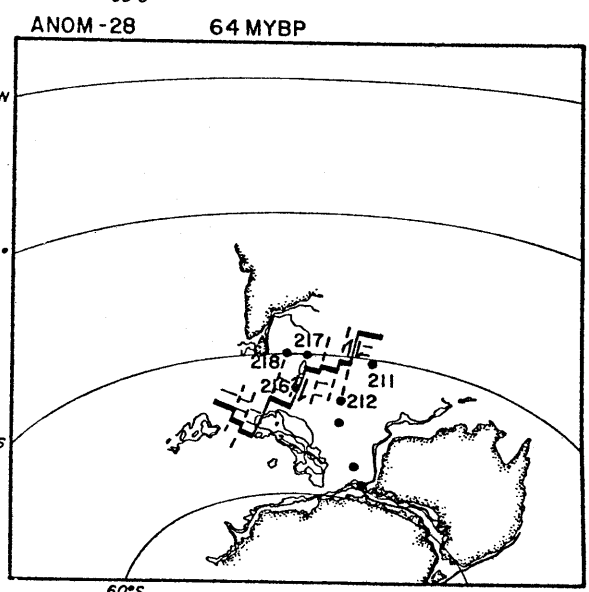
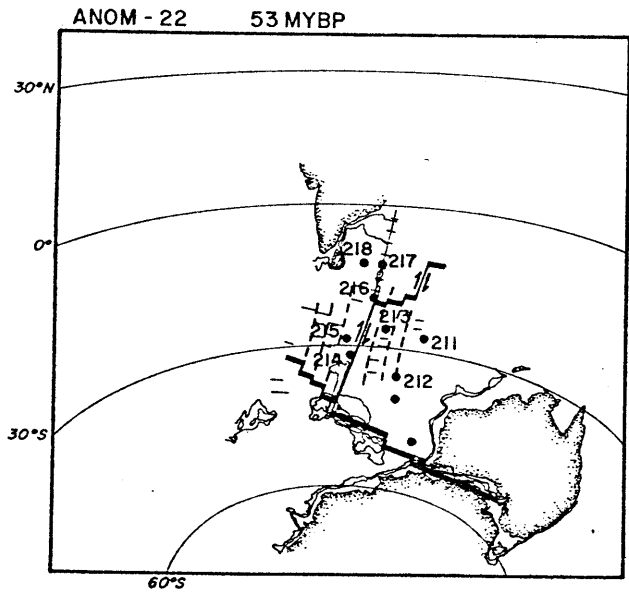
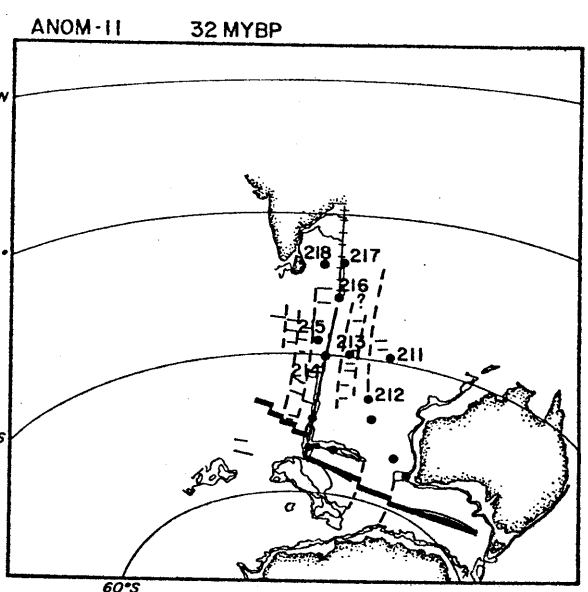
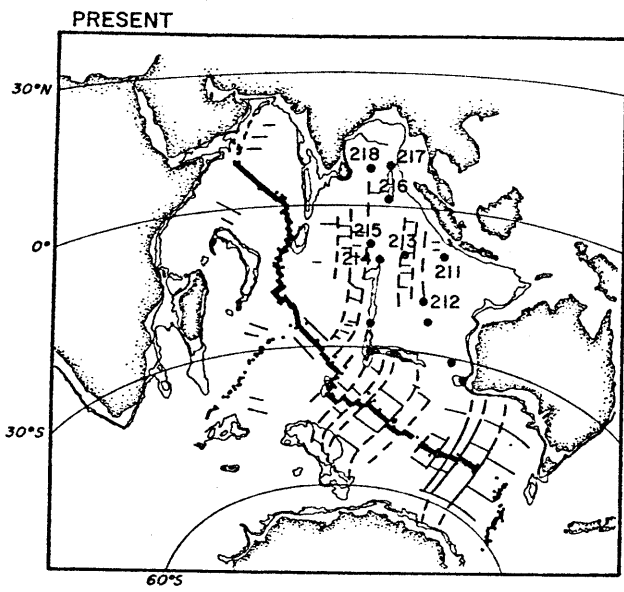
-  ANOM. 16-20
-  ANOM. 20-24
-  ANOM. 24-28
-  ANOM. 28-33b

FIGURE 3

Reconstructions of the relative positions of India, Australia, and Antarctica from the present back to 100 mybp. Reconstructions are relative to a fixed Antarctica, and the paleolatitude parallels are drawn to agree with the paleomagnetic data for Australia. The small black dots are seismic epicenters on mid-ocean ridges. The large dots represent DSDP sites, and those from Leg 22 are numbered. Thick black lines indicate spreading centers; heavy continuous lines are transform faults; heavy broken lines are fracture zones; and short east-west lines are identified magnetic anomalies. (From Sclater and Fisher, 1974).



subducted in the Java Trench. When this spreading ceased (anomaly 17 or earlier, Sclater and Fisher, 1974), the Indian plate and the Wharton Basin healed together and became the Australian plate as it is today.

Previous evidence for northward motion

The paleontology and palynology of the DSDP sites on the Ninetyeast Ridge is marked by two distinctive trends: (1) a shallow, or sometimes subaerial, to deep water facies change up section, and (2) a transition from high latitude temperate assemblages to low latitude tropical assemblages up section (Gartner et al., 1974; Pimm et al., 1974; Harris, 1974; Kemp and Harris, 1975).

The present depths of the Ninetyeast Ridge increase systematically to the north in rough accordance with the shape of the empirical age-depth curve for the ocean basins (Sclater et al., 1971; Bowin, 1973; Sclater and Fisher, 1974). Much of the ridge was originally above sea level (Luyendyk and Davies, 1974; Pimm et al., 1974; Kemp and Harris, 1975; Sclater et al., in press, 1976). Previously published paleomagnetic results from the basalts indicate a high southern latitude origin for the southern end of the ridge (Peirce et al., 1974), but the associated confidence interval was very large (Peirce, in press, 1976). A well constrained

paleolatitude has been reported by Cockerham et al. (1975) which confirms this conclusion. Paleomagnetic data from other parts of the Indian plate also indicate positions in high southern latitudes in the Cretaceous (McElhinny, 1968, 1973; Wellman and McElhinny, 1970; Blow and Hamilton, 1975).

Reconstructions of the Gondwanaland continents (Smith and Hallam, 1970; McElhinny, 1970; McElhinny and Luck, 1970) place the Antarctic, Australian, and Indian continents in close proximity. Using Australian paleomagnetic data (Wellman et al., 1969) for paleolatitude control, Sclater and Fisher (1974) have reconstructed the evolution of the eastern Indian Ocean from magnetic anomalies (Figure 3). Their reconstructions also indicate southern latitudes for the Ninetyeast Ridge as it formed.

Basalt Paleolatitudes

Paleolatitudes are calculated from the paleomagnetic data at sites 213, 214, 215, and 216. Sites 214 and 216 are on the Ninetyeast Ridge, and both paleolatitudes lie near 50°S. Site 213 is 400 km east of the Ninetyeast Ridge in the Wharton Basin. The basement at this site formed near the northern end of the old Ninetyeast transform fault, hence its low paleolatitude of 18°S. The difference between the paleolatitudes at sites 213 and 214 is $32^\circ \pm 16^\circ$, implying

that the Ninetyeast Transform Fault was some 3500 km long.

Site 215 lies to the west of the Ninetyeast Ridge, and it is slightly older than site 214. Its paleolatitude of 64°S is not consistent with the Ninetyeast Ridge data or with the results from the overlying sediments. Because the magnetic directions at this site were often characterized by unstable behavior (see discussion below), this paleolatitude is not considered reliable.

The paleolatitudes and associated confidence intervals are calculated according to the method developed by Cox (in prep., 1976). Using this procedure, the data are averaged by cooling unit, and the size of the confidence interval is determined by: (1) the modelled secular variation at the estimated paleolatitude; (2) the within unit dispersion of the paleomagnetic directions; (3) and the number of independent cooling units. Independent cooling units are those which represent independent samplings of the geomagnetic vector at the site.

Ideally, several tens of independent cooling units spaced over at least 50,000 years are needed to completely average the secular variation of the geomagnetic field. In practice, many adjacent geologic cooling units have very similar inclinations, suggesting that they are not independent.

Consequently, I have considered cooling units to be independent only when the mean inclination of one unit lies more than two standard errors of the mean away from the mean inclination of the adjacent units. Similar methods have been used to identify separate cooling units on DSDP Leg 37 (Ade-Hall et al., 1975; Hall and Ryall, in press, 1976). Units with inclinations of opposite sign have always been assumed to be independent as all of these paleolatitudes lie far from the equator. As a result of this method, the number of independent cooling units at a given DSDP site is relatively few (to date always less than 10), and the confidence interval of the paleolatitude remains highly dependent on it. Because my interpretation of cooling unit independence is crucial to an evaluation of the paleolatitude reliabilities, a description of it is included below in the discussion of the data quality at each site.

The paleolatitudes and their associated statistics are listed in Table I. The values listed here are revisions of the preliminary results reported by Peirce (in press, 1976). The differences in the paleolatitudes are small, but the confidence intervals are often larger because of more strict criteria for cooling unit independence. The paleomagnetic directions of the individual specimens are listed in Appendix I,

and the uncorrected paleolatitudes for each cooling unit are plotted in Figure 4.

The total number of basalt specimens measured was 143. Of these, 44 were partially demagnetized in alternating fields (AF) in a stepwise manner up to 800 oersteds as pilot samples from the inferred cooling units. The directional behavior and normalized intensity curves for a representative set of these are included in Appendix II.

About 10% of the basalt specimens exhibited unstable behavior or anomalous directions, and these were omitted from the data set used for paleolatitude calculations. Most of these were from site 215 where back to back specimens sampled from the same piece of core often exhibited discordant directions. The criteria used for rejecting basalt specimen directions were as follows:

1. If the paleomagnetic direction did not stabilize to less than a 5° change between two successive demagnetizing steps (NRM, 100, 150, 200, and 400 oersteds), it was rejected. Exceptions to this rule were made only when back to back specimens showed similar inclinations (within 10°) and similar declinations (within 20°).
2. If two back to back specimens showed discordant directions, both were rejected.

All of the specimens were partially demagnetized at at least three different cleaning fields, usually 100, 150, and 200 oersteds. The directions chosen for the paleo-latitude calculations were those which showed the least angular change from the previous direction, and the maximum stability index with respect to the previous magnetic vector ($SI = 1 - (\vec{J}_1 - \vec{J}_2)/\vec{J}_1$, Briden, 1972). When these two criteria were not met simultaneously, it was usually because of a large intensity change, and the minimum angular change criterion was given more weight.

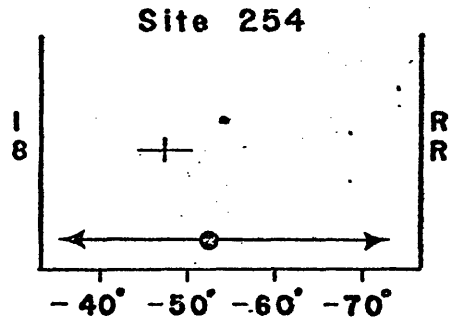
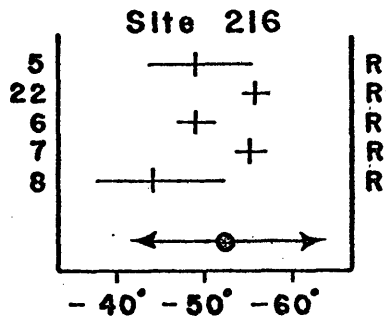
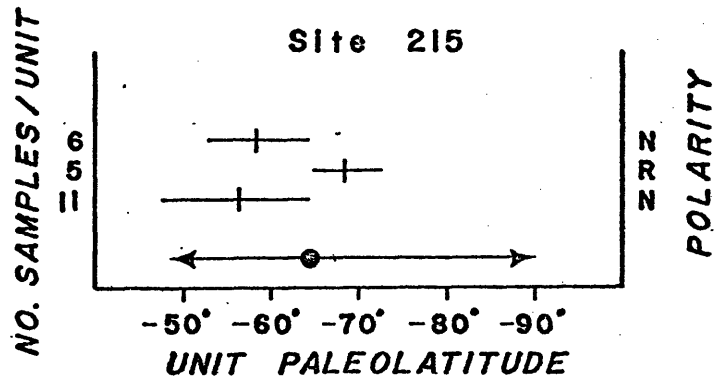
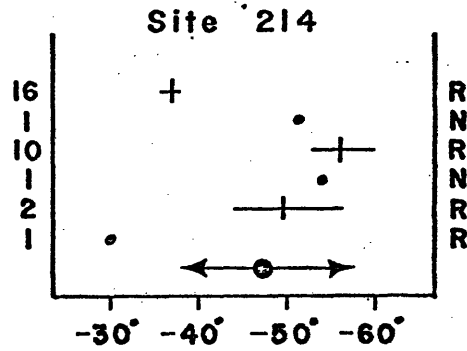
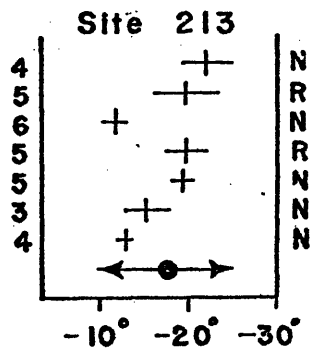
Geology of the basalt sections

The 95% confidence interval for the paleolatitude is primarily dependent on the number of independent cooling units identified at each site. The identification of cooling unit boundaries is difficult when one only has a core about 6 cm in diameter to work with. In some cases the presence of graded textural changes (glass to vesicular to fine grained to coarse grained) is a clear indication of a cooling unit. Sometimes possible subaerial weathering zones were indicated by oxidized, vesicular flow (?) tops (e.g. Site 216). However, more often, possible cooling unit boundaries are indicated only by chilled margins, and there

FIGURE 4

The uncorrected virtual geomagnetic latitudes of the independent basalt units of sites 213, 214, 215, 216, and 254 are shown arranged in stratigraphic order. The numbers to the left are the number of samples in each unit, and the letters N and R on the right denote whether the unit was normally or reversely polarized. The length of the horizontal bar of each unit indicates the range of two standard errors of the mean of the paleolatitudes. Units with only one sample are indicated by an open circle. The corrected paleolatitude and 95% confidence interval from Table 1 is shown by the star and arrows.

UNCORRECTED PALEOLATITUDES OF BASALT COOLING UNITS



is no way to distinguish whether these represent individual pillows from the same eruption, or whether they represent different cooling units from different eruptions. In Tables 2-5, I have listed the geological evidence suggesting cooling unit boundaries, the paleomagnetic inclinations associated with each of these units, and my interpretation of which units I considered independent. In one case (Site 215), I inferred a cooling unit boundary between cores 18 and 19 on the basis of an observed reversal of inclination. In another case (Site 216), I inferred a cooling unit boundary in core 38 (section 2, 38 cm) on the basis of significant change in inclination. This inferred boundary coincides with a zone of alteration and chlorite veins which I had previously discarded as a possible boundary. In all the other cases, significant changes of inclination only occurred on either side of a boundary previously identified on geological criteria alone. However, the majority of the previously identified boundaries did not separate zones of significantly different magnetic inclinations. In such cases, adjacent cooling units were not considered independent, and they are presumed to be either pillows from the same eruption or units from eruptions closely spaced in time.

Site 213

The basalt section at site 213 consists of a series of weathered basalt units separated by glassy palagonitized zones (Table II). The shipboard scientists described the section as "a succession of at least eleven basaltic flows", (von der Borch, Sclater et al., 1974, p. 88). I identified fifteen separate cooling units on the basis of chilled margins. Of these, three were unsuitable for sampling because of insufficient recovery of orientable pieces. Of the remaining twelve units, six are considered to be independent, and at least four well established reversals were observed (Figure 4a).

Most of the specimens exhibited good stability on cleaning (see Appendix II). Five samples reversed polarity on cleaning. Three of these were discarded, because they did not stabilize, and the directions of the remaining two migrated to values very similar to those measured in back to back specimens. An additional sample was discarded because it displayed an extremely anomalous direction and an anomalously soft coercive force spectrum. Nine pairs of back to back specimens were taken. The cleaned directions of six of the pairs agreed very well, two of them agreed moderately well, and the stability of one of the specimens in the ninth pair was considered doubtful (Appendix I).

The oldest clearly dated sediments from site 213 are placed in the D. multiradiatus zone (53.5-56.6 m.y.B.P., according to Berggren, 1972). However, sediments removed ultrasonically from some of the basalt pieces gave a slightly older age (von der Borch, Sclater et al., 1974, p. 92; Gartner, 1974). The site was drilled on the beginning of anomaly 26 (von der Borch, Sclater et al., 1974, p. 92), giving an age of 64 m.y.B.P. according to the Heirtzler et al. (1968) time scale or 60 m.y.B.P. according to the revised time scale of Sclater et al. (1974).

At all of these sites I have considered five million years to be a conservative estimate for the possible age range of the basalts when the age of the overlying sediment is reasonably well controlled. For site 213 I have assigned an age of 58-63 m.y.B.P. as the best compromise between the paleontologic age and the two ages from the different time scales.

Site 214

The basalt section at site 214 is quite variable (Table III). The top three units have a fine grained trachytic texture and are quite fresh. The reversed directions here are

very tightly grouped, and I considered these three apparent units to be one independent unit. Hekinian (1974) describes these units as oceanic andesites which are more differentiated than the basalts deeper in the hole. The shipboard scientists interpreted them as sills (von der Borch, Sclater et al., 1974, p. 122). Unit 5 is a normally magnetized unit located below a tuff, and above a sand and debris layer. The four lowermost units appear to be thin flows which may be subaerial, and they are each considered to be independent (Figure 4b). The flow (?) tops are marked by very coarse (up to 10 mm) vesicular zones.

No specimens exhibited unstable behavior, and no directions were rejected for any reason. Nine sets of back to back specimens showed excellent directional agreement.

The oldest sediments at site 214 are assigned NP5 (H. kleinPELLI, lower P4, 57-58 m.y.B.P.) of the Berggren (1972) time scale (von der Borch, Sclater et al., 1974, p. 126). This age was confirmed by Berggren et al. (1974). As this age seems well established, and yet as site 214 is clearly somewhat younger than site 215 to the west, a narrow age band of 57-60 m.y.B.P. is assigned.

Site 215

The basalt section at site 215 consists of a sequence of closely spaced chilled margins which probably represent a pillow sequence (Table IV). Because of the presence of reversely magnetized units in core 19, my interpretation is that three distinctive eruptive episodes are represented in the section (Figure 4c). The shipboard scientists interpreted this section as a sequence of 14 pillows, based on the frequent occurrence of glass, palagonite, and numerous cross-cutting veins (von der Borch, Sclater et al., 1974, p. 196).

Numerous samples exhibited anomalous directions. Some of these anomalous directions are probably due to movement within the pillow pile after the lava had cooled through the Curie point, but the frequent occurrence of discordant directions in back to back specimens at this site casts doubt on the validity of the paleolatitude. Four pairs of back to back specimens were rejected because of discordant directions. Five other pairs of specimens showed concordant directions, and two pairs showed roughly concordant directions. Four specimens which reversed on cleaning and one other specimen direction did not stabilize. These directions were rejected. An additional direction (20-2-120) was omitted because it was of opposite polarity to the adjacent specimens and there was no

evidence of cooling unit boundaries on either side of it. This specimen came from a piece of core which was too long to be inverted during the drilling process, but it may have been accidentally inverted by careless handling.

The oldest sediments at site 215 are assigned to zone NP5 (F. tympaniformis, upper P3, 58-59 m.y.B.P.) of the Berggren (1972) time scale (von der Borch, Sclater et al., 1974, p. 198). The site is located between two anomalies tentatively identified as 24 and 25 by Sclater and Fisher (1974). If these identifications are correct, they also give an age of about 58 m.y.B.P. according to the Sclater et al. (1974) time scale. The Heirtzler et al. (1968) time scale predicts an age of 61-62 m.y.B.P. I have assigned an age range of 58-63 m.y.B.P.

Site 216

The basalt section at site 216 consists primarily of units which are characterized by an oxidized, pale red, vesicular or scoriaceous top (Table V). The oxidized nature of these tops suggest that they may have been subaerially erupted. Ninety centimeters of loosely cemented tuff and two thin basalt units lie at the top of the section. Of the several units sampled, five are considered independent (Figure 4d).

All of the specimens had very stable directions, and those from the flows (?) with the scoriaceous tops were very tightly grouped. Two alteration zones, characterized by clearly visible weathering fronts, were sampled. These specimens showed no significant difference in their magnetic properties from the fresher appearing specimens. Sixteen groups of back to back specimens were taken, and all of them had concordant directions.

The oldest sediments at site 216 which are clearly dated (core 33) are placed in the uppermost Maastrichtian (N. frequens zone of Bukry, 1974; von der Borch, Sclater et al., 1974, p. 219) with an age of 65-67 m.y.B.P. A poorly preserved Maastrichtian assemblage was found in cores 34 and 35 which included an unidentified species of Nephrolithus (loc. cit.). Therefore an age bracket of 67-72 m.y.B.P. is assigned to the basalts to include the first five million years of the Maastrichtian.

Sediment Paleolatitudes

Paleolatitudes are calculated from the sediment data at various horizons at site 215, 216 and 217. The paleolatitudes for sites 216 and 217 show a consistent pattern of northward motion for the Ninetyeast Ridge. At

site 215, to the west of the ridge, the sediment paleolatitude is inconsistent with that of the underlying basalts as well as the results from the Ninetyeast Ridge (Figure 6). No reliable sediment paleolatitudes were measured at sites 213 or 214.

The paleolatitudes and their associated confidence intervals are calculated according to the method developed by Cox (in prep., 1976), as modified by Peirce (in press, 1976) for use with DSDP sediments. Using this method, each sample direction is considered to be an independent sampling of the geomagnetic secular variation. The size of the confidence interval is determined only by the modelled secular variation at the observed paleolatitude and by the number of samples. The dispersion of the observed directions is not considered because tightly grouped data are usually an indication of inadequate sampling of secular variation. On the other hand, a large amount of dispersion is probably indicative of bad data. Consequently, data are considered reliable only when there are sufficient samples to guarantee some averaging of secular variation and when the standard deviation of the observed inclinations is less than 10° (an empirical cutoff, from Peirce (in press, 1976)).

The paleolatitudes and their associated statistics are listed in Table VI. The cleaned directions of the individual specimens are listed in Appendix III, and the distributions of the uncorrected paleolatitudes at each horizon are plotted in Figure 5.

A total of 388 sediment samples were measured from DSDP sites 213, 214, 215, 216 and 217. Most of the specimens were drilled from indurated pieces of core, using a diamond rock drill. Relative declinations were preserved when several specimens came from the same piece of core. At sites 213, 215, and the uppermost horizons at sites 214, 216, and 217, specimens were taken using a DSDP plastic sample cutter inserted with a miniature piston core sampling device. The specimens were then capped in the plastic, top and bottom, with an epoxy which cured at room temperature. Measurements were made on the cryogenic magnetometers at the University of Texas (C.E. Helsley) and at the University of Rhode Island (N.D. Watkins).

Basal sediments were sampled at all the sites. Attempts to sample up core at younger horizons were made at all sites. However, suitable material undisturbed by the drilling process was not present up core at site 213 and 215, and it occurred only sparsely at site 214. The biostratigraphic

horizons which were sampled, the paleolatitudes and their associated statistics, and the assigned ages are listed in Table VI. The directions of individual samples are listed in Appendix III for those horizons at which paleolatitudes were calculated. The directional behavior and the normalized AF demagnetization curves for several representative pilot specimens are shown in Appendix IV.

Sixty-one pilot specimens were progressively AF demagnetized to determine proper cleaning fields. About half of the remaining specimens were cleaned only at either 100 oersteds or at 150 oersteds. Upon reduction of the data, it became apparent that many of these specimens might need further cleaning, and they were remeasured and then cleaned at higher fields after an interval of a few months. All of these specimens had acquired sufficient viscous remanent magnetization (VRM) in the intervening months to completely dominate the natural remanent magnetization (NRM). Only at site 215 could this secondary remanence be even partially removed before totally erasing the original direction. Many of these samples exhibited rapidly decaying magnetic components when they were placed in the field free region inside the magnetometer.

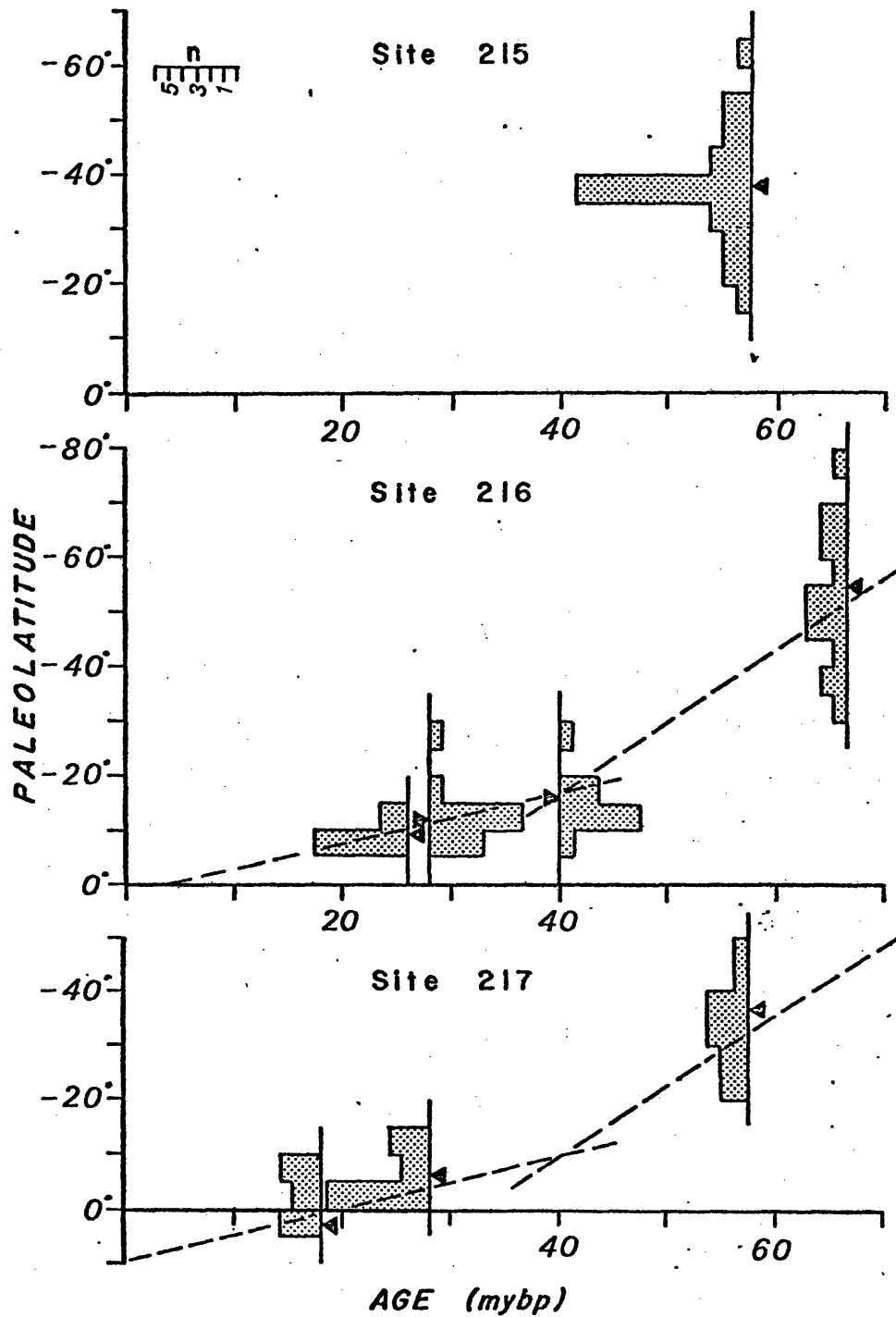
A second set of samples, acquired for more up core data at sites 216 and 217, were all measured at several

FIGURE 5

The uncorrected virtual geomagnetic latitudes of the sediment samples from sites 215, 216, and 217 are shown in histogram form. Each baseline is positioned according to age along the horizontal axis. Two histograms in the middle figure are inverted to avoid overlaps.

The triangles point to the corrected paleolatitudes given in Table 6. The dashed lines indicate the paleomotion of the site based on all the paleomagnetic data (see Figure 6).

UNCORRECTED PALEOLATITUDES OF SEDIMENT SPECIMENS



cleaning fields (100, 150 and 200 oersteds) within a few hours of their initial cleaning. None of these specimens exhibited behavior characteristic of a large VRM component.

From this experience, it appears that the process of partially demagnetizing a specimen in some way activates the magnetic domains and makes VRM easier to acquire than if no cleaning had occurred. Perhaps the cleaning process moves many domain walls into positions which are barely stable, and in the presence of an applied field these gradually move into more stable positions, aligning such domains in the direction of the applied field in the process. However, there appears to be a great deal of variability in the response of VRM to AF demagnetization (Dunlop, 1973). Lowrie and Kent (1976) observed the opposite effect in DSDP Leg XXXIV basalts. Thus these ideas must be considered speculative until supported by experimental data from several rock types.

I do not feel that VRM acquisition was a significant component in any of the cleaned measurements made soon after the original cleaning. All directions which were measured after a significant delay beyond the original cleaning were rejected as unreliable.

At many of the horizons sampled, the directions which were considered reliable (see discussion of acceptance criteria below) were too scattered or too few to compute a

paleolatitude. In most cases, scattered directions were observed in very weakly magnetized sediments ($< 1 \times 10^{-6}$ emu/cc). However, in core 8 of site 217, sediments with cleaned magnetizations $< 1 \times 10^{-7}$ emu/cc produced very stable, well grouped directions which were confirmed by frequent back to back sampling.

It is unclear why some sediments appear to be reliable paleomagnetic recorders, as characterized by coherent directions in a group of samples, while others of apparently similar lithology and magnetization are not reliable. I have made an attempt to make magnetic separates of several specimens using heavy liquids. These were examined under a scanning electron microscope fitted with an energy dispersive X-ray attachment to detect elemental composition, but the results were inconclusive.

Individual specimen directions were rejected as unreliable for several reasons. All specimen directions whose cleaned intensity was $< 1 \times 10^{-6}$ emu/cc were rejected unless that direction could be confirmed in both inclination and declination by a specimen sampled from the same indurated piece of core. This intensity cutoff is not a function of the cryogenic magnetometers, which have a practical sensitivity of about 1×10^{-8} emu/cc, but rather it is based on the empirical observation that most groups of specimens with such low magnetizations do not have well grouped directions. At only two horizons (cores 8 and 10,

site 217) was this poor grouping not observed. However, in those cases, every direction used in the paleolatitude calculation was confirmed by at least one other back to back specimen.

Specimen directions were rejected as unreliable when they did not stabilize to less than 10° angular change between successive demagnetization steps unless such a direction was confirmed by that from another back to back specimen. When only one cleaned direction was available, the 10° angular change criteria was not applied.

Paleolatitudes were calculated only when at least four samples at a given horizon met the direction acceptance criteria. Paleolatitudes based on less than eight directions are considered marginally reliable, and they are listed in parentheses in Table VI.

The ages assigned in Table VI are drawn from the site reports in von der Borch, Sclater et al. (1974), as well as the following shipboard and shore laboratory studies: nannofossils, Gartner (1974) and Bukry (1974); foraminifera, McGowran (1974) and Berggren (1974); and radiolaria, Johnson (1974). The absolute ages of the biostratigraphic horizons are those assigned by Berggren (1972). Generally, all the paleontologic

ages agree well except in the lower Oligocene where the radiolaria show discordant ages a few million years older than those from the nannofossils. In these cases, when both the nannofossil and foraminiferal ages are in agreement, I have used them. If no foraminiferal age was available (usually because of dissolution), I have assigned an age range including the nannofossil and the radiolarian ages.

Magnetic stability of sediments

The confidence intervals given in Table VI are a function of the number of samples and the observed paleolatitude. As such, they cannot reflect certain characteristics of a particular data set which may detract from its reliability as subjectively evaluated. Because such subjective assessments can provide an unquantifiable insight beyond that offered by the statistics in some cases, a brief discussion of the data quality is given below for each site.

Site 213:

The specimens all appeared to be stably magnetized. However, in the absence of observable bedding in the sampled part of the core, I interpret the tremendous scatter of inclinations as an indication of severe disturbance of the mud by the drilling process.

Site 214:

Most of the specimens above the basal section had weak magnetizations ($< 1 \times 10^{-6}$ emu/cc) and the inclinations were very scattered. One pilot specimen from the tuff in core 41 exhibited an extremely high median destructive field (MDF) which extrapolated to > 3000 oersteds. Its most stable inclination was 49.3° before thermal cleaning. The entire tuff behaved in an unstable manner when thermally demagnetized.

There were five specimens in the basal section which met the acceptance criteria. Four of these were paired back to back specimens. Four other back to back specimen directions were rejected because of discordant directions. In view of the high rejection percentage (58%) at this horizon and the inconsistency with the basalt paleolatitude, this paleolatitude is considered unreliable.

Site 215:

The directions from site 215 were stably magnetized and well grouped (see Appendices III and IV). There is no a priori reason to disbelieve this data. However, the measured paleolatitude is inconsistent with that from the basalts which are of similar age. Although the quality of

the basalt data is not high, and might be disregarded, the sediment paleolatitude also radically diverges from the more abundant data from the Ninetyeast Ridge if one assumes that there has been no relative motion between the site and the ridge. One possible explanation is that the paleolatitude is the result of chemical remanent magnetization (CRM) acquired about 10 m.y. after the sediment was deposited. As there is no other evidence to support relative motion between the site and the ridge or the existence of CRM to support such motion, the sediment paleolatitude remains a well defined but unexplained anomaly.

Site 216:

The magnetic stability of specimens from site 216 is quite variable from horizon to horizon. The demarcation between stable and unstable zones is usually quite clear, as for example between core sections 9-1 and 9-2, and also in core section 16-2 (Appendices III and IV). The calculated paleolatitudes are based on specimens which did not exhibit unstable behavior. They are self-consistent in the upper part of the hole. The basalt paleolatitude is 6° further south than the sediment paleolatitude, but there is good overlap of the 95% confidence intervals (Figure 7).

In core 16, two adjacent specimens (16-2-89 and 93) had NRM intensities more than two orders of magnitude greater than those of the adjacent specimens. I interpret this sharp intensity change as probably indicating an ash layer which is not visible. The coercivity of these two specimens (Appendix IV) reveals that over 80% of the total NRM was contained in a narrow coercivity band between 160 and 180 oersteds. One explanation for this unusually coherent coercivity distribution is that the remanance is contained in the particles of a very well sorted ash layer where all the magnetic grains are of the same size and mineralogy.

Site 217:

The entire section at Site 217 is calcareous and weakly magnetized. Very few specimens show a high degree of stability, and none of the paleolatitudes is considered to be of high quality. The paleolatitudes for zones N-5 and P-1 are based on only four samples out of much larger data sets which show generally poor stability. They are considered unreliable. The paleolatitudes for zones P-21 and P-11-12 are based on weakly magnetized material, and either may be in error. However, the directions at both horizons are based only on specimens oriented with respect to at least one other

specimen, and there is good correspondence between adjacent specimens. Therefore, they are interpreted as probably reliable. As the paleolatitude from zone P-11-12 is based on only six samples, it is considered less reliable than the one from P-21. Most of the specimens from zone P-4 have MDF's < 100 oersteds. The directions from back to back specimens are generally concordant, but one pair of discordant directions was observed. The P-4 paleolatitude is also interpreted as probably reliable.

Paleomotion of the Ninetyeast Ridge

The basalt paleolatitudes and the sediment paleolatitudes are combined into one graph of the paleomotion for the Ninetyeast Ridge in Figure 6. All the data shown in Figure 6 is "reduced" to site 216 by assuming that there has been no relative motion between the sites on the ridge and applying a correction to the paleolatitudes equal to the present latitude difference between the sites. Thus, the graph can be made applicable to any point on the ridge by the addition of an offset equal to the present latitude difference between that point and site 216.

These paleolatitudes indicate that the Ninetyeast Ridge and, by implication, the Indian plate were moving northward

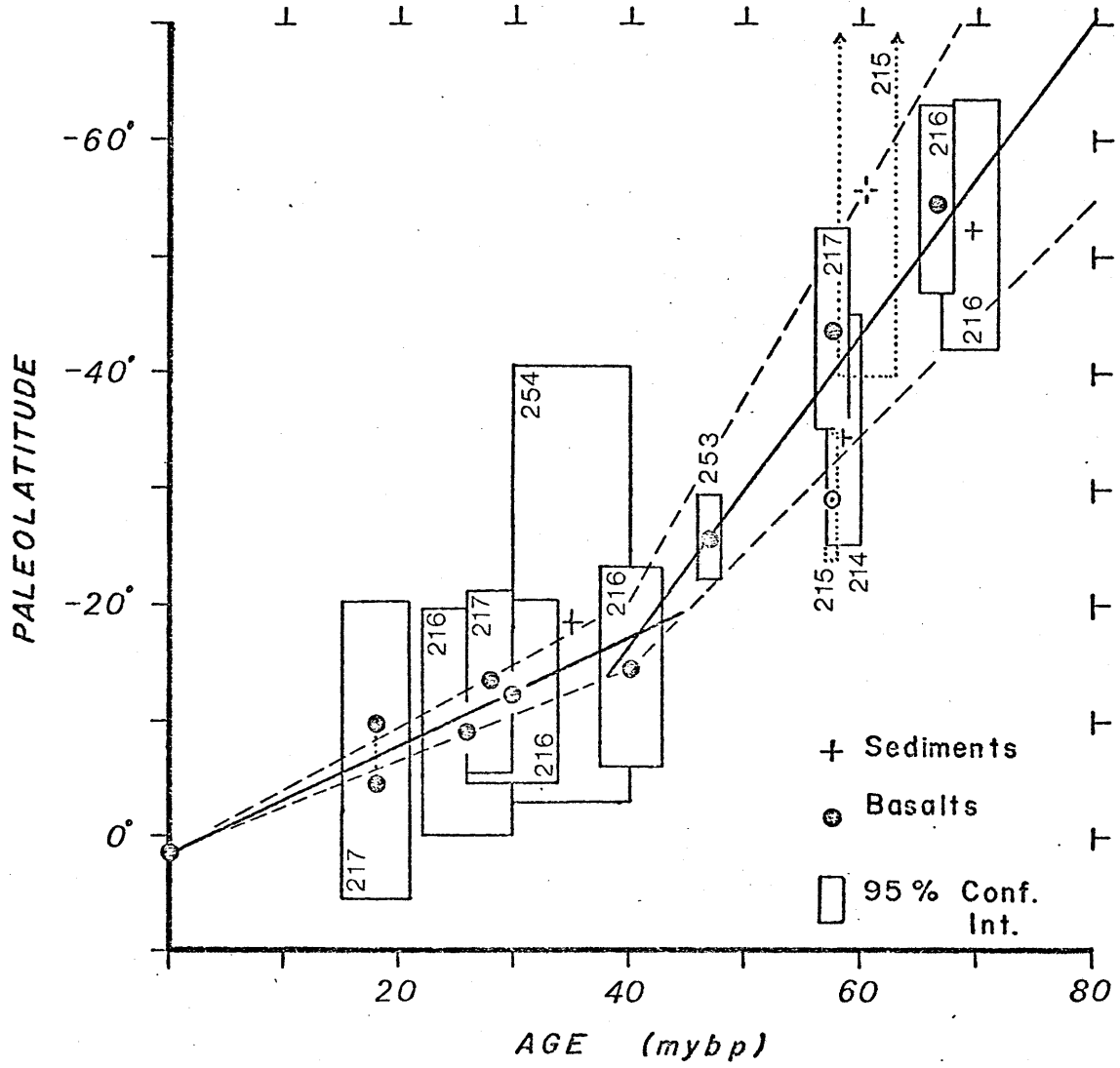
FIGURE 6

Paleomotion of DSDP Site 216 based on paleolatitudes from all the sites on the Ninetyeast Ridge. Boxes indicate the 95% confidence intervals of each paleolatitude and the best estimate of the associated age. Crosses indicate basalt data; solid circles indicate sediment data; and numbers indicate the site. Only paleolatitudes based on at least eight samples are plotted.

For sites other than 216, a correction equal to the present latitude difference from Site 216 was applied. Site 215 data are not consistent with those from the Ninetyeast Ridge sites and they have been dotted in. The solid lines indicate

rates of northward motion of India obtained by weighted least squares linear regression. The dashed lines indicate the 95% confidence region for the position of Site 216, assuming Student t-statistics apply to the rates of motion. The calculated rates are: 0-40 mybp, $5.2 \pm .8$ cm/yr (N = 6, through the origin); and 40 - 70 mybp, 14.9 ± 4.5 cm/yr (N = 6).

PALEOMOTION OF DSDP SITE 216



with respect to the south pole at 14.9 ± 4.5 cm/yr from 70 to 40 mybp. At about 40 mybp the rate of the northward flight slowed to $5.2 (\pm .8)$ cm/yr. This slowing was most likely a rapid but smooth deceleration, not the abrupt change obtained by the linear regressions in Figure 6. This slowing of India roughly coincides with the time of spreading reorganization in the Indian Ocean and the beginning of the collision of the Indian subcontinent and Eurasia (Molnar and Tapponnier, 1975).

The rates of absolute northward motion of India derived from the paleomagnetic data are in excellent agreement with the relative rate of closing between Asia and India calculated by Molnar and Tapponnier (1975). Using the assumption that Eurasia had negligible absolute motion, they calculated relative closing rates of 10.0-18.4 cm/yr between Eurasia and India for the first time period 80-38 mybp. (The range of linear rates is due to the different distances of parts of India from the pole of rotation.) After 38 mybp, their calculated rate is 4.5-6.4 cm/yr. This correlation between the rates of relative and absolute motion implies that the pole of relative motion for Eurasia/India and the pole of absolute motion for India were nearly coincident during this time. Implicit in this coincidence is the conclusion that India had no significant

longitudinal component of absolute motion. Such a component is undetectable by paleomagnetic techniques. The implication of coincident poles is valid only to the extent that the assumption of a nearly stationary Eurasia is correct. However, it is an important point to which I shall return in the discussion of the origin of the Ninetyeast Ridge.

The DSDP data can be compared to the Indian continental paleomagnetic data by correcting for any relative motion or rotation between the Ninetyeast Ridge and the continental sites. Paleolatitudes calculated from the paleomagnetic pole positions for the Deccan Traps (McElhinny, 1973; Molnar and Francheteau, 1975a) lie very close to the best fit line through the Ninetyeast Ridge data (Figure 7). On the other hand, the lower Siwalik beds of Miocene age indicate a more southerly paleolatitude (Wensink, 1972a,b) than the DSDP data yield. However, the Siwaliks are in a tectonically complicated area and there is some doubt as to the validity of that pole for India (Hall, personal communication, 1976).

The paleomagnetic data from Australia are extensive and well-documented (McElhinny et al., 1974). One can use the Australian paleomagnetic poles to predict the motion of site 216 by removing the relative motion components (as

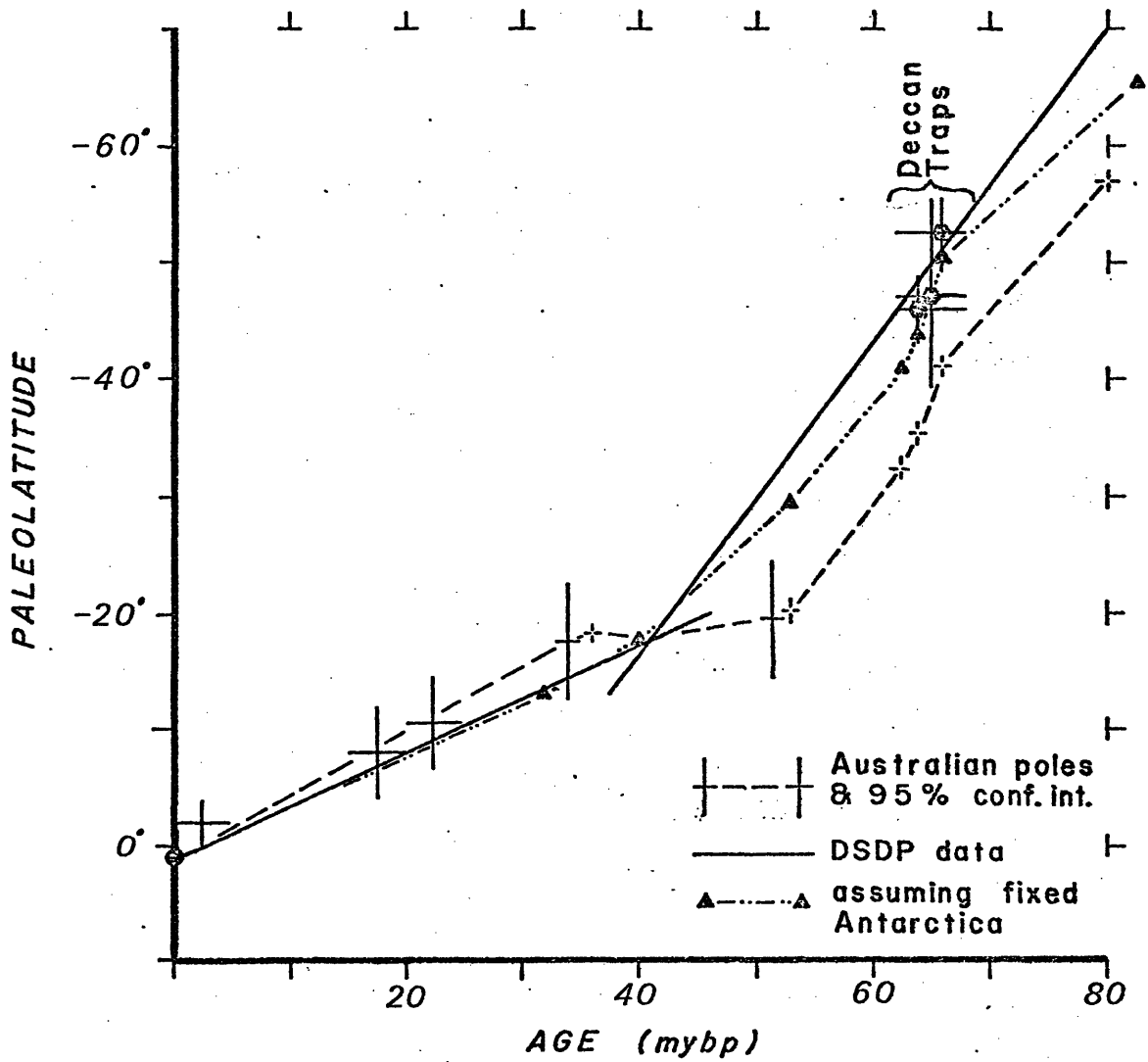
FIGURE 7

Estimates of the paleomotion of DSDP Site 216 using different assumptions. The solid lines indicate the rates determined in Figure 6. The triangles show the positions of Site 216 assuming that Antarctica has remained fixed and using the India/Antarctica poles of relative motion from Table 7. The crosses show the positions of the site based on Australian paleomagnetic data and using the poles of relative motion for India/Antarctica and Australia/Antarctica from Table 7. The size of the crosses indicate the accuracy of the Australian data. The small dashed crosses indicate ages where paleomagnetic poles were inferred from the apparent polar wandering path

for Australia (McElhinney et al., 1974). Also shown are positions of Site 216 based on three paleomagnetic poles from the Deccan Traps (poles 11.1-11.3, McElhinney, 1973; age 65 mybp, Molnar and Francheteau, 1975b).

Note the discrepancy between the positions of Site 216 indicated by the Australian and Indian plate data sets prior to 40 mybp.

ESTIMATES OF THE PALEOMOTION OF DSDP SITE 216



estimated from magnetic anomalies), much as Sclater and Fisher (1974) did in their reconstruction maps. To do this for a given age one rotates site 216 (India) back to its position relative to Antarctica, Antarctica (and India) back to its position relative to Australia, and Australia (and Antarctica and India) back to its position relative to the south pole. Mathematically, this rotation is expressed as

$$-(\omega_{216 \text{ Ant}} + \omega_{\text{Ant Aus}} + \omega_{\text{Aus S. Pole}}) = \omega_{\text{S. Pole 216}}$$

The results of such rotations for the ages corresponding to the Australian paleomagnetic poles are plotted on Figure 7. Note that the indicated rate of motion for India 70 mybp is the same as is indicated by the DSDP data, but the paleolatitudes disagree by 13°. Furthermore, using this method suggests that the northward motion of India came to an abrupt halt at about 51 mybp before resuming again 17 million years later at a rate approximately equal to the measured rate. The directly measured motion of India (DSDP data) is less complicated.

The source of this discrepancy must lie either in the paleomagnetic data or in the relative motion estimates for India/Antarctica and Australia/Antarctica. As both sets of

paleomagnetic data are self-consistent and well defined, and as the Australia/Antarctica motion seems relatively straightforward (Weissel and Hayes, 1972), the logical place to look for an error is in the more complicated Indian/Antarctic relative motion (Sclater and Fisher, 1974; Schlich, 1975).

As a way of checking this possibility, I assumed that the Antarctic plate has remained fixed with respect to the South Pole, and then I calculated the paleomotion of site 216 by rotating India back to Australia using Sclater and Fisher's (1974) poles of rotation. The results (Figure 7) show good agreement with the measured paleolatitudes, and, most importantly, they do not show the break in motion which was indicated by using Australia as the reference point.

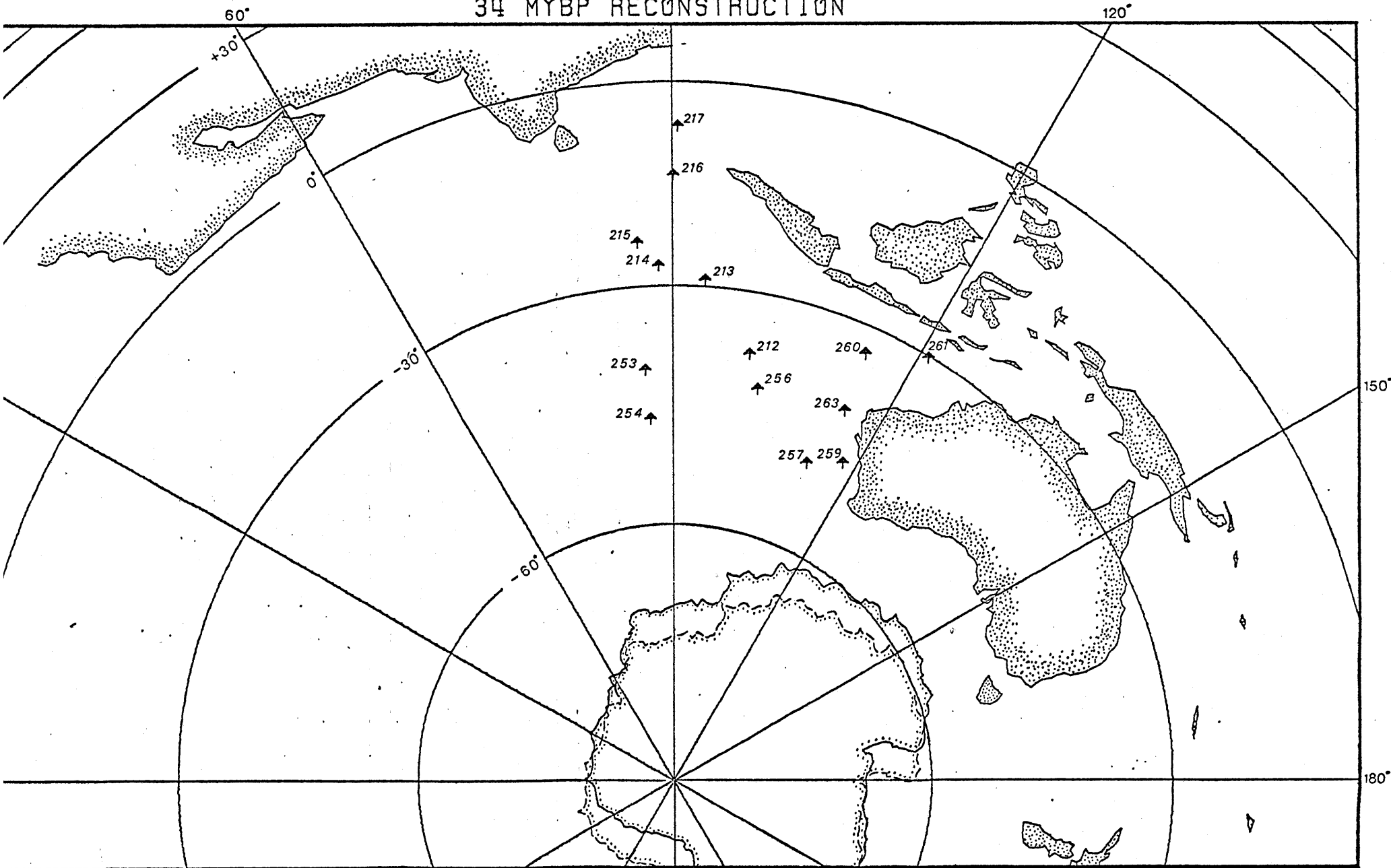
We are left in a quandry: the position of the Antarctic plate as defined by its motion with respect to India and the absolute motion of India does not agree with its position as defined by the motion of Antarctica with respect to Australia and the absolute motion of Australia. The scale of the mismatch is demonstrated in Figures 8a and 8b. Here I have assumed that all the errors in matching are the positions of Antarctica, and its positions are plotted with respect to India and to Australia for 34 MYBP and 51.5 MYBP. The match

FIGURES 8a AND 8b

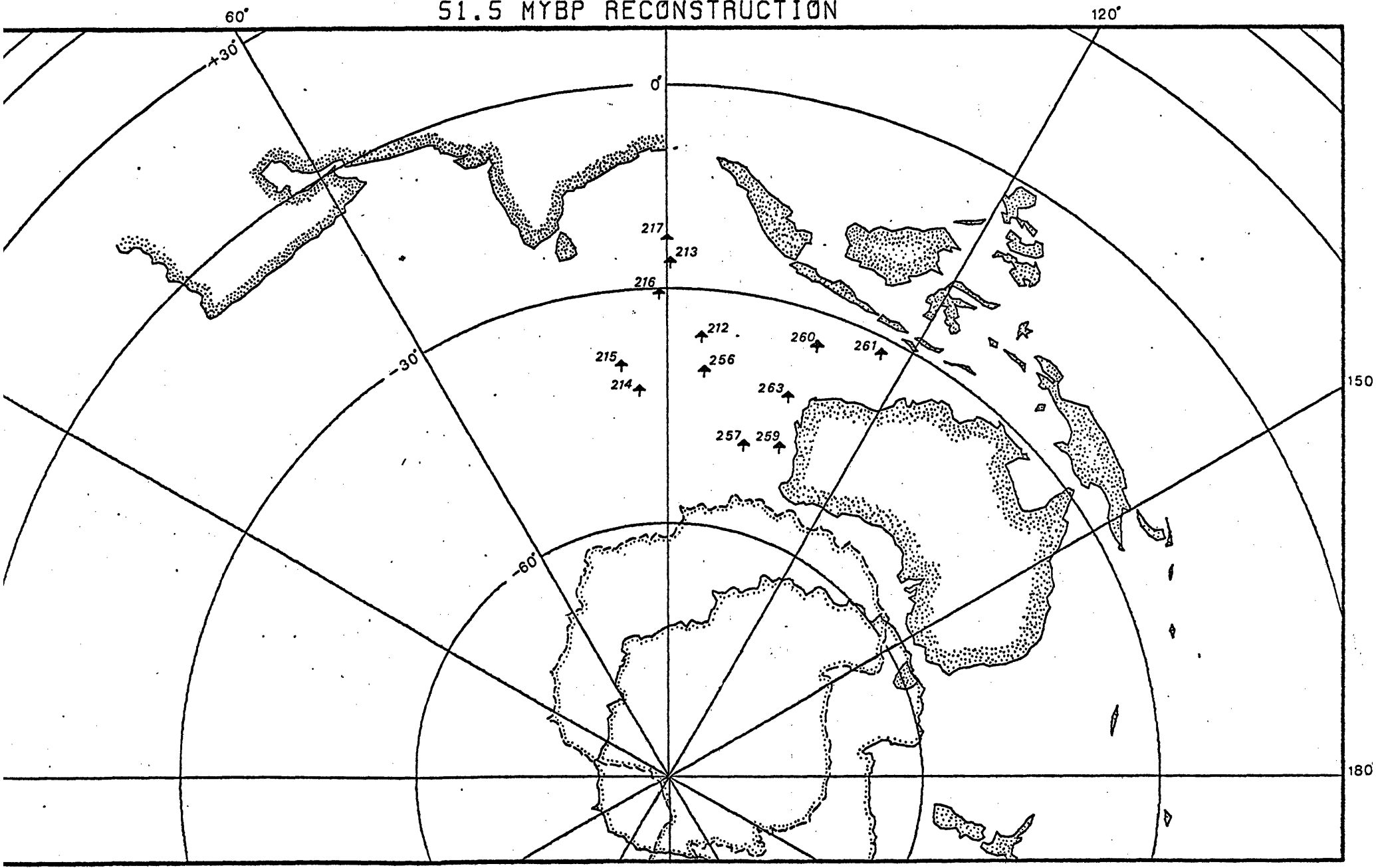
Reconstructions of the Indian Ocean for 34 and 51.5 mybp. The position of India and the DSDP sites on the Ninetyeast Ridge relative to the South Pole were computed from the paleomotion curve for Site 216 in Figure 6. The positions of Australia and the remaining DSDP sites were computed from the Australian paleomagnetic data (McElhinney et al. 1974).

Two positions are shown for Antarctica to demonstrate the magnitude of the discrepancy noted in Figure 7. The solid outlines are the positions using the Ninetyeast Ridge paleomagnetic data and the relative motion poles from Table 7. The dashed outlines are the positions using the Australian paleomagnetic data and the poles from Table 7. The projections are Lambert equal area, centered at the South Pole.

34 MYBP RECONSTRUCTION



51.5 MYBP RECONSTRUCTION



of the positions is fairly close at 34 MYBP and it is terrible at 51.5 MYBP. There are undoubtedly some errors in the paleomagnetic data, but it is unlikely that these could account for more than about 5° of mismatch.

More than one paleomagnetic pole must be in error to resolve the discrepancy, and the errors must all be in the same direction. As all of the error occurs between 40 and 50 mybp and as the indicated rates of paleomotion prior to that time are the same for both data sets, it seems most likely that the error lies in the estimates of the relative motions of the three plates involved. Additional relative motion between India and Antarctica during this time would neatly resolve the discrepancy. However, the key magnetic anomalies are clearly identifiable, and no reasonable interpretation allows this simple solution to the problem.

Skewness of Magnetic Anomalies

One potential means of checking on the DSDP paleolatitudes is to estimate the skewness of the magnetic anomalies and then compute a lune of possible paleomagnetic pole positions (Schouten and Cande, 1976). Implicit in the use of this method for the Ninetyeast Ridge is the assumption that there is a negligible difference in the

ages and the original latitudes between the Ninetyeast Ridge sites and the anomalies to the west on the Indian plate. All the tracks used for picking the skewness of anomalies run nearly north/south, and the anomalies strike $N95^{\circ}E$. The quantity of suitable tracks is low, and the variability of the measured skewnesses is usually $10-20^{\circ}$ and occasionally more (see Appendix V). Both of these factors contribute to the widths of the lunes plotted in figures 9-11.

The edge of the lune for anomalies 22-26 (Figure 9a) intersects the small circles of possible pole positions defined by the Ninetyeast Ridge paleomagnetic data, but the width of the lune is such that it provides no further constraint on the paleolatitude.

There are two wide lunes for anomalies 25-33 (Figure 9b). The intersection of these lunes corresponds well with the paleomagnetic data, but again the width of the lunes precludes further constraint of the paleolatitude. Furthermore, Sclater and Fisher (1974) estimated an $8-9^{\circ}$ left lateral offset along the 86° fracture zone (which lies between some of the anomalies and the Ninetyeast Ridge), and no allowance has been made for any offset in Figure 10.

FIGURE 9

Lunes of confidence for the possible positions of paleomagnetic poles for the plates and ages shown, calculated using the method of Cande (1976).

(a) Based on tracks CIRCE 5 A and B and VEMA 19 A (see Figure 11 and Appendix V). $\theta = 69.2^\circ \pm 13.4$ (two standard deviations, $N = 13$). The lune is compared to the small circles of possible pole positions defined by the paleomotion curve for Site 216 from Figure 6. The width of the small circles is based only on the age range of the anomalies for which the lune has been calculated. The error range of the paleomagnetic data has not been included.

(b) One lune based on track CIRCE 5 A.

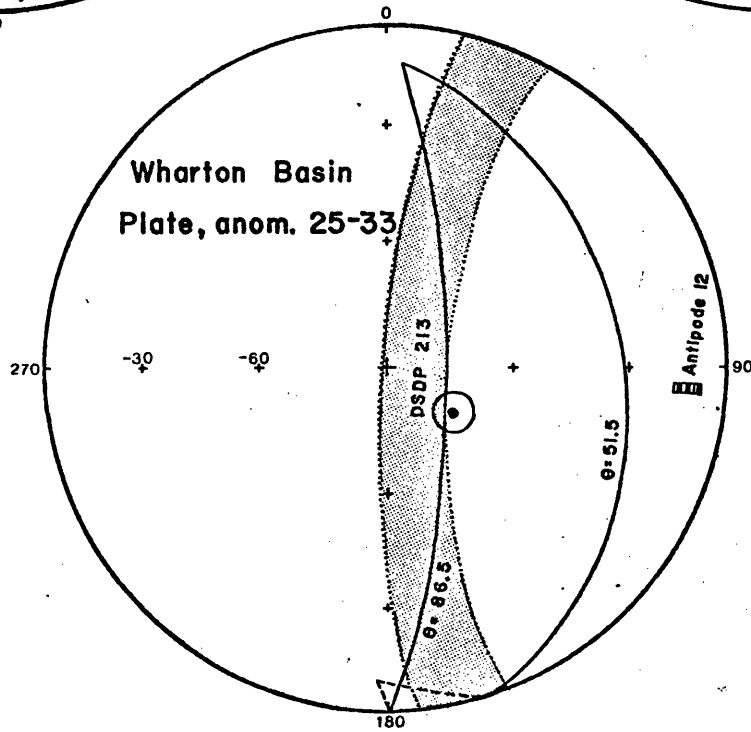
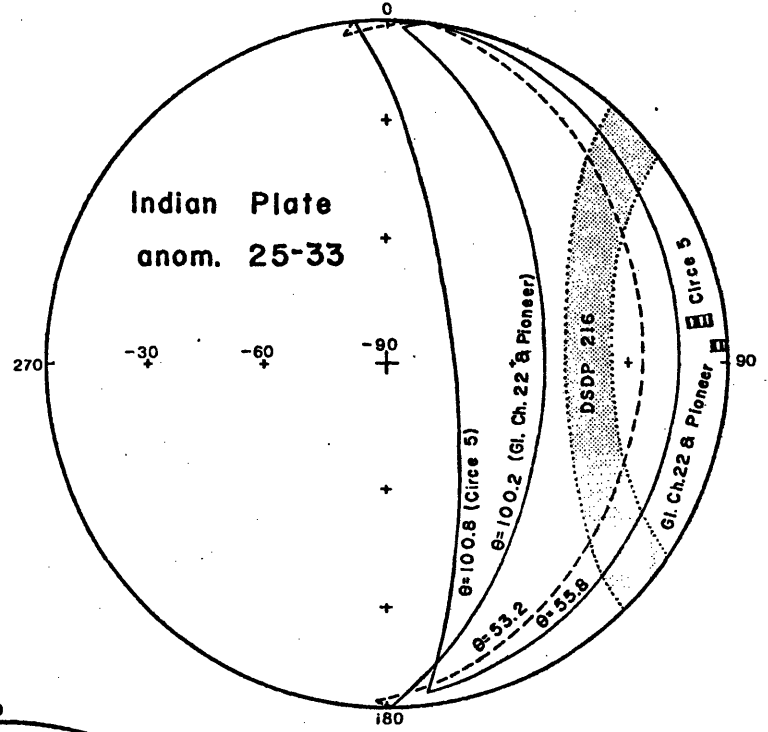
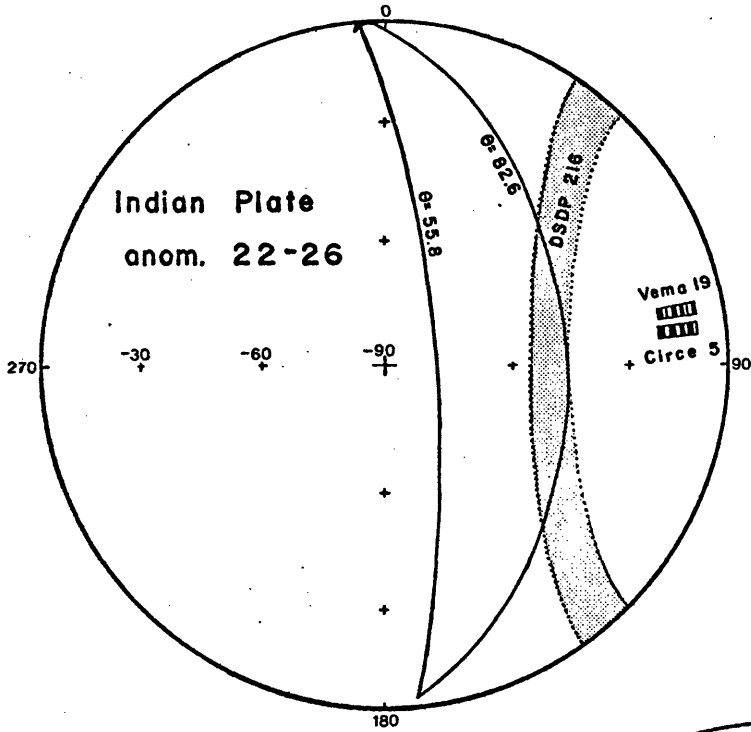
$\theta = 78.3^\circ \pm 22.5$ (N = 7). Second lune based on tracks GLOMAR CHALLENGER 22 and PIONEER B.

$\theta = 76.7^\circ \pm 23.5$ (N = 9, dashed edge on far hemisphere). The comparison with Site 216 is the same as in (a), except that it is for a different age range.

(c) Based on tracks ANTIPODE 12 A and B.

$\theta = 69.5^\circ \pm 17.5$ (N = 10). The lune is compared with the small circles of possible pole positions defined by the 95% confidence intervals of the basalt paleolatitude for DSDP Site 213 (Table 1). Also shown is the paleomagnetic pole for Barrington volcano (51.5 mybp) (McElhinney et al., 1974), which is the Australian paleomagnetic pole nearest in age to the anomalies in question.

LUNES OF CONFIDENCE FOR PALEOLATITUDES



To the east of the Ninetyeast Ridge, the skewness of anomalies 25-33 define another wide lune. When compared to the DSDP data for the Wharton Basin (Figure 9c), the two estimates of paleopole positions do not overlap. As an additional point of comparison, the Australian paleomagnetic pole of that age is plotted, and it lies between the two estimates. This comparison is weak evidence contradicting the suggestion that there may have been left lateral motion between the Wharton Basin and Australia since the Cretaceous (Peirce, in press, 1976).

As the data for each of these lunes comes from only one limb of the spreading center, there is no way of estimating any anomalous skewness. When a deskewed anomaly has a different phase shift angle, θ , than the same anomaly has when it is reduced to the pole ($\theta = 0^\circ$), the difference is called anomalous skewness. Cande (1976) has found such anomalous skewness in anomalies 27-32 in the southwest Pacific, and he suggests that it is caused by geomagnetic field behavior. If this is the case, then the sign of the skewness anomaly can be predicted if one knows the age gradient of the anomalies. In the cases cited here, the presence of any anomalous skewness would move the lunes away from the magnetic anomalies (towards the center of the figure)

for those anomalies west of the Ninetyeast Ridge, and it would move the lunes towards the anomalies for those east of the ridge because the age gradient is opposite to that west of the ridge.

Anomaly Identification

The discussion of Indian Ocean tectonics at the beginning of this paper was based primarily on the anomaly identifications of Sclater and Fisher (1974). Deskewing the anomalies removes the distortions from their shapes and makes them easier to identify. The deskewed anomalies used for this study are plotted along track in figure 10. The observed data are presented in the same format by Sclater and Fisher (1974) for all the tracks except PIONEER 1964. My identifications of these anomalies generally agree with those of Sclater and Fisher (1974), and they confirm the overall pattern of spreading rate changes postulated by them.

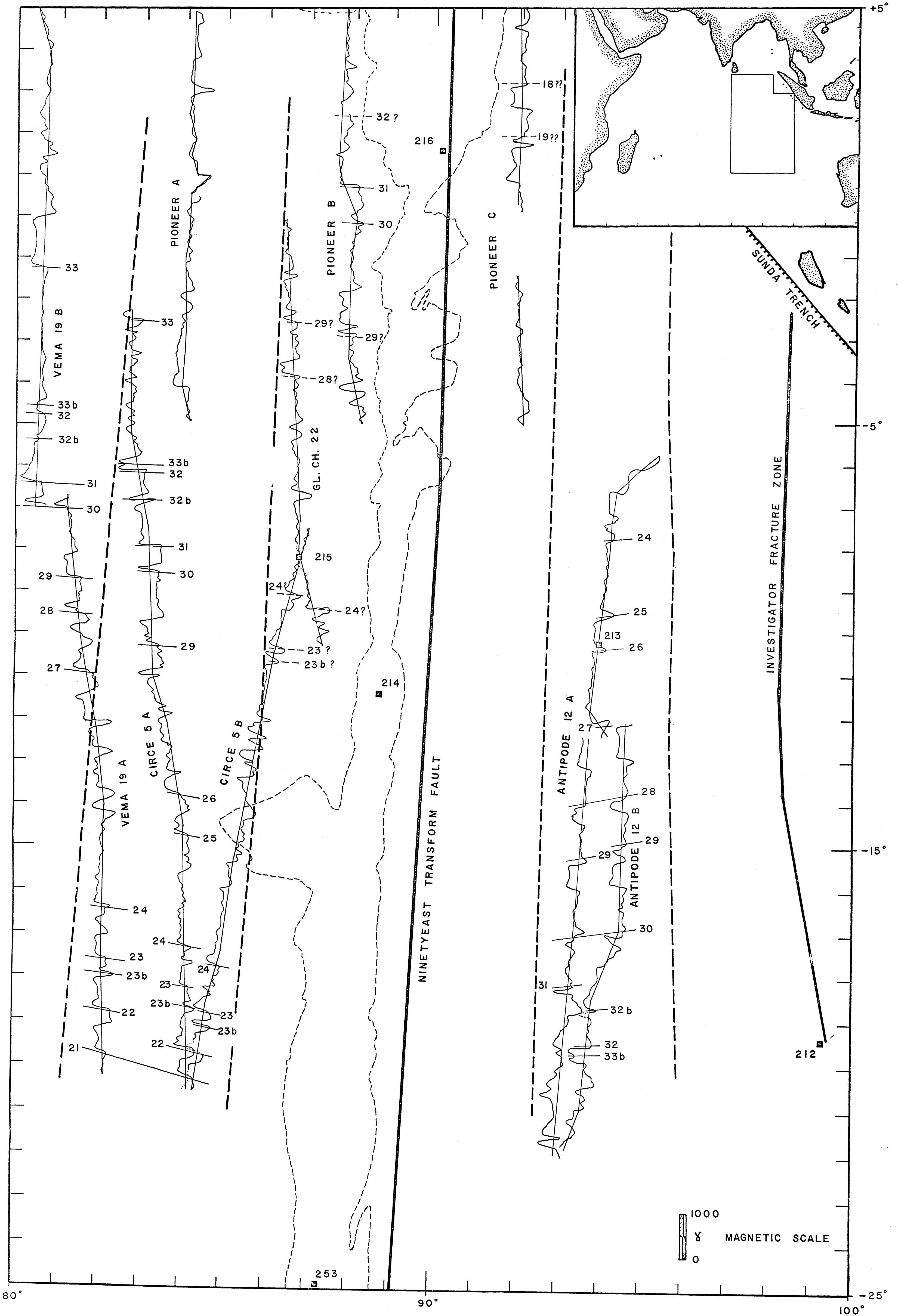
The PIONEER 1964 track confirms the previous tentative identification of anomaly 30 (Sclater and Fisher, 1974) between 86°E and 90°E , and it clearly establishes the existence of an $8-9^{\circ}$ left lateral offset on the 86°E fracture zone for that age. Throughout all the profiles west of the

FIGURE 10

Deskewed magnetic anomalies in the east central Indian Ocean, plotted perpendicular to track. The straight lines are the approximate ship tracks. Representative phaseshifts were chosen for each data set; plots of several different phaseshifts and the original data are included in Appendix V.

Phaseshifts used: ANTIPODE 12 A, -65° ; ANTIPODE 12 B, -60° ; CIRCE 5 A, -75° ; CIRCE 5 B, -70° ; GLOMAR CHALLENGER 22, -80° ; PIONEER A and B, -80° ; PIONEER C, -90° ; VEMA 19 A, -70° ; VEMA 19 B, -80° .

DESKEWED MAGNETIC ANOMALIES



Ninetyeast Ridge, the time between anomalies 24 and 30 is marked by poorly correlatable anomalies. In the slice of crust between 86°E and 90°E the record is by no means straightforward, and it consists of basically one track. Nevertheless, I agree with Sclater and Fisher's (1974) tentative identification of anomaly 24 there, primarily on the basis of its position with respect to anomaly 30. Furthermore, I tentatively identify anomaly 23 on the CIRCE 5 track just to the south (Fig. 10).

If these tentative identifications are correct, then the 11° of extra crust between 86°E and the ridge must lie south of site 214. Unfortunately, only east-west tracks cross this area. Sclater et al. (1976) identified anomalies 18-22 in the area just north and west of site 253. Although I feel that these anomaly identifications were made on extremely tenuous grounds, the possibility exists that between 11° and 22°S there is a captured portion of the Antarctic plate. However, it is more likely, in my opinion, that some of these tentative anomaly identifications are wrong and that the 11° of extra crust has been broken up into small pieces by a series of small ridge jumps.

To the east of the Ninetyeast Ridge, the PIONEER 1964 data add coverage between the ridge and 93°E . North of the

Equator the anomalies seem clear and distinct. These might be anomalies 18-20, but the track is short and these identifications should be regarded as very tenuous. South of the Equator, the anomalies seem quite different in character and they seem indistinct. Unfortunately, the ship was diverted for a station in the transition between the two anomaly types.

Previous Ninetyeast Ridge Models and Their Predicted Paleolatitudes

There are three models for the origin of the Ninetyeast Ridge which are compatible with the existing data. They are, in chronological order, the hotspot model (Morgan, 1972a, 1972b), the migrating spreading center-transform fault junction model (Sclater and Fisher, 1974), and the two hotspot model (Rennick and Luyendyk, 1975; Luyendyk and Rennick, in press, 1976). Basically, the differences are that the hotspot model predicts a fixed (or nearly fixed) paleolatitude for the basement rocks along the length of the ridge. The migrating spreading center-transform junction model assumes that the position of the spreading center is free to migrate in latitude (and longitude) to keep itself in a median position between India and Antarctica. The two hotspot model assumes that the spreading

center is free to migrate and that it is independent of the position of the Amsterdam-St. Paul (AMSP) and Kerguelen (KER) hotspots. It considers the effects of the plate boundary passing back and forth over this pair of hotspots. The predicted paleolatitudes of each model are discussed in detail below.

1. Migrating spreading center-transform junction model.

According to the model developed by Sclater and Fisher (1974) on the basis of magnetic anomaly reconstructions (Figures 2 and 3), site 217 formed at about 55°S some 80 mybp. As the spreading system moved north site 216 was formed at about 40°S about 57 mybp. Around 58-63 mybp, when site 216 was near 30°S, site 215 formed west of the Ninetyeast Ridge near 40°S, and site 213, east of the ridge, formed near 30°S. Shortly thereafter, site 214 formed on the ridge near 35°S. Thus the difference in the paleolatitudes at the bottom of holes 213 and 214 should indicate the length of the Ninetyeast transform fault before the spreading center immediately west of the Ninetyeast Ridge jumped or migrated 11° to the south at about 53 mybp. The combination of the southerly jump of the spreading center and the southward motion of the Antarctic

plate during the next few million years means that site 253 (age 46-51 mybp) must have formed near 45°S, further south than either 214 or 216. Site 254 (age 30-40 mybp) should have formed still further south near 50°S if the Sclater and Fisher (1974) model were correct (Figure 8). A shortcoming of this model was that one would expect some of the excess volcanics to accumulate on the Antarctic plate and form a "mirror image" ridge. At the time the model was proposed no such ridge was suggested (but see model 3 below).

2. Hotspot model.

On the other hand, if Morgan's (1972a, 1972b) hypothesis were correct, namely that the Ninetyeast Ridge formed by a deep seated hotspot fixed with respect to the Earth's spin axis, then the DSDP site paleolatitudes from the Ninetyeast Ridge should be all the same. If the hotspot were not absolutely fixed, but instead had moved slowly (say 1 cm/yr) with respect to the spin axis, then the ridge paleolatitudes should show a slow steady change with age. Over a time span of forty million years, 1 cm/yr of hotspot motion would produce no more than 4° change in paleolatitude. Thus, this model predicts that all the basement paleolatitudes for sites on the Ninetyeast Ridge should lie near 40°S if the

Amsterdam-St. Paul hotspot formed the ridge, or near 50°S if the Kerguelen hotspot formed the ridge.

This model, as originally presented, did not predict any age relationship between the Ninetyeast Ridge and the adjacent Indian plate to which it is attached. The results of DSDP Legs 22 and 26 (von der Borch, Sclater et al., 1974; Davies, Luyendyk et al., 1974) showed that the ridge is of very nearly the same age as the ocean crust just to the west. A further shortcoming is that it offers no explanation for the curious coincidence of the strikes of the Ninetyeast Ridge and of the Ninetyeast Transform Fault. This second point is not inconsistent with the hotspot model, it is merely an unlikely coincidence. Bowin (1973) attempted to explain this suggested that the volcanic source was not deep seated in the mantle but was in some way being carried along with India, but at a slower rate.

3. Two hotspot model.

Luyendyk and Rennick (in press, 1976) and Rennick and Luyendyk (1975) favor a two hotspot model for the origin of the ridge to overcome the shortcomings of the earlier ones. The model considers the effects of a spreading system migrating northwards towards the Kerguelen and Amsterdam/

St. Paul hotspots, passing over Kerguelen, then jumping south of it when the 11° ridge jump occurred (Sclater and Fisher, 1974), and finally passing northwards over it once again. It predicts that basement formed near 40° at sites 216 and 217, and that it formed near 50° S at sites 253 and 254. The predicted paleolatitude of site 214 is ambiguous, between 40° S and 50° S, because the site may have formed during the 11° ridge jump in their interpretation.

They showed that the Kerguelen-Gaussberg Ridge on the Antarctic plate is the "mirror image" ridge to the Ninetyeast Ridge if the Ninetyeast Ridge is assumed to be a hotspot trace. Broken Ridge, now on the Australian plate, was once part of the Kerguelen-Gaussberg complex. This finding overcomes the previous objection to the migrating spreading center-transform junction model, but it requires the assumption of a contradictory model to do it! The two hotspot model explains the age correlation between the Ninetyeast Ridge and the Indian plate because one or the other hotspot is always near the spreading center. Luyendyk and Rennick (in press, 1976) explain the coincident strike of the hotspot traces and the fault by postulating that the spreading pattern was constrained to follow the line between

the two hotspots. This presumed line of weakness has the same strike as those of the Ninetyeast Ridge and the Ninetyeast Transform Fault.

The predicted paleolatitudes are compared with the measured basal paleolatitudes in Figure 11. The only model which fits the measured paleolatitudes is the Kerguelen hotspot model. It is the only model which predicts a paleolatitude near 50°S for site 216. As the basalt and sediment paleolatitudes have 95% confidence intervals which lie wholly south of 40°S, this is strong evidence in favor of the Kerguelen hotspot model. The other basement paleolatitudes on the Ninetyeast Ridge also lie near 50°S. Thus these data indicate that the volcanic source of the Ninetyeast Ridge was fixed, or nearly fixed in latitude for 30-40 million years.

Implications for the origin of the Ninetyeast Ridge

The paleomagnetic evidence strongly supports the hypothesis that the Kerguelen hotspot was the source of the Ninetyeast Ridge. What other geologic and geophysical evidence can be cited which is relevant to the fixed volcanic source idea? In the discussion below I will show that none of the available geologic and geophysical data

contradicts the hotspot model as it was originally proposed by Morgan (1972a, 1972b). There is room for other interpretations, but it is this model which best satisfies all of the available data.

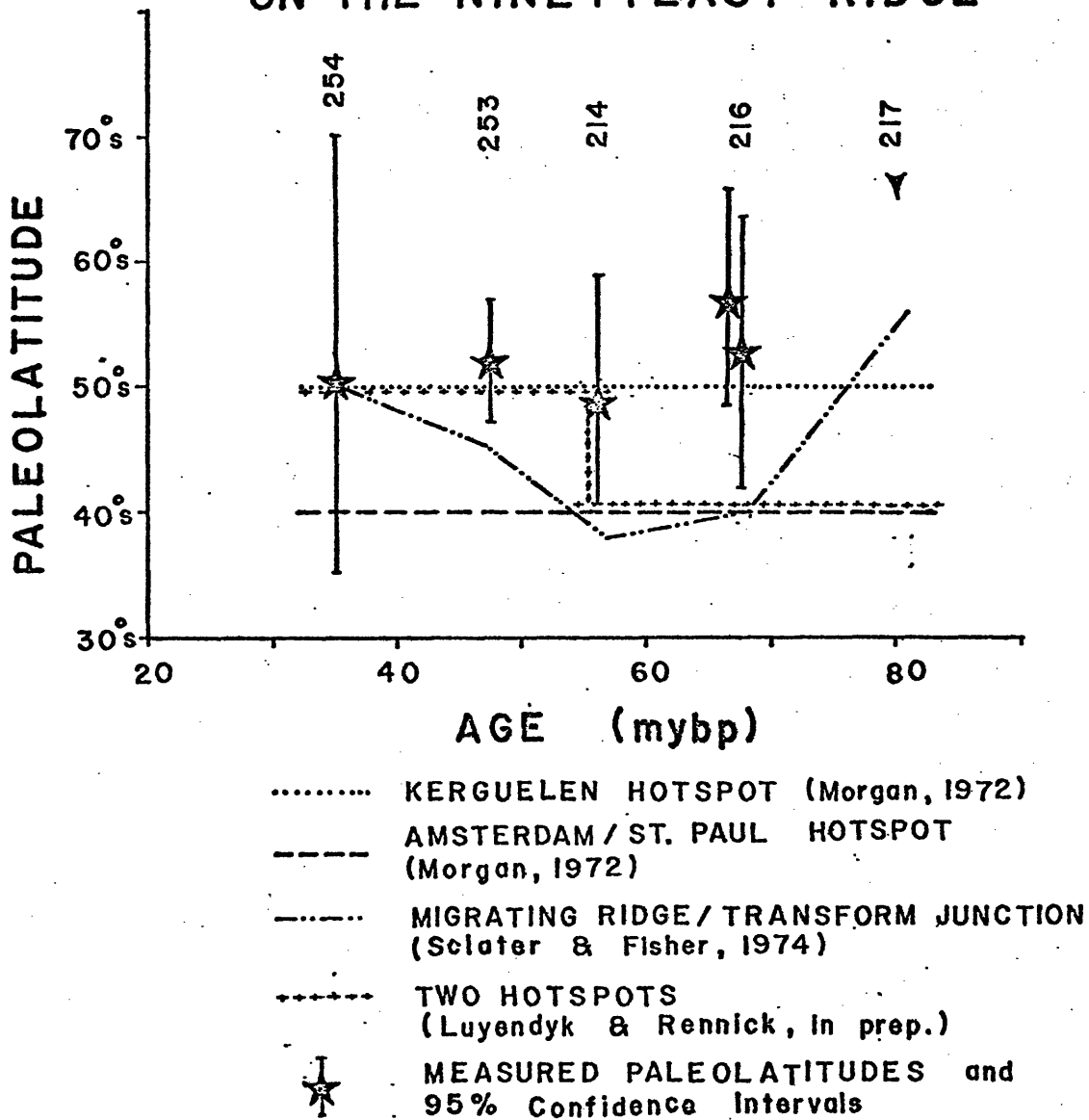
A large number of authors have worked on the petrology and the geochemistry of the Ninetyeast Ridge rocks (Hekinian, 1974a, 1974b; Frey and Sung, 1974; Kempe, 1974; Thompson et al., 1974; and Frey et al., in press, 1976). At the three sites with significant basalt recovery (214, 216 and 254), the basalts were generally enriched with large ion lithophile elements such as Ba, K, Hf, Sr and Zr. They also showed a negative slope in the rare earth pattern, indicating enrichment of the lighter rare earths (Frey and Sung, 1974; Fleet and Kempe, 1974), although this pattern was not universal (Frey et al., in press, 1976). The overall suite of rock types indicated a similarity between the petrogenic processes under oceanic islands and a dissimilarity with "normal" mid-ocean ridge processes (Frey and Sung, 1974), indicating an affinity with the rocks from other hypothesized hotspot traces.

Because the Ninetyeast Ridge has a free air gravity anomaly near zero and no major flanking faults to the west, Bowin (1973) argued that the ridge has always been nearly

FIGURE 11

Comparison of the measured and predicted basal paleolatitudes at the DSDP sites on the Ninetyeast Ridge. The measured paleolatitudes and 95% confidence intervals (Tables 1 and 6) are shown by the stars and error bars. No basement paleolatitude is available for Site 217. The paleolatitudes predicted by various models discussed in the text are shown by the indicated symbols. Note that all the basal paleolatitudes lie near 50°S and that only the Kerguelen hotspot model predicts all of them.

COMPARISON OF MEASURED AND PREDICTED PALEOLATITUDES ON THE NINETYEAST RIDGE



in isostatic equilibrium. In order to accomplish this and to provide the 7-8 km/sec material detected by seismic refraction (Francis and Raitt, 1967), he proposed that a mixture of gabbro and serpentized peridotite was emplaced at depth at the same time the volcanic pile was being built near sea level. Such high velocity rocks could provide both the isostatic compensation required by the gravity data and the observed uplift. He favored a modification of Morgan's (1972a, 1972b) hotspot model as the mechanism to accomplish this emplacement.

Much of the geology, paleontology, and palynology of the Ninetyeast Ridge indicates that it was once near or above sea level, as discussed above. As the topography of the ridge roughly follows the shape of the age-depth curve (Sclater et al., 1971) for oceanic basins, it is reasonable to suppose that the basement at the Ninetyeast Ridge drill sites was formed very close to an active spreading center. If the Ninetyeast Ridge is a hotspot trace and if it is slightly younger than the Indian plate to the west, then there should be no "mirror image" ridge on the Antarctic plate, unless there are two hotspots, as proposed by Luyendyk and Rennick (in press, 1976). On the other hand, if it is exactly the same age as the Indian plate, that

indicates that it formed at the Indian-Antarctic plate boundary, and there should be a complimentary ridge on the Antarctic plate. The available data cannot resolve this age question.

Luyendyk and Rennick (in press, 1976) showed that a "mirror image" ridge does exist. They did reconstructions of the Indian Ocean using marine magnetic anomalies and the Australian paleomagnetic data in a manner very similar to that of Sclater and Fisher (1974). They assumed that the Ninetyeast Ridge was a hotspot trace, and therefore they constrained the longitude of their reconstructions to keep the Amsterdam-St. Paul hotspot under the Ninetyeast Ridge until 53 m.y.B.P. Because the trace of the Ninetyeast Ridge can be approximated by an equatorial pole of rotation, a corollary to this assumption is that India has experienced no absolute longitudinal rotation. The most important result of their work was that they demonstrated that the Kerguelen-Gaussberg/Broken Ridge complex forms a hotspot trace on the Antarctic plate from the Kerguelen hotspot. These two features were subsequently rifted apart during the reorganization of spreading in the Indian Ocean about 40 m.y.B.P. As none of their assumptions constrain the motion of the Antarctic plate relative to the Kerguelen hotspot,

their work demonstrates that there may indeed be a "mirror image" ridge to the Ninetyeast Ridge. Thus, if one accepts the hypothesis advanced above that the Ninetyeast Ridge is the trace of one fixed volcanic source, Luyendyk and Rennick's (in press, 1976) reconstructions show that it must have formed at the Indian-Antarctic spreading center and created traces on both plates.

The existence of a worldwide network of hotspots with little or no relative motion between them remains in doubt. Hey (1975) has shown that the Galapagos hotspot is fixed with respect to Hawaii. Duncan and McDougall (in press, 1976) have shown that the Society, Austral, Marquesas, and Pitcairn-Gambier Island chains have rates and trends of volcanic migration which predict the same motion for the Pacific plate as is predicted by the Hawaii-Midway chain. Thus the existence of a Pacific network of hotspots relatively fixed with respect to one another seems probable. Whether or not this network can be extended to include Kerguelen is problematic (Molnar and Atwater, 1973). Because the Kerguelen hotspot appears to be essentially fixed in latitude, one would like to infer that it is also fixed with respect to Hawaii. However, there is no conclusive evidence that it is. It is clear that the Atlantic hotspots cannot have remained fixed with respect

to the Indian Ocean hotspots if they all created the hotspot traces usually ascribed to them (Molnar and Francheteau, 1975a). Relative motions up to 2 cm/yr are required to satisfy all of the available constraints.

Thus the weight of evidence strongly supports the concept that the Ninetyeast Ridge is the volcanic trace of the Kerguelen hotspot which is fixed with respect to latitude. However, an apparent contradiction exists in the arguments presented above. The volcanic source of the ridge was nearly fixed in latitude, and yet it appears to have remained under the Indian-Antarctic spreading center from the initial rifting of India and the Antarctic until spreading reorganized in the central Indian Ocean about 40 m.y.B.P. Considering that the measured spreading rates during that time (up to 12.0 cm/yr one limb rate, Sclater and Fisher, 1974) are among the highest ever observed, it seems to be an artificial constraint to suggest that the spreading center did not migrate quite freely with respect to latitude. This implies that the spreading center, if it were spreading symmetrically, must have been migrating northwards with respect to the south pole at $12 \text{ cm/yr} \pm$ any motion of Antarctica with respect to the South Pole.

In his discussion of the hotspot hypothesis Morgan (1972a) suggests that if one plate of a rifting two plate

system were fixed by forces external to those causing the rifting, a hotspot under the spreading center might cause asymmetric spreading. I suggest that the Kerguelen hotspot has caused asymmetric accretion (symmetric spreading with repeated spreading center jumps in the same direction (see Hey (1975) and Hey et al. (in press, 1976)) in the Indian Ocean, and furthermore that this asymmetric accretion was, at least in part, the cause of the extreme length of the Ninetyeast Transform Fault.

There is no relevant paleomagnetic data from East Antarctica, but there are several poles of Cretaceous and Lower Tertiary age from West Antarctica and from Australia (McElhinny, 1973) which suggest that Antarctica was indeed moving very little with respect to the spin axis of the earth during the period from the middle Cretaceous to the Paleocene (also see Figure 3 and Luyendyk and Rennick (in press, 1976), figure 8d). Perhaps the geometry of other plate motions held the Antarctic nearly fixed in much the same manner as it appears to be today. Thus if the Ninetyeast Ridge is a hotspot trace we might expect to find asymmetric spreading or asymmetric accretion between the Indian and Antarctic plates for the reasons suggested by Morgan (1972a). Sclater and Fisher (1974) have documented an 11° southerly jump of the spreading center at the

southwestern end of the Ninetyeast Ridge. There is a data gap through the region of the jump, and the equivalent anomalies on the Antarctic plate have not yet been described, so the exact nature of the jump is unknown. Its existence cannot be doubted, however, as anomalies 27-30 are offset 8-9° left laterally and the anomalies younger than anomaly 15 are offset 2-3° right laterally along the same fracture zone. This jump may have occurred as a series of small jumps or as one large jump, but the net effect was to cause asymmetric accretion with the Indian plate growing much faster than the Antarctic plate between the 86°E fracture zone and the Ninetyeast Ridge. It is possible that the Antarctic plate did not grow at all during the time of the jumping and that the integrated effect of this asymmetric accretion process was entirely one sided. This jumping must have predated the reorganization of spreading south of the Ninetyeast Ridge as the crust involved is bounded by the north striking 86°E and 90°E transform faults. Thus it cannot have been caused by the westward migration of the spreading pattern which separated Australia from Antarctica (Bowin, 1974).

A very similar process has been documented for a small section of crust south of Australia (Weissel and Hayes, 1972).

There the spreading seems to be truly asymmetric, at least within the resolution of the data. Even though there is no direct evidence of a hotspot in this area, Hayes (1976) has used a very similar model to mine to explain the asymmetric spreading and the scale of the asymmetry, both in time and in space. He points out that the asymmetry occurs only along a short section (200 km) of the spreading ridge. This indicates that if a hotspot causes such asymmetry, its effect is local in scope and it apparently cannot upset the overall symmetry of the entire plate boundary.

Part of the Galapagos spreading system also behaves similarly. Hey et al. (in prep., 1976) showed that the Galapagos volcanic source was fixed with respect to Hawaii. They also showed that one part of the Galapagos spreading system has been spreading symmetrically but accreting asymmetrically. The spreading process itself has been symmetric and continuous, but the ridge has jumped south towards the hotspot at discrete times, making the accretion process discontinuous and asymmetric.

There is no a priori reason why the absolute motion vector of a plate should coincide with its relative rotation vector with respect to some other plate. Neither is there any reason why they should not coincide. If the Ninetyeast

Ridge is indeed a hotspot trace, then its strike parallel to the Ninetyeast Transform Fault implies that the absolute rotation vector of India and the relative motion vector for Antarctica/India were nearly coincident. As mentioned above, Molnar and Tapponnier's (1975) analysis of the relative motion of Eurasia/India agrees well with the foregoing analysis of India's northward motion. This is independent circumstantial evidence supporting the possibility of coincident absolute and relative motion vectors.

The paleomagnetic data presented in the beginning of this paper suggested that the Ninetyeast Ridge might be a hotspot trace. The foregoing discussion has shown that there is no other data in conflict with this hypothesis and, indeed, the hypothesis predicts some of the unusual geometric relationships observed. Two hotspots are not needed to explain the presence of both the Ninetyeast Ridge and the Kerguelen-Gaussberg Ridge/Broken Ridge complex if one accepts the paleomagnetic evidence for an essentially stationary Antarctic plate and the causal relationship between the hotspot position and the position of the spreading center.

Summary

Paleomagnetic data have been presented for several sites on and near the Ninetyeast Ridge. These data, combined with previously published data, indicate that the Indian plate moved northwards with respect to the south pole at a rate of 14.9 ± 4.5 cm/yr between 70 and 40 mybp. Near 40 mybp, presumably in response to the closing of the Tethys, the rate slowed to $5.2 \pm .8$ cm/yr from then until the present.

Furthermore, these data show that the volcanic source of the Ninetyeast Ridge has remained essentially fixed in latitude near 50°S , supporting the hypothesis that the ridge is the trace of the Kerguelen hotspot on the Indian plate (Morgan, 1972a, 1972b). Note, however, that nothing can be said about any possible longitudinal motion of the hotspot. The paleontology, palynology and subsidence history of the drilled sections indicate that the ridge was formed at or near sea level in high southern latitudes. The petrology of the basalts is generally, but not always, more similar to oceanic island rock suites than it is to "typical" mid-ocean ridge rock suites.

The existence of a "mirror image" ridge on the Antarctic plate indicates that the volcanic source must have remained very near to the Indian-Antarctic plate boundary.

This implication, together with the fixed latitude constraint, implies a causal relationship between the positions of the hotspot and the plate boundary. It is suggested that Antarctica was held relatively fixed by forces external to those controlling the Indian-Antarctic separation, and that, as a result, the hotspot caused asymmetric accretion of crust between 86°E and 90°E near the southern end of the Ninetyeast Ridge in a manner similar to that predicted by Morgan (1972a) in his original discussion of the hotspot hypothesis. A similar process has been observed south of Australia (Weissel and Hayes, 1972; Hayes, 1976). The existence of such asymmetric accretion near the Ninetyeast Ridge is postulated on the basis of an inferred 11° southerly migration or jump of the spreading center at the southwest end of the ridge. This probably occurred between anomalies 23 and 15 (55-38 mybp).

In addition, several north-south tracks of magnetic anomalies were deskewed to estimate the position of the paleomagnetic poles as a check against the DSDP data. Unfortunately, the paucity of tracks and the variability of the skewnesses of the anomalies combined to make the lunes of possible pole positions too wide to provide any additional paleolatitude constraints. However, they did confirm the overall pattern of previous anomaly identifications and spreading rate changes (Sclater and Fisher, 1974).

Two reconstructions are presented to demonstrate the incompatibility of the Indian plate and Australian plate paleomagnetic data sets when they are used in conjunction with the estimates of the relative motions of India/Antarctica and Australia/Antarctica to predict the position of Antarctica. At present, there is no explanation for the discrepancy.

Table I

Basalt Paleolatitudes

Site	Age (m.y.b.p.)	N ¹	\bar{I}	$\pm 2 SM^2$	Corr. ² Paleolat.	95% ¹ C.I.	Rating	Comments
213	58-63	35/38	± 31.6	7.6	-17.5	-9.7 -25.2	B*	5 normal and 2 reversed units; consistent with other Wharton Basin paleolatitudes
214	57-60	30/30	± 63.7	9.1	-47.3	-37.9 -57.6	B?	2 normal and 4 reversed units; roughly consistent with other Ninetyeast Ridge paleolatitudes
215	58-63	24/34	± 74.8	13.6	-65.0	-49.2 -90.0	C?	2 normal and 1 reversed unit; disagrees with basal sediment paleolatitude; many discordant directions omitted from calculation
216	67-72	42/42	± 67.6	10.2	-52.0	-41.2 -63.9	C*	5 reversed units; consistent with basal sediment paleolatitudes
254	30-40	9/9	± 67.8	16.2	-52.3	-35.3 -73.0	D*	2 reversed units; consistent with other Ninetyeast Ridge paleolatitudes (Peirce et al., 1974)

1. The first number is the number of sample directions which passed the acceptance criteria (see text). The second number is the total number of cleaned sample directions.
2. See Peirce (in press, 1976) for definition of these parameters. After the rating, * implies that the data are consistent with other independent data; ° implies dubious consistency, and ? implies inconsistency.

Table II
Apparent Cooling Units, DSDP Site 213

Unit #	Top	Bottom	N ¹	\bar{T}	S.D. ²	Comments
1	17-1-109	17-2-005	0	-	-	Weathered basalt and glass, not sampled.
2	17-2-005	17-2-091	3/4	-40.2	2.4	Weathered basalt bounded by palagonitized glass
3	17-2-091	17-2-130	2/2	-36.7	4.5	Same as unit 2
4	17-2-130	17-3-070	5/6	+35.7	6.1	Weathered basalt and glass over partially weathered porphyritic basalt
5	17-3-070	17-cc	4/4	-24.6	2.5	Weathered basalt and glass with 15 cm of partially weathered porphyritic basalt
6	18-1-100	18-2-005	2/2	-20.5	3.3	Partially weathered basalt
7	18-2-005	18-2-055	0	-	-	Zone of alteration and glass; not sampled
8	18-2-055	18-3-005	6/6	+35.7	3.7	Weathered glass over partially weathered basalt. One short piece apparently inverted
9	18-3-005	18-3-033	2/2	-34.6	.6	Weathered basalt
10	18-3-033	18-3-072	3/4	-35.6	3.3	Weathered basalt and glass over partially weathered basalt

Table II (continued)

Unit #	Top	Bottom	N ¹	\bar{I}	S.D. ²	Comments
11	18-3-072	18-3-101	3/3	-28.7	3.4	Weathered glass over partially weathered basalt
12	18-3-101	18-3-142	2/2	-23.1	1.2	Weathered basalt and glass over partially weathered basalt
13	18-3-142	19-1-135	0	-	-	Weathered basalt and glass over coarse grained basalt (125 cm void); not sampled
14	19-1-135	19-2-010	0	-	-	Weathered basalt and glass over coarse grained basalt not sampled
15	19-2-010	19-2-150	2/2	-26.1	.8	Glass over a vesicular zone over coarse grained basalt. One short piece apparently inverted.

Units 2-3, 4, 5-6, 8, 9-10, 11, 12-15 are interpreted as being independent.

1. N as in Table 1.
 2. Standard deviation of inclinations.
-

Table III
 Apparent Cooling Units, DSDP Site 214

Unit #	Top	Bottom	N ¹	\bar{I}	S.D. ²	Comments
1	48-1-000	48-2-010	4/4	+55.2	2.4	Fine grained over medium grained basalt
2	48-2-010	48-cc	6/6	+56.5	1.0	Vesicular over fine grained basalt
3	49-top	51-1-120	6/6	+57.1	2.0	Fine grained basalt with chilled bottom
4	51-1-120	53-1-010	0	-	-	Lignite and weathered lapilli tuff; too friable to sample
5	53-1-010	53-1-150	1	-68.0	-	Fine grained, glassy basalt over coarser grained basalt
6	53-2-020	53-cc	0	-	-	Basaltic sand and debris; not sampled
7	54-1-035	54-2-140	10/10	+71.5	3.5	Coarse amygdalar basalt over very coarse grained basalt
8	54-2-140	54-3-056	1	-70.0	-	Vesicular over amygdalar basalt
9	54-3-056	54-3-134	2	+67.0	-	Vesicular over amygdalar over coarse grained basalt
10	54-3-134	54-cc	1	+49.1	-	Vesicular over amygdalar basalt

1. N as in Table I.

2. Standard deviation of inclinations.

Table III (continued)

Units 1-3, 5, 7, 8, 9, and 10 are interpreted as being independent.

Hekinian (1974a) describes cores 48-51 as an "intermediate differentiated flow", an "oceanic andesite" on petrologic evidence.

Table IV
 Apparent Cooling Units, DSDP Site 215

Unit #	Top	Bottom	N ¹	\bar{I}	S.D. ²	Comments
1	17-1-110	17-cc	0	-	-	Four small pieces of weathered glass, palagonite and weathered basalt. Bounded by unre-crystallized chalks; not sampled.
2	18-1-000	18-cc	6/10	-72.9	4.3	Mostly weathered fine grained basalt; glassy zones occur at 18-1-000, 130, 18-2-055, 068, 140.
3	19-1-000	19-cc	5/7	+79.0	2.2	Relatively fresh, coarse grained basalt; glassy zones occur at 19-2-050 and 130.
4	20-1-070	20-cc	13/17	-72.6	9.8	Mostly weathered fine grained basalt; glassy zones occur at 20-2-73, 130, 20-3-003 (with interbedded limestone), 20-3-042, 100, 20-4-013, 040, 060.

Unit 1 may be part of Unit 2. Unit 3 distinguished from units 2 and 4 on the basis of polarity. The three independent units are interpreted as three sets of pillow structures.

1. N as in Table I.

2. Standard deviation of inclinations.

Table V
Apparent Cooling Units, DSDP Site 216

Unit #	Top	Bottom	N ¹	\bar{I}	S.D. ²	
1	36-3-115	36-3-150	0	-	-	Amygdalar basalt; separated from unit 2 by 10 cm of sediment.
2	36-4-110	36-4-040	3/3	+66.2	4.9	Amygdalar basalt.
3	36-4-040	36-4-130	2/2	+67.0	6.6	Coarse grained tuff.
4	36-4-130	37-3-100	10/10	+70.8	1.9	Oxidized, pale red scoriaceous zone over fine grained basalt.
5	37-3-100	38-2-030	12/12	+71.3	2.3	Oxidized, pale red vesicular zone over fine grained basalt; two alteration zones at 37-4-100-150 and 38-1-30-50.
6	38-2-030	38-3-040	6/6	+66.5	2.0	Alteration zone with chlorite veins over fresh fine grained basalt. Distinguished from unit 5 on the basis of magnetic inclinations.
7	38-3-040	38-4-012	5/5	+71.0	1.1	Oxidized, pale red scoriaceous zone over vesicular basalt over fine grained basalt.
8	38-4-012	38-4-085	4/4	+62.7	4.7	Vesicular basalt over amygdalar basalt over vesicular basalt (cc).

Units 2-3, 4-5, 6, 7, 8 are interpreted as independent.

1. N as in Table 1.

2. Standard deviation of inclinations.

Table VI

Sediment Paleolatitudes

Site	Cores	Horizon ¹	Age	N ²	\bar{I}	S.D. ³	2SM ⁴	Corr. P. Lat. ⁴	95% C.I. ⁴	Rating ⁴	Comments
213	16-4	D. multi-radiatus (N) P5 (F)	54-56	4/4	38.8	26.2	-	-	-	-	Individual specimen directions stable but no grouping. Material probably disturbed by drilling.
214	6-2	D. surculus (N) S. pentas (R) N20 (F)	2.8-3.8	0/3	-	-	-	-	-	-	$< 1 \times 10^{-6}$
214	22-3,4	S. belemnos (N) N5 (F)	18-21	0/5	-	-	-	-	-	-	$< 1 \times 10^{-6}$
214	32-2,3 34-6	C. alatus to D. lodoensis (N) P11 to P7 (F)	46-51	3/6	34.9	10.0	-	-	-	-	Others $< 1 \times 10^{-6}$
214	36-4	H. kleinPELLI (N) P4 (F)	57-58	1/4	33.6	-	-	-	-	-	Others $< 1 \times 10^{-6}$
214	41-2,3	C. robusta (N) ??	57-60	0/9	-	-	-	-	-	-	Tuff; thermal demag. used but no stable directions found; generally $< 1 \times 10^{-6}$

Table VI (continued)

Site	Cores	Horizon	Age	N	\bar{I}	S.D.	2SM	Corr. P. Lat.	95% C.I.	Rating	Comments
214	44-1 46-3	Barren	57-60	5/12	44.9	4.6	(12.8)	(-27.0)	(-13.9) (-40.1)	C°	Inconsistent with basalts.
215	15- 4,5 16- 1, 4,5	H. klein- pelli (N) P4 (F)	57-58	29/32	56.3	8.7	5.4	-38.5	-33.0 -44.1	B°	Inconsistent with basalts. Inconsistent with Ninety- east Ridge data.
216	5-2 6-3	S. belemnos and below C. virginis (R) N5-N6 (F)	16-21	3/7	19.2	7.1	-	-	-	-	Others < 1 x 10 ⁻⁶
216	9- 1,2 10-1	S. cipro- ensis (N) D. ateuchus (R) N4 (F)	22-30	9/16	17.8	5.0	9.3	- 9.3	+ .1 -18.8	B*	All directions in section 9-1 discordant; sections 9-2 and 10-1 concord- ant; See Fig. 7.
216	13-1 14-1, 2,3	S. distensus (N) T. tuberosa (R) P19-21 (F)	26-34	13/14	23.4	7.2	7.8	-12.6	- 4.5 -20.5	B*	See Fig. 7.
216	15-3 16- 1,2	D. barbad- iensis (N) T. bromia (R)	37.5- 43	11/16	27.5	8.5	8.5	-15.1	- 6.5 -23.8	B*	5 back to back samples un- stable and < 1 x 10 ⁻⁶ ; see Fig. 7.

Table VI (continued)

Site	Cores	Horizon	Age	N	\bar{I}	S.D.	2 SM	Corr. P. Lat.	95% C.I.	Rating	Comments
216	21-1 22- 1,2	D. mohleri (N) P4 (F)	56-58	8-14	64.0	13.0	-	-	-	-	Others unstable
216	23-2 24- 2,3	C. danicus to N. frequens (N) P1 to G. mayaroensis (F)	62-67	10/30	56.0	13.0	-	-	-	-	Others unstable
216	34- 1,2 35- 2,3	N. frequens or older (N) Maastrichtian (F)	65-68	3/16	51.4	28.9	-	-	-	-	Mostly $< 1 \times 10^{-6}$ and poor stability
216	36- 1,2	N. frequens or older (N) Maastrichtian (F)	65-68	16/16	68.5	8.9	7.1	-54.7	-46.8 -62.9	B*	See Fig. 7
216	36-3	N. frequens or older (N) Maastrichtian	65-68	0/9	-	-	-	-	-	-	Unstable
217	4-3	D. neohamatus (N) O. antepenul- timus (R) N16 (F)	7-10	1/4	28.5	-	-	-	-	-	Others unstable

Table VI (continued)

Site	Cores	Horizon	Age	N	\bar{I}	S.D.	2 SM	Corr. P. Lat.	95% C.I.	Rating	Comments
217	6-3, 4,6	S. hetero- morphus to S. belemnos (N) C. virginis (R) N5 (F)	15-21	8/20	5.2	9.6	9.9	+ 2.7	+12.8 -12.8	B*	Others discordant and unstable.
217	7-2, 3	S. ciproensis (N) D. ateuchus (R)	24-30	3/10	6.5	2.2	-	-	-	-	Others unstable and < 1 x 10 ⁻⁶
217	8-3, 4,5	S. distensus (N) T. tuberosa (R) P-21 (F)	26-30	13/17	11.3	8.4	7.8	- 5.9	+ 2.0 -13.8	B*	Intensities < 1 x 10 ⁻⁶ ; directions based on back to back sampling.
217	9-2	S. predisten- sus to D. bar- badiensis (N)	30-40	7/8	6.1	9.3	(10.5)	(-3.8)	(+ 6.7) (-14.6)	C°	< 1 x 10 ⁻⁶ ; incon- sistent with other core 9 data.
	9-3, 4,5, 6	T. tuberosa to T. bromia (R) P20-P16 (F)	30-40	4/16	27.9	3.1	(15.3)	(-15.0)	(+ 0.5)	D°	Inconsistent with other core 9 data.
217	10- 1,2, 4,6	C. alatus (N) P. mitra to T. triacantha (R) P11-12	45.5-48	6/8	16.9	5.5	(11.4)	(-8.8)	(+ 2.7) (-20.4)	C*	< 1 x 10 ⁻⁷

Table VI (continued)

Site	Cores	Horizon	Age	N	\bar{I}	S.D.	2 SM	Corr. P. Lat.	C.I.	Rating	Comments
217	14-1, F. tympani- 5 formis (N) 15-1, P4 (F) 2		56-59	12/14	52.0	7.7	8.4	-36.3	-27.7 -45.0	B*	See Fig. 7.
217	16-3, C. helis (N) 5,6 P1 (F)		63-65	10/14	13.1	12.2	-	-	-	-	
217	18-2 N. frequens 19-1, to L. quad- 2,3 ratus (N) G. mayaroen- sis (F)		65-70	13/17	46.0	13.3	-	-	-	-	Wide scatter
217	33-2, E. augustus (N) 3 34-1 Companian (F)		73-76	11/83	25.0	14.7	-	-	-	-	Wide scatter
253	? D. tani nodifer (N)		46-48	49/55	67.6	10	3.3	-51.9	-48.3 -55.8	A*	See Fig. 7; (Cockerham and Luyendyk, 1975)

1. Paleontologic horizons taken from site reports and other paleontologic studies in the Initial Reports. See text for references. Age correlations from Berggren (1972).
2. N as in Table I.
3. Standard deviation of inclination.
4. As in Table I. See Peirce (in press, 1976) for definitions.

TABLE VII

Poles of Relative Rotation

INDIA/ANTARCTICA				AUSTRALIA/ANTARCTICA			
Time	Lat.	Lon.	Angle	Time	Lat.	Lon.	Angle
0-32	4.9	36.4	18.3	0-32	4.9	36.4	18.3
32-34	-16.0	27.4	1.28	32-34	-17.2	51.5	1.21
0-34	3.66	35.62	19.49	0-34	3.43	37.07	19.39
32-36	-16.00	27.4	2.56	32-36	-17.2	51.5	2.43
0-36	2.56	34.93	20.68	0-36	2.11	37.67	20.5
32-40	-16.0	27.4	5.11	36-40	-20.6	42.7	2.83
0-40	.72	33.78	23.10	0-40	-.67	37.76	23.13
40-51.5	-16.0	27.4	11.76	36-51.5	-20.6	42.7	11.29
0-51.5	-4.45	30.56	34.48	0-51.5	-6.19	37.93	31.19
40-53	-16.0	27.4	13.29	36-53	-20.6	42.7	12.38
0-53	-4.88	30.28	35.98	0-53	-6.70	37.94	32.24
53-62.5	4.0	357.0	12.43				
0-62.5	-.10	22.82	46.75				
62.5-64	4.0	357.0	3.17				
0-64	.80	21.42	49.61				
64-66.5	-2.0	8.0	7.27				
0-66.5	1.21	19.65	56.70				
66.5-80	-2.0	8.0	17.91				
0-80	1.9	16.63	74.30				

SOUTH POLE/INDIA			
Time	Lat.	Lon.	Angle
0-34	1.32	1.92	-18.36
0-36	.62	6.74	-19.59
0-40	1.83	11.40	-19.63
0-51.5	2.80	25.54	-23.25
0-53	2.81	26.15	-24.29
0-62.5	6.31	24.21	-38.54
0-64	6.74	23.58	-41.99
0-66.5	5.96	22.84	-49.73
0-80	3.46	23.08	-69.5

TABLE VII

(continued)

SOUTH POLE/AUSTRALIA

Time	Lat.	Lon.	Angle	
0-5	0	356.3	-3.4	composite pole
0-17.5	0	336.0	-10.6	composite pole
0-22.5	0	20.9	-12.6	composite pole
0-30	0	2.4	-21.1	composite pole
0-34	0	5.5	-18.9	Liverpool volc.
0-36	0	9.1	-19.0	inferred
0-40	0	15.8	-19.1	inferred
0-51.5	0	35.6	-19.5	Barrington vol.
0-53	0	36.7	-20.1	inferred
0-62.5	0	43.4	-23.7	inferred
0-64	0	44.5	-24.4	inferred
0-66.5	0	46.3	-25.4	inferred
0-80	0	53.0	-29.5	inferred

Notes to Table VII.

Australia and India are assumed to be one plate from 0-32 mybp, and the rotation pole from Sclater and Fisher (1974) is used. India/Antarctica poles are taken from Sclater and Fisher (1974) with adjustments in the rate of opening to match the observed changes in spreading rate. Australia/Antarctica poles are taken from Weissel and Hayes (1972) except that the ages have been changed to conform to the Sclater et al. (1974) time scale.

The South Pole/Australia poles have been calculated from the paleomagnetic poles for Australia given by McElhinny et al. (1974). Inferred poles have been estimated from the apparent polar wandering curve in that paper. The South Pole/India poles have been calculated from the two relative motion poles and the South Pole/Australia poles. See text for method of calculation.

These poles have been used to calculate the paleolatitude of site 216 with respect to the Australian paleomagnetic data and with respect to a fixed Antarctica (Figure 7).

References

- Ade-Hall, J.M., R.D. Hyndman, W.G. Melson, M. Bougault, L. Dmitrev, J. Fisher, P.T. Robinson, T.L. Wright, G.A. Miles, M.T. Flower and R.C. Howe, Sources of magnetic anomalies on the Mid-Atlantic Ridge, Nature, 255, 389-390, 1975.
- Berggren, W.A., A Cenozoic time-scale - Some implications for regional geology and paleogeography, Lethaia, 5, 195-215, 1972.
- Berggren, W.A., G.P. Lohmann and R.Z. Poore, Shore laboratory report on Cenozoic planktonic foraminifera: Leg 22, in von der Borch, C.C., J.G. Sclater et al., Initial Reports of the Deep Sea Drilling Project, XXII, Washington (U.S. Gov't Printing Office), 635-656, 1974.
- Blow, R.A. and N. Hamilton, Paleomagnetic evidence from DSDP cores of northward drift of India, Nature, 257, 570-572, 1975.
- Bowin, C.O., Origin of Ninetyeast Ridge from studies near the equator, Jour. Geophys. Research, 78, 6029-6043, 1973.
- Bowin, C.O., Migration of a pattern of plate motion, Ear. Plan. Sci. Ltrs., 21, 400-404, 1974.

- Briden, J.C., A stability index of remanent magnetism,
J. Geophys. Res., 47, 1401-1405, 1972.
- Bukry, D., Coccolith and silicoflagellate stratigraphy,
Eastern Indian Ocean, Deep Sea Drilling Project:
Leg 22, in von der Borch, C.C., J.G. Sclater et al.,
Initial Reports of the Deep Sea Drilling Project,
XXII, Washington (U.S. Gov't Printing Office),
601-608, 1974.
- Burakova, M., ed., Indiiskii Okean, Glavnoe Upravlenie,
Geodezii i Kartografii, Pri Sovette Ministrov SSSR,
Moskva. (Bathymetric chart of Indian Ocean, no
publication data, 5th printing).
- Cande, S.C., A paleomagnetic pole from Late Cretaceous
marine magnetic anomalies in the Pacific, Geophys.
J.R. astr. Soc., 44, 547-566, 1976.
- Cockerham, R.S., B.P. Luyendyk, and R.D. Jarrard,
Paleomagnetic study of sediments from site 253 DSDP,
Ninetyeast Ridge, EOS Trans. Am. Geophys. Un., 56,
978, 1975.
- Cox, A., Paleolatitudes determined from paleomagnetic data
from vertical cores, in preparation, 1976.
- Davies, T.A., B.P. Luyendyk, et al., Initial Reports of the
Deep Sea Drilling Project, XXVI, Washington, D.C.
(U.S. Gov't Printing Office), 982 p., 1974.

- Duncan, R.A. and I. McDougall, Linear volcanism in French Polynesia, Volc. and Geoth. Res., in press, 1976.
- Dunlop, D.J., Theory of magnetic viscosity of lunar and terrestrial rocks, Rev. of Geophys. and Sp. Phys., 11, 855-901, 1973.
- Fleet, A.J. and D.R.C. Kempe, Preliminary geochemical studies from DSDP Leg 26, Southern Indian Ocean, in Davies, T.A., B.P. Luyendyk, et al., Initial Reports of the Deep Sea Drilling Project, XXVI, Washington, D.C. (U.S. Gov't Printing Office), 541-552, 1974.
- Francis, T.J.G. and R.W. Raitt, Seismic refraction measurements in the southern Indian Ocean, Jour. Geophys. Research, 72, 3015-3041, 1967.
- Frey, F.A. and C.M. Sung, Geochemical results for basalts from sites 253 and 254, in Davies, T.A., B.P. Luyendyk et al., Initial Reports of the Deep Sea Drilling Project, XXVI, Washington, D.C. (U.S. Gov't Printing Office), 567-572, 1974.
- Frey, F.A., J.S. Dickey, G. Thompson and W.B. Bryan, Eastern Indian Ocean DSDP sites: correlations between petrography, geochemistry, and tectonic setting, in Heirtzler, J.R., ed., Special Paper, Geol. Soc. of Am., in press, 1976.

Gartner, S., Nannofossil biostratigraphy, Leg 22, Deep Sea Drilling Project, in von der Borch, C.C., J.G. Sclater et al., Initial Reports of the Deep Sea Drilling Project, XXII, Washington, D.C. (U.S. Gov't Printing Office), 577-600, 1974.

Gartner, S., D.A. Johnson and B. McGowran, Paleontology synthesis of Deep Sea Drilling results from Leg 22 in the Northeastern Indian Ocean, in von der Borch, C.C., J.G. Sclater et al., Initial Reports of the Deep Sea Drilling Project, XXII, Washington, D.C. (U.S. Gov't Printing Office), 805-813, 1974.

Hall, J.M. and P.J.C. Ryall, Paleomagnetism of basement rocks, Leg 37, in Melson, W.G. et al., Initial Reports of the Deep Sea Drilling Project, XXXVII, Washington, D.C. (U.S. Gov't Printing Office), in press, 1976.

Harris, W.K., Palynology of Paleocene sediments at site 214, Ninetyeast Ridge, in von der Borch, C.C., J.G. Sclater et al., Initial Reports of the Deep Sea Drilling Project, XXII, Washington, D.C. (U.S. Gov't Printing Office), 503-520, 1974.

Hayes, D.E., Nature and implications of asymmetric sea-floor spreading - "Different rates for different plates", Bull. Geol. Soc. Am., 87, 994-1002, 1976.

- Heirtzler, J.R., G.O. Dickson, E.M. Herron, W.C. Pitman III, and X. LePichon, Marine magnetic anomalies, geomagnetic reversals, and motions of the ocean floor and continents, J. Geophys. Res., 73, 2119-2136, 1968.
- Hekinian, R., Petrology of igneous rocks from Leg 22 in the northeastern Indian Ocean, in von der Borch, C.C., J.G. Sclater et al., Initial Reports of the Deep Sea Drilling Project, XXII, Washington, D.C. (U.S. Gov't Printing Office), 413-448, 1974a.
- Hekinian, R., Petrology of the Ninetyeast Ridge (Indian Ocean) compared to other aseismic ridges, Contr. Mineral. and Petrol., 43, 125-147, 1974b.
- Hey, R.N., Tectonic evolution of the Cocos-Nazca rise, Ph.D. Thesis, Department of Geol. and Geophys. Sci., Princeton Univ., 169 p., 1975.
- Hey, R.N., G.L. Johnson and A. Lowrie, Recent tectonic evolution of the Galapagos area and plate motions in the East Pacific, in preparation, 1976.
- Kemp, E.M. and W.K. Harris, The vegetation of Tertiary Islands on the Ninetyeast Ridge, Nature, 258, 303-307, 1975.
- Kempe, D.R.C., The petrology of the basalts, Leg 26, in Davies, T.A., B.P. Luyendyk et al., Initial Reports of the Deep Sea Drilling Project, XXVI, Washington, D.C. (U.S. Gov't Printing Office), 465-504, 1974.

- Johnson, D.A., Radiolaria from the eastern Indian Ocean, DSDP Leg 22, in von der Borch, C.C., J.G. Sclater et al., Initial Reports of the Deep Sea Drilling Project, XXII, Washington, D.C. (U.S. Gov't Printing Office), 521-575, 1974.
- Laughton, A.S., D.H. Matthews, and R.L. Fisher, The structure of the Indian Ocean, in Maxwell, A.E., ed., The Sea: Ideas and Observations, Vol. 4, Pt. II, New York, John Wiley and Sons, Inc., 543-586, 1971.
- LePichon, X. and J.R. Heirtzler, Magnetic anomalies in the Indian Ocean and sea floor spreading, Jour. Geophys. Research, 73, 2101-2117, 1968.
- Lowrie, W. and D.V. Kent, Viscous remanent magnetization in basalt samples, in Hart, S.R. and A.S. Yeats et al., Initial Reports of the Deep Sea Drilling Project, XXXIV, Washington, D.C. (U.S. Gov't Printing Office), 479-484, 1976.
- Luyendyk, B.P., Deep sea drilling on the Ninetyeast Ridge: synthesis and a tectonic model, in Heirtzler, J.R., ed., Special Paper, Geol. Soc. Am., in press, 1976.
- Luyendyk, B.P. and T.A. Davies, 1974, Results of DSDP Leg 26 and the geologic history of the Southern Indian Ocean, in Davies, T.A., B.P. Luyendyk et al., Initial Reports of the Deep Sea Drilling Project, XXVI, Washington, D.C. (U.S. Gov't Printing Office), 909-943.

- Luyendyk, B.P. and W. Rennick, The tectonic origin of aseismic ridges in the Eastern Indian Ocean, submitted to Bull. Geol. Soc. Am., in preparation, 1976.
- McElhinny, M.W., Northward drift of India - Examination of recent paleomagnetic results, Nature, 217, 342-344, 1968.
- McElhinny, M.W., Formation of the Indian Ocean, Nature, 228, 977-979, 1970.
- McElhinny, M.W., Paleomagnetism and Plate Tectonics, Cambridge Univ. Press (Cambridge), 359 pp., 1973.
- McElhinny, M.W., B.J.J. Embleton, and P. Wellman, A synthesis of Australian Cenozoic paleomagnetic results, Geophys. Jour. Roy. astr. Soc., 36, 141-151, 1974.
- McElhinny, M.W. and G.R. Luck, Paleomagnetism and Gondwanaland, Science, 168, 830-832, 1970.
- McGowran, B., Foraminifera, in von der Borch, C.C., J.G. Sclater et al., Initial Reports of the Deep Sea Drilling Project, XXII, Washington, D.C. (U.S. Gov't Printing Office), 609-628, 1974.
- McKenzie, D. and J.G. Sclater, The evolution of the Indian Ocean since the Late Cretaceous, Geophys. J.R. astr. Soc., 25, 437-528, 1971.

- Molnar, P. and T.M. Atwater, Relative motion of hotspots in the mantle, Nature, 246, 288-291, 1973.
- Molnar, P. and J. Francheteau, The relative motions of "hotspots" in the Atlantic and Indian Oceans during the Cenozoic, Geophys. J.R. astr. Soc., 43, 763-774, 1975a.
- Molnar, P. and J. Francheteau, Plate tectonic and paleomagnetic implications for the age of the Deccan Traps and the magnetic anomaly time scale, Nature, 255, 128-130, 1975b.
- Molnar, P. and P. Tapponnier, Cenozoic tectonics of Asia: effects of a continental collision, Science, 189, 419-426, 1975.
- Morgan, W.J., Deep mantle convection plumes and plate motions, Amer. Assoc. Pet. Geol. Bull., 56, 203-213, 1972a.
- Morgan, W.J., Plate motions and deep mantle convection, in Shagam, R. and others, eds., Studies in earth and space sciences (Hess volume), Geol. Soc. America Mem. 132, 7-22, 1972b.
- Peirce, J.W., Assessing the reliability of DSDP paleolatitudes, J. Geophys. Res., in press, 1976.

- Peirce, J.W., C.R. Denham, and B.P. Luyendyk, Paleomagnetic results of basalt samples from DSDP Leg 26, southern Indian Ocean, in Davies, T.A., B.P. Luyendyk et al., Initial Reports of the Deep Sea Drilling Project, XXVI, Washington, D.C. (U.S. Gov't Printing Office), 517-527, 1974.
- Pimm, A.C., B. McGowran, and S. Gartner, Early sinking history of Ninetyeast Ridge, Northeastern Indian Ocean, Bull. Geol. Soc. of Am., 85, 1219-1224, 1974.
- Rennick, W.L. and B.P. Luyendyk, Tectonic origin of aseismic ridges in the Eastern Indian Ocean (abstract), EOS Trans. Am. Geophys. Un., 56, 1065, 1975.
- Schlich, R., Structure et age de l'océan Indien Occidentale. Mém. hors-série Soc. géol. de France, no. 6, 102 pp., 1975.
- Schouten, H. and S.C. Cande, Paleomagnetic poles from marine magnetic anomalies, Geophys. J. R. astr. Soc., 44, 567-575, 1976.
- Sclater, J.G., D. Abbott, and J. Thiede, The paleobathymetry and sediments of the Indian Ocean, in Heirtzler, J.R., ed., Special Paper, Geol. Soc. Am., in press, 1976.
- Sclater, J.G., R.N. Anderson, and M.L. Bell, The elevation of ridges and the evolution of the central eastern Pacific, Jour. Geophys. Research, 76, 7888-7915, 1971.

- Sclater, J.G. and R.L. Fisher, The evolution of the east central Indian Ocean, with emphasis on the tectonic setting of the Ninetyeast Ridge, Geol. Soc. Amer. Bull., 85, 683-702, 1974.
- Sclater, J.G., R. Jarrard, B. McGowran, and S. Gartner, Jr., A comparison of the magnetic and biostratigraphic time scales, in von der Borch, C.C., J.G. Sclater et al., Initial Reports of the Deep Sea Drilling Project, XXII, Washington, D.C. (U.S. Gov't Printing Office), 381-386, 1974.
- Sclater, J.G., B.P. Luyendyk and L. Meinke, Magnetic lineations in the southern part of the Central Indian Basin, Bull. Geol. Soc. Am., 87, 371-378, 1976.
- Smith, A.G. and A. Hallam, The fit of the southern continents, Nature, 225, 139-144, 1970.
- Thompson, G., W. Bryan, F. Frey and C.M. Sung, Petrology and geochemistry of basalts and related rocks from sites 214, 215, 216, DSDP Leg 22, Indian Ocean, in von der Borch, C.C., J.G. Sclater et al., Initial Reports of the Deep Sea Drilling Project, XXII, Washington, D.C. (U.S. Gov't Printing Office), 459-468, 1974.
- von der Borch, C.C., J.G. Sclater et al., Initial Reports of the Deep Sea Drilling Project, XXII, Washington, D.C. (U.S. Gov't Printing Office), 890 pp., 1974.

- Weissel, J.K. and D.E. Hayes, Magnetic anomalies in the southeast Indian Ocean, in Hayes, D.E., ed., Antarctic oceanology II: the Australian-New Zealand sector, Washington, D.C., Am. Geophys. Union, Antarctic Research Series, 19, 165-196, 1972.
- Wellman, P. and McElhinny, M.W., K-Ar age of the Deccan Traps, India, Nature, 227, 595-596, 1970.
- Wellman, P., M.W. McElhinny, and I. McDougall, On the polar-wander path for Australia during the Cenozoic, Geophys. J.R. astr. Soc., 18, 371-395, 1969.
- Wensink, H., A note on the paleomagnetism of the Lower Siwaliks near Choa Saiden Shak, Potwar Plateau, West Pakistan, Pakistan Sci. and Ind. Res. Bull., 1972a.
- Wensink, H., The paleomagnetism of the salt pseudomorph beds of middle Cambrian age from the Salt Range, West Pakistan, Ear. and Plan. Sci. Ltrs., 16, 189-194, 1972b.

Appendix I

BASALT SPECIMEN DIRECTIONS

APPENDIX I

BASALT SPECIMEN DIRECTIONS

Unit	Specimen	Field	Incl. ¹	Decl. ²	MDF ³	Comments
<u>Site 213</u>						
2	17-2-029	150	-39.8		288	
	17-2-036	200	(-34.0)		88	Reversed on demag; unstable
	17-2-048	200	-42.8		376	Pilot
	17-2-066	100	+38.0		132	Long piece of core probably was inverted during handling
3	17-2-102	100	-33.5		330	
	17-2-127	150	-39.9		291	
4	17-2-132	200	+37.1	174.0	139	Pilot
	17-2-136	100	+27.3	211.6	>200	Pilot; unstable intensity at 400 oe.
	17-3-013	100	+33.8	76.0	307	
	17-3-019	400	+36.0	55.7	287	Reversed on demag.
	17-3-047	400	(+48.3)		148	Reversed on demag.; unstable
	17-3-063	200	+44.3		560	Pilot
5	17-3-102	150	-21.5		264	
	17-3-114	400	-23.6	264.4	>800	Pilot; reversed on demag.
	17-3-117	150	-26.4	262.4	400	Pilot
	17-3-123	200	-26.7		287	
6	18-1-129	100	-22.8	170.4	274	Pilot
	18-1-142	100	-18.2	154.3	240	Pilot
8	18-2-026	150	+40.1	257.3	333	
	18-2-032	150	+36.1	257.3	(425)	
	18-2-075	100	+35.2		400	
	18-2-119	200	+28.9		573	Pilot
	18-2-137	150	+37.4		>800	
	18-3-003	100	+36.4		583	
9	18-3-008	200	-34.2	293.7	246	Pilot
	18-3-013	150	-35.0	296.3	283	

Appendix I (continued)

Unit	Specimen	Field	Incl.	Decl.	MDF	Comments
<u>Site 213 (cont.)</u>						
10	18-3-056	150	-39.2	158.9	784	
	18-3-060	100	-34.9	154.7	277	Pilot
	18-3-065	400	-32.8	305.1	400	Pilot
	18-3-069	400	(-22.8)	(318.5)	568	Pilot; reversed on demag.; unstable
11	18-3-083	150	-31.9		200	
	18-3-094	200	-29.1	69.5	325	
	18-3-098	150	-25.2	71.1	314	
12	18-3-136	150	-22.3	248.1	198	
	18-3-139	100	-24.0	242.0	226	Pilot
15	19-2-043	200	-26.5		250	Pilot; one of these short pieces probably was inverted during drilling or handling
	19-2-058	200	+25.7		710	
<u>Site 214</u>						
1	48-1-036	200	+53.7	206.3	(225)	
	48-1-039	200	+52.6	208.1	(250)	
	48-1-142	150	+56.6	118.9	218	Pilot
	48-1-145	200	+57.8	121.5	253	Pilot
2	48-2-027	200	+57.2	299.0	(275)	
	48-2-030	150	+57.7	297.1	(250)	
	48-2-087	150	+55.2		(250)	
	48-2-093	150	+56.6	284.0	(250)	
	48-2-096	150	+55.7	281.0	(250)	
	48-2-099	200	+56.7	287.9	(250)	
3	49-1-123	200	+56.5	184.5	333	Pilot
	49-1-126	200	+57.3	189.6	(275)	
	49-2-069	150	+54.9		(350)	
	49-2-087	200	+57.0		(400)	
	50-1-108	400	+56.2		385	Pilot
	51-1-101	200	+60.9		(325)	
5	53-1-131	150	-68.0		197	

Appendix I (continued)

Unit	Specimen	Field	Incl.	Decl.	MDF	Comments
<u>Site 214 (cont.)</u>						
7	54-1-062	200	+70.0		(225)	
	54-1-113	150	+64.6	323.9	(275)	
	54-1-128	200	+67.4	320.7	(325)	
	54-1-130	150	+71.2	319.0	259	Pilot
	54-1-142	200	+75.3	310.5	121	Pilot
	54-2-029	200	+70.9	310.0	124	
	54-2-032	200	+74.6	298.8	119	
	54-2-092	150	+74.9	149.6	91	
	54-2-104	150	+72.9	161.6	136	
	54-2-108	200	+73.1	137.0	98	
8	54-3-038	200	-70.0		200	
9	54-3-060	150	+69.6	327.3	295	Pilot
	54-3-068	100	+64.4	322.5	142	Pilot
10	54-3-142	200	+49.1		94	
<u>Site 215</u>						
2	18-1-020	100	-69.0		197	
	18-1-056	100	-76.5		324	Pilot
	18-1-079	100	(-58.4)		129	Pilot; reversed on demag.; unstable
	18-1-122	150	-66.6		(225)	
	18-3-018	150	(-44.6)	(238.9)	(250)	018 and 021 directions discordant
	18-3-021	150	(+16.1)	(245.6)	>> 200	
	18-3-051	100	-75.0	279.3	>>200	
	18-3-057	150	-72.8	277.4	>>200	
	18-3-059	100	-77.5	270.0	>>200	
	18-3-079	150	(-17.9)		(350)	Unstable
3	19-1-040	100	+80.8	257.3	284	Pilot
	19-1-042	100	+80.4	253.5	412	Pilot
	19-1-067	200	+75.3		>>200	
	19-1-102	150	+79.1	330.6	>>200	
	19-1-110	150	+79.4	321.0	(250)	
	19-2-098	200	(+80.4)	(352.9)	>>200	098 and 103 directions discordant
	19-2-103	200	(-69.9)	(358.2)	>>200	

Appendix I (continued)

Unit	Specimen	Field	Incl.	Decl.	MDF	Comments
<u>Site 215 (cont.)</u>						
4	20-1-097	150	-53.6	59.2	(275)	097 and 099 directions barely concordant
	20-1-099	150	-78.4	50.2	(300)	
	20-1-121	100	(+80.2)	(320.0)	775	Pilot; 121 and 135 directions discordant
	20-1-135	200	(-74.7)	(222.4)	300	
	20-2-013	150	-76.2		>>200	Pilot
	20-2-092	200	-81.2		176	
	20-2-102	150	-79.3	161.6	>>200	102 and 108 directions barely concordant
	20-2-108	150	-54.6	198.4	>>200	
	20-2-120	150	+79.3		>>200	Long piece of core probably was inverted during handling
	20-3-056	200	-82.1	130.4	(300)	
	20-3-064	150	-70.5	171.9	(250)	056 and 064 directions barely concordant
	20-3-076	200	-77.0		>>200	
	20-3-138	200	-61.5		(250)	
	20-4-002	200	-74.0		171	
	20-4-015	50	(-60.1)	(62.9)	92	Pilot; 015 and 022 directions discordant
	20-4-022	150	(-80.8)	(309.8)	249	
	20-4-094	150	-75.7		(250)	Pilot
<u>Site 216</u>						
2	36-4-022	150	+71.9	219.1	(300)	Pilot
	36-4-026	150	+63.7	221.2	426	
	36-4-028	150	+63.0	217.0	(250)	
3	36-4-093	150	+62.3		222	Pilot; tuff
	36-4-109	100	+71.7		193	Tuff
4	37-1-084	400	+71.8		557	Pilot
	37-1-119	150	+70.4	143.7	(425)	
	37-1-122	150	+72.9	141.2	(425)	
	37-2-005	150	+71.3	280.9	379	Pilot
	37-2-017	150	+69.6	285.4	305	Pilot
	37-2-103	100	+69.8		115	Pilot; alteration zone
	37-3-043	150	+67.6	292.8	94	
	37-3-046	200	+68.9	290.1	122	
	37-3-070	100	+72.1	59.2	147	
	37-3-079	150	+73.6	40.8	96	

Appendix I (continued)

Unit	Specimen	Field	Incl.	Decl.	MDF	Comments	
<u>Site 216</u> (cont.)							
5	37-3-113	150	+67.2	100.5	(250)		
	37-3-121	200	+74.8	102.9	(350)		
	37-4-054	200	+73.5	140.6	(250)		
	37-4-059	200	+73.2	149.3	(250)		
	37-4-099	200	+72.3	228.9	319	Pilot	
	37-4-104	150	+68.5	217.4	345	Pilot; alteration zone	
	37-4-106	150	+71.7	235.0	349	Pilot; alteration zone	
	37-4-142	100	+68.8		(250)		
	38-1-058	150	+71.9	140.8	(250)		
	38-1-060	200	+73.1	137.7	(275)		
	38-1-100	150	+70.0	146.9	(450)		
	38-1-102	150	+70.5	146.6	(475)		
	6	38-2-032	200	+68.6		617	
		38-2-131	200	+67.8	289.0	279	Pilot
38-2-134		100	+67.9	284.5	273	Pilot	
38-3-031		200	+66.4	162.9	(425)		
38-3-037		150	+64.0	163.7	(425)		
38-3-040		150	+64.3	169.9	176		
7	38-3-047	150	+72.6	239.5	(450)		
	38-3-054	100	+69.8	258.2	555	Pilot	
	38-3-133	100	+71.6	256.3	557	Pilot	
	38-3-145	100	+70.7	256.8	554	Pilot	
	38-3-147	200	+70.1	257.8	(500)		
8	38-4-030	150	+67.3	266.6	756	Pilot	
	38-4-032	100	+68.5	258.9	778	Pilot	
	38-4-054	200	+56.7	308.8	475		
	38-4-056	200	+58.1	306.9	450		

Appendix I notes:

- 1) The most stable cleaned directions are listed for all samples. Directions given in parentheses were not used in paleolatitude calculations for the reasons discussed in the text.
- 2) Declinations are fiducial only, and they do not indicate "true" declination. Declinations are given only for those specimens which were drilled from one coherent piece of core. The vertical bar denotes which specimens came from one piece.
- 3) MDF is median destructive field, the field at which the NRM intensity is reduced by 50%. MDF's given in parentheses are extrapolated values, given to the closest 25 oe.

Appendix II

STEREONET PLOTS
AND ALTERNATING FIELD DEMAGNETIZATION CURVES
FOR REPRESENTATIVE BASALT PILOT SPECIMENS

Appendix II

Stereonet Plots and Alternating Field Demagnetization Curves
for Representative Basalt Pilot Specimens

Semi-logarithmic plots of progressive alternating field cleaning are given for twenty-six pilot basalt specimens. Normalized intensity is plotted on the vertical axis and peak field strength (RMS) is plotted in the horizontal axis. Single measurements are indicated by a cross; replicate measurements are indicated by a vertical bar.

The directions observed after each cleaning step are plotted on an equal area stereonet. Where the points are tightly grouped an expanded scale is used and overlapping points are often omitted for clarity. Solid symbols and lines indicate the lower hemisphere (+ inclination) and open symbols and dashed lines indicate the upper hemisphere (- inclination). Symbols used: NRM - hexagon; 50 Oersted - small circle (often omitted); 100 Oe - square; 200 Oe - triangle; 400 Oe - diamond, 800 Oe - large circle; and 1200 Oe - star.

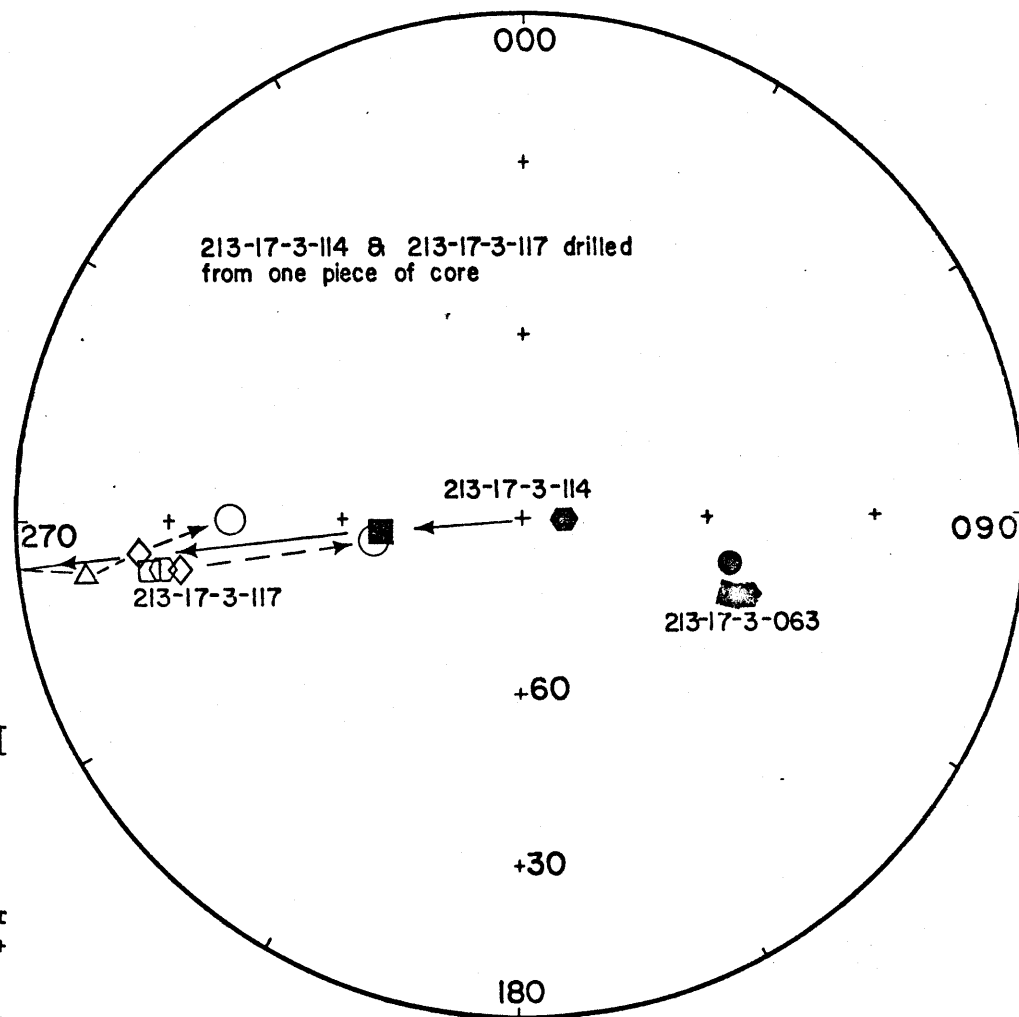
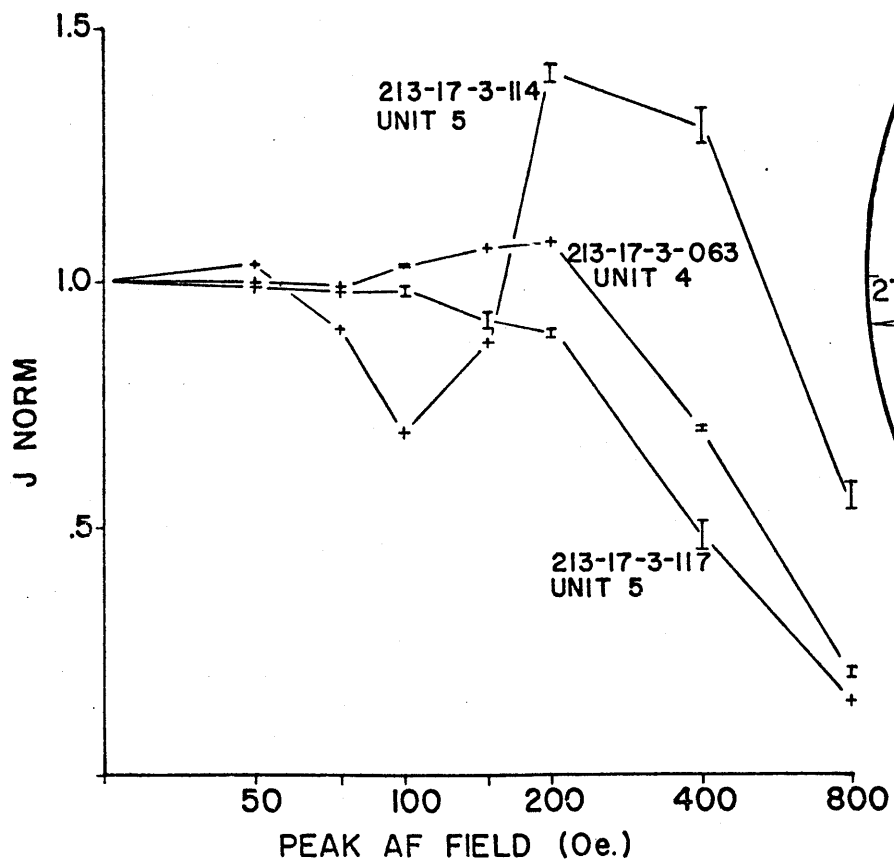
Note that many specimens were subsampled from an intact piece of drill core. Relative declinations were preserved between such specimens.

Data for the following specimens are plotted:

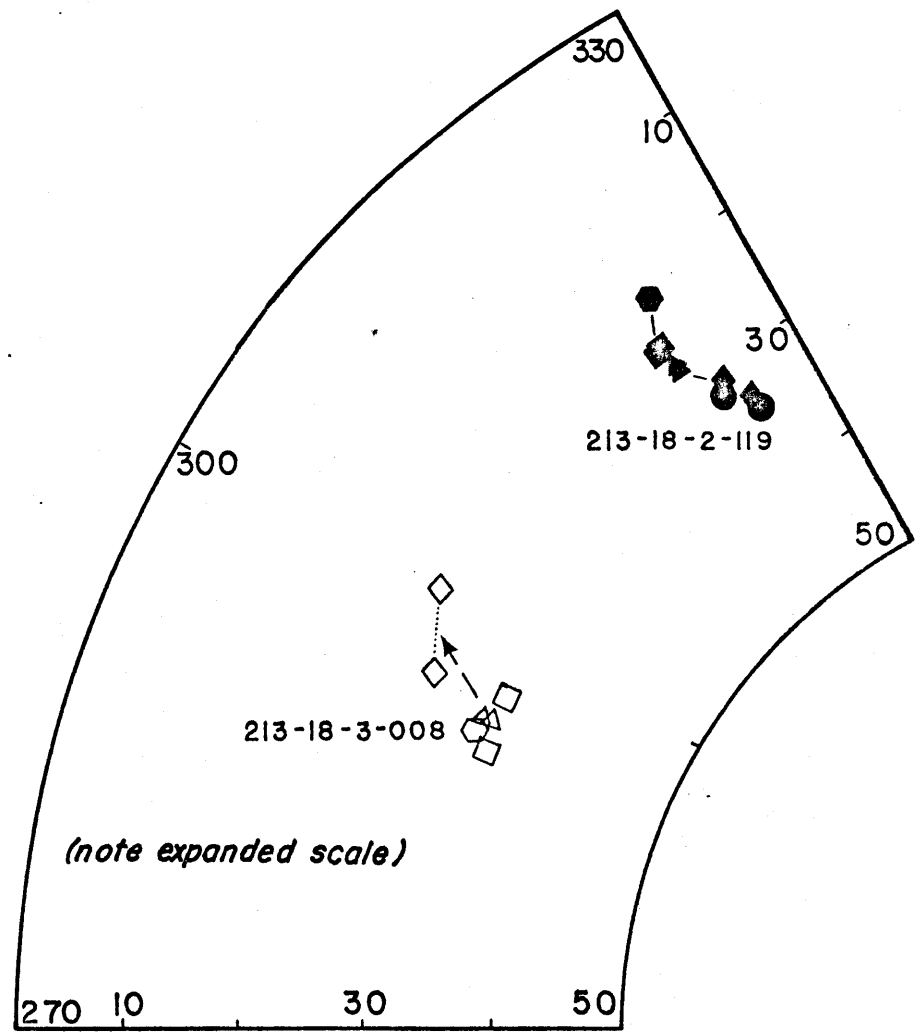
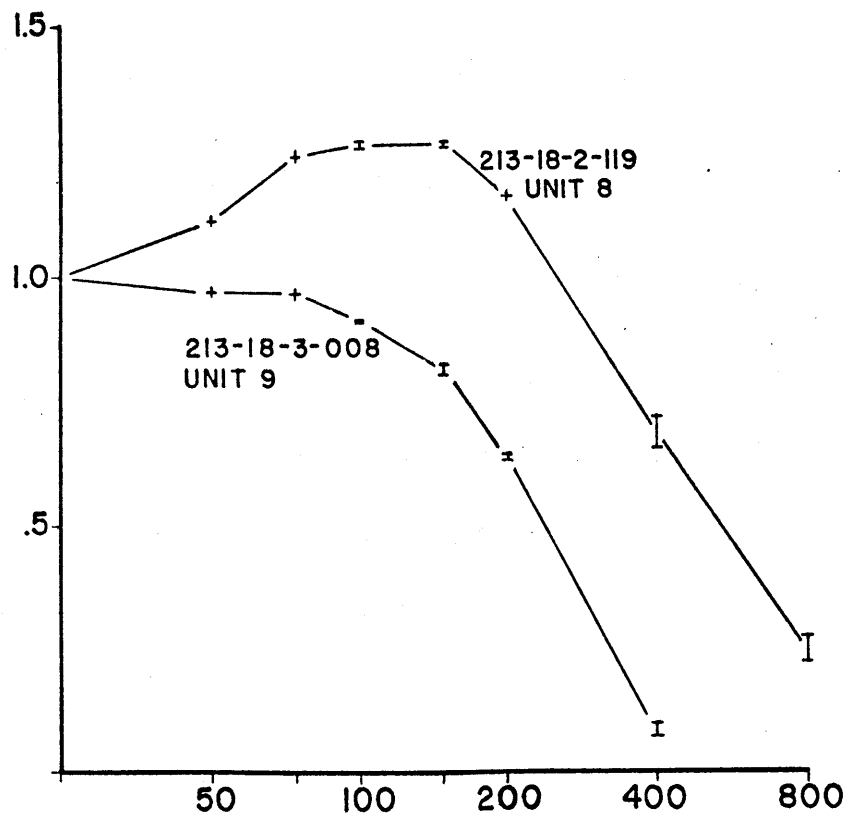
- | | | |
|----|--------------------------------------|------------------|
| 1. | 213-17-3-063
213-17-3-114 and 117 | Unit 4
Unit 5 |
| 2. | 213-18-2-119
213-18-3-008 | Unit 8
Unit 9 |
| 3. | 214-48-1-142 and 145 | Unit 1 |

- | | | |
|-----|---------------------------|--------------------------|
| 4. | 214-54-3-060 and 068 | Unit 9 |
| 5. | 215-18-1-056 | Unit 2 |
| | 215-18-1-079 | Unit 2 |
| 6. | 215-19-1-040 and 042 | Unit 3 |
| 7. | 215-20-1-121 and 135 | Unit 4 |
| 8. | 216-36-4-026 | Unit 2 |
| | 216-36-4-093 | Unit 3 |
| 9. | 216-37-1-084 | Top, unit 4 |
| | 216-37-2-005 and 017 | Unit 4 |
| | 216-37-2-103 | Local alteration, unit 4 |
| 10. | 216-37-4-99, 104, and 106 | Unit 5 |
| | 216-38-2-131 and 134 | Unit 6 |

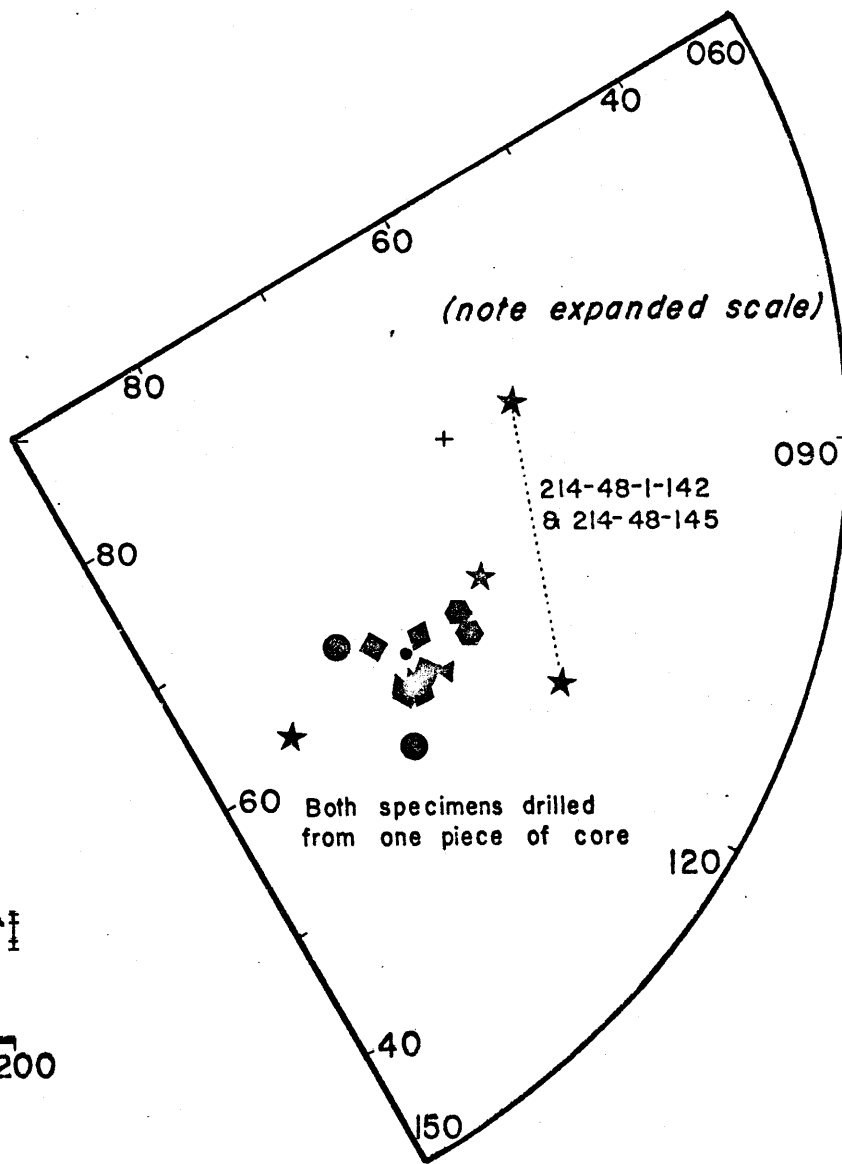
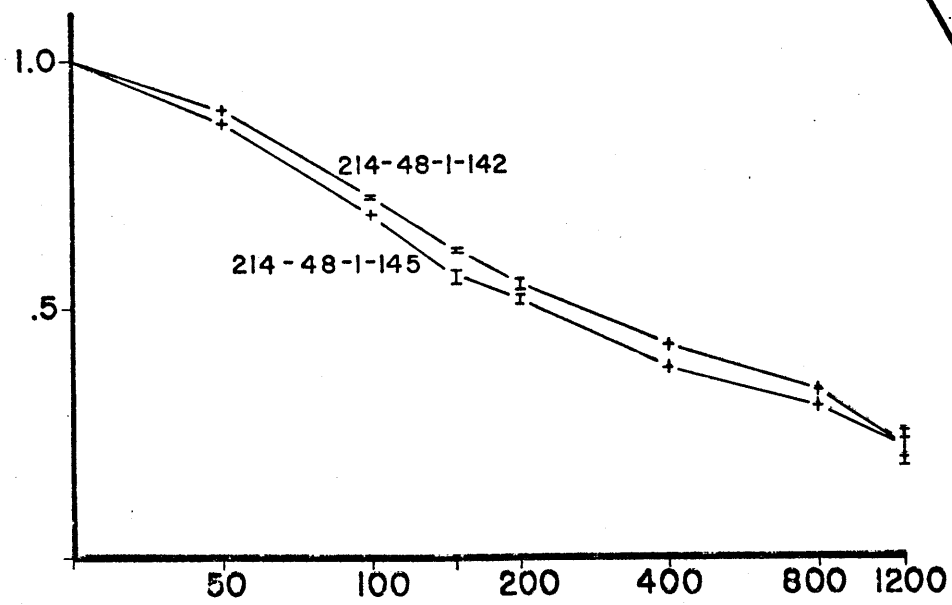
DSDP SITE 213
COOLING UNITS 4 AND 5



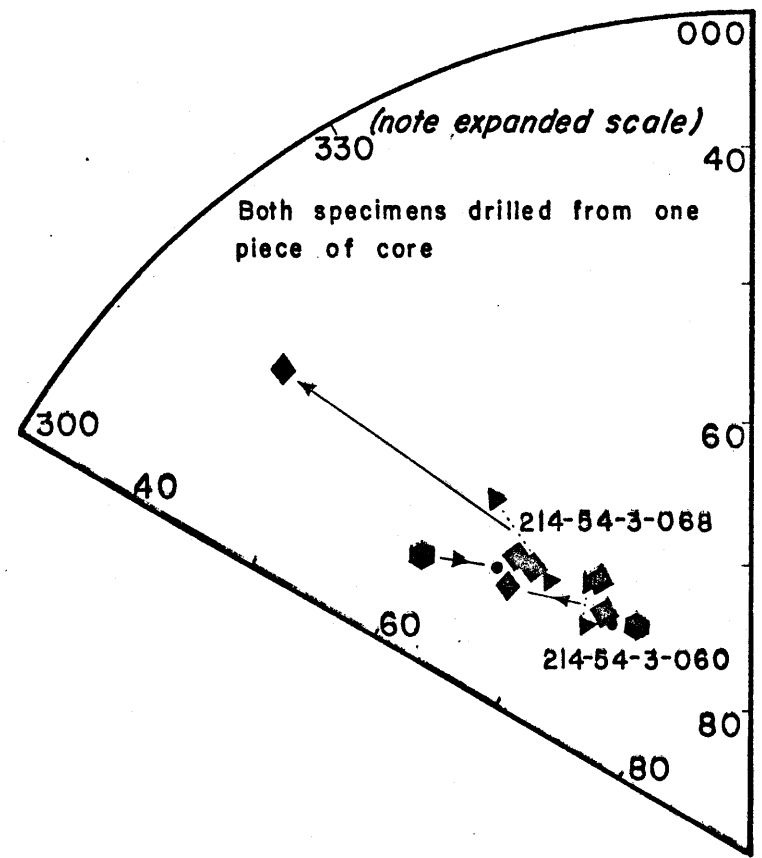
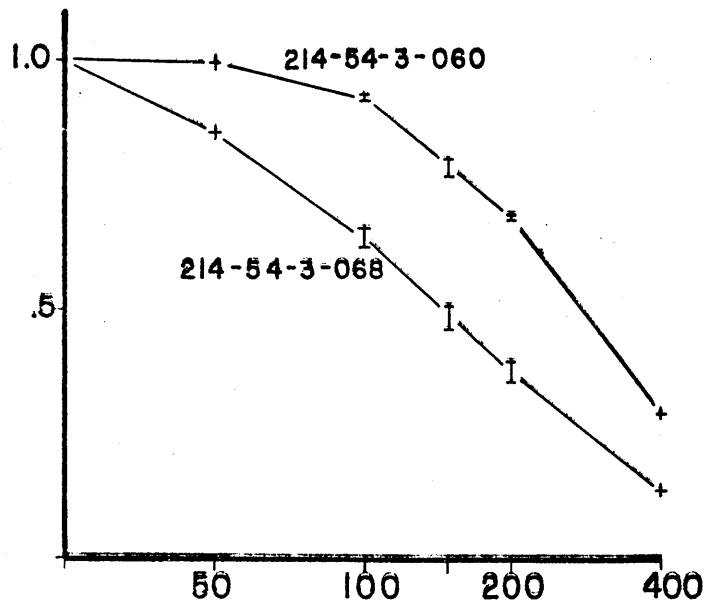
DSDP SITE 213
COOLING UNITS 8 AND 9



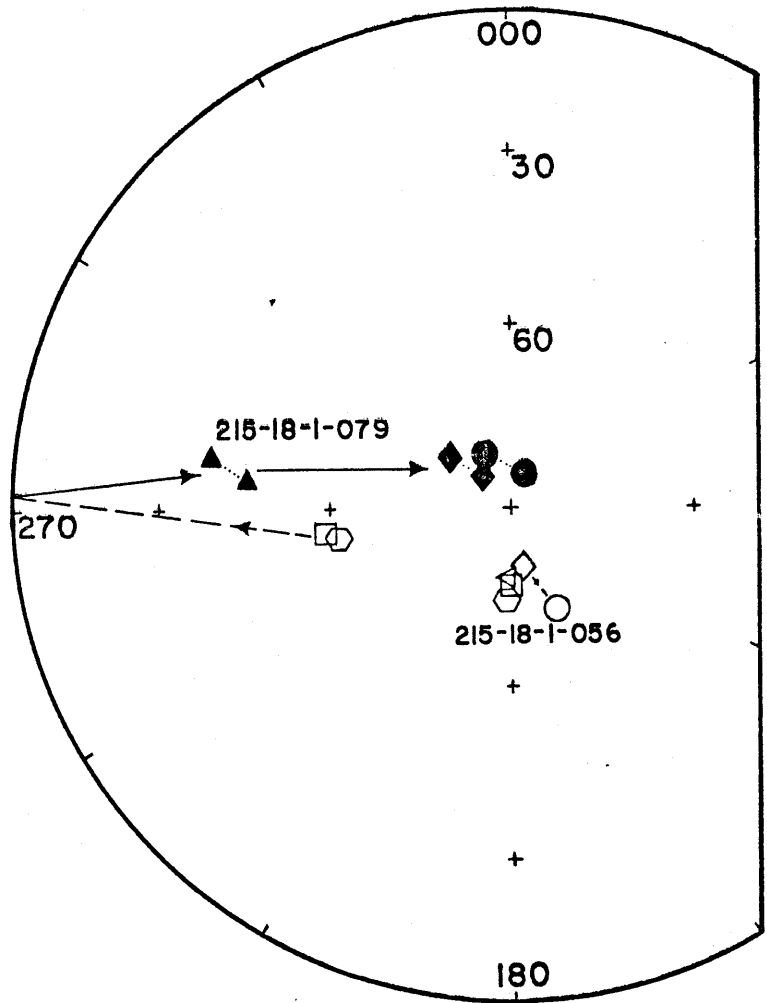
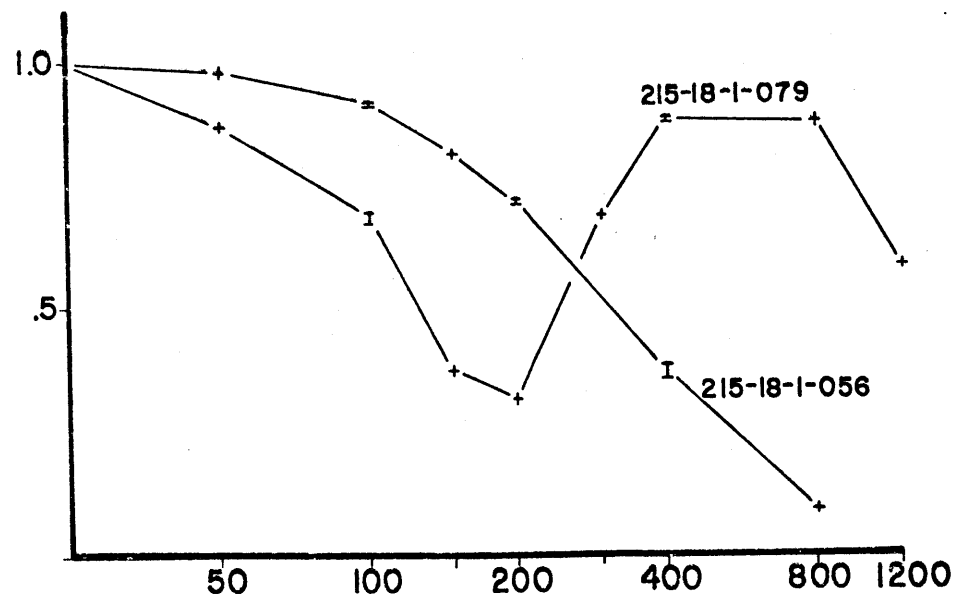
DSDP SITE 214
COOLING UNIT I



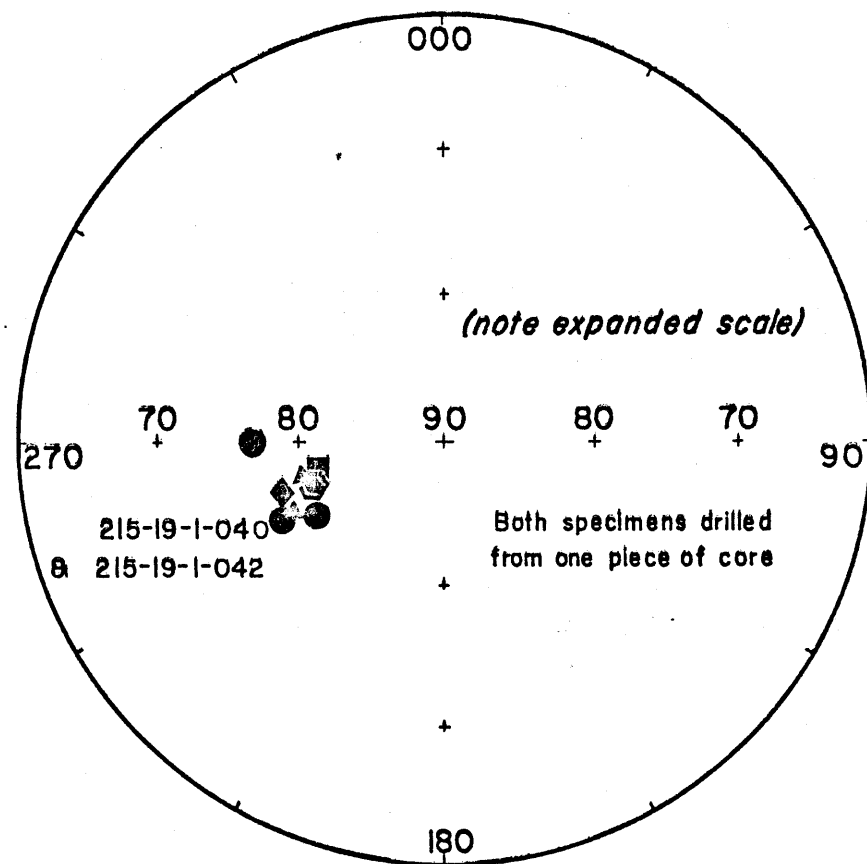
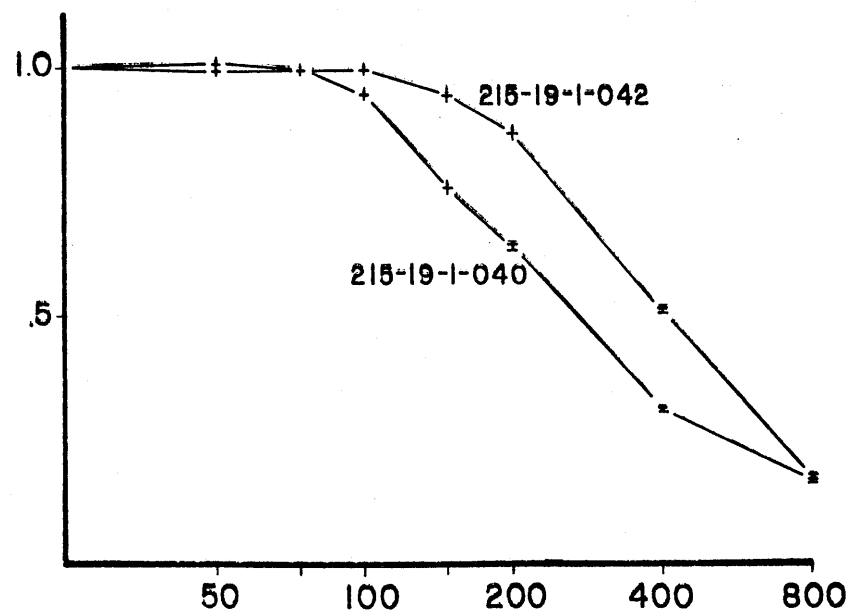
DSDP SITE 214
COOLING UNIT 9



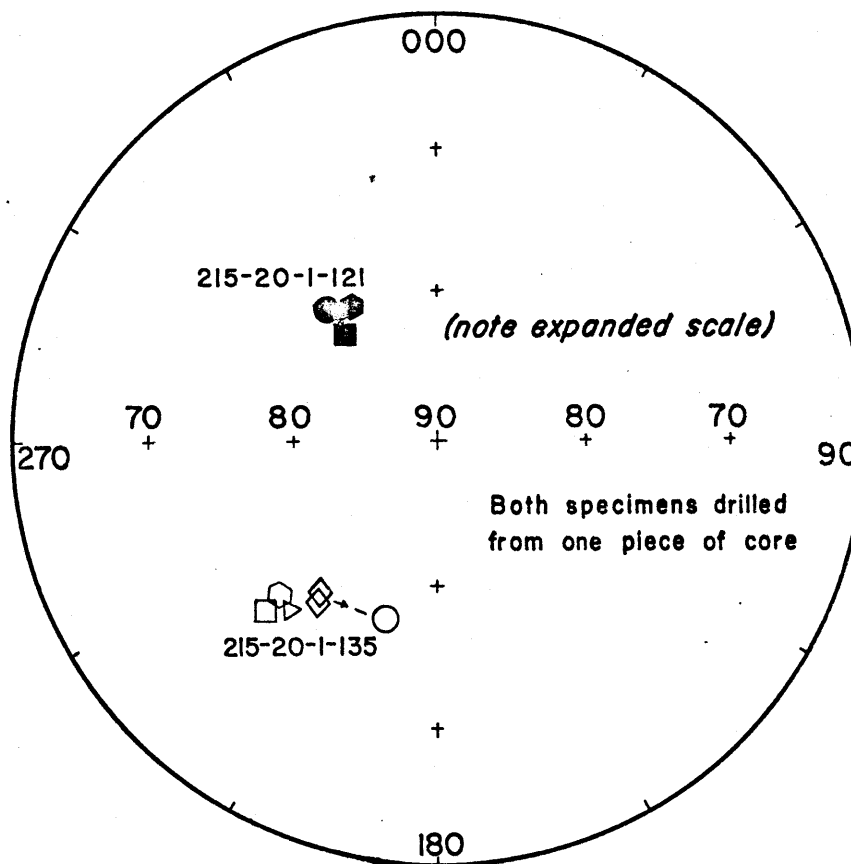
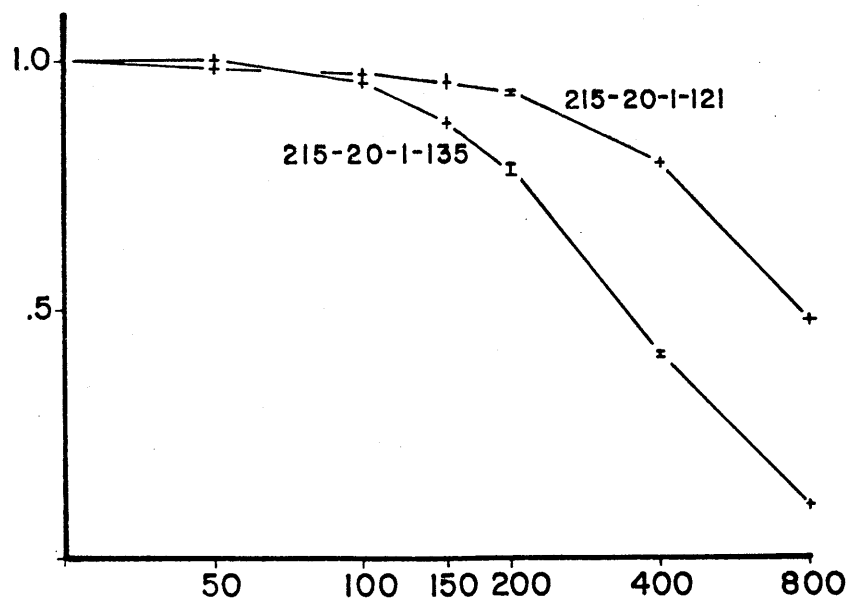
DSDP SITE 215
COOLING UNIT 2



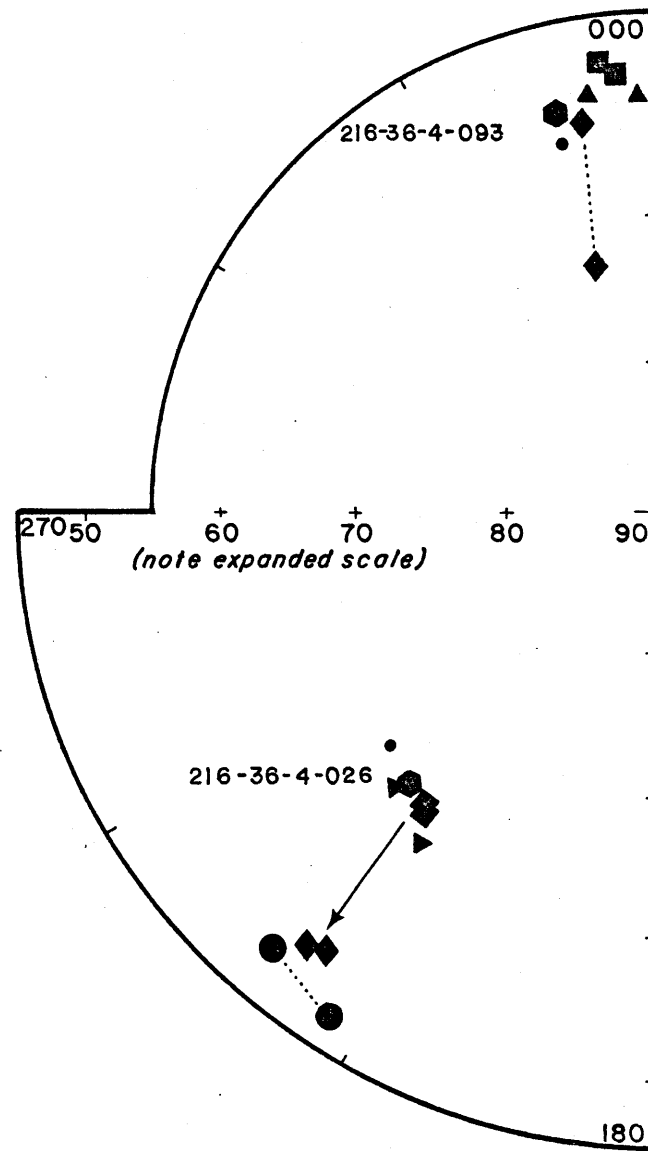
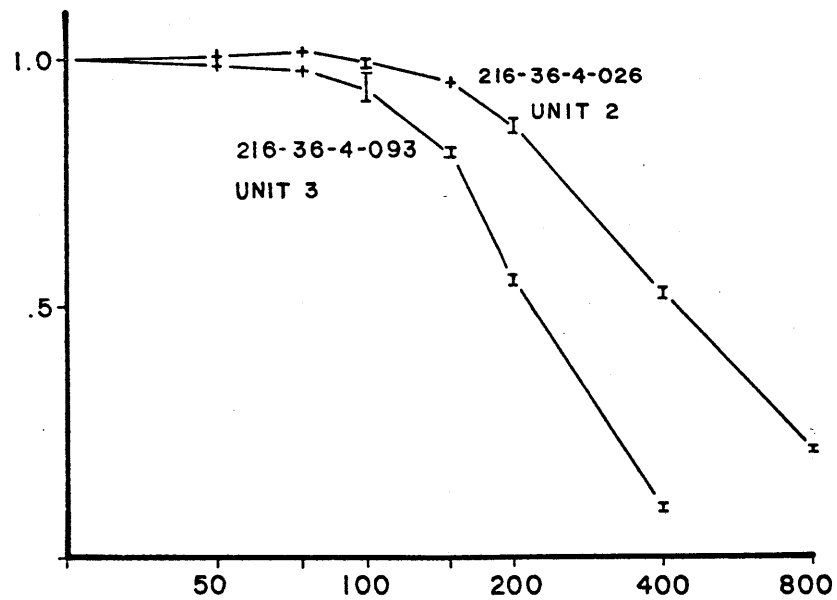
DSDP SITE 215
COOLING UNIT 3



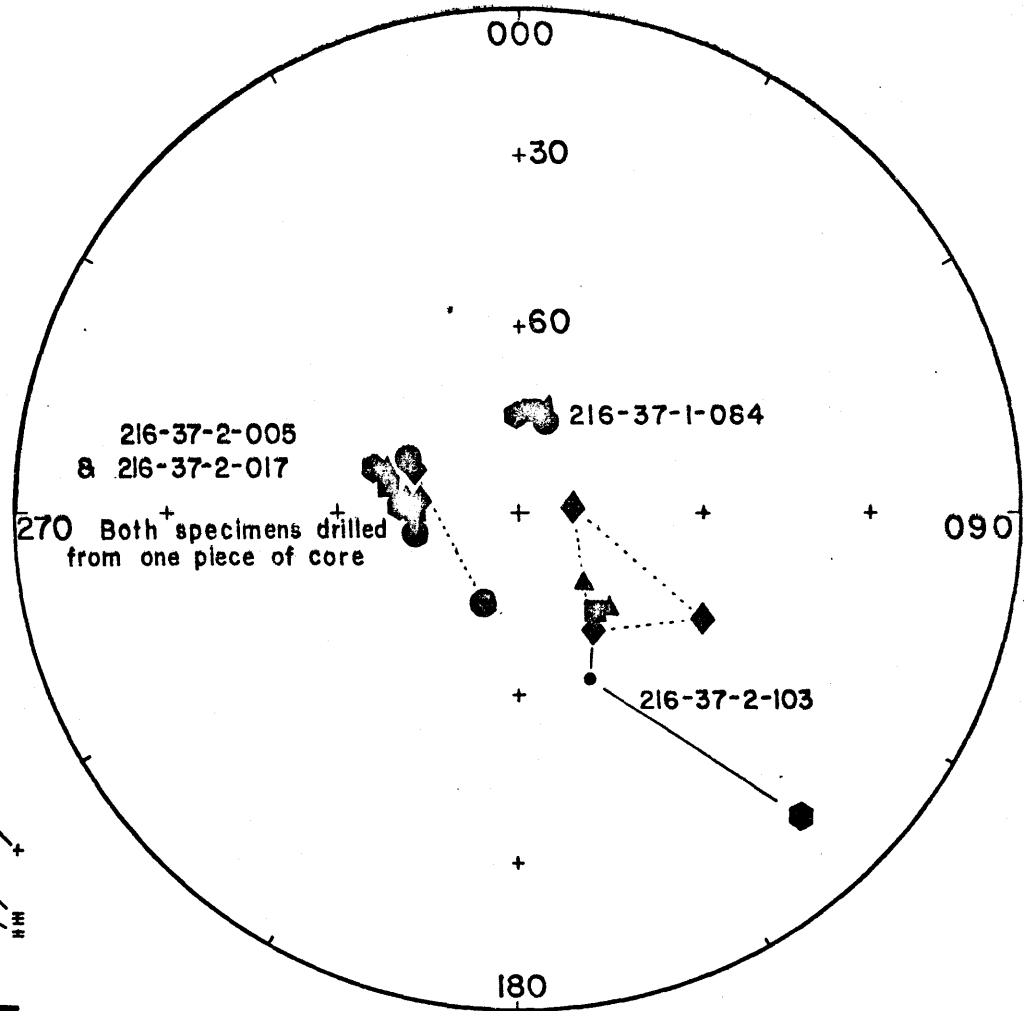
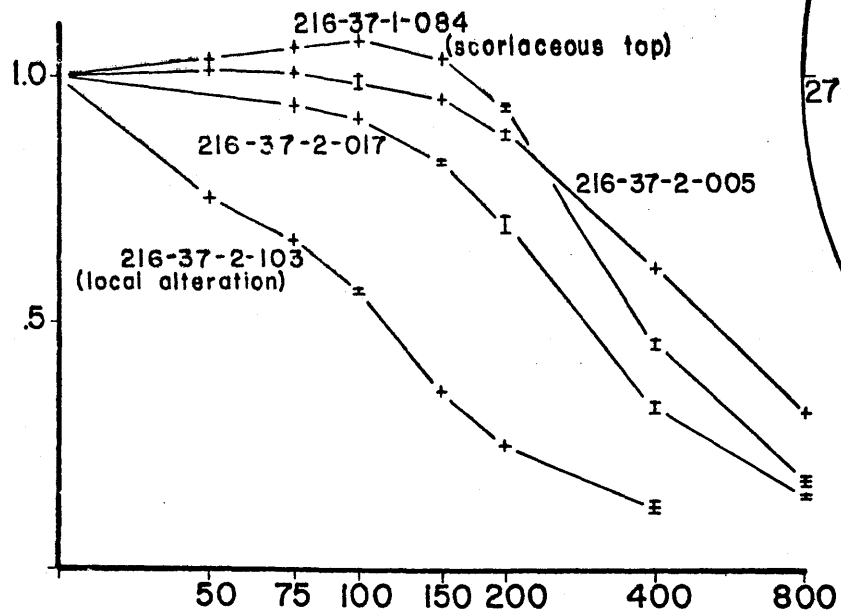
DSDP SITE 215
COOLING UNIT 4



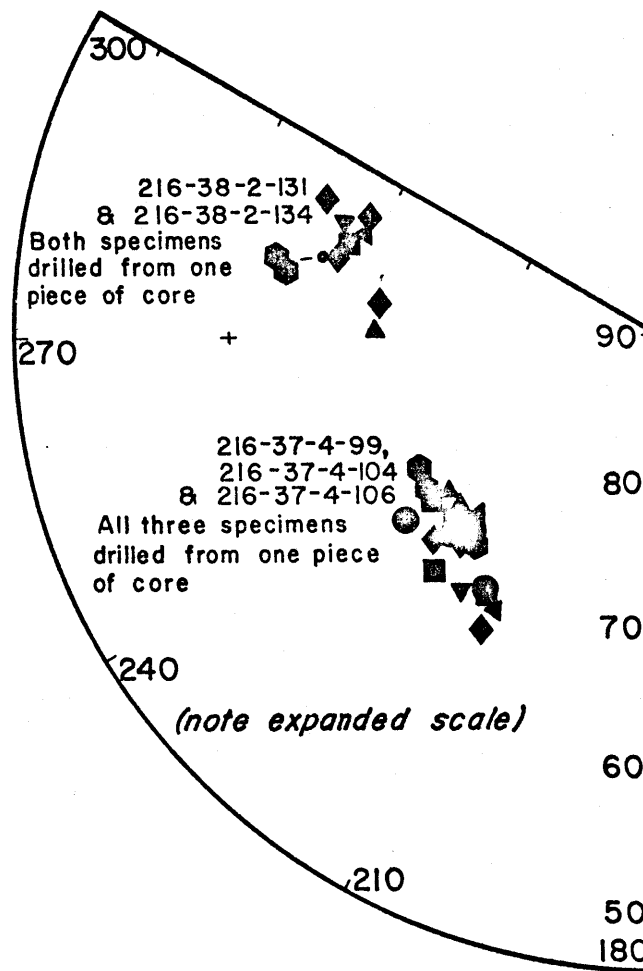
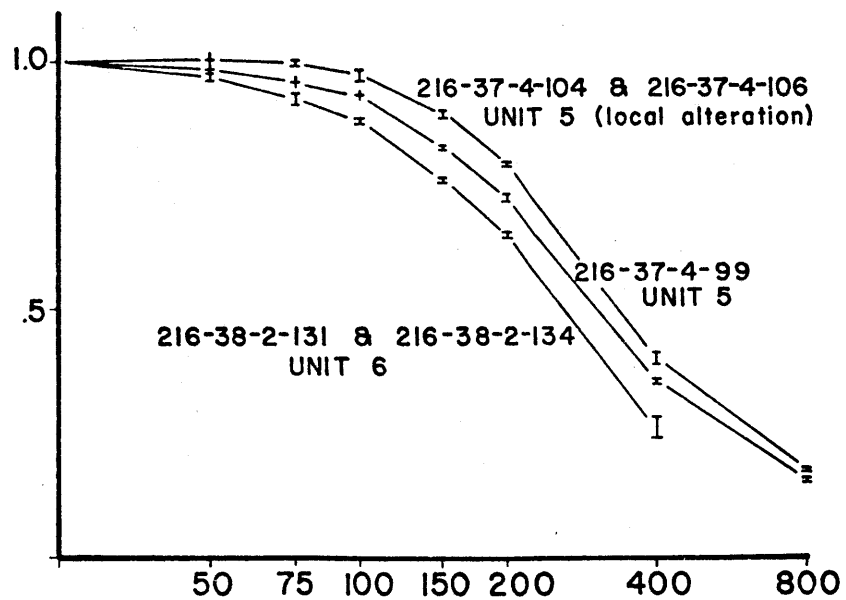
DSDP SITE 216 COOLING UNITS 2 AND 3



DSDP SITE 216
COOLING UNIT 4



DSDP SITE 216
COOLING UNITS 5 AND 6



Appendix III

SEDIMENT SPECIMEN DIRECTIONS

APPENDIX III

SEDIMENT SPECIMEN DIRECTIONS

Site	1 Age	Specimen	Field	2 Incl.	3 Decl.	Comments
214	57-60	44-1-014	100	(+1.2)	(255.4)	014, 018 and 021 directions discordant
		44-1-018	100	(+60.8)	(1.5)	
		44-1-021	100	(+49.1)	(16.0)	
		44-1-071				No cleaned direction
		44-1-086	200	+44.8	211.5	Pilot
		44-1-090	100	+46.1	219.2	
		44-1-103	100	(-20.2)		< 1 x 10 ⁻⁶
		44-1-126	100	+45.4	274.7	
		44-1-129	100	+37.6	264.6	
		44-1-132	100	(-11.5)	(183.1)	Discordant direction
		46-3-014	100	+50.5		
		46-3-073				No cleaned direction
		46-3-092	100	(+8.4)		Pilot; < 1 x 10 ⁻⁶
		46-3-098	100	(+77.5)		< 1 x 10 ⁻⁶
215	57-58	15-4-104	100	-57.3		
		15-4-114	100	-68.0		
		15-5-045	100	-55.9		
		15-5-095	150	-56.0		Pilot
		15-5-114	200	(+46.7)		Pilot; reversed on demag.; < 1 x 10 ⁻⁶
		15-5-133				No cleaned direction
		15-5-139				No cleaned direction
		16-1-091	150	+66.9		
		16-1-098	150	+52.4		
		16-1-106	150	+47.5		
		16-1-109	150	+42.8		
		16-1-117	150	-35.1		
		16-1-120	150	(-63.8)		Pilot; < 1 x 10 ⁻⁶
		16-1-126	200	+58.9		Pilot
		16-1-128	150	+75.8		
		16-1-131	150	+67.1		

Appendix III (continued)

Site	Age	Specimen	Field	Incl.	Decl.	Comments
215 (con.)	57-58	16-4-028	150	+56.4		
		16-4-128	150	+54.9	280.5	
		16-4-131	150	(+25.5)	29.3	Anomalous direction unrelated to 128
		16-5-011	150	+57.2		
		16-5-051	150	+51.5		
		16-5-057	150	+58.3		
		16-5-060	150	+55.3		
		16-5-071	150	+57.2		
		16-5-085	150	+44.6		
		16-5-095	150	+40.9		
		16-5-100	150	+57.0		
		16-5-110	150	+55.6		
		16-5-113	150	+51.2		
		16-5-120	150	+61.6		
		16-5-125	150	+55.3		
		16-5-128	200	+63.3		Pilot
		16-5-138	150	+60.3		
16-4-140	200	+67.4		Pilot		
216	22-30	9-1-040	120	(0.0)	(322.4)	040, 045, and 051 < 1×10^{-6} and concordant, but discordant with core 9-2
		9-1-045	170	(-1.0)	(314.0)	
		9-1-051	120	(-0.5)	(303.3)	
		9-1-085	120	(-8.3)	(220.8)	085, 091 and 104 discordant and
		9-1-091	170	(-54.0)	(226.5)	< 1×10^{-6}
		9-1-104	120	(-5.6)	(280.7)	
		9-2-062	120	+19.3		
		9-2-084	120	+15.3	297.2	
		9-2-089	120	+14.3	295.9	
		9-2-093	120	+12.3	294.7	
		9-2-101	120	+14.8	293.5	
		9-2-107	120	+15.3	295.6	
		10-1-086	120	(+51.7)	(355.8)	Pilot; < 1×10^{-6}
		10-1-091	120	-17.0	81.3	Pilot
		10-1-130	120	-26.9	211.9	130 and 135 directions concordant; < 1×10^{-6}
10-1-135	120	+24.9	218.3			

Appendix III (continued)

Site	Age	Specimen	Field	Incl.	Decl.	Comments
216 (con.)	26-34	13-1-144	120	(-1.7)		< 1 x 10 ⁻⁶
		14-1-147	220	+2 .3		
		14-2-057	170	+17.6	206.8	
		14-2-062	120	+23.0	204.8	Pilot
		14-2-069	120	+20.9	203.1	Pilot
		14-2-115	220	+43.6	287.5	
		14-2-120	120	+23.0	284.0	
		14-2-125	170	+22.4	282.7	
		14-2-131	170	+19.4	280.5	
		14-3-077	120	+21.0	182.1	077, 081 and 087 directions concordant; < 1 x 10 ⁻⁶
		14-3-081	120	+28.0	182.0	
		14-3-087	170	+23.6	185.7	
		14-3-115	220	+17.5	261.4	
		14-3-120	220	-15.5	225.5	
216	37.5-43	15-3-099	120	+34.8	153.7	099, 104, 110, 117 directions concordant; < 1 x 10 ⁻⁶
		15-3-104	170	+35.5	164.7	
		15-3-110	120	+32.8	154.5	
		15-3-117	120	+44.9	151.4	
		16-1-098	120	+22.2	129.7	
		16-1-105	170	+25.9	131.5	
		16-1-111	120	+24.1	135.1	
		16-1-117	120	+24.2	139.8	
		16-2-009	120	(-52.7)	(338.4)	009, 013, 016, 023 directions discordant, < 1 x 10 ⁻⁶
		16-2-013	120	(-41.2)	(235.1)	
		16-2-016	170	(-45.0)	(272.3)	
		16-2-019	120	(-34.6)	(328.0)	
		16-2-023	120	(-0.6)	(350.7)	
		16-2-085	120	+22.9	240.9	
16-2-089	120	+20.4	240.9	Pilot		
16-2-093	120	+15.2	242.0	Pilot		

Appendix III (continued)

Site	Age	Specimen	Field	Incl.	Decl.	Comments
216 (con.)	65-68	36-1-042	100	+65.9	118.8	
		36-1-046	100	+54.9	123.7	
		36-1-054	100	+64.9	141.1	
		36-1-060	100	+51.8	152.5	
		36-1-122	150	+60.4	294.8	
		36-1-128	150	+58.8	317.0	
		36-1-136	200	+77.3	242.1	Pilot
		36-1-144	200	+75.0	224.0	Pilot
		36-2-003	100	-66.5		Pilot
		36-2-052	175	+70.1	22.4	Pilot
		36-2-057	175	+69.9	17.9	Pilot
		36-2-079	100	+83.3	31.8	
		36-2-085	100	+79.0	26.3	
		36-2-101	100	+68.2		
		36-2-107	100	+76.6		
		36-2-141	100	+73.1		Pilot
		217	15-21	6-3-028	100	(+62.8)
6-3-031	100			(+80.3)	(317.5)	
6-3-041	200			+17.3	228.9	Pilot
6-3-047	200			+15.3	212.0	Pilot
6-3-079	150			(+18.4)	(59.3)	079, 083, 087, and 090 directions discordant; 087 and 090 $< 1 \times 10^{-6}$
6-3-083	100			(+40.2)	(65.5)	
6-3-087	100			(+21.7)	(294.1)	
6-3-090	100			(+5.0)	(326.6)	
6-4-008	100			+14.0		
6-4-011	100			+6.8		
6-4-048	100			-0.9	280.6	
6-4-052	100			-4.8	280.8	
6-6-015	100			1.4	123.7	
6-6-019	100			-7.4	130.5	
6-6-026	100			(+12.8)		$< 1 \times 10^{-6}$
6-6-075	100			(-18.5)	(181.2)	075, 078, 081, 084 and 087 directions dis- cordant; $< 1 \times 10^{-6}$
6-6-078	100			(+8.3)	(22.8)	
6-6-081	100			(+55.6)	(318.4)	
6-6-084	100			(+28.9)	(66.2)	
6-6-087	100	(+18.1)	(195.2)			

Appendix III (continued)

Site	Age	Specimen	Field	Incl.	Decl.	Comments
217 (con.)	26-30	8-3-109	100	-8.1	80.9	109 and 114 directions concordant; $< 1 \times 10^{-7}$
		8-3-114	100	-10.3	79.8	
		8-3-133	150	-25.3	69.1	133, 136, 140, 144, and 147 directions concordant; $< 1 \times 10^{-7}$
		8-3-136	150	-20.2	54.8	
		8-3-140	150	-28.4	50.4	
		8-3-144	150	(-20.5)	(10.8)	
		8-3-147	100	(-7.8)	(348.1)	
		8-4-020	200	-8.3	272.8	020, 023, 027, 031, 034, 039 directions concordant; $< 1 \times 10^{-6}$
		8-4-023	200	-0.5	272.3	
		8-4-027	200	-9.2	264.8	
		8-4-031	200	-8.3	273.6	
		8-4-034	100	-6.7	270.9	
		8-4-039	200	-1.3	275.9	
		8-4-113	100	(+56.2)	(8.7)	113 and 118 directions discordant; $< 1 \times 10^{-7}$
		8-4-118	150	(+34.7)	(223.7)	
		8-5-129	100	-7.4	256.3	129 and 135 directions concordant; $< 1 \times 10^{-6}$
		8-5-135	100	-12.7	255.2	
217	30-40	9-2-024	150	+16.0	44.2	024, 029, 037 directions concordant; $< 1 \times 10^{-7}$
		9-2-029	100	-4.9	36.3	
		9-2-037	150	+14.9	29.5	
		9-2-053	100	-5.1	95.1	053, 062, 067, 071 directions concordant; 058 discordant; all except 058 $< 1 \times 10^{-6}$

Appendix III (continued)

Site	Age	Specimen	Field	Incl.	Decl.	Comments	
217 (con.)	30-40	9-2-058	100	(+0.2)	(237.2)	↑	
		9-2-062	100	+6.1	97.0		
		9-2-067	100	+1.1	90.3		
		9-2-071	100	-14.8	82.9		
		9-3-074	100	(-13.6)	(30.7)		074 and 083 directions discordant; < 1 x 10 ⁻⁶
		9-3-083	100	(+28.2)	(67.7)		
		9-3-128	100	+24.5	157.0		128 and 137 directions concordant; < 1 x 10 ⁻⁶
		9-3-137	100	+28.3	154.5		
		9-3-083	100	(+42.4)	(48.1)		083, 087, 104 and 111 directions discordant; < 1 x 10 ⁻⁶
		9-4-087	100	(+33.6)	(326.5)		
		9-4-104	100	(+24.0)	(-42.0)		
		9-4-111	150	(+24.3)	(69.3)		
		9-5-034	150	(-45.1)	(242.4)		034 and 041 directions discordant; < 1 x 10 ⁻⁶
		9-5-041	100	(-18.3)	(159.0)		
		9-5-068	100	(+33.9)	(346.6)		068, 071, 076, 080 directions discordant; < 1 x 10 ⁻⁶
		9-5-071	100	(+34.0)	(86.0)		
		9-5-076	150	(+18.0)	(104.2)		
		9-5-080	100	(+45.4)	(343.4)		
		9-5-120	100	+31.8	144.3		120 and 126 directions concordant; 120 < 1 x 10 ⁻⁶
		9-5-126	100	+26.8	141.9		

Appendix III

Site	Age	Specimen	Field	Incl.	Decl.	Comments		
217 (con.)	45.5-48	10-1-130	200	-22.5	248.9	130 and 136 directions concordant; < 1×10^{-7} ; pilots		
		10-1-136	200	-17.0	252.7			
		10-2-140	100	-16.4	354.0	140 and 146 directions concordant; < 1×10^{-7}		
		10-2-146	100	+23.4	357.1			
		10-4-038	100	-9.1	87.4	038 and 043 directions concordant; < 1×10^{-6}		
		10-4-043	100	-13.0	88.6			
		10-6-023	100	+34.8	261.7	023 and 029 directions discordant; < 1×10^{-8}		
		10-6-029	100	+49.0	141.1			
		217	56-59	14-1-003	100	+52.1	187.9	Pilot
				14-1-009	100	+58.4	204.9	Pilot
14-5-136	100			+39.5	175.0			
14-5-144	100			+47.2	176.6	Pilot		
14-5-147	100			+40.6	180.8	Pilot		
15-1-103	100			+50.1	276.6			
15-1-107	100			+47.6	292.1			
15-2-110	100			(+72.4)	(28.8)	110 and 113 directions discordant		
15-2-113	100			(+59.2)	(262.1)			
15-2-120	100			+63.5	66.2			
15-2-124	100			+55.8	61.4			
15-2-128	100			+51.5	62.2			
15-2-133	100			+54.6	50.1			
15-2-139	100	+62.9	71.6					

Notes to Appendix III

- 1) Age in mybp, according to Berggren (1972) time scale.
- 2) The most stable cleaned directions are listed for all samples. Directions given in parentheses were not used in paleolatitude calculations for the reasons discussed in the text.
- 3) Declinations are fiducial only, and they do not indicate "true" declination. Declinations are given only for those specimens which were drilled from one coherent piece of core. The vertical bar denotes which specimens came from one piece.

Appendix IV

STEREONET PLOTS
AND ALTERNATING FIELD DEMAGNETIZATION CURVES
FOR REPRESENTATIVE SEDIMENT PILOT SPECIMENS

Appendix IV

Stereonet Plots and Alternating Field Demagnetization Curve
for Representative Sediment Pilot Specimens

Semi-logarithmic plots of progressive alternating field cleaning are given for twenty pilot sediment specimens. Normalized intensity is plotted on the vertical axis and peak field strength (RMS) is plotted in the horizontal axis. Single measurements are indicated by a cross; replicate measurements are indicated by a vertical bar.

The directions observed after each cleaning step are plotted on an equal area stereonet. Where the points are tightly grouped an expanded scale is used and overlapping points are often omitted for clarity. Solid symbols and lines indicate the lower hemisphere (+ inclination) and open symbols and dashed lines indicate the upper hemisphere (- inclination). Symbols used: NRM - hexagon; 25 Oersted - small square; 50 Oe - small circle; 75 or 150 Oe - small dot (omitted except in cases of large motions); 100 Oe - square; 200 Oe - triangle; 400 Oe - diamond.

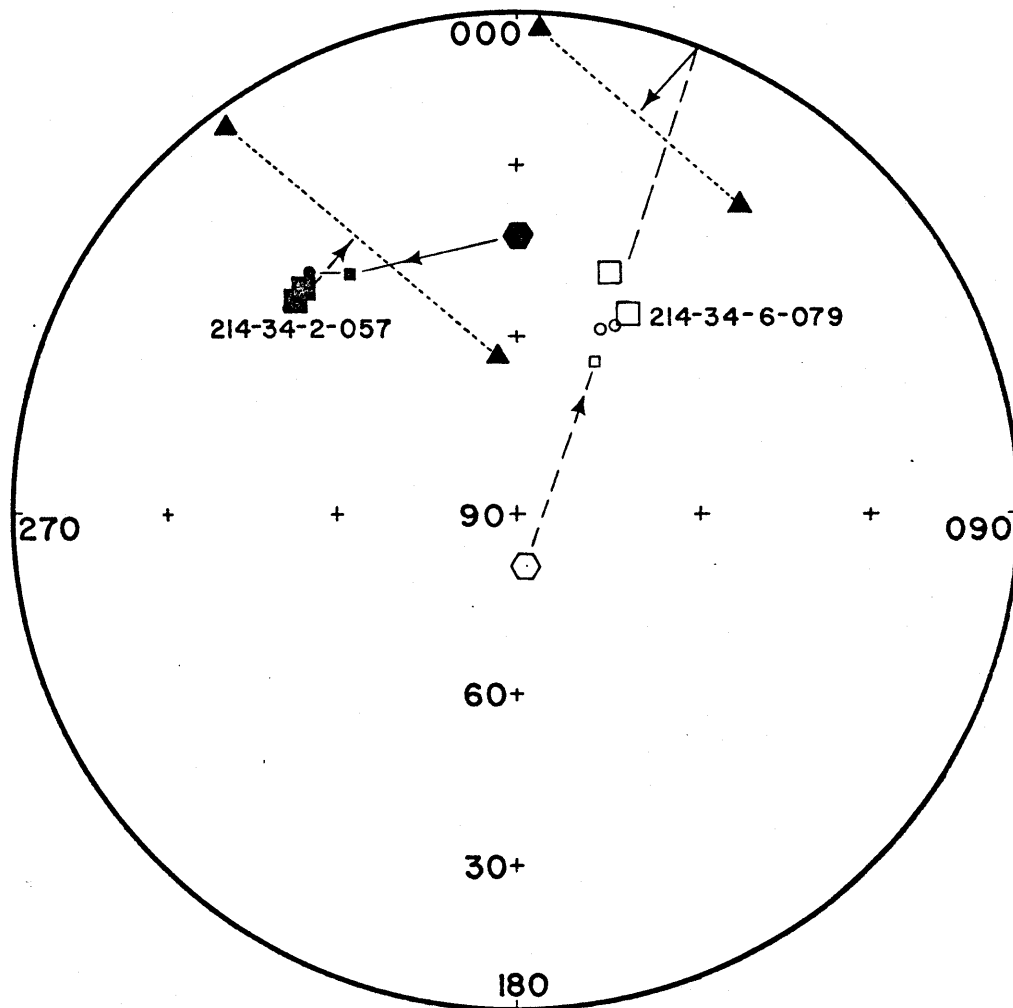
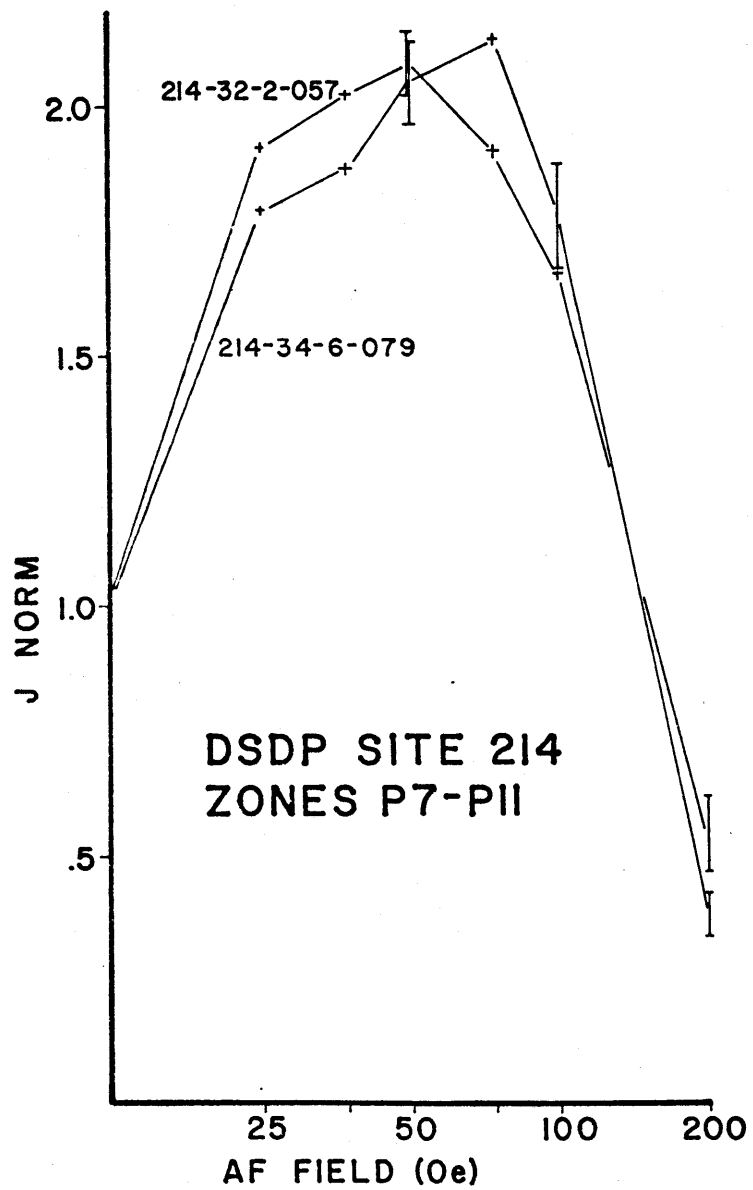
Note that many specimens were subsampled from an intact piece of drill core. Relative declinations were preserved between such specimens.

Data for the following specimens are plotted:

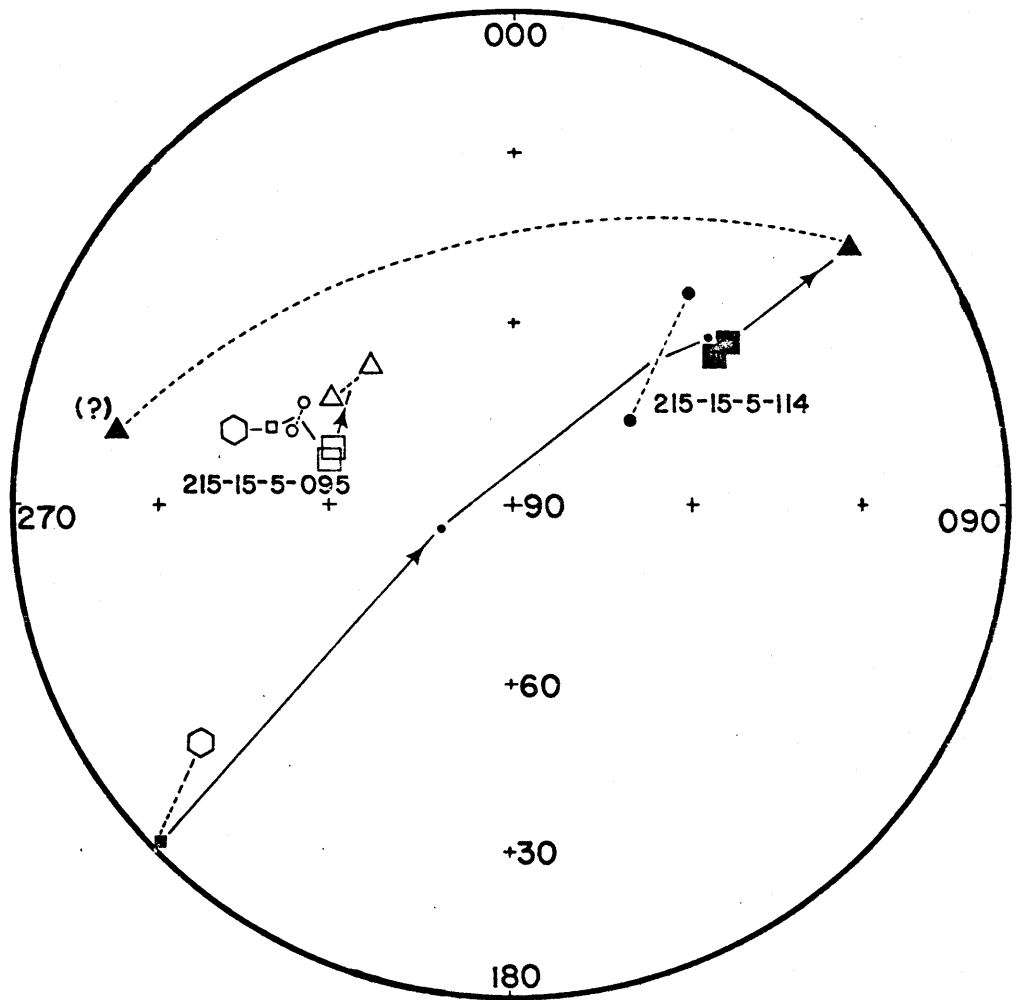
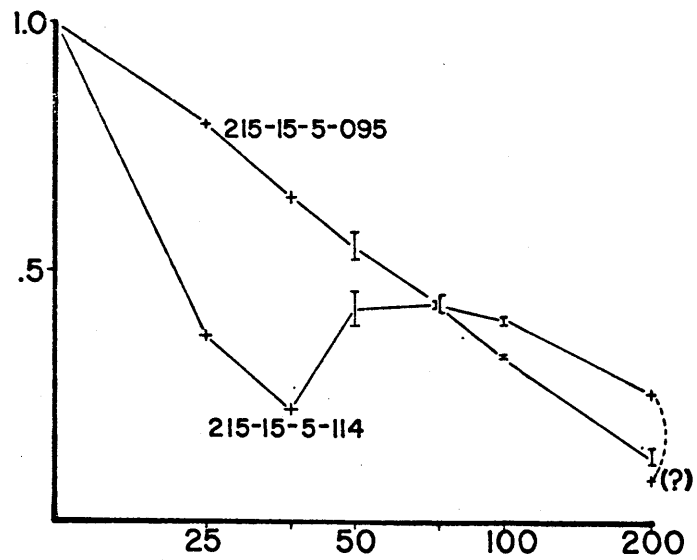
- | | | |
|----|------------------------------|--------------|
| 1. | 214-32-2-057
214-34-6-079 | Zones P7-P11 |
| 2. | 215-15-5-095
215-15-5-114 | Zone P4 |
| 3. | 215-16-5-128
215-16-5-140 | Zone P4 |

- | | | |
|-----|-------------------------------|------------------|
| 4. | 216-05-2-082*
216-05-2-096 | S. belemnos zone |
| 5. | 216-10-1-086 and 091 | Zone N4 |
| 6. | 216-14-2-062 and 069 | Zones P19-P21 |
| 7. | 216-36-1-136 and 144 | Maastrichtian |
| 8. | 217-6-3-041 and 047 | Zone N5 |
| 9. | 217-14-2-062 and 069 | Zone P21 |
| 10. | 217-14-5-144 and 147 | Zone P4 |

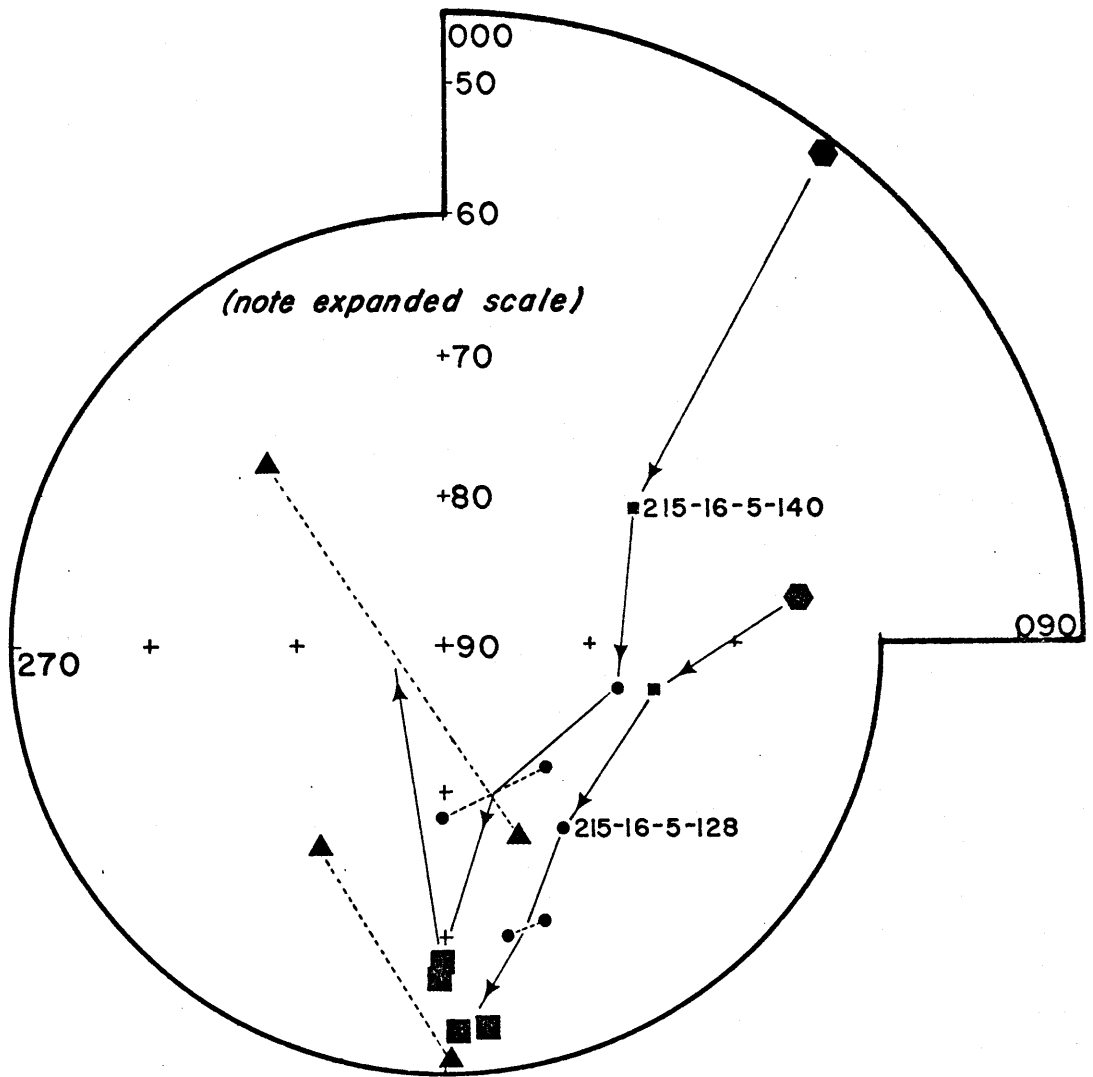
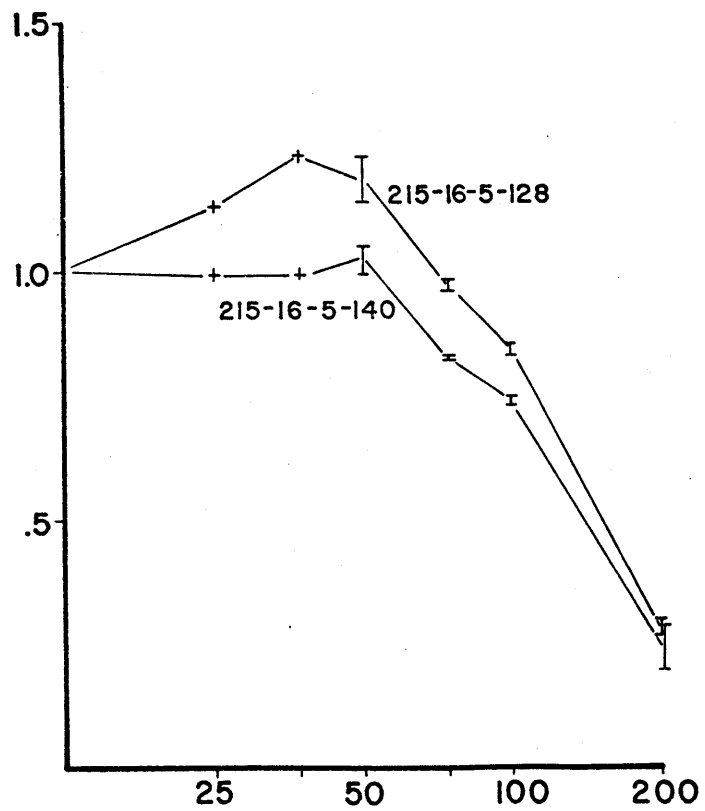
* These specimens were incorrectly referenced as 216-16-2-089 and 093 on page 164.



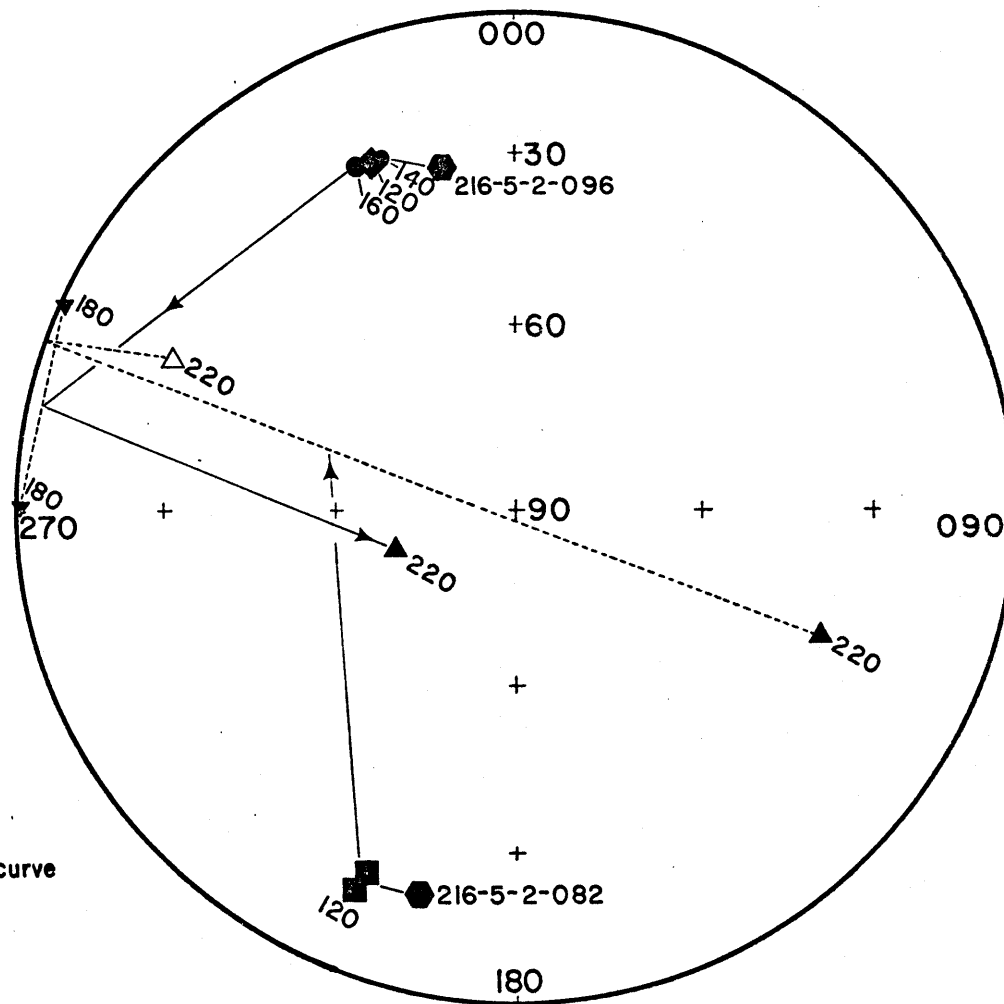
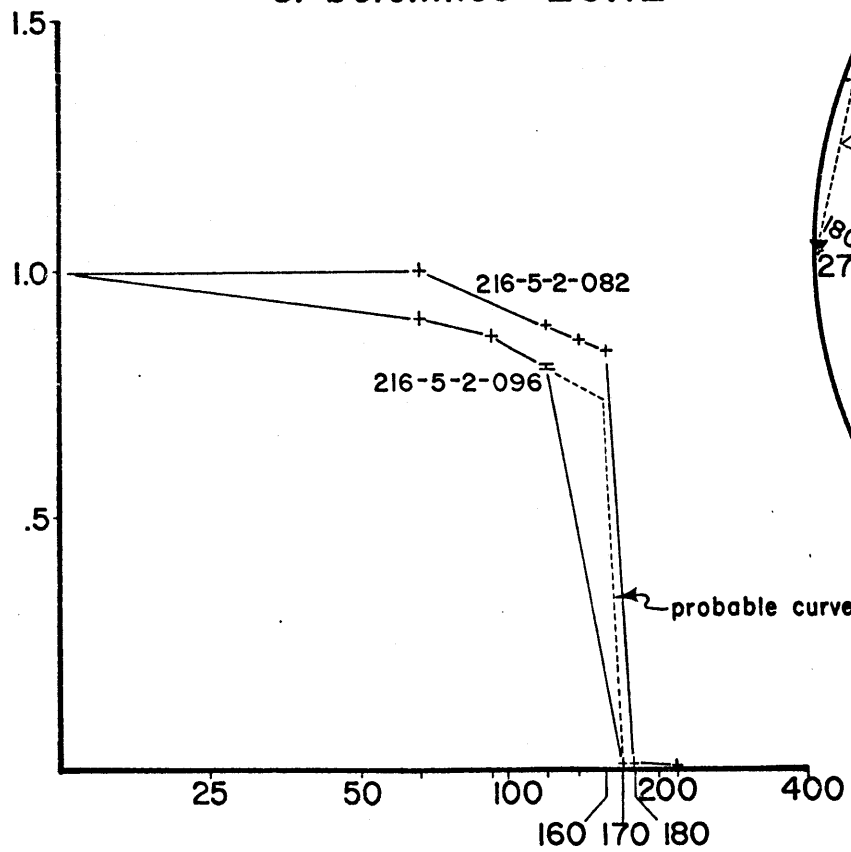
DSDP SITE 215
ZONE P4



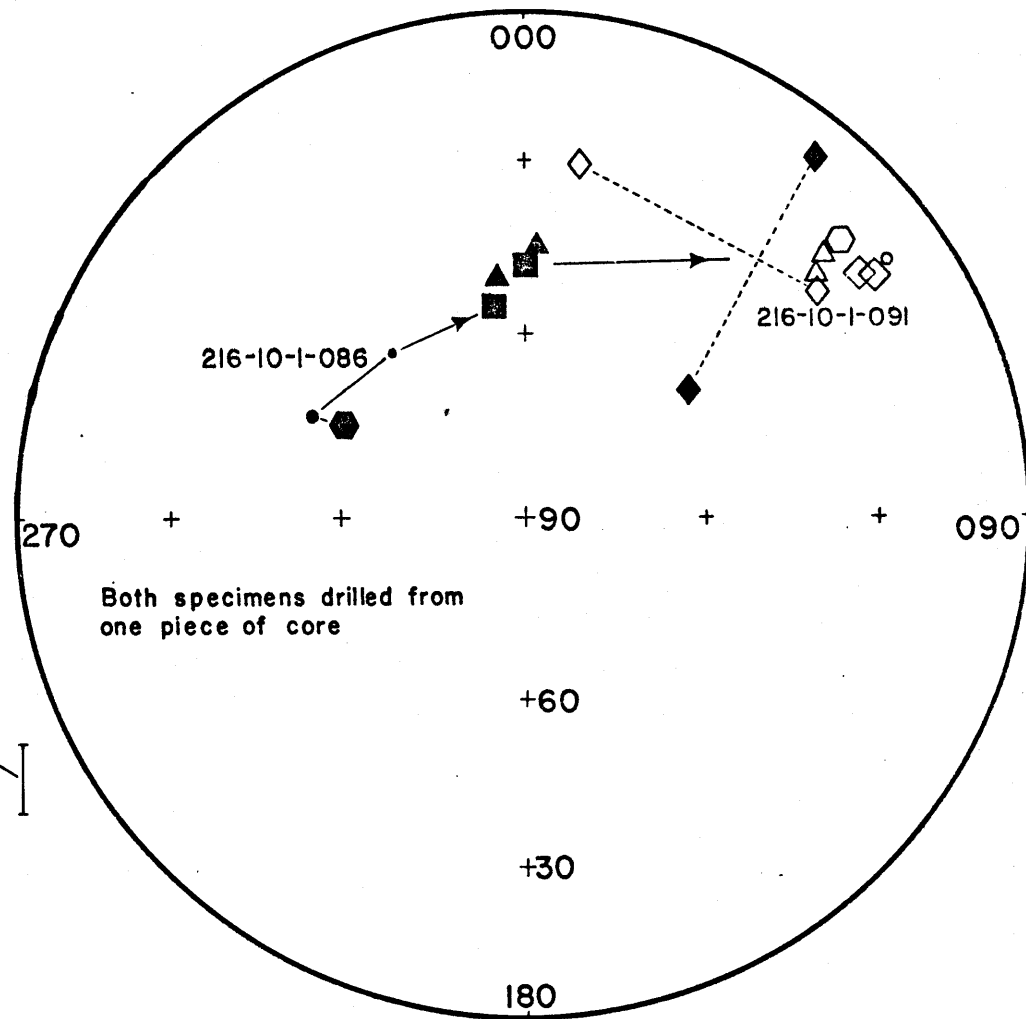
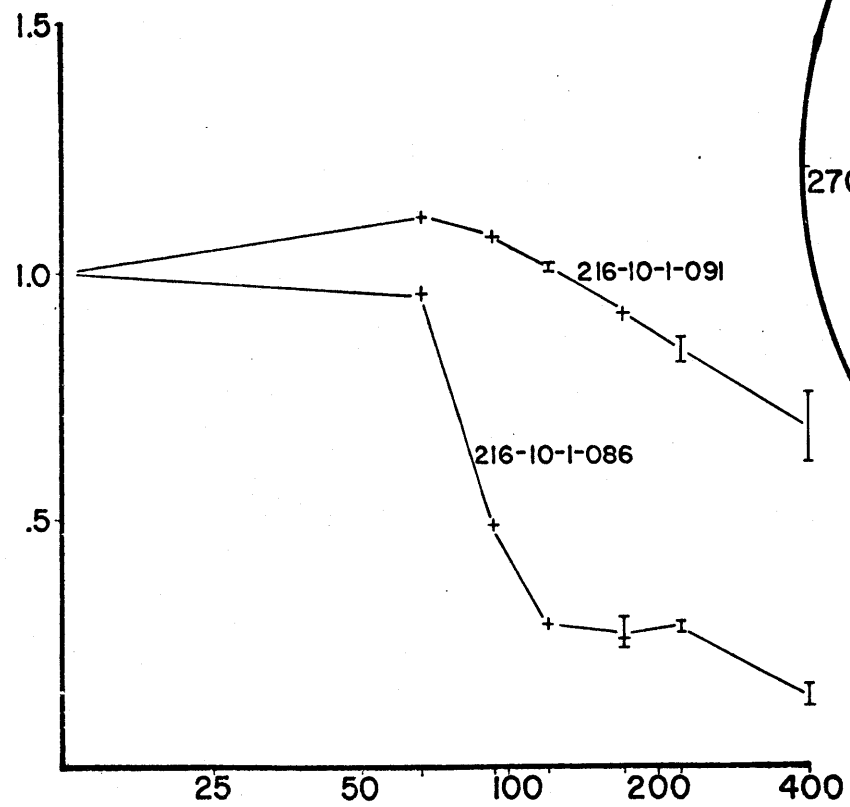
DSDP SITE 215
ZONE P4



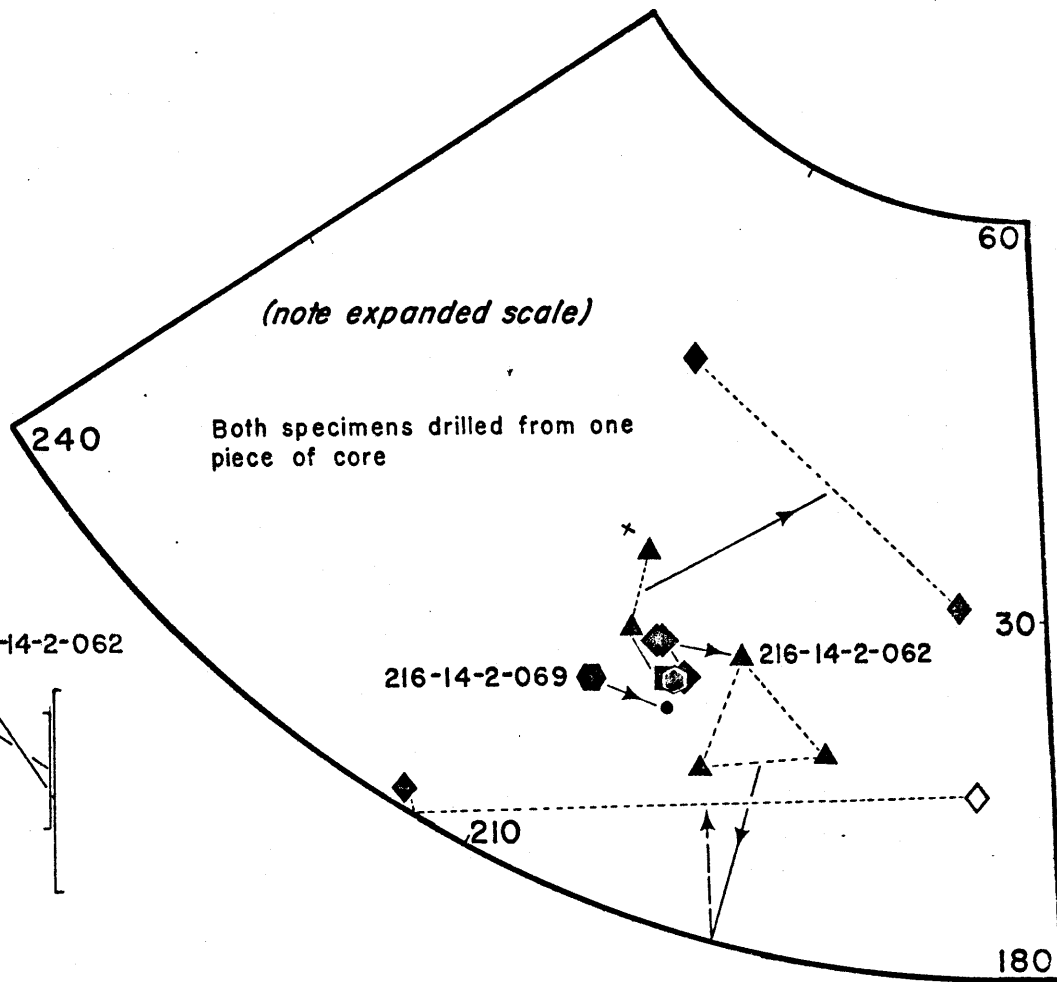
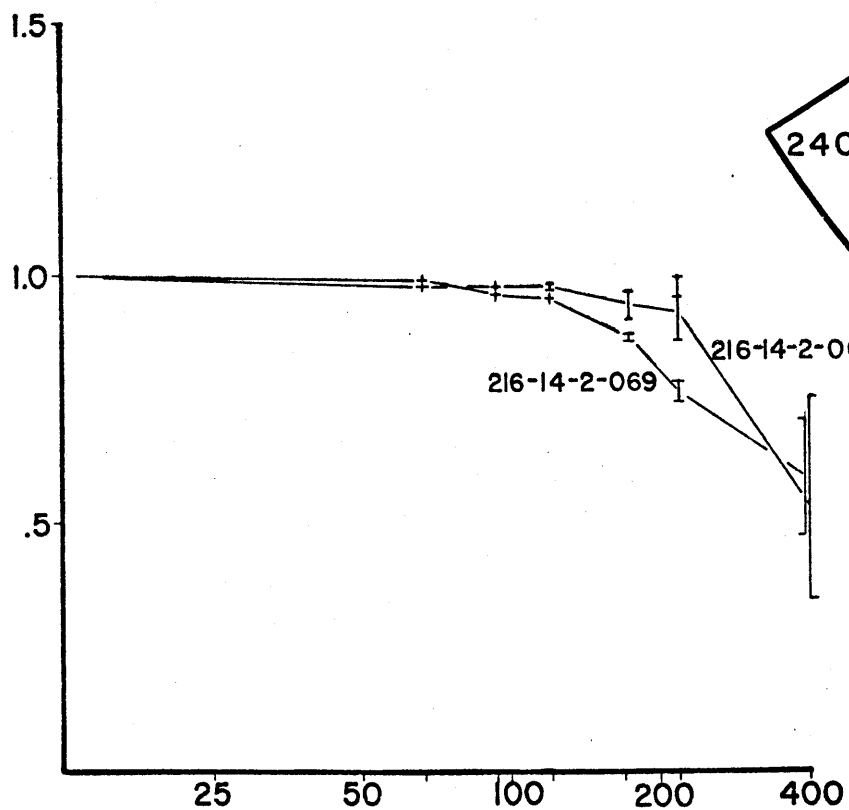
DSDP SITE 216
S. belemnites ZONE



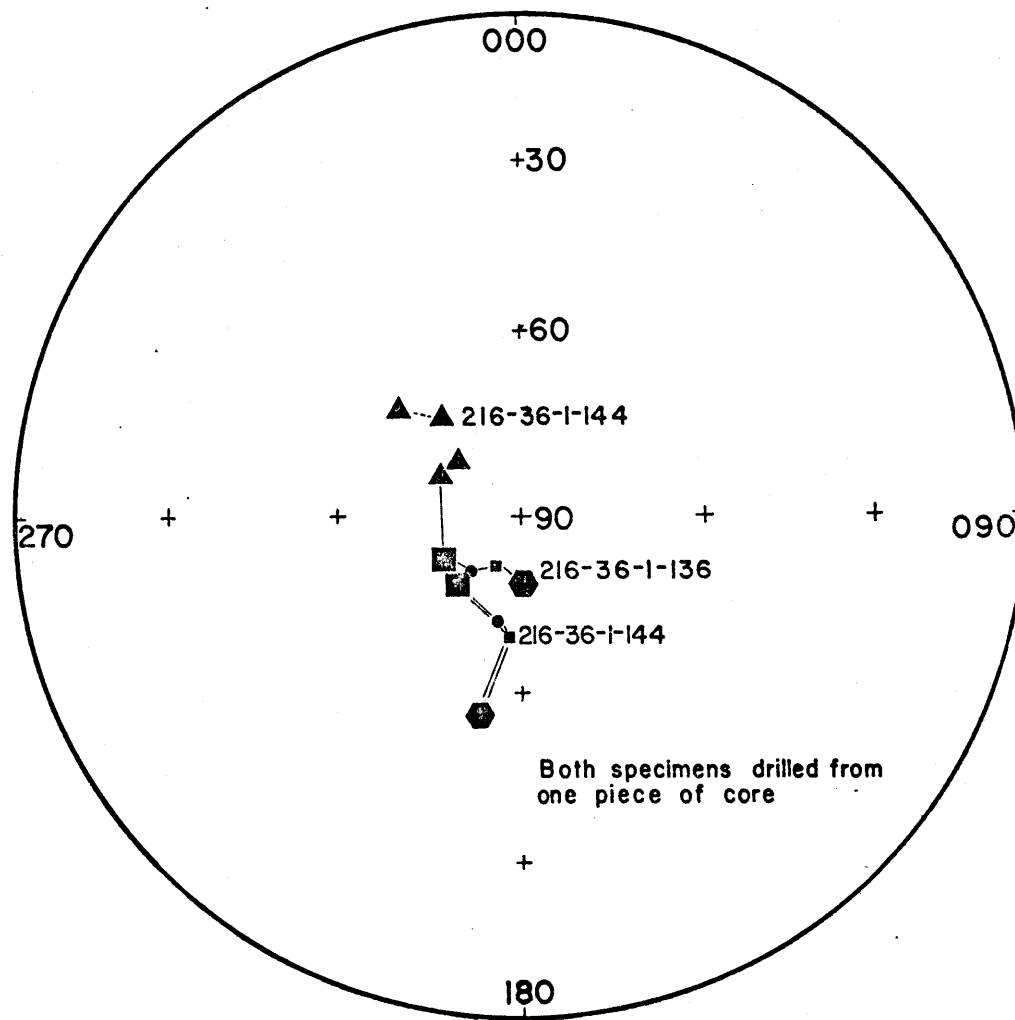
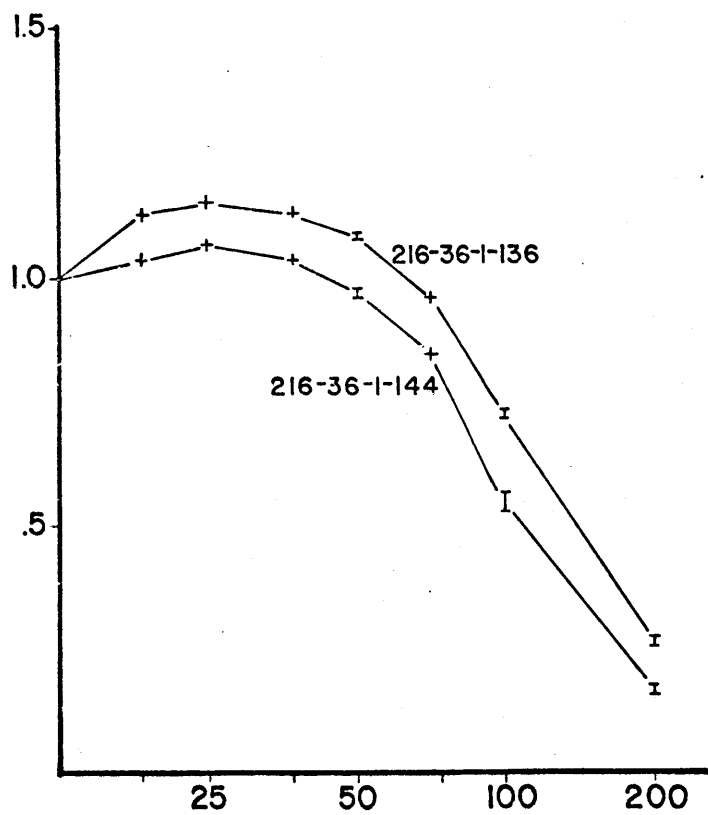
DSDP SITE 216
 ZONE N4



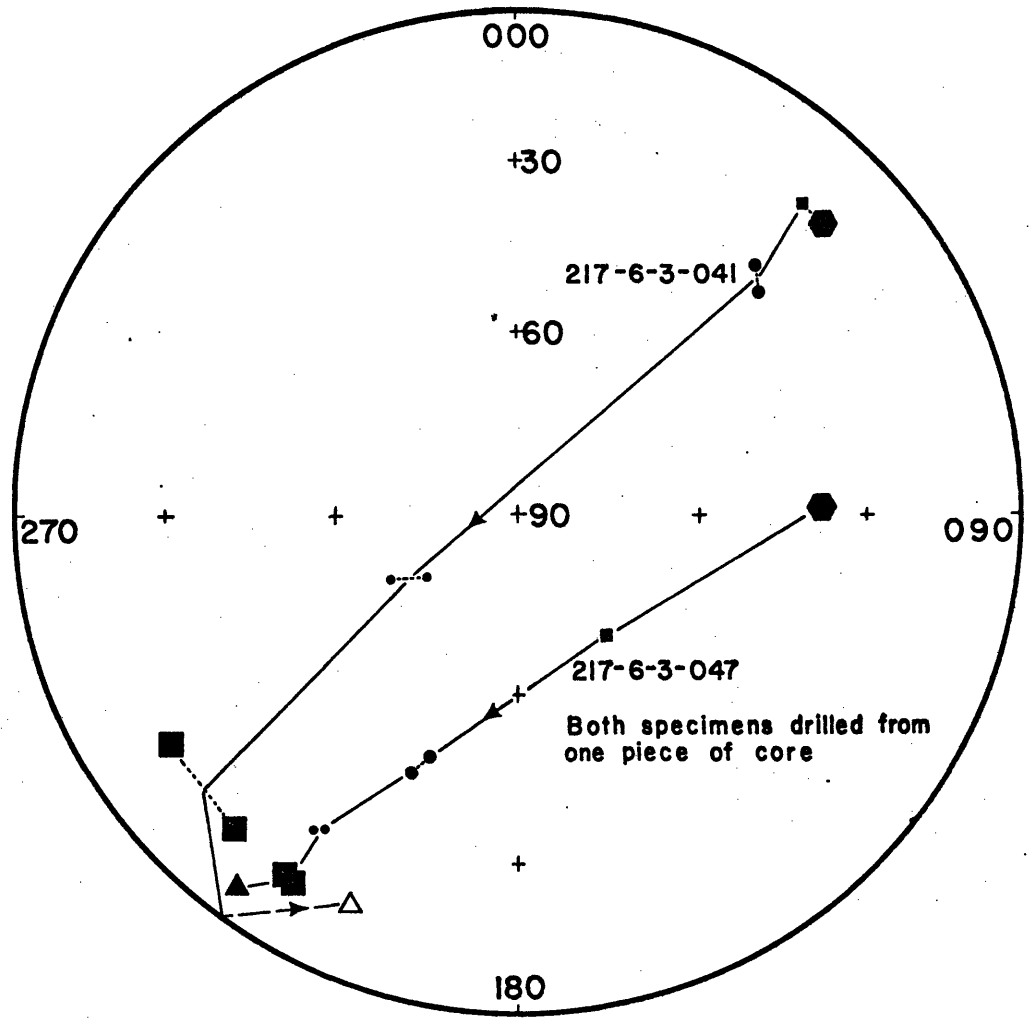
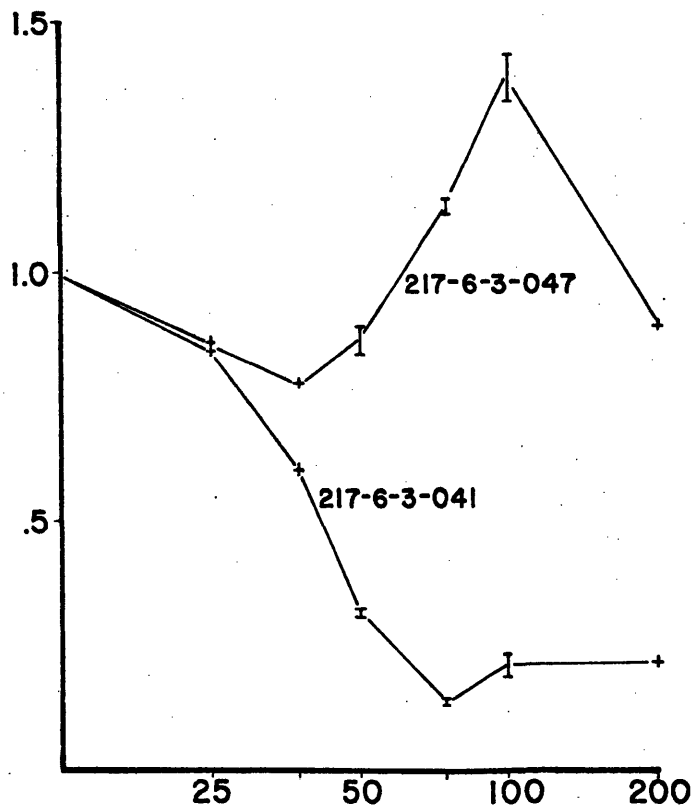
DSDP SITE 216
ZONES P19-P21



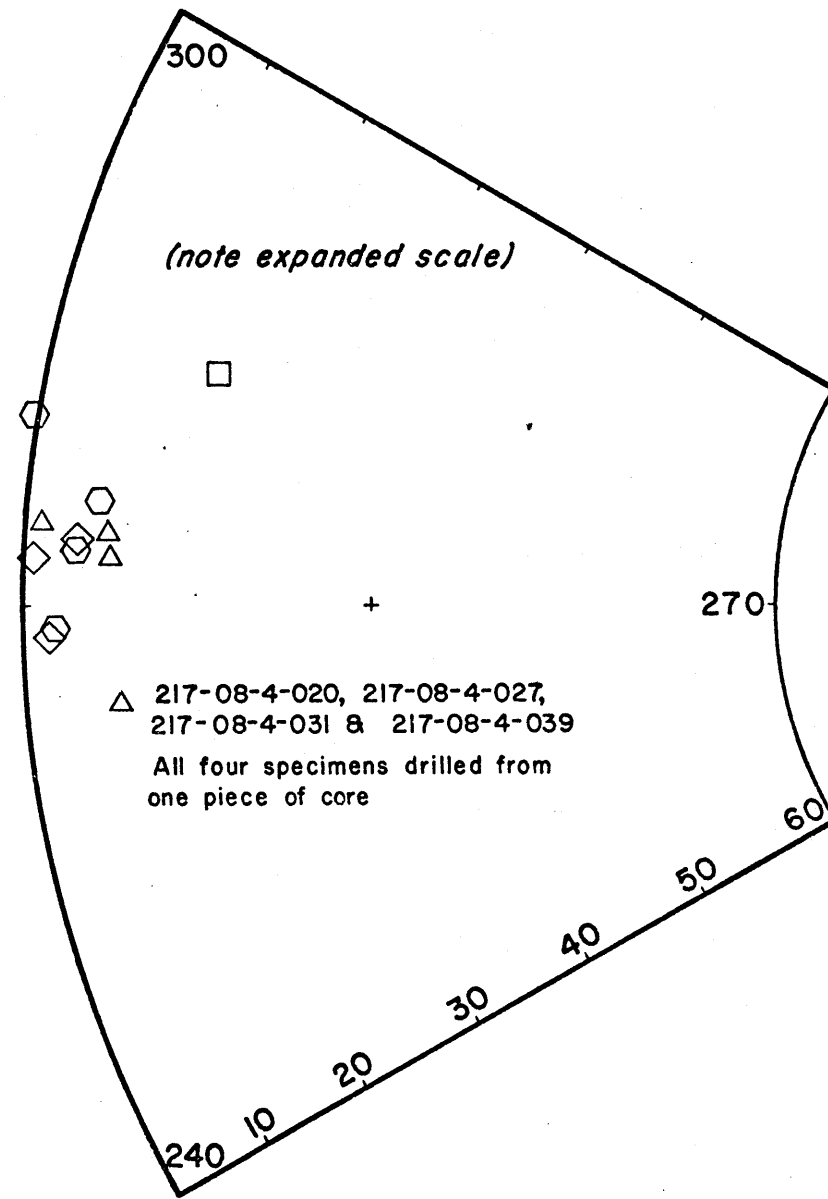
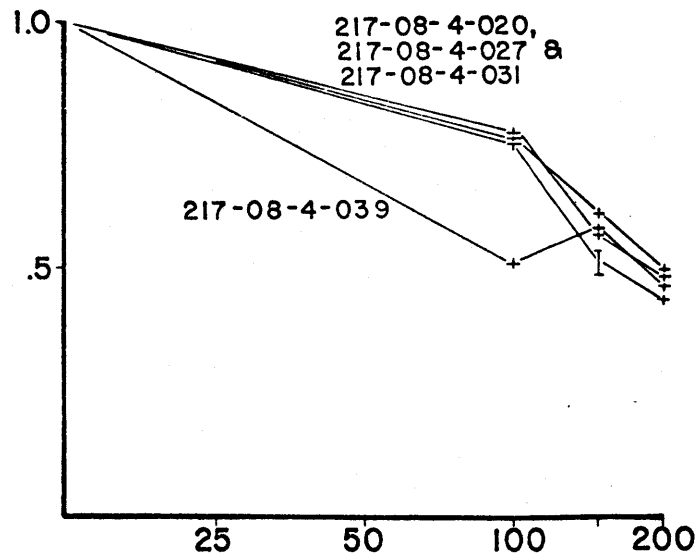
DSDP SITE 216
Maastrichtian



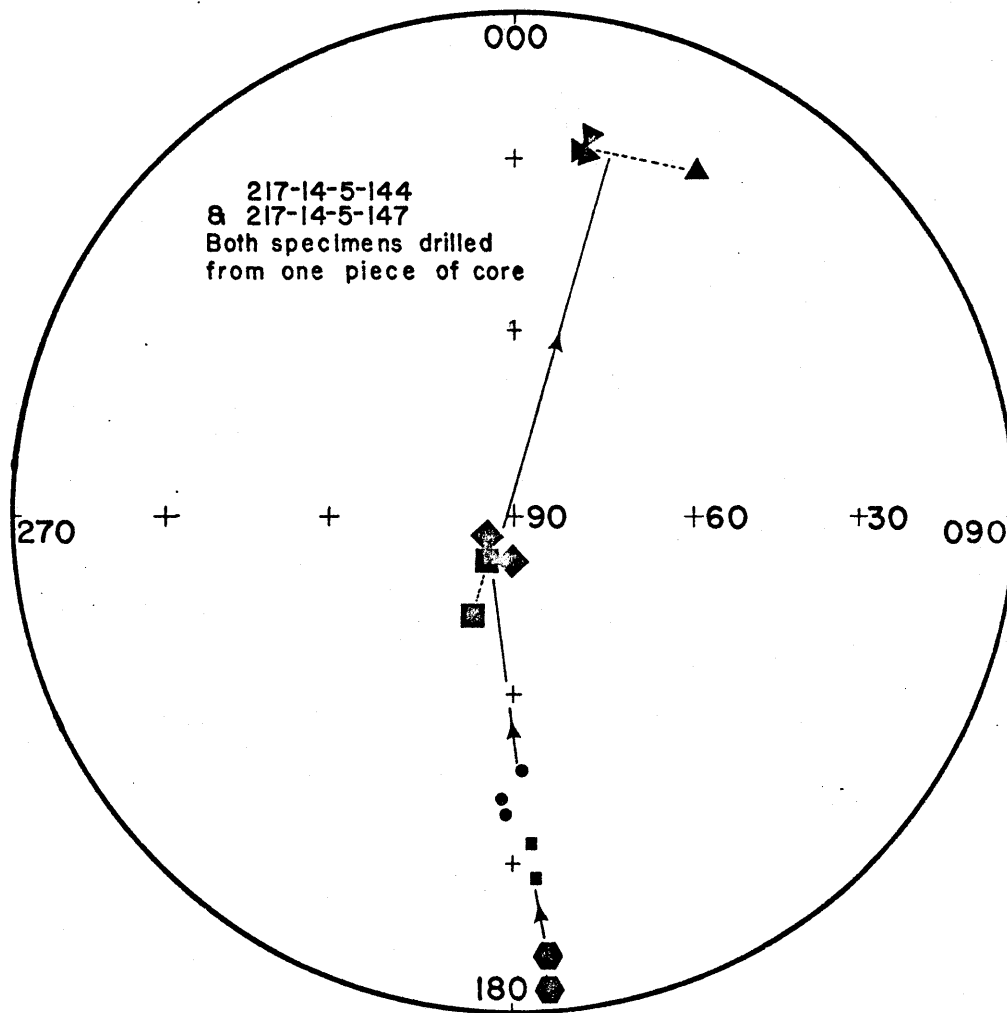
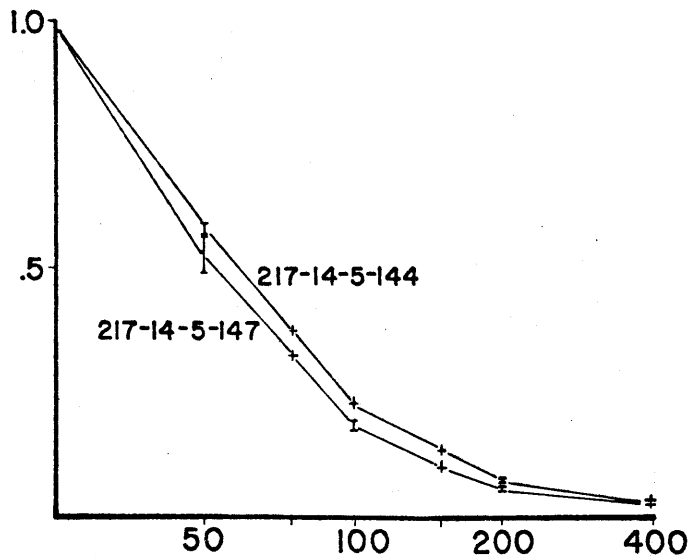
DSDP SITE 217
 ZONE N5



DSDP SITE 217
ZONE P21



DSDP SITE 217
 ZONE P4



Appendix V

DESKEWED MAGNETIC ANOMALIES
FROM THE EAST CENTRAL INDIAN OCEAN

This Appendix presents several approximately north-south tracks of magnetic anomaly data in the east central Indian Ocean. All data have been projected onto a north-south line and interpolated at a one mile interval. The observed interval was five minutes. In each figure the observed data are plotted at the bottom and five plots of phaseshifted data are shown above it. All data are plotted with north to the right. These phaseshifted data show the deskewed form of the anomalies and the variability of skewness along any one track.

Representative phaseshifts ($\Delta\theta$) have been chosen for each track, and a composite picture of all the data plotted perpendicular to track is given in Figure 10, Chapter IV. Lunes of confidence for paleomagnetic pole positions are presented in Figure 9, Chapter IV.

The following tracks are included, in alphabetical order:

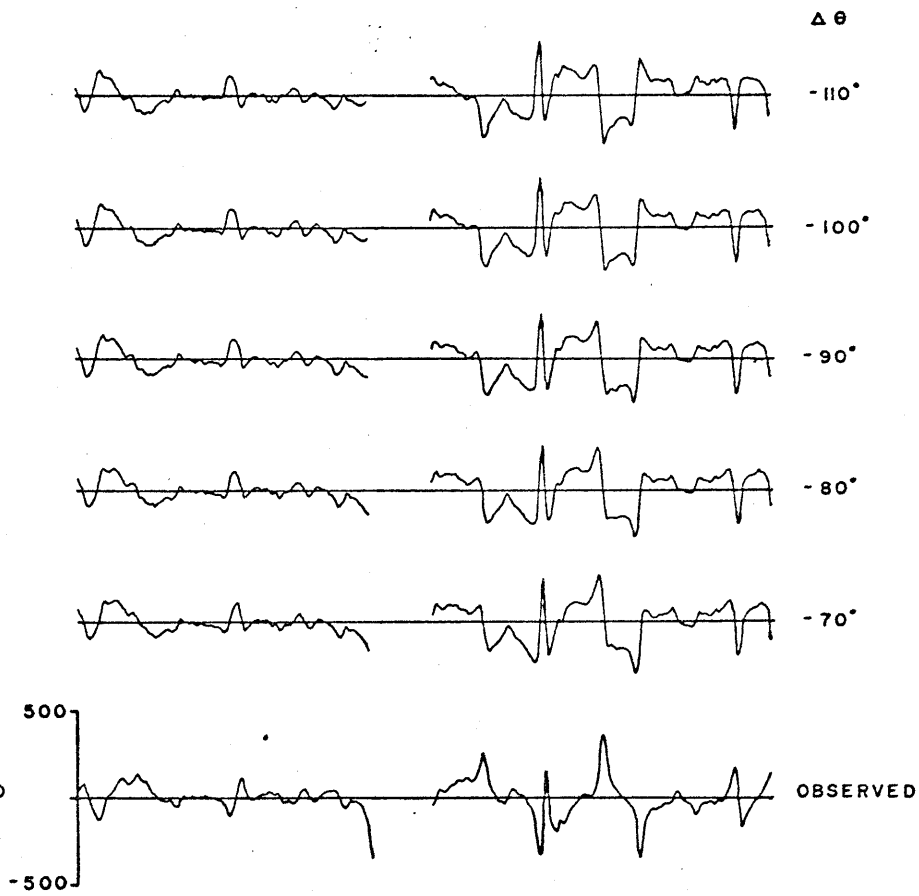
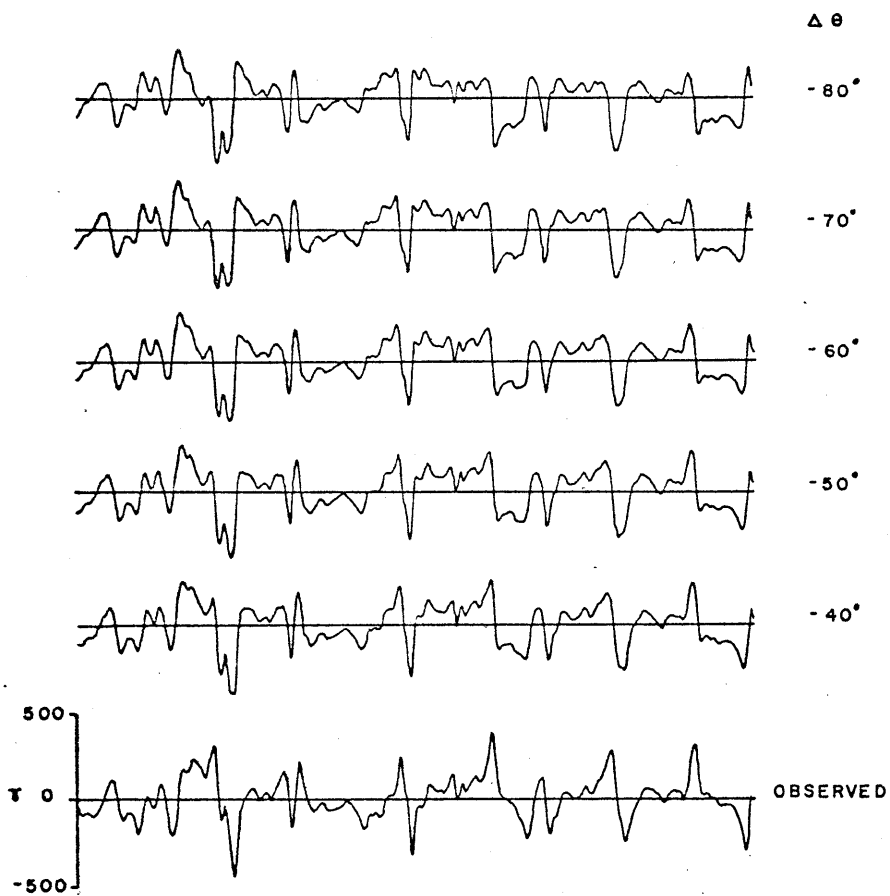
Track	South Lat.	North Lat.	Approximate $\Delta\theta$ to deskew
ANTIPODE 12 A	-22°	-6°	-65°
ANTIPODE 12 B	-22°	-16°	-60°
CIRCE 5 A	-20°	-2.5°	-75°
CIRCE 5 B	-20°	-8°	-70°
GLOMAR CHALLENGER 22	-10°	0°	-80°
PIONEER A	-5°	+5°	-80°
PIONEER B	-5°	+5°	-80°
PIONEER C	-5°	+5°	-90°
VEMA 19 A	-20°	-6°	-70°
VEMA 19 B	-7°	+3°	-80°

ANTIPODE 12 A

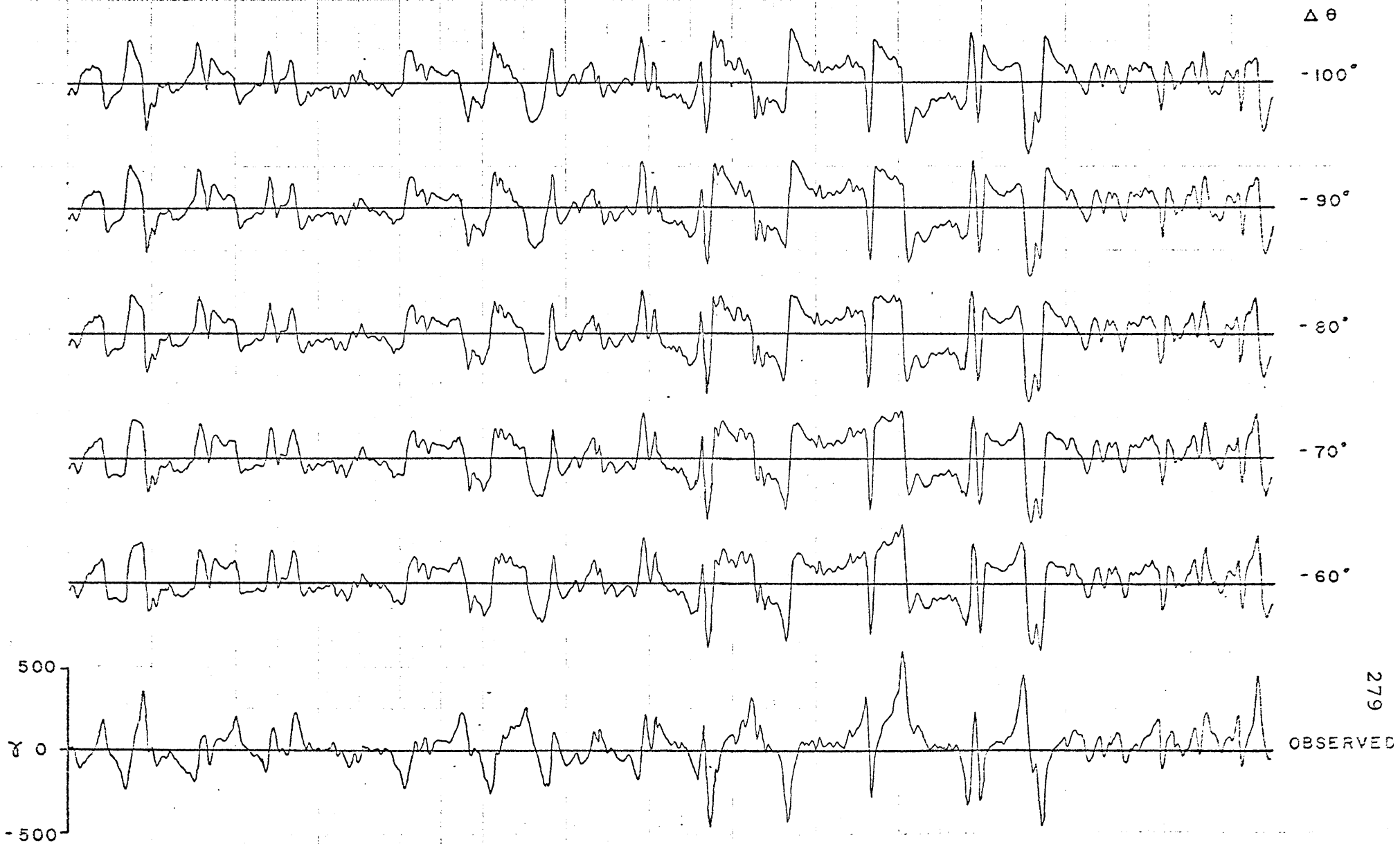


ANTIPODE i2 B

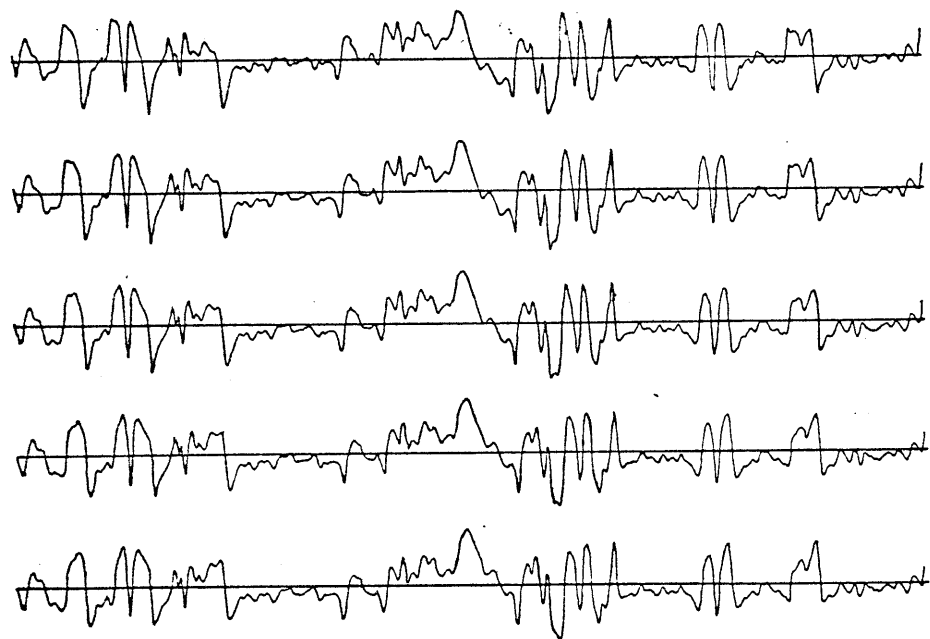
PIONEER C



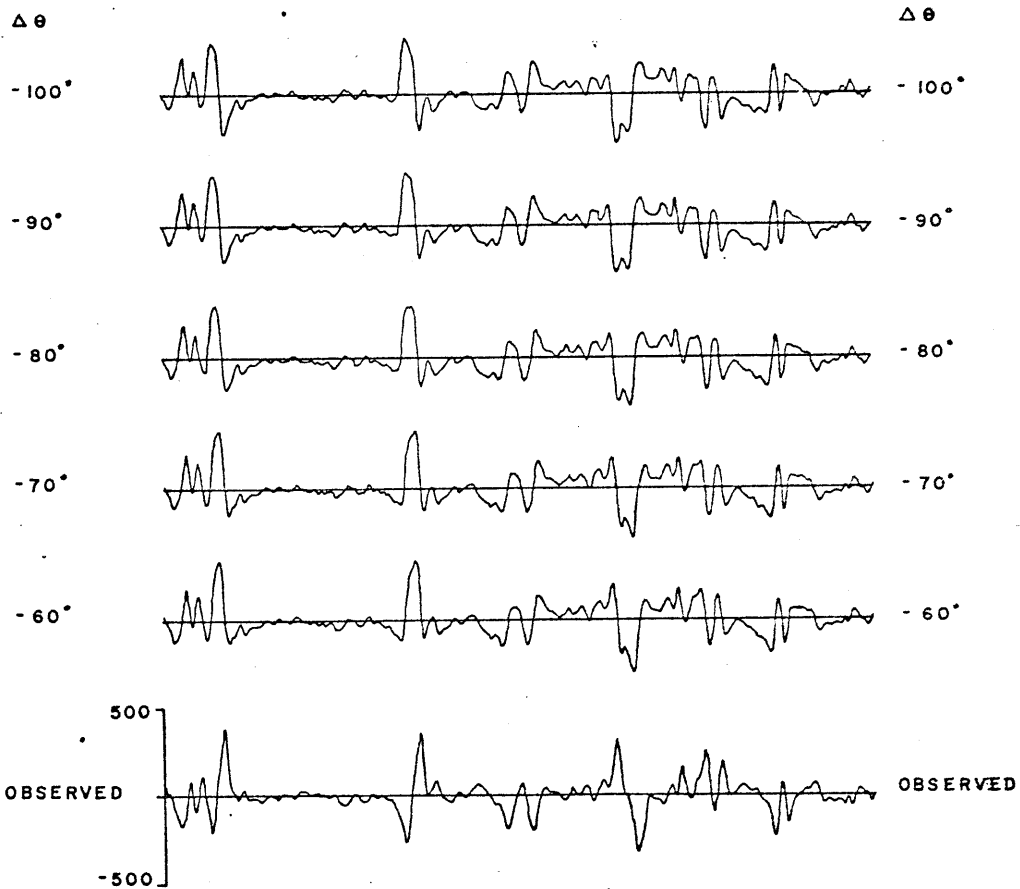
CIRCE 5 A



CIRCE 5 B

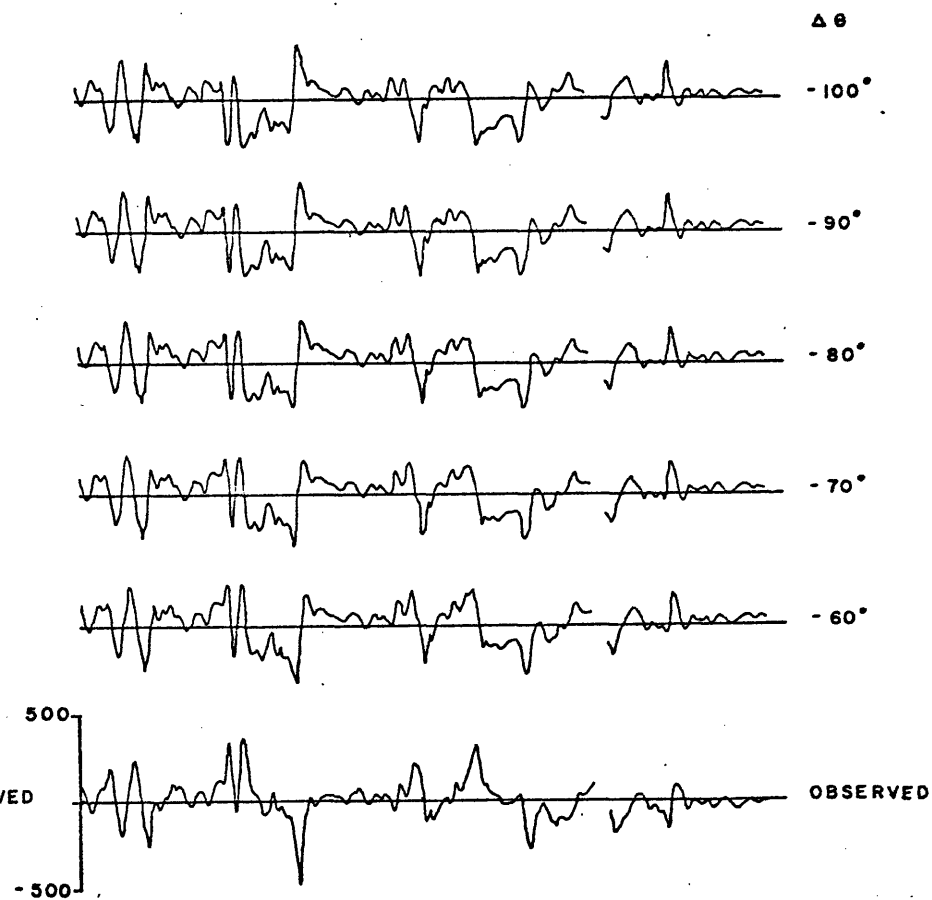
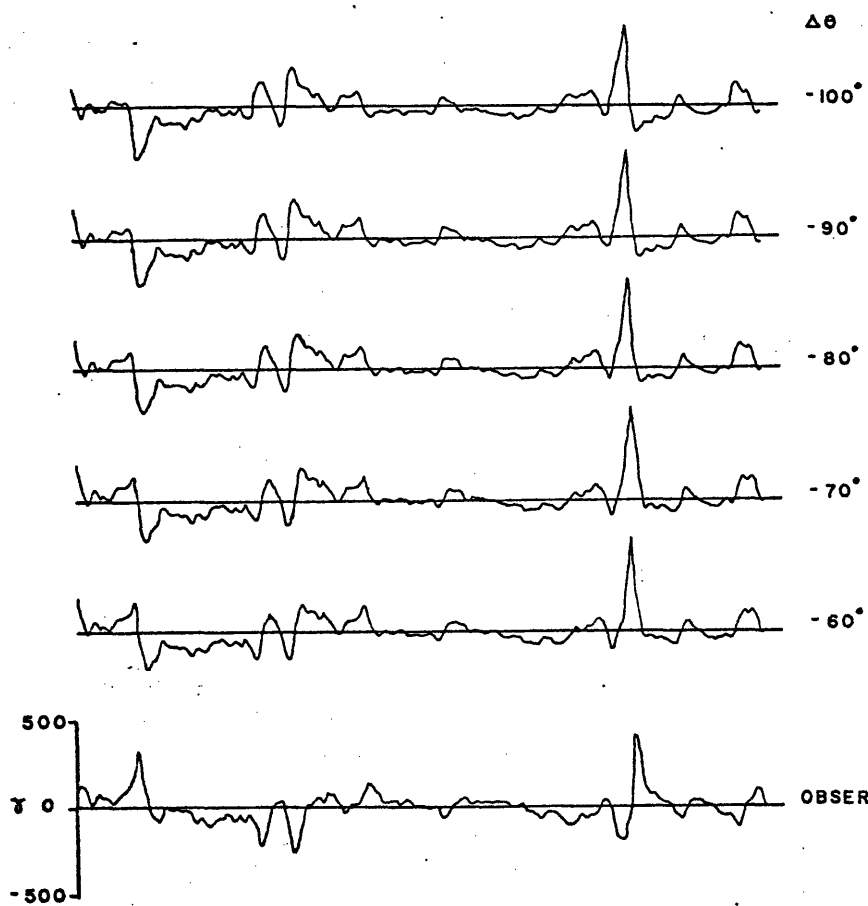


GLOMAR CHALLENGER 22

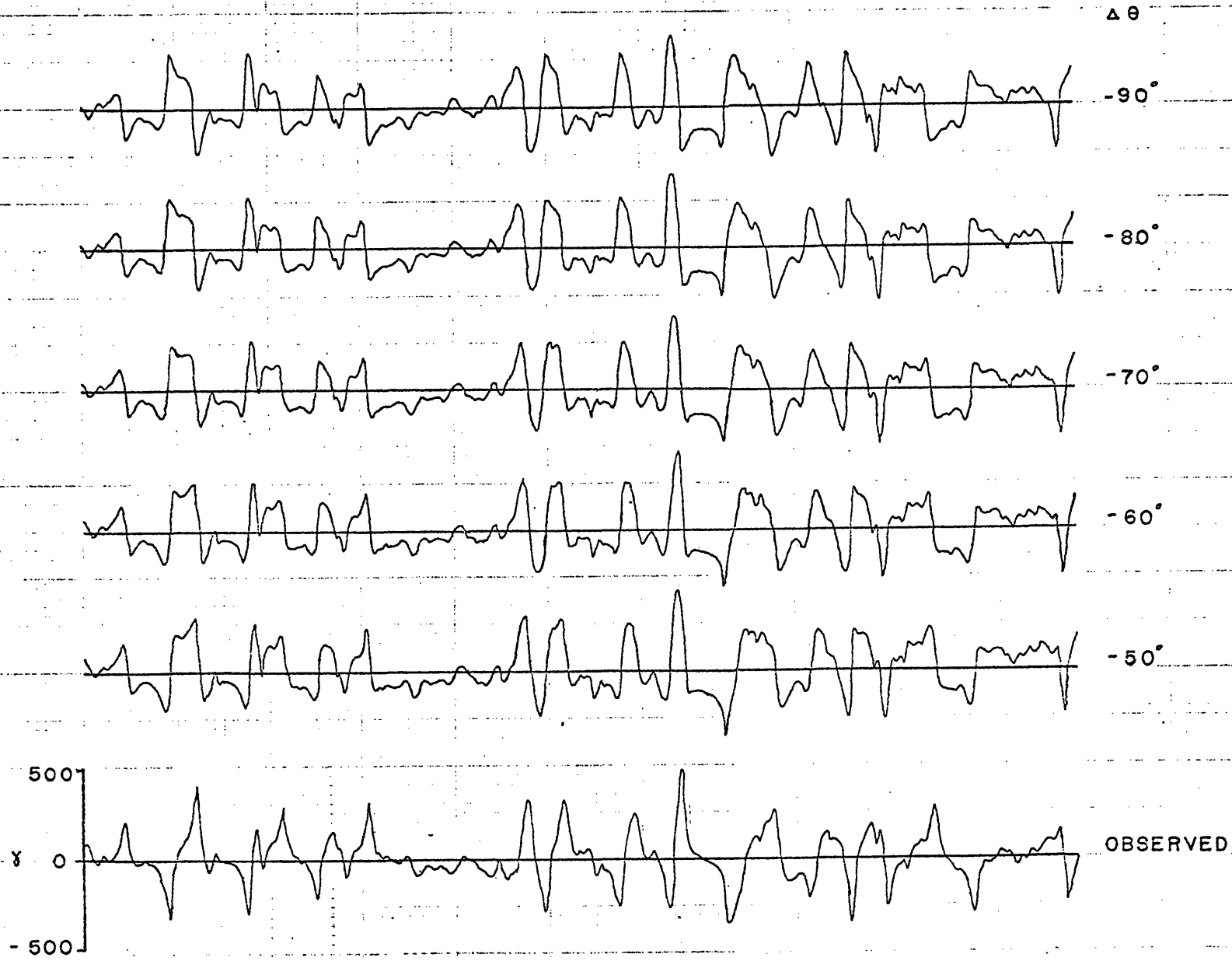


PIONEER A

PIONEER B



VEMA 19 A



VEMA 19 B

